E-ISSN: 2148-6247

Turkish Journal of PHARMACEUTICAL SCIENCES

An Official Journal of the Turkish Pharmacists' Association, Academy of Pharmacy

Volume: 21 Issue: 4 August 2024

www.turkjps.org

Emerging Sources Citation Index · PubMed Central · PubMed · Scopus · TR Dizin

galenos Publishing House

Turkish Journal of
PHARMACEUTICAL SCIENCES

Turkish Journal of
PHARMACEUTICAL SCIENCES

Prof. Robert Rapoport, Ph.D.
ORCID: orcid.org/0000-0001-8554-1014
Cincinati University Faculty of Pharmacy, Department of Pharmacology and Cell Biophysics, Cincinati, USA
robertrapoport@gmail.com

Prof. Tayfun Uzbay, Ph.D.
ORCID: orcid.org/0000-0002-9784-5637
Üsküdar University Faculty of Medicine, Department of Medical Pharmacology, İstanbul, Türkiye
tayfun.uzbay@uskudar.edu.tr

Prof. Wolfgang Sadee, Ph.D.
ORCID: orcid.org/0000-0003-1894-6374
Ohio State University, Center for Pharmacogenomics, Ohio, USA
wolfgang.sadee@osumc.edu

Advisory Board

Turkish Journal of
PHARMACEUTICAL SCIENCES

Please refer to the journal's webpage (https://www.turkjps.org/) for "Editorial Policy" and "Instructions to Authors".

The editorial and publication process of the **Turkish Journal of Pharmaceutical Sciences** are shaped in accordance with the guidelines of ICMJE, WAME, CSE, COPE, EASE, and NISO. The Turkish Journal of Pharmaceutical Sciences is indexed in **PubMed, PubMed Central, Thomson Reuters / Emerging Sources Citation Index, Scopus, ULAKBİM, Türkiye Atıf Dizini, Embase, EBSCO Host, Türk Medline, Cabi, CNK**I.

The journal is published online.

Owner: Turkish Pharmacists' Association, Academy of Pharmacy

Responsible Manager: Mesut Sancar

galenos yayınevi

Publisher Contact
Address: Molla Gürani Mah. Kaçamak Sk. No: 21/1
34093 İstanbul, Türkiye
Phone: +90 (530) 177 30 97
E-mail: info@galenos.com.tr/yayin@galenos.com.tr
Web: www.galenos.com.tr | **Publisher Certificate Number:** 14521

Publication Date: August 2024
E-ISSN: 2148-6247
International scientific journal published bimonthly.

Turkish Journal of
PHARMACEUTICAL SCIENCES

CONTENTS

Original Articles

Turk J Pharm Sci 2024;21(4):259-266
DOI: 10.4274/tjps.galenos.2023.47650

ORIGINAL ARTICLE

Altered Levels of Gene Expression of Drug Metabolism Enzymes in Rat Brain Following Kainic Acid Treatment

Ayfer YALÇIN[1]*, Ezgi TURUNÇ[2], Güliz ARMAĞAN[1], Lütfiye KANIT[3]

[1]Ege University Faculty of Pharmacy, Department of Biochemistry, İzmir, Türkiye
[2]İzmir Katip Çelebi University Faculty of Pharmacy, Department of Biochemistry, İzmir, Türkiye
[3]Ege University Faculty of Medicine, Department of Physiology, İzmir, Türkiye

ABSTRACT

Objectives: Previous studies have shown that gene expressions can be regulated in the hippocampus of rats after seizures induced by kainic acid (KA). The aim of this study was to examine the potential regulatory impact of KA administration on gene expression levels of enzymes responsible for drug metabolism in rat hippocampal tissue.

Materials and Methods: Rats received intraperitoneal injections of KA and saline at a dose of 10 mg/kg. Behavioral changes were observed in experimental animals following the administration of KA. Four hours after receiving treatments, all rats were decapitated, and the brains were removed. Hippocampal tissues were used for total RNA isolation, and cDNA synthesis was performed by reverse transcription polymerase chain reaction (PCR). Gene expression levels of enzymes responsible for drug metabolism were determined by quantitative PCR using the RT^2 Profiler PCR Array Rat Drug Metabolism PCR array system containing the relevant primers for a total of 84 genes. The gene expression levels of drug-metabolizing enzymes were quantified using the comparative Ct ($2^{-\Delta\Delta(\text{delta delta})Ct}$) method. The Student's t-test was used for data analysis.

Results: Our results indicate that KA treatment caused significant changes in the gene expression levels of metallothionein 3, glucose phosphate isomerase, adenosine triphosphate-binding cassette protein C1, cytochrome P450 enzymes (Cyp2c6v1, Cyp3a23/3a1, Cyp2c7), glutathione peroxidase 1, 4, and 5, glutamic acid decarboxylase 1 and 2, paraoxonase 2, carbohydrate sulfotransferase 1, glutathione S-transferases (Gsta3, Gstm1, Gstm4), microsomal glutathione S-transferase 3, carboxylesterase 2C, fatty acid amide hydrolase, pyruvate kinase-muscle, arachidonate 5-lipoxygenase, apolipoprotein E, cytochrome b5 reductase 5, xanthine dehydrogenase, N-acetyltransferase 1, glucokinase regulator, hexokinase 2, myristoylated alanine rich protein kinase C substrate, and stannin in the hippocampus compared with the control ($p < 0.05$).

Conclusion: As a conclusion, it can be said that the seizure activity triggered by KA has the potential to change the gene expression levels of the enzymes responsible for drug metabolism in the hippocampus of rats.

Keywords: Kainic acid, status epilepticus, hippocampus, drug metabolism, gene expression, PCR array

INTRODUCTION

Kainic acid (KA) is an analog of glutamate, an excitatory amino acid. The treatment of rodents with KA results in seizures and neuronal death in specific brain regions such as the hippocampus.[1-3] Neuropathological changes induced in the brain by KA are similar to the changes detected in the hippocampus region of patients with temporal lobe epilepsy (TLE).[4]

Different enzyme classes that are in charge of the biochemical alteration of medicinal compounds participate in drug metabolism. Drug-metabolizing enzymes (DMEs) are also found in extrahepatic tissues, such as the brain, despite the liver being the primary organ of metabolism in the body.[5,6]

Prior research has demonstrated that KA-induced seizures or status epilepticus (SE) can alter gene expression in the rat brain.[7-10] There appear to be few studies examining the impact of KA administration on DMEs. Conducting research on potential genetic controls of KA-induced SE on DMEs in rat brains was deemed advantageous in this context. This approach might also

*Correspondence: ayfer.yalcin@ege.edu.tr, Phone: +90 232 311 13 55, ORCID-ID: orcid.org/0000-0003-0407-3218
Received: 14.04.2023, Accepted: 14.07.2023

be helpful for identifying the gene profile of potential molecular targets in KA-induced seizures. According to these stated goals, the objective of our investigation was to determine how KA administration affected the relative expression levels of DMEs, which include drug transporters, P-glycoproteins, and Phase I and Phase II DMEs.

MATERIALS AND METHODS

Animals and in vivo treatments

Twelve male adult Sprague-Dawley rats weighed 200-230 g were used in this study. The rats were housed under identical laboratory settings of lighting (14:10 h light-dark) and temperature (24 ± 2 °C) and had free access to normal laboratory food and tap water. Every attempt was made to minimize animal suffering and the number of animals employed. The procedure for the experiments was approved by Ege University Faculty of Pharmacy, Experimental Animal Ethics Committee (2006/6-1, date: 22.06.2006).

KA [2-carboxy-4-isopropenyl-pyrrolidin-3-acetic acid] was obtained from Ocean Products International (Canada). Rats received intraperitoneal injections of KA and saline at a dose of 10 mg/kg each according to previous studies.[10,11] Behavioral changes were observed in experimental animals following the administration of KA. KA promotes seizures and selective excitotoxic cell death, primarily in the limbic structure, in rodents when administered systemically.[2] Once the KA was administered, it resulted in a series of behavioral alterations that were clearly characterized. After 45 minutes, the rats' rigidity and immobility were replaced by "staring spells", which were then followed by wet dog shakes and repetitive head nodding, and finally by rearing and falling. A generalized tonic-clonic seizure with ongoing convulsions eventually developed in rats. Four hours after receiving treatment, all rats were decapitated. The brains were removed and the hippocampus tissues were dissected. The effect of KA on the expression of DMEs was investigated using the RT^2 profiler polymerase chain reaction (PCR) Array Rat Drug Metabolism (SABiosciences, Qiagen, Maryland, USA) in accordance with the manufacturer's guidelines. Each array contained five housekeeping genes and a panel of 84 target genes related to drug metabolism and transport.

Hippocampal tissues were used for total RNA isolation with Trizol (Invitrogen, USA), followed by phenol chloroform extraction and isopropanol precipitation chloroform.[12] The complementary DNA (cDNA) was synthesized from total RNA using a reverse transcription PCR RT^2 PCR array first strand kit. The real-time PCR mixture, which contained RT^2 master mix, nuclease-free H_2O, and cDNA, was loaded onto a PCR plate. PCR amplification was conducted with an initial step at 95 °C for 10 minutes, followed by 40 cycles of 15 s at 95 °C and 1 minute at 60 °C. Threshold cycles were detected for all genes, and the data obtained were examined using PCR Array Data Analysis Software (SABiosciences, USA). The gene levels of DMEs were determined using the comparative Ct ($2^{-\Delta\Delta Ct}$) method.[13,14] Gene expression was normalized using β-actin, ribosomal protein large P1, ribosomal protein L13A, hypoxanthine phosphoribosyltransferase-1, and lactate dehydrogenase A as reference genes, which were included in the PCR array kit.

Statistical analysis

Statistical analysis was performed using SPSS statistical software version 16.0 (SPSS Inc., Chicago, IL, USA), and the data were evaluated using the Student's t-test, and $p < 0.05$ was considered statistically significant.

RESULTS

Metallothionein 3 (Mt3), ATP-binding cassette protein C1, and glucose phosphate isomerase (Gpi) gene expression levels were considerably lower after KA treatment compared to control ($p < 0.05$) (Figure 1, Table 1). When compared to controls,

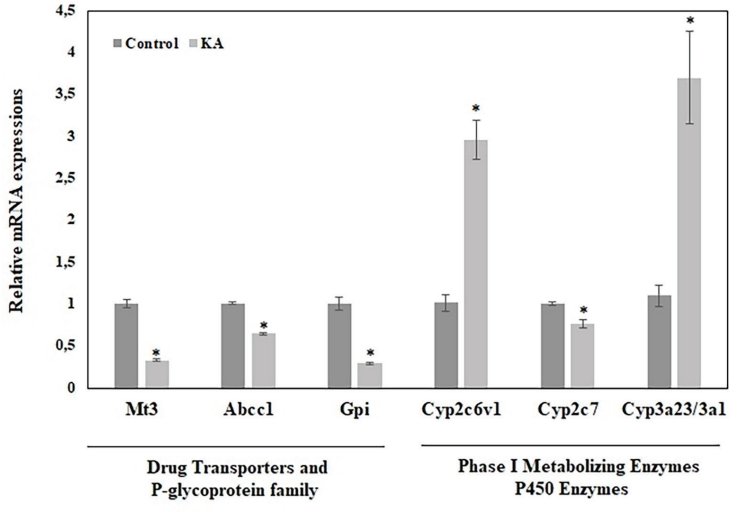

Figure 1. Effects of KA treatment on mRNA expression levels of drug transporters, P-glycoprotein family, and Phase I metabolizing enzymes in the hippocampus. Data are expressed as mean ± standard error. *$p < 0.05$ vs. control in hippocampus (n= 6 for each group)

KA: Kainic acid

KA administration significantly upregulated Cyp2c6v1, Cyp3a23/3a1, and downregulated Cyp2c7 gene expressions ($p < 0.05$) (Figure 1, Table 2). When compared to the control, KA administration significantly changed the expression of the genes glutathione peroxidase 1 (Gpx1), genes glutathione peroxidase 5 (Gpx5), paraoxonase 2 (Pon2), carbohydrate sulfotransferase 1 (Chst1), Gsta3, microsomal glutathione S-transferase 3, and lowered the expression of the genes carboxylesterase 2C, glutamic acid decarboxylase (Gad) 1, Gad2, Gpx4, fatty acid amide hydrolase (Faah), pyruvate kinase-muscle (Pkm2), arachidonate 5-lipoxygenase, apolipoprotein E (Apoe), cytochrome b5 reductase 5, Gstm1, Gstm4, xanthine dehydrogenase, N-acetyltransferase 1, glucokinase regulator, hexokinase 2, myristoylated alanine rich protein kinase C substrate (Marcks), and stannin (Snn) ($p < 0.05$) (Figure 2, Table 3).

DISCUSSION

Effects of KA on drug transporters and P-glycoproteins

The Mt1, Mt2, and Mt3 isoforms may be controlled differentially in the rat brain depending on their roles in cell type-dependent cellular responses to KA-induced damage.[15] In line with this finding, we found that KA treatment reduced the level of Mt3 expression in the hippocampus. The enzyme Gpi, also known as neuroleukin, is reportedly involved in metabolic activities. It has also been shown that focal ischemia-induced brain injury results in a decrease in Gpi protein expression levels.[16]

Table 1. Regulated levels of drug transporters and P-glycoproteins gene expressions in the hippocampus of rats after KA treatment. Gene expression levels are stated as n-fold change normalized to the control group. Each sample is tested in triplicate

Gene symbol	Drug metabolism enzymes	Expression levels
Drug transporters and P-glycoprotein family		
Mt3	Metallothionein 3	0.332 ± 0.014*
Abcb1b	ATP-binding cassette, sub-family B (MDR/TAP), member 1B	1.014 ± 0.075
Abcb1a	ATP-binding cassette, sub-family B (MDR/TAP), member 1A	0.889 ± 0.116
Abcb4	ATP-binding cassette, sub-family B (MDR/TAP), member 4	1.357 ± 0.252
Abcc1	ATP-binding cassette, sub-family C (CFTR/MRP), member 1	0.655 ± 0.014*
Abp1	Amiloride binding protein 1 (amine oxidase, copper-containing)	2.219 ± 0.791
Gpi	Glucose phosphate isomerase	0.297 ± 0.017*

*p <0.05, KA: Kainic acid, ATP: Adenosine triphosphate

Table 2. Regulated levels of Phase I metabolizing enzymes (P450 family) in the hippocampus of rats after KA treatment. Gene expression levels are stated as n-fold change normalized to the control group. Each sample is tested in triplicate

Gene symbol	Drug metabolism enzymes	Expression levels
Phase I metabolizing enzymes-P450 family		
Cyp17a1	Cytochrome P450, family 17, sub-family a, polypeptide 1	3.227 ± 1.893
Cyp19a1	Cytochrome P450, family 19, sub-family a, polypeptide 1	0.012 ± 0.005
Cyp1a1	Cytochrome P450, family 1, sub-family a, polypeptide 1	3.580 ± 1.772
Cyp1a2	Cytochrome P450, family 1, sub-family a, polypeptide 2	2.603 ± 1.468
Cyp1b1	Cytochrome P450, family 1, sub-family b, polypeptide 1	1.000 ± 0.095
Cyp27b1	Cytochrome P450, family 27, sub-family b, polypeptide 1	2.567 ± 1.324
Cyp2b15	Cytochrome P450, family 2, sub-family b, polypeptide 15	0.928 ± 0.086
Cyp2b6	Cytochrome P450IIB3	0.986 ± 0.099
Cyp2c13	Cytochrome P450, family 2, sub-family c, polypeptide 13	1.717 ± 0.614
Cyp2c6v1	Cytochrome P450, family 2, sub-family c, polypeptide 6	2.969 ± 0.235*
Cyp2c7	Cytochrome P450, family 2, sub-family c, polypeptide 7	0.775 ± 0.049*
Cyp2e1	Cytochrome P450, family 2, sub-family e, polypeptide 1	1.591 ± 0.487
Cyp3a23/3a1	Cytochrome P450, family 3, sub-family a, polypeptide 23/polypeptide 1	3.706 ± 0.555*
Cyp4b1	Cytochrome P450, family 4, sub-family b, polypeptide 1	0.012 ± 0.006

*p <0.05, KA: Kainic acid

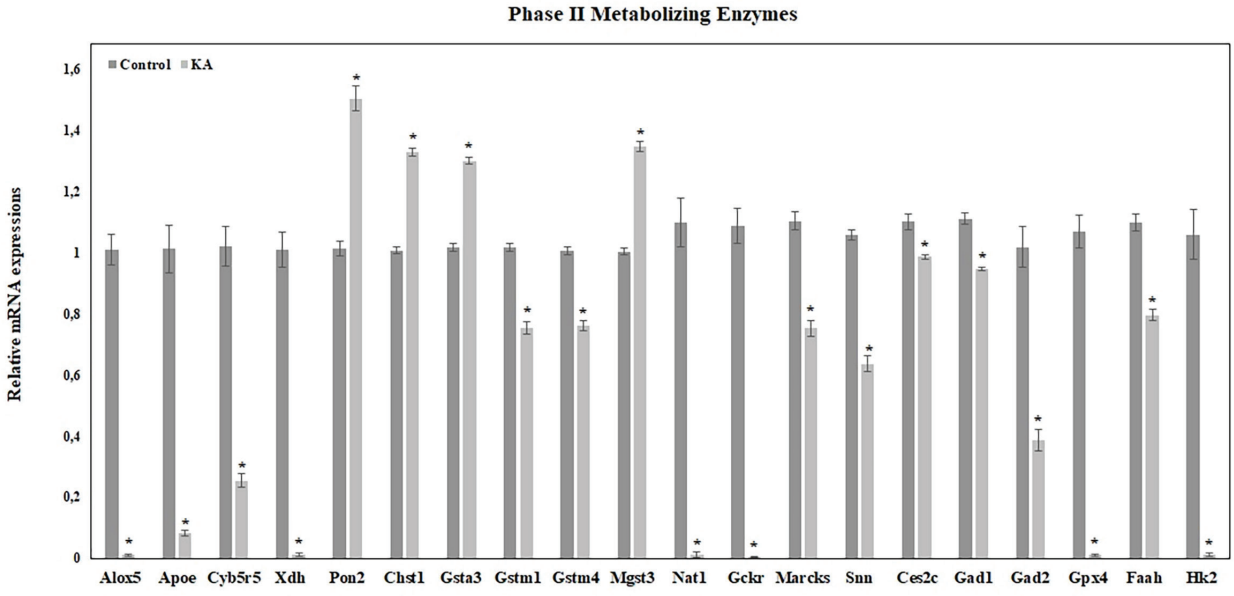

Figure 2. Effects of KA treatment on mRNA expression levels of Phase II metabolizing enzymes in the hippocampus. Data are expressed as mean ± standard error. *$p < 0.05$ vs control in hippocampus (n= 6 for each group)

KA: Kainic acid

Table 3. Regulated levels of Phase II metabolizing enzymes in the hippocampus of rats after KA treatment. Gene expression levels are stated as n-fold change normalized to the control group. Each sample is tested in triplicate

Gene symbol	Drug metabolism enzymes	Expression levels
Phase II metabolizing enzymes		
Lipoxygenases		
Alox15	Arachidonate 15-lipoxygenase	1.866 ± 0.539
Alox5	Arachidonate 5-lipoxygenase	0.012 ± 0.004*
Apoe	Apolipoprotein E	0.083 ± 0.009*
Oxidoreductases		
Blvra	Biliverdin reductase A	2.657 ± 1.215
Blvrb	Biliverdin reductase B (flavin reductase (NADPH)	2.732 ± 1.483
Cyb5r5	Cytochrome b5 reductase 5	0.255 ± 0.021*
Gsr	Glutathione reductase	2.639 ± 1.367
Mthfr	Methylenetetrahydrofolate reductase (NAD(P)H)	2.313 ± 1.088
Nos2	Nitric oxide synthase 2, inducible	2.317 ± 1.002
Nos3	Nitric oxide synthase 3, endothelial cell	2.462 ± 1.245
Nqo1	NAD(P)H dehydrogenase, quinone 1	3.031 ± 1.626
Srd5a1	Steroid-5-alpha-reductase, alpha polypeptide 1 (3-oxo-5 alpha-steroid delta 4-dehydrogenase alpha 1)	2.014 ± 0.997
Xdh	Xanthine dehydrogenase	0.012 ± 0.005*
Paraoxonases		
Pon1	Paraoxonase 1	4.922 ± 2.096
Pon2	Paraoxonase 2	1.505 ± 0.039*
Pon3	Paraoxonase 3	1.717 ± 0.567

Table 3. Continued

Gene symbol	Drug metabolism enzymes	Expression levels
Glutathione S-transferases		
Chst1	Carbohydrate (keratan sulfate Gal-6) sulfotransferase 1	1.329 ± 0.012*
Gsta3	Glutathione S-transferase A3	1.301 ± 0.009*
Gsta4	Glutathione S-transferase alpha 4	2.514 ± 1.494
Gstm1	Glutathione S-transferase mu 1	0.753 ± 0.021*
Gstm2	Glutathione S-transferase mu 2	2.144 ± 1.128
Gstm3	Glutathione S-transferase mu 3	0.742 ± 0.283
Gstm4	Glutathione S-transferase mu 4	0.763 ± 0.017*
Gstm5	Glutathione S-transferase, mu 5	1.141 ± 0.135
Gstp1	Glutathione S-transferase pi 1	1.125 ± 0.112
Gstt1	Glutathione S-transferase theta 1	4.258 ± 2.999
Mgst1	Microsomal glutathione S-transferase 1	2.657 ± 1.386
Mgst2	Microsomal glutathione S-transferase 2	4.469 ± 3.015
Mgst3	Microsomal glutathione S-transferase 3	1.347 ± 0.016*
Transferases		
Nat1	N-acetyltransferase 1	0.012 ± 0.008*
Comt1	Catechol-O-methyltransferase	1.840 ± 0.784
Ggt1	Gamma-glutamyltransferase 1	2.603 ± 1.372
Other genes related to drug metabolism		
Arnt	Aryl hydrocarbon receptor nuclear translocator	1.613 ± 0.493
Ahr	Aryl hydrocarbon receptor	1.548 ± 0.401
Asna1	ArsA arsenite transporter, ATP-binding, homolog 1 (bacterial)	0.914 ± 0.065
Gckr	Glucokinase (hexokinase 4) regulator	0.004 ± 0.002*
Marcks	Myristoylated alanine rich protein kinase C substrate	0.753 ± 0.027*
Smarcal1	Swi/SNF related matrix associated, actin dependent regulator of chromatin, sub-family a-like 1	1.198 ± 0.126
Snn	Stannin	0.637 ± 0.025*
Carboxylesterases		
Ces1e	Carboxylesterase 1E	2.695 ± 1.571
Ces2c	Carboxylesterase 2C	0.986 ± 0.007*
Decarboxylases		
Gad1	Glutamic acid decarboxylase 1	0.946 ± 0.005*
Gad2	Glutamic acid decarboxylase 2	0.387 ± 0.034*
Dehydrogenases		
Adh1	Alcohol dehydrogenase 1 (class I)	3.011 ± 1.568
Adh4	Alcohol dehydrogenase 4 (class II), pi polypeptide	3.272 ± 1.923
Alad	Aminolevulinate, delta-, dehydratase	0.500 ± 0.396
Aldh1a1	Aldehyde dehydrogenase 1 family, member A1	1.765 ± 0.582
Hsd17b1	Hydroxysteroid (17-beta) dehydrogenase 1	2.099 ± 1.115
Hsd17b2	Hydroxysteroid (17-beta) dehydrogenase 2	3.011 ± 1.679
Hsd17b3	Hydroxysteroid (17-beta) dehydrogenase 3	2.297 ± 1.107

Table 3. Continued

Gene symbol	Drug metabolism enzymes	Expression levels
Glutathione peroxydases		
Gpx1	Glutathione peroxidase 1	1.110 ± 0.085
Gpx2	Glutathione peroxidase 2	2.071 ± 0.899
Gpx3	Glutathione peroxidase 3	1.580 ± 0.414
Gpx4	Glutathione peroxidase 4	0.012 ± 0.003*
Gpx5	Glutathione peroxidase 5	1.043 ± 0.021
Lpo	Lactoperoxidase	2.042 ± 0.902
Mpo	Myeloperoxidase	2.549 ± 1.318
Hydrolases		
Ephx1	Epoxide hydrolase 1, microsomal	0.732 ± 0.266
Faah	Fatty acid amide hydrolase	0.796 ± 0.019*
Fbp1	Fructose-1,6-bisphosphatase 1	2.514 ± 1.297
Kinases		
Hk2	Hexokinase 2	0.012 ± 0.005*
Pklr	Pyruvate kinase, liver and RBC	0.865 ± 0.154
Pkm2	Pyruvate kinase, muscle	0.859 ± 0.031*

*p <0.05, KA: Kainic acid, ATP: Adenosine triphosphate, RBC: Red blood cells

Therefore, it can be concluded that the lower levels of Gpi found in our study may be linked to a potential metabolic constraint that could emerge from KA-induced neuronal injury.

Effects of KA on phase I DMEs

The cytochrome P450 (CYP) superenzyme family, particularly in the liver, is involved in biotransformation activities in the brain.[17] Disruptions in CYP-related biotransformation systems in the brain have been hypothesized to be a factor in metabolic decline or the development of drug toxicity.[18] Additionally, it has been observed that a number of antiepileptic medications are known to induce CYP isoenzymes.[19]

Our findings indicate that after KA treatment, a major portion of P450 enzymes showed statistically insignificant high or low results in terms of gene expression levels. However, within the parameters of our findings, it was also observed that KA treatment significantly upregulated Cyp2c6v1, Cyp3a23/3a1, and Cyp2c7 expression levels.

Therefore, it is possible to state that KA administration may regulate the gene expression of P450 enzymes in the hippocampus of rats.

Effects of KA on phase II DMEs

The enzymes glutathione-S-transferase, which use glutathione in their activities, are known to be involved in detoxification processes and to provide protection against oxidative stress. In a prior study, it was found that the expression of Gsta4 increased in correlation with neuronal damage following oxidative stress caused by substances like paraquat or zinc.[20] In this case, the increase in Gsta4 gene expression levels detected in our study can be explained by the fact that KA is also an agent that causes the emergence of reactive oxygen species.[11]

It has been reported that glutathione peroxidase enzymes provide protection against various neurotoxic agents.[21] In addition, it has been reported that there is an increase in Gpx1 levels in the brain tissue of patients with mesial TLE patients.[22] In this context, in our study, gene expression levels of all GPx enzymes, except Gpx4, were increased following KA treatment, which is a neurotoxic agent. However, the increase in gene expression levels of only Gpx1 and Gpx5 among these enzymes was relatively low.

In a microarray study aiming to reveal the transcriptome profile of the hippocampal CA1 region after preconditioning due to early life seizure, it was reported that the Gad1 gene was overexpressed within the scope of neuroprotective genes after 3h KA treatment.[23] In our study, Gad1 and Gad2 gene expression levels were found to be significantly reduced in the hippocampus tissue after KA was administered at a dose of 10 mg/kg to rats, which may be an indicator of the regulatory effect of KA on these genes.

In a study on mice, it was reported that Cyb5r3 overexpression reduced oxidative damage, improved mitochondrial function, and inhibited proinflammatory pathways.[24] According to our results, Cybr5 gene expression was found to be significantly decreaseing due to the potential neurotoxic effects of KA in the hippocampus.

It has been suggested that Pon2 is a neuroprotective enzyme due to its antioxidant and anti-inflammatory properties.[25] According to our findings, Pon1, Pon2, and Pon3 gene expression levels

were all upregulated by KA treatment; however, only Pon2's increase reached a statistically significant level.

Apoe plays a role in various CNS disorders by modulating microglial activation.[26] There have also been some studies showing that Apoe can modulate hippocampal damage induced by KA.[27] In addition, it has been suggested that Apoe deficiency increases microglial activation and hippocampal damage in mice exposed to KA.[26] Consistent with this observation, our results suggest that decreased Apoe levels may be an indicator of neuronal damage that may be caused by KA in the hippocampus.

In our study, all pyruvate kinase enzyme levels were found to be low, which is critical for fundamental metabolic pathways. However, only Pkm2 levels were significantly reduced among these enzymes, which could be explained by the neurotoxic effect of KA on the metabolic pathways.

In a transgenic mouse study, it was found that KA administration increased the level of chondroitin 6-sulfation in the hippocampus and cerebral cortex and that transgenic mice overexpressing chondroitin 6-sulfate chains were more sensitive to KA-induced seizures than wild-type mice.[28] The Chst1 enzyme is also involved in the sulfation of carbohydrates. In this context, increased Chst1 levels, as detected in our study, could indicate neuronal damage caused by KA.

A previous study found that a 25 mg/kg dose of KA increased Marcks protein expression in microglial cells.[29] In our study, it was observed that KA administration at a dose of 10 mg/kg significantly decreased Marcks gene expression levels in the hippocampus tissue, which can be interpreted as a dose-dependent effect.

It has been proposed that Snn is a protein involved in mitochondrial responses as part of the mechanisms that cause brain damage.[30] In our study, we found a significant decrease in Snn gene expression levels after KA-induced seizures, which is thought to be an indication of possible mitochondrial damage caused by KA.

It was previously reported in a study with Faah enzyme inhibitors that some specific inhibitors protect against brain damage after KA treatment.[31] However, in our study, there was a decrease in Faah gene expression levels after KA treatment, which is thought to be related to the level of neuronal damage caused by KA.

Study limitations

Our research has some limitations. By adding additional animals to the experimental groups, we could improve the efficacy of our gene expression analysis results. We were unable to examine the amounts of proteins or the activity of the enzymes involved in drug metabolism. Finding gene expression levels may not always provide an accurate estimate of a protein's concentration. Thus, for a more thorough examination, protein quantification and enzyme activity measurements are needed.

CONCLUSION

In conclusion, our findings suggest that KA treatment may alter gene expression levels of enzymes involved in drug metabolism in rat hippocampus tissue. Furthermore, our findings may contribute to the gene expression profile previously revealed after KA treatment in the context of various neurotoxic or neurodegenerative conditions.

Ethics

Ethics Committee Approval: The procedure for the experiments was authorized by Ege University Faculty of Pharmacy, Experimental Animal Ethics Committee (2006/6-1, date: 22.06.2006).

Informed Consent: Not required.

Authorship Contributions

Surgical and Medical Practices: L.K., Concept: A.Y., Design: A.Y., Data Collection or Processing: A.Y., E.T., G.A., Analysis or Interpretation: A.Y., E.T., G.A., Literature Search: A.Y., E.T., G.A., L.K., Writing: A.Y.

Conflict of Interest: The authors declare no potential conflicts of interest with respect to the research, authorship, and/or publication of this article.

Financial Disclosure: This study was partially supported by Ege University Science and Technology Centre (EBİLTEM) 2008/EBILTEM/001.

REFERENCES

1. Sperk G, Lassmann H, Baran H, Seitelberger F, Hornykiewicz O. Kainic acid-induced seizures: dose-relationship of behavioural, neurochemical and histopathological changes. Brain Res. 1985;338:289-295.
2. Sperk G. Kainic acid seizures in the rat. Prog Neurobiol. 1994;42:1-32.
3. Coyle JT, Puttfarcken P. Oxidative stress, glutamate, and neurodegenerative disorders. Science. 1993;262:689-695.
4. Lévesque M, Avoli M. The kainic acid model of temporal lobe epilepsy. Neurosci Biobehav Rev. 2013;37:2887-2899.
5. Lewis D. Cytochrome P450, Structure, function and mechanism. Bristol; Taylor&Francis; 1996:122-123.
6. Miksys S, Tyndale RF. Brain drug-metabolizing cytochrome P450 enzymes are active *in vivo*, demonstrated by mechanism-based enzyme inhibition. Neuropsychopharmacology. 2009;34:634-640.
7. Asai Y, Tanaka H, Nadai M, Katoh M. Status Epilepticus Decreases Brain Cytochrome P450 2D4 Expression in Rats. J Pharm Sci. 2018;107:975-978.
8. Asai Y, Tanaka H, Nadai M, Katoh M. Effect of status epilepticus on expression of brain UDP-glucuronosyltransferase 1a in rats. Biopharm Drug Dispos. 2018;39:75-82.
9. Boussadia B, Ghosh C, Plaud C, Pascussi JM, de Bock F, Rousset MC, Janigro D, Marchi N. Effect of status epilepticus and antiepileptic drugs on CYP2E1 brain expression. Neuroscience. 2014;5:124-134.
10. Chung SY, Han SH. Melatonin attenuates kainic acid-induced hippocampal neurodegeneration and oxidative stress through microglial inhibition. J Pineal Res. 2003;34:95-102.

11. Turunc E, Kanit L, Yalcin A. Effect of gamma-glutamylcysteine ethylester on the levels of c-fos mRNA expression, glutathione and reactive oxygen species formation in kainic acid excitotoxicity. J Pharm Pharmacol. 2010;62:1010-1017.
12. Chomczynski P. A reagent for the single-step simultaneous isolation of RNA, DNA and proteins from cell and tissue samples. Biotechniques. 1993;15:532-537.
13. Armagan G, Bojnik E, Turunc E, Kanit L, Gündüz Çinar O, Benyhe S, Borsodi A, Yalcin A. Kainic acid-induced changes in the opioid/nociceptin system and the stress/toxicity pathways in the rat hippocampus. Neurochem Int. 2012;60:555-564.
14. Naserpour Farivar T, Nassiri-Asl M, Johari P, Najafipour R, Hajiali F. The Effects of Kainic Acid-Induced Seizure on Gene Expression of Brain Neurotransmitter Receptors in Mice Using RT^2 PCR Array. Basic Clin Neurosci. 2016;7:291-298.
15. Kim D, Kim EH, Kim C, Sun W, Kim HJ, Uhm CS, Park SH, Kim H. Differential regulation of metallothionein-I, II, and III mRNA expression in the rat brain following kainic acid treatment. Neuroreport. 2003;14:679-682.
16. Sung JH, Shah FA, Gim SA, Koh PO. Identification of proteins in hyperglycemia and stroke animal models. J Surg Res. 2016;200:365-373.
17. Hedlund E, Gustafsson JA, Warner M. Cytochrome P450 in the brain; a review. Curr Drug Metab. 2001;2:245-263.
18. Ghosh C, Hossain M, Solanki J, Dadas A, Marchi N, Janigro D. Pathophysiological implications of neurovascular P450 in brain disorders. Drug Discov Today. 2016;21:1609-1619.
19. Brodie MJ, Mintzer S, Pack AM, Gidal BE, Vecht CJ, Schmidt D. Enzyme induction with antiepileptic drugs: cause for concern? Epilepsia. 2013;54:11-27.
20. Kumar A, Ahmad I, Shukla S, Singh BK, Patel DK, Pandey HP, Singh C. Effect of zinc and paraquat co-exposure on neurodegeneration: Modulation of oxidative stress and expression of metallothioneins, toxicant responsive and transporter genes in rats. Free Radic Res. 2010;44:950-965.
21. Klivenyi P, Andreassen OA, Ferrante RJ, Dedeoglu A, Mueller G, Lancelot E, Bogdanov M, Andersen JK, Jiang D, Beal MF. Mice deficient in cellular glutathione peroxidase show increased vulnerability to malonate, 3-nitropropionic acid, and 1-methyl-4-phenyl-1,2,5,6-tetrahydropyridine. J Neurosci. 2000;20:1-7.
22. Yüzbaşioğlu A, Karataş H, Gürsoy-Ozdemir Y, Saygi S, Akalan N, Söylemezoğlu F, Dalkara T, Kocaefe YC, Ozgüç M. Changes in the expression of selenoproteins in mesial temporal lobe epilepsy patients. Cell Mol Neurobiol. 2009;29:1223-1231.
23. Friedman LK, Mancuso J, Patel A, Kudur V, Leheste JR, Iacobas S, Botta J, Iacobas DA, Spray DC. Transcriptome profiling of hippocampal CA1 after early-life seizure-induced preconditioning may elucidate new genetic therapies for epilepsy. Eur J Neurosci. 2013;38:2139-2152.
24. Martin-Montalvo A, Sun Y, Diaz-Ruiz A, Ali A, Gutierrez V, Palacios HH, Curtis J, Siendones E, Ariza J, Abulwerdi GA, Sun X, Wang AX, Pearson KJ, Fishbein KW, Spencer RG, Wang M, Han X, Scheibye-Knudsen M, Baur JA, Shertzer HG, Navas P, Villalba JM, Zou S, Bernier M, de Cabo R. Cytochrome b_5 reductase and the control of lipid metabolism and healthspan. NPJ Aging Mech Dis. 2016;12:16006.
25. Costa LG, de Laat R, Dao K, Pellacani C, Cole TB, Furlong CE. Paraoxonase-2 (PON2) in brain and its potential role in neuroprotection. Neurotoxicology. 2014;43:3-9.
26. Duan RS, Chen Z, Dou YC, Concha Quezada H, Nennesmo I, Adem A, Winblad B, Zhu J. Apolipoprotein E deficiency increased microglial activation/CCR3 expression and hippocampal damage in kainic acid exposed mice. Exp Neurol. 2006;202:373-380.
27. Grootendorst J, Mulder M, Haasdijk E, de Kloet ER, Jaarsma D. Presence of apolipoprotein E immunoreactivity in degenerating neurones of mice is dependent on the severity of kainic acid-induced lesion. Brain Res. 2000;868:165-175.
28. Yutsudo N, Kitagawa H. Involvement of chondroitin 6-sulfation in temporal lobe epilepsy. Exp Neurol. 2015;274:126-133.
29. Eun SY, Kim EH, Kang KS, Kim HJ, Jo SA, Kim SJ, Jo SH, Kim SJ, Blackshear PJ, Kim J. Cell type-specific upregulation of myristoylated alanine-rich C kinase substrate and protein kinase C-alpha, -beta I, -beta II, and -delta in microglia following kainic acid-induced seizures. Exp Mol Med. 2006;38:310-319.
30. Billingsley ML, Yun J, Reese BE, Davidson CE, Buck-Koehntop BA, Veglia G. Functional and structural properties of stannin: roles in cellular growth, selective toxicity, and mitochondrial responses to injury. J Cell Biochem. 2006;98:243-250.
31. Mikheeva IB, Shubina L, Matveeva N, Pavlik LL, Kitchigina VF. Fatty acid amide hydrolase inhibitor URB597 may protect against kainic acid-induced damage to hippocampal neurons: Dependence on the degree of injury. Epilepsy Res. 2017;137:84-94.

Turk J Pharm Sci 2024;21(4):267-273
DOI: 10.4274/tjps.galenos.2023.23890

ORIGINAL ARTICLE

A Preliminary Study on the Effect of Deferoxamine on the Disruption of Bacterial Biofilms and Antimicrobial Resistance

Aybala TEMEL[1]*, Zinnet Şevval AKSOYALP[2]

[1]İzmir Katip Çelebi University Faculty of Pharmacy, Department of Pharmaceutical Microbiology, İzmir, Türkiye
[2]İzmir Katip Çelebi University Faculty of Pharmacy, Department of Pharmacology, İzmir, Türkiye

ABSTRACT

Objectives: Antiviral therapy approaches have become significant strategies to combat antibiotic resistance. Metal ions, particularly iron, play crucial roles in metabolic activities and virulence of bacteria. Loading iron into siderophore molecules could potentially circumvent antimicrobial resistance. This study aimed to evaluate the antibiofilm and antimicrobial effects of deferoxamine (DFO), an iron chelator and natural siderophore, on antibiotic susceptibility in clinical methicillin-resistant *Staphylococcus aureus* (MRSA) and carbapenem-resistant *Acinetobacter baumannii* (CRAB) isolates.

Materials and Methods: The *in vitro* antibacterial activity of DFO alone and in combination with vancomycin [VAN (30 µg)], amoxicillin (25 µg), colistin (10 µg), and imipenem (10 µg), was investigated against MRSA and CRAB isolates using the disk diffusion method. The spectrophotometric microplate method was used to detect the *in vitro* antibiofilm effect of DFO.

Results: DFO exhibited a synergistic effect with VAN, amoxicillin, and colistin and significantly disrupted mature biofilm formation in MRSA and CRAB isolates. Notably, the antibiofilm effect of DFO was more pronounced in CRAB strains.

Conclusion: These findings highlight the potential of DFO as an antibiofilm agent candidate and suggest that it can enhance the antibiotic susceptibility of certain microorganism species.

Keywords: Antibiofilm, deferoxamine, iron chelator, non-antibiotics, synergism

INTRODUCTION

Bacterial antimicrobial resistance poses a significant global public health challenge[1] and renders various antibiotics ineffective. The World Health Organization has identified several microorganisms, including *Staphylococcus aureus* and *Acinetobacter baumannii*, as antibiotic-resistant "priority pathogens".[2] Methicillin-resistant *Staphylococcus aureus* (MRSA) is classified as a high-priority pathogen,[2] with vancomycin (VAN) and daptomycin suggested as first-line treatments.[2,3] Carbapenem-resistant *Acinetobacter baumannii* (CRAB) is listed as a critical priority pathogen[2] and has limited treatment options because of higher resistance rates. Polymyxins [polymyxin B and colistin (COL)] and tetracycline derivatives (minocycline, doxycycline, and tigecycline) are used to treat drug-resistant *Acinetobacter* infections.[4]

The ability of these pathogens to form biofilms is one of the key reasons for their antimicrobial resistance.[5,6] Bacterial biofilms, the adherence of microbial cells to biotic or abiotic surfaces, represent a target for multidrug-resistant pathogens.[5,6] The role of iron in biofilm formation, crucial for the survival of both host and pathogen, has garnered significant attention.[7] Iron chelation has been proposed as a strategy to enhance the antimicrobial activity of antibiotics by disrupting bacterial biofilms.[8,9] Considering the potential effects of iron chelators on infections, it is argued that iron chelators may be of benefit in combination with antibiotics, but pathogen-specific chelators should be

*Correspondence: aybala.temel@ikcu.edu.tr, Phone: +90 232 329 35 35/61 61, ORCID-ID: orcid.org/0000-0003-1549-7219
Received: 30.05.2023 , Accepted: 29.07.2023

utilized.[10] Deferoxamine (DFO), an iron chelator and natural siderophore, is used to treat iron overload and intoxication. Originally discovered in *Streptomyces pilosus*, DFO is also produced by various terrestrial and marine actinomycetes species.[11] Siderophores enhance permeability by depleting iron and may facilitate the entry of antibiotics into cells.[12]

The urgent need for new antibiotics has prioritized the development of novel medications. However, developing new drugs is both time-consuming and expensive. Repurposing approved medications has gained attention as an accelerated approach to overcoming antibiotic resistance. Additionally, combining antibiotics with non-antibiotic drugs may exhibit synergistic effects against antibiotic resistance. Therefore, our objective was to investigate the potential synergistic effect of DFO and antibiotics against CRAB and MRSA and to explore the antibiofilm effect of DFO on mature biofilm.

MATERIALS AND METHODS

Bacterial strains and culture conditions

Clinical methicillin-resistant *S.aureus* (n= 5) and carbapenem-resistant *A. baumannii* isolates (n= 4), are part of the collection of our laboratory. The main reason for choosing methicillin- and carbapenem-resistant bacterial isolates in this study was to investigate the interactions of DFO with commonly used antibiotics against drug-resistant isolates [such as imipenem (IMP) and COL], even though DFO alone has low antibacterial activity. MRSA and CRAB isolates were selected from those previously identified using the automated *VITEK® 2* Compact system (bioMérieux). *Pseudomonas aeruginosa* ATCC 27853 and *Escherichia coli* ATCC 25922 were used as internal quality control strains, and *Enterococcus faecalis* ATCC 29212 served as a positive control for biofilm assays. All bacterial isolates were stored in brain-heart infusion broth containing 10% glycerin (Merck, Darmstadt, Germany) at 20 °C. Mueller-Hinton Agar (MHA) (Merck, Darmstadt, Germany) and tryptic soy broth with 2.5% glucose (TSBG) medium (Oxoid, UK) were used for antimicrobial activity tests and biofilm experiments, respectively. As a result of the biofilm production assays, two MRSA and one CRAB isolates that were found not to be strong biofilm producers were excluded from the study. The antibacterial and antibiofilm effects of DFO were evaluated against six isolates (MRSA3, MRSA6, MRSA21, CRAB35, CRAB50, CRAB89) in the disc diffusion and antibiofilm experiments.

Iron chelators and antimicrobials

DFO mesylate, commercially available (Desferal®, Novartis, Switzerland), was procured in powder form. The preparation of DFO solutions was performed as described in the package insert. Briefly, 500 mg DFO in each vial was reconstituted in 2 mL sterile distilled water at a concentration of 380 mM. These freshly prepared DFO solutions whose concentration after reconstitution was 213 mg/mL (the indicated concentration for the intramuscular route) were used in the experiments. The commercial antibiotic discs were utilized for the antimicrobial susceptibility and synergy testing in this study. The antibiotics used were VAN-30 µg, amoxicillin (AX-25 µg), COL-10 µg, and IMP-10 µg from Bioanalyse®, Türkiye.

Determination of the in vitro antimicrobial effect of DFO

The *in vitro* antimicrobial effect of DFO against MRSA and CRAB isolates was assessed using the disk diffusion method, following the criteria outlined by the European Committee on Antimicrobial Susceptibility Testing.[13] The bacterial strains were cultured on MHA and incubated overnight. Subsequently, bacterial suspensions in sterile physiological saline were adjusted to 0.5 McFarland turbidity standard (approximately 1-2 x 10^8 colony-forming units/mL) using a densitometer device (Biosan, DEN-1). The suspensions were then evenly spread on MHA plates using sterile swab sticks. 10 µL of the DFO solution was loaded onto both blank and antibiotic disks. In the following inoculation, the standard antibiotic disks (VAN, AX, COL, and IMP), DFO disks, and antibiotic and DFO disks were placed on the MHA plates. The plates were incubated at 37 °C for 18 ± 2 hours, and the inhibition zones surrounding each disk were measured.[12,13]

Detection of the biofilm-forming capacities of bacterial strains

The biofilm-forming capacities of bacterial isolates were quantified using the spectrophotometric microplate method with crystal violet (CV) staining.[14,15] The bacterial strains were cultured on MHA and incubated at 37 °C overnight. Following incubation, bacterial suspensions adjusted to a 0.5 McFarland turbidity standard were prepared in TSBG medium (3 mL) using the direct colony suspension method. Then, 180 µL of TSBG medium and 20 µL of the bacterial suspension were added to each well of a sterile 96-well flat-bottom microplate. As controls, TSBG (200 µL) medium without bacterial suspension was added to designated wells. The microplates were incubated at 37 °C for 24 hours to allow biofilm formation. After incubation, the contents of the wells were aspirated and washed with sterile phosphate-buffered saline (200 µL) (Oxoid, UK) to remove nonadherent bacteria. Following the washing steps, the microplates were allowed to dry at 25 °C. The remaining attached microorganisms were fixed by adding 200 µL of methanol and waiting for 15 minutes. After discarding the methanol, 200 µL of 0.1% CV solution was added to each well, and the mixture was incubated for 15 minutes at room temperature. Subsequently, the wells were aspirated and gently rinsed with tap water until colorless. After drying at room temperature, each well was destained with 200 µL of 95% ethanol for 10 minutes.[14,15]

Spectrophotometric measurements were performed at a wavelength of 570 nm using a microplate reader (*CLARIOstar* Plus Microplate Reader, BMG LabTech, Cary NC). The optical density (OD) of the wells containing only the TSBG medium was used as the negative control. *E. faecalis* ATCC 29212 was used as a positive control for biofilm production. The cut-off ODc was defined as three standard deviations above the mean OD of the negative controls.

In vitro antibiofilm effect of DFO

The *in vitro* antibiofilm effect of DFO on MRSA and CRAB biofilms was assessed using the spectrophotometric microplate method. First, each bacterial strain was allowed to form mature biofilms on the bottom of the sterile F-bottom 96-well

microplates. TSBG medium (180 µL) and bacterial suspension (20 µL) were added to the wells. The microplates were then incubated at 37 °C for 24 hours to induce biofilm formation. Following aspiration of the well contents, 200 µL of DFO was added directly to each well, forming the mature bacterial biofilm layer. The microplates were further incubated for 24 hours. After the incubation period, the well contents were aspirated, and the microplates were subjected to CV staining as described above. Spectrophotometric measurements were performed to obtain the OD values. To determine the percentages of biofilm disruption, OD values were calculated using the following formula: percentage of biofilm disruption (%) = (OD_A – OD_B) / OD_A × 100 (OD_A: the OD of biofilm control well without DFO, OD_B : the OD in the presence of DFO).

Statistical analysis

All experiments were performed in triplicate to ensure reproducibility. The data obtained from the experiments were assumed to follow a normal distribution. To compare the two groups, a Student's t-test was applied. Statistical analyses were performed using GraphPad Prism 9 Software (San Diego, CA, USA).

The biofilm production capacities of MRSA and CRAB isolates were categorized based on the following criteria: OD ≤ ODc: no biofilm production, ODc < OD ≤ (2 × ODc): weak biofilm producer, (2 × ODc) < OD ≤ (4 × ODc): moderate biofilm producers, and (4 × ODc) < OD: strong biofilm producer.

RESULTS

Antibacterial activity of DFO

Considering the results of biofilm detection experiments for nine isolates, two MRSA and one CRAB isolates, which were determined not to be strong biofilm producers, were excluded from the study. The antibacterial effect of DFO was evaluated against six isolates (MRSA3, MRSA6, MRSA21, CRAB35, CRAB50, CRAB89) in a disc diffusion test. Based on the results of the disk diffusion test, the inhibitory zone diameters of DFO, AX and DFO, VA and DFO, COL and DFO, and IMP and DFO against clinical MRSA and CRAB isolates varied between 8 and 22 mm. The zone diameters after exposure to DFO, antibiotics, and their combinations are listed in Table 1.

Representative examples of inhibition zones in the presence of DFO, antibiotics, and combinations of these for MRSA6 and CRAB35 isolates are shown in Figure 1.

Antibiofilm activity of DFO

Of the nine tested strains, MRSA3, MRSA6, MRSA21, CRAB35, CRAB50, and CRAB89 were identified as strong biofilm producers using the CV method. The results indicated that DFO exerted a significant antibiofilm effect on the mature biofilms of the five isolates Figure 2. Antibiofilm activity of DFO was not observed for MRSA21 and therefore this result is not included in Figure 2. The percentage of biofilm disruption caused by DFO ranged from 38.1% to 72.3%. DFO exerted a stronger disruptive effect on the biofilms formed by CRAB isolates than MRSA isolates. The percentages of biofilm disruption by DFO were 38.1% for MRSA3, 42.1% for MRSA6, 62.9% for CRAB35, 72.3% for CRAB50, and 66.5% for CRAB89. The OD values and corresponding percentage of biofilm disruption in the presence of DFO for each isolate are presented in Figure 2.

DISCUSSION

The development of resistance to VAN and COL, the last-resort antibiotics for MRSA and CRAB, respectively, leads to the need for combination therapy. Therefore, the primary aim of this study was to investigate the effect of DFO on the susceptibility of clinical MRSA and CRAB isolates to these last-resort antibiotics. Additionally, the study aimed to assess whether the presence of DFO could alter the susceptibility of these isolates, which were confirmed to be resistant to AX and IML. Furthermore, the secondary objective was to evaluate the antibiofilm effect of DFO against these resistant isolates. The main findings of our preliminary study are as follows: (a) DFO exerted a synergistic effect when combined with AX, VAN, and COL, but did not exert an antibacterial effect alone; (b) DFO significantly disrupted the mature biofilm formed by both MRSA and CRAB isolates.

The pathogenesis of bacterial infections involves various factors, including antimicrobial resistance gene expression,

Table 1. Susceptibility of MRSA and CRAB isolates to DFO alone and in combination with antibiotics

	Zone of inhibition (diameter in mm)				
Isolate number	**DFO**	**AX**	**AX and DFO**	**VAN**	**VAN and DFO**
MRSA3	0	20	22	19	21
MRSA6	0	15	17	20	22
MRSA21	0	15	17	19	21
Isolate number	**DFO**	**IMP**	**IMP and DFO**	**COL**	**COL and DFO**
CRAB35	0	12	9	13	15
CRAB50	0	11	8	13	15
CRAB89	0	11	10	13	14

AX: Amoxicillin (25 µg), COL: Colistin (10 µg), CRAB: Carbapenem-resistant *Acinetobacter baumannii*, DFO: Deferoxamine, IMP: Imipenem (10 µg), MRSA: Methicillin-resistant *Staphylococcus aureus*, VAN: Vancomycin (30 µg)

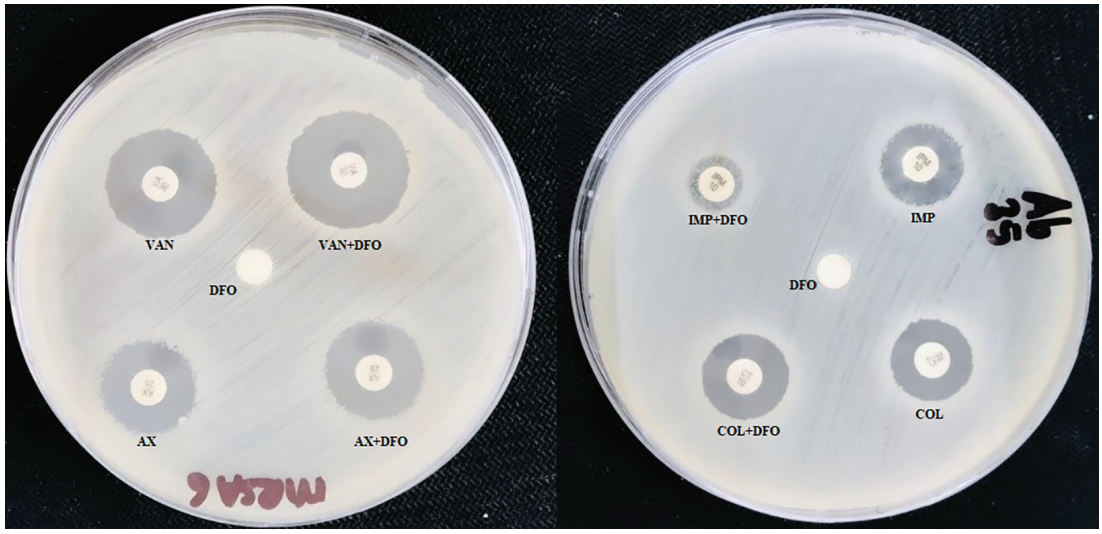

Figure 1. Inhibition zones in the presence of DFO, antibiotics, and combinations of these for MRSA6 and CRAB35

AX: Amoxicillin, COL: Colistin, CRAB: Carbapenem-resistant *Acinetobacter baumannii*, DFO: Deferoxamine, IMP: Imipenem, MRSA: Methicillin-resistant *Staphylococcus aureus*, VAN: Vancomycin

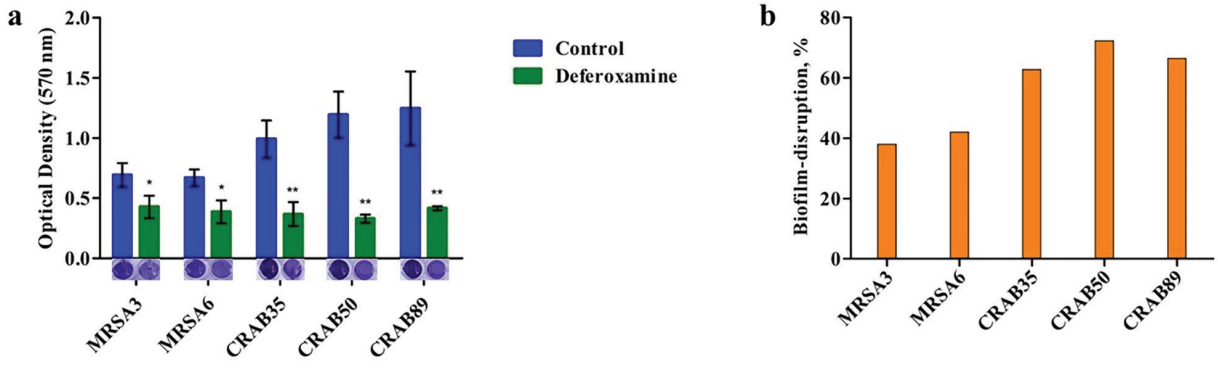

Figure 2. (A) Optical densities of mature biofilms formed by bacterial strains and mature biofilms exposed to deferoxamine. (B) Percentage of the biofilm disruption effect of deferoxamine, quantified as a percentage relative to the control using crystal violet staining

CRAB: Carbapenem-resistant *Acinetobacter baumannii*, MRSA: Methicillin-resistant *Staphylococcus aureus*

iron uptake mechanisms, and biofilm formation. Iron metabolism is closely linked to quorum sensing signaling and biofilm formation, which influence bacterial colonization, antibiotic susceptibility, and essential functions within the bacteria.[10,16] Critical iron-dependent proteins are vital for bacterial growth and multiplication, including ribonucleotide reductase, which is involved in DNA synthesis, and cytochromes, which are essential for energy metabolism.[12] In the absence of sufficient iron, these critical proteins are unable to function, leading to growth inhibition. Iron chelators are believed to exert antimicrobial effects by targeting iron-dependent pathways, enzymes, and proteins in bacteria.[11] DFO was the first iron chelator approved for use in humans and is widely used for the treatment of iron overload.[17] DFO has a higher affinity for Fe^{3+} than deferiprone and deferasirox. However, due to its siderophore nature, DFO has the potential to stimulate bacterial growth.[18] In our study, we found that DFO alone did not exhibit antibacterial activity in the disk diffusion method. However, when combined with VAN, AX, or COL, DFO enhanced the inhibitory effects of these antibiotics, as evidenced by larger zone diameters (2 mm) compared with the antibiotic discs alone. This suggests a synergistic interaction between DFO and these antibiotics.

Considering the limited literature on the effects of DFO against bacteria species, there are noteworthy findings that indicate a synergistic interaction between DFO and antibiotics, which is in line with our findings. Gokarn and Pal[12] investigated the effects of exogenous siderophore (exochelin-*Mycobacterium smegmatis* and DFO-B) in combination with antibiotics against various resistant bacteria, including MRSA. They reported that siderophore-antibiotic (ampicillin, cefdinir, IMP, and meropenem) combinations inhibited the growth of a significant proportion (50-75%) of MRSA isolates.[12] Similarly, DFO-B exhibited a bacteriostatic effect on 30-50% of the tested isolates at relatively higher concentrations.[12] In parallel to our findings, this siderophore alone did not show zones of inhibition in the disk diffusion method.[12] Another study by van Asbeck et al.[19] demonstrated the synergic interaction between DFO and antibiotics (gentamicin, chloramphenicol, cephalothin, cefotiam,

or cefsulodin) against *S. aureus, Staphylococcus epidermidis, E. coli, Klebsiella pneumoniae, Proteus mirabilis, Pseudomonas,* and *Providencia.*[19] In contrast, a study investigating the effects of iron chelators (DFO, deferiprone, Apo6619, and VK28) on the growth of nosocomial pathogens reported that DFO did not exhibit an inhibitory effect [minimum inhibitory concentration (MIC) ≥ 512 g/mL for all bacteria tested]. In contrast, other chelators inhibited bacterial growth in standard mediums.[20] These discrepancies may be attributed to variations in the bacterial species, experimental conditions, and concentrations of the iron chelators.

Indeed, the lack of an inhibitory effect of DFO observed in the disc diffusion method, including in our study, can be attributed to several factors. Previous studies using broth microdilution have demonstrated the inhibitory effect of DFO.[12,16] The most obvious explanation is that siderophores have easier access to iron in liquid media and are better at iron sequestration.[12,21] Most siderophore sequester Fe^{3+} at low concentrations under aerobic and neutral pH conditions.[22] DFO, with its hydroxamic functional groups surrounding the ferric ion, has a higher affinity for Fe^{3+} and forms a neutral and more stable octahedral complex.[11] However, the antibacterial effect of iron-bound DFO is lower than that of hydrophobic chelating agents like deferiprone, primarily because of its hydrophilic nature and limited penetration into lipid membranes.[21,23,24] Nevertheless, the role of DFO in iron bioavailability and virulence can vary depending on the specific bacterial species and infection models. Arifin et al.[25] found that DFO increased iron bioavailability and enhanced virulence of bacteria in a murine systemic infection model with community-associated MRSA. Similarly, DFO may play a promoting role in systemic infections of *Yersinia enterocolitica* in humans.[26] These findings highlight the complex interplay between iron chelators, bacterial pathogens, and host responses. The antibacterial effect of iron chelators alone or in combination with antibiotics can be influenced by various factors. The concentration of the iron chelator, the type and virulence characteristics of the bacteria, the mechanism of action of antibiotics, the diversity of mechanisms for iron uptake in bacteria, and the presence of siderophore with different iron binding capacities and chemical structures can contribute to the observed variability in antibacterial effects. The iron content of the culture media can vary, which can also influence the availability of iron and response to iron chelators.[27] Furthermore, DFO may facilitate the delivery of iron to bacteria through the receptors of their cognate siderophore, potentially augmenting the virulence of pathogenic bacteria.[28] On the other hand, iron deprivation induced by iron chelators can impair essential functions and increase the effectiveness of antibiotics against bacteria.[29] Although the precise mechanism underlying the synergistic interactions between siderophore and antibiotics has not been completely elucidated, it is noted that this effect may arise from the heightened permeability of the cell membrane resulting from iron deficiency.[30] This could explain the synergistic inhibition of MRSA isolates by DFO with antibiotic combinations observed in our study, as well as in previous studies with similar findings.

One of the important mechanisms contributing to antibiotic resistance is the production of metallo-beta-lactamase enzymes.[31] These enzymes inactivate beta-lactam antibiotics (such as penicillins, cephalosporins, and carbapenems) by cleaving the beta-lactam ring in their chemical structure, and they rely on the presence of Zn^{2+} ions for their enzymatic activity.[31] DFO has a high affinity for both Zn^{2+} and Fe^{3+} ions because of its specific chemical groups.[32] This affinity can result in the depletion of Zn^{2+} ions in the media, leading to the inactivation of metallo-beta-lactamases and increased susceptibility of bacteria to -lactam antibiotics. This effect is believed to be responsible for the observed synergistic effect, especially in resistant bacterial isolates in the presence of DFO. In this study, although DFO showed synergy with three of the tested antibiotics, no synergy was observed with IMP against CRAB isolates. This discrepancy may be attributed to both the chemical structure of the IMP and the expression of bacterial membrane proteins.[33] In response to *in vitro* iron loading or restriction, the expression of proteins responsible for various metabolic functions, including cell division, antibiotic resistance, and iron acquisition, particularly membrane proteins, changes in bacterial cells.[34] A previous proteomic study indicated that the membrane proteins and metabolism of *Acinetobacter* respond differently to the presence of iron, especially CRAB.[35] Hence, the presence of multiple proteins, which are also associated with carbapenem resistance, and the differentiation of their expression levels under iron-limited conditions may be the potential reasons for the different results in CRAB.

Bacterial biofilms are among the leading causes of morbidity and mortality associated with infectious diseases.[36] Biofilms are bacterial layers that form on the surfaces of medical devices like catheters and heart valve prostheses, contributing to nosocomial infections and preventing access to antimicrobial drugs to bacteria, resulting in reduced susceptibility to treatment.[36] Therefore, the detection of pathogen biofilm-forming capacity and the discovery of antibiofilm compounds play crucial roles in effective treatment strategies. In this context, we examined the impact of iron depletion via DFO on preformed biofilms *in vitro*. The biofilm-forming capacities of MRSA and CRAB isolates were evaluated using the spectrophotometric microplate method, and the isolates were found to be strong biofilm producers. DFO exhibited significant disruption in the mature biofilms, especially in CRAB strains, leading to a reduction in optical densities by > 60%. Similar studies have been conducted to explore the antibiofilm effects of DFO, deferasirox, and deferiprone against different bacterial and fungal species.[20,29] In one study, combined treatment with tobramycin and iron chelators (DFO or deferasirox) resulted in an approximately 90% reduction in preformed *P. aeruginosa* biofilm biomass and a 7-log units decrease in bacterial viability.[9] Gentile et al.[37] reported that iron starvation did not affect the biofilm-forming capacity of *A. baumannii* strains isolated from veterinary and clinical sources. Conversely, DFO had lower efficacy against *Protovella intermedia* biofilm formation than deferasirox.[38] Nazik et al.[39] reported that DFO had no inhibitory or stimulant effect on planktonic growth in their study examining the effects of DFO on *Aspergillus fumigatus*. Consequently, our

findings indicate that DFO disrupted mature biofilm formation in clinical MRSA and CRAB isolates, suggesting its potential as an antibiofilm agent.

Study limitations

The present study has some limitations in terms of the comprehensive understanding of the antibacterial and synergistic effects of DFO. The reason for preferring the disc diffusion method to the broth microdilution method (BMD) is that the liquid medium used for MIC determination contains iron and other cations. This was considered to be an important factor that could influence the antibacterial potential of DFO. Although iron-rich and iron-poor media have been used in the BMD method in previous studies to investigate the effect of DFO, it is considered that this situation in the experimental design may be disadvantageous in terms of reflecting *in vivo* conditions. Future studies are planned to determine the minimum inhibitory concentrations in iron-poor and iron-rich environments. In addition, the antibiofilm effect of DFO at different concentrations will be investigated against various bacterial species causing biofilm-associated infections and with a greater number of isolates.

CONCLUSION

In conclusion, our findings suggest that DFO can enhance antibiotic efficacy and combat biofilm-associated infections caused by CRAB and MRSA. The prevalence of high rates of antibiotic resistance and the rapid evolution of resistance to the latest antimicrobials indicate the urgent need for innovative therapeutic approaches to combat infections. In an era of limited antibiotic discovery and antibiotic resistance posing global health concerns, that, the importance of drug repositioning studies has become increasingly evident. Iron chelation is a promising antiviral strategy for combating drug-resistant bacteria. In light of the results of previous studies and our study, iron chelators have significant potential for off-label use to enhance susceptibility to antibacterial drugs. Further research is warranted to explore the mechanistic aspects and clinical applications of DFO in the context of antimicrobial resistance and biofilm control. Conducting further studies on the impact of iron chelators on microorganisms and their interaction with antibiotics will contribute to the fight against infections. The combination of iron chelators with antibacterial agents can potentially provide clinical benefits in the treatment of resistant infections by augmenting the susceptibility of antibacterial agents.

Ethics

Ethics Committee Approval: Not applicable.

Informed Consent: Not applicable.

Authorship Contributions

Surgical and Medical Practices: A.T., Z.Ş.A., Concept: A.T., Z.Ş.A., Design: A.T., Z.Ş.A., Data Collection or Processing: A.T., Z.Ş.A., Analysis or Interpretation: A.T., Z.Ş.A., Literature Search: A.T., Z.Ş.A., Writing: A.T., Z.Ş.A.

Conflict of Interest: No conflict of interest was declared by the authors.

Financial Disclosure: The authors declared that this study received no financial support.

REFERENCES

1. Antimicrobial Resistance Collaborators. Global burden of bacterial antimicrobial resistance in 2019: a systematic analysis. Lancet. 2022;399:629-655.
2. World Health Organization (WHO). WHO publishes list of bacteria for which new antibiotics are urgently needed. Accessed 25.01.2023, Available from: https://www.who.int/en/news-room/detail/27-02-2017-who-publishes-list-of-bacteria-for-which-new-antibiotics-are-urgently-needed
3. Mahjabeen F, Saha U, Mostafa MN, Siddique F, Ahsan E, Fathma S, Tasnim A, Rahman T, Faruq R, Sakibuzzaman M, Dilnaz F, Ashraf A. An update on treatment options for methicillin-resistant *Staphylococcus aureus* (MRSA) bacteremia: a systematic review. Cureus. 2022;14:e31486.
4. Kanafani Z, Kanj SJU. Acinetobacter infection: treatment and prevention. Accessed 25.01.2023, Available from: https://www.uptodate.com/contents/acinetobacter-infection-treatment-and-prevention/print#H5.
5. Silva V, Almeida L, Gaio V, Cerca N, Manageiro V, Caniça M, Capelo JL, Igrejas G, Poeta P. Biofilm formation of multidrug-resistant MRSA strains isolated from different types of human infections. Pathogens. 2021;10:970.
6. Yang CH, Su PW, Moi SH, Chuang LY. Biofilm formation in *Acinetobacter baumannii*: genotype-phenotype correlation. Molecules. 2019;24:1849.
7. Oliveira F, Rohde H, Vilanova M, Cerca N. The emerging role of iron acquisition in biofilm-associated infections. Trends Microbiol. 2021;29:772-775.
8. Coraça-Huber DC, Dichtl S, Steixner S, Nogler M, Weiss G. Iron chelation destabilizes bacterial biofilms and potentiates the antimicrobial activity of antibiotics against coagulase-negative *Staphylococci*. Pathog Dis. 2018;76.
9. Moreau-Marquis S, O'Toole GA, Stanton BA. Tobramycin and FDA-approved iron chelators eliminate *Pseudomonas aeruginosa* biofilms on cystic fibrosis cells. Am J Respir Cell Mol Biol. 2009;41:305-13.
10. Aksoyalp ZŞ, Temel A, Erdogan BR. Iron in infectious diseases friend or foe?: The role of gut microbiota. J Trace Elem Med Biol. 2023;75:127093.
11. Bellotti D, Remelli M. Deferoxamine B: a natural, excellent and versatile metal chelator. Molecules. 2021;26:3255.
12. Gokarn K, Pal RB. Activity of siderophores against drug-resistant Gram-positive and Gram-negative bacteria. Infect Drug Resist. 2018;11:61-75.
13. The European Committee on Antimicrobial Susceptibility Testing (EUCAST). Disk diffusion method for antimicrobial susceptibility testing version 11.0. Accessed 01.03.2023, Available from: www.eucast.org
14. Temel A, Erac B. Investigating biofilm formation and antibiofilm activity using real time cell analysis method in carbapenem resistant *Acinetobacter baumannii* strains. Current Microbiology. 2022;79:256.
15. Stepanović S, Vuković D, Hola V, Di Bonaventura G, Djukić S, Cirković I, Ruzicka F. Quantification of biofilm in microtiter plates: overview of testing conditions and practical recommendations for assessment of biofilm production by *Staphylococci*. APMIS. 2007;115:891-899.
16. Nair A, Perry A, Perry JD, Gould FK, Samuel J. In vitro effects of combined iron chelation, antibiotics and matrix disruption on clinical isolates of *Pseudomonas aeruginosa*. J Antimicrob Chemother. 2020;75:586-592.

17. Bellanti F, Del Vecchio GC, Putti MC, Cosmi C, Fotzi I, Bakshi SD, Danhof M, Pasqua OD. Model-based optimisation of deferoxamine chelation therapy. Pharm Res. 2016;33:498-509.

18. Zhu CF, Qiu DH, Kong XL, Hider RC, Zhou T. Synthesis and *in vitro* antimicrobial evaluation of a high-affinity iron chelator in combination with chloramphenicol. J Pharm Pharmacol. 2013;65:512-520.

19. van Asbeck BS, Marcelis JH, Marx JJ, Struyvenberg A, van Kats JH, Verhoef J. Inhibition of bacterial multiplication by the iron chelator deferoxamine: potentiating effect of ascorbic acid. Eur J Clin Microbiol. 1983;2:426-431.

20. Thompson MG, Corey BW, Si Y, Craft DW, Zurawski DV. Antibacterial activities of iron chelators against common nosocomial pathogens. Antimicrob Agents Chemother. 2012;56:5419-5421.

21. Cahill C, O'Connell F, Gogan KM, Cox DJ, Basdeo SA, O'Sullivan J, Gordon SV, Keane J, Phelan JJ. The iron chelator desferrioxamine increases the efficacy of bedaquiline in primary human macrophages infected with BCG. Int J Mol Sci. 2021;22:2938.

22. Kiss T, Farkas E. Metal-binding ability of desferrioxamine B. Journal of inclusion phenomena and molecular recognition in chemistry. 1998;32:385-403.

23. Cronjé L, Edmondson N, Eisenach KD, Bornman L. Iron and iron chelating agents modulate Mycobacterium tuberculosis growth and monocyte-macrophage viability and effector functions. FEMS Immunol Med Microbiol. 2005;45:103-112.

24. Pereira M, Chen TD, Buang N, Olona A, Ko JH, Prendecki M, Costa ASH, Nikitopoulou E, Tronci L, Pusey CD, Cook HT, McAdoo SP, Frezza C, Behmoaras J. Acute iron deprivation reprograms human macrophage metabolism and reduces inflammation *in vivo*. Cell Rep. 2019;28:498-511.

25. Arifin AJ, Hannauer M, Welch I, Heinrichs DE. Deferoxamine mesylate enhances virulence of community-associated methicillin resistant *Staphylococcus aureus*. Microbes Infect. 2014;16:967-972.

26. Lesic B, Foulon J, Carniel E. Comparison of the effects of deferiprone versus deferoxamine on growth and virulence of *Yersinia enterocolitica*. Antimicrob Agents Chemother. 2002;46:1741-1745.

27. Hartmann A, Braun V. Iron uptake and iron limited growth of *Escherichia coli* K-12. Arch Microbiol. 1981;130:353-356.

28. Fekri K, Khoshdel A, Rasoulynezhad M, Kheiri S, Malekpour A, Zamanzad B. *In vitro* effect of iron chelators on the growth of *Escherichia coli*, *Staphylococcus epidermidis*, *Staphylococcus aureus*, *Yersinia enterocolitica*, and *Pseudomonas aeruginosa* strains. J Shahrekord Univ Med Sci. 2019;21:244-249.

29. Visca P, Bonchi C, Minandri F, Frangipani E, Imperi F. The dual personality of iron chelators: growth inhibitors or promoters? Antimicrob Agents Chemother. 2013;57:2432-2433.

30. Stapleton PD, Taylor PW. Methicillin resistance in *Staphylococcus aureus*: mechanisms and modulation. Sci Prog. 2002;85:57-72.

31. Bush K. Past and present perspectives on β-lactamases. Antimicrob Agents Chemother. 2018;62:e01076-18.

32. Hernlem BJ, Vane LM, Sayles GD. Stability constants for complexes of the siderophore desferrioxamine B with selected heavy metal cations. Inorganica Chimica Acta. 1996;244:179-184.

33. Krewulak KD, Vogel HJ. Structural biology of bacterial iron uptake. Biochim Biophys Acta. 2008;1778:1781-804.

34. Eijkelkamp BA, Hassan KA, Paulsen IT, Brown MH. Investigation of the human pathogen *Acinetobacter baumannii* under iron limiting conditions. BMC Genomics. 2011;12:126.

35. Tiwari V, Rajeswari MR, Tiwari M. Proteomic analysis of iron-regulated membrane proteins identify FhuE receptor as a target to inhibit siderophore-mediated iron acquisition in *Acinetobacter baumannii*. Int J Biol Macromol. 2019;125:1156-1167.

36. Blackledge MS, Worthington RJ, Melander C. Biologically inspired strategies for combating bacterial biofilms. Curr Opin Pharmacol. 2013;13:699-706.

37. Gentile V, Frangipani E, Bonchi C, Minandri F, Runci F, Visca P. Iron and *Acinetobacter baumannii* biofilm formation. Pathogens. 2014;3:704-719.

38. Moon JH, Kim C, Lee HS, Kim SW, Lee JY. Antibacterial and antibiofilm effects of iron chelators against Prevotella intermedia. J Med Microbiol. 2013;62:1307-1316.

39. Nazik H, Penner JC, Ferreira JA, et al. Effects of iron chelators on the formation and development of *Aspergillus fumigatus* biofilm. Antimicrob Agents Chemother. 2015;59:6514-6520.

Turk J Pharm Sci 2024;21(4):274-283
DOI: 10.4274/tjps.galenos.2023.44459

ORIGINAL ARTICLE

Evaluation of Drug-Related Problems of Intensive Care Unit Patients by Clinical Pharmacists: A Retrospective Study

Ahmet ÇAKIR[1], Hasan MEMİŞ[1]*, Zeynep Ülkü GÜN[1], Murat BIÇAKCIOĞLU[2]

[1]İnönü University Faculty of Pharmacy, Department of Clinical Pharmacy, Malatya, Türkiye
[2]İnönü University Faculty of Medicine, Department of Anaesthesiology and Reanimation, Malatya, Türkiye

ABSTRACT

Objectives: The study aimed to identify drug-related problems (DRPs) and risk factors associated with the emergence of DRPs in intensive care unit (ICU) patients.

Materials and Methods: This retrospective study included patients in the anesthesiology and reanimation ICU of a university-affiliated tertiary care hospital. DRPs identified by clinical pharmacists were classified using the Pharmaceutical Care Network Europe Classification for DRPs version 9.1. The association between various patient-related factors, and having DRPs were evaluated.

Results: In total, 222 patients were included in the study, 128 of which were male (57.7%). The number of DRPs was 388 in 135 patients (1.75 ± 2.47 DRPs per patient). The group in which at least 1 DRP was identified, the duration of hospitalization was longer than in the group in which no DRP was identified ($p < 0.001$). In the groups in which there was the presence of mechanical ventilation support at admission or mortality, the mean DRP count was significantly higher than that in the other group ($p < 0.05$). Age, duration of hospitalization, and the Acute Physiology and Chronic Health Evaluation (APACHE) II score at admission had positive relationships with the DRP count, but the Glasgow Coma Scale (GCS) showed a negative relationship ($p < 0.05$). According to the binary logistic regression analysis ($p < 0.001$), in which the age of the patient, GCS score, APACHE II score at admission, duration of hospitalization, and presence of mechanical ventilation support at admission were included, only the APACHE II score at admission and duration of hospitalization significantly affected the emergence of DRPs. The major problem was related to treatment effectiveness (47.9%), followed by treatment safety problems (29.9%). The major causes of these problems were dose selection (44.0%) and drug selection (36.8). Interventions were made at the drug (97.2%) and prescriber level (2.3%). The acceptance rate of interventions and resolution rate of the DRPs were 93.6% and 85.1%, respectively. The top three medications that caused DRPs the most were as follows: meropenem, colistin, and piperacillin/tazobactam.

Conclusion: Clinical pharmacists can detect and treat DRPs quickly. Our analysis shows that clinical pharmacy services are needed in high-DRP wards like ICU.

Keywords: Clinical pharmacist, critical illness, intensive care units, medication errors

INTRODUCTION

According to the Pharmaceutical Care Network Europe Association (PCNE), a drug-related problem (DRP) is defined as "an event or circumstance involving drug therapy that actually or potentially interferes with desired health outcomes".[1] Drug-drug interactions, adverse drug events (ADEs), and medication errors can be classified as DRPs.[2] DRPs and ADEs are frequently encountered in intensive care units (ICUs).[3] Treatments administered to critically ill patients may put them at risk in terms of these types of medical errors.[4] A previously conducted study claims that almost half of the hospitalizations are related to DRPs and ADEs.[5] A systematic review conducted in 2007 shows that 46.5% of the ADEs are preventable, and 16.0% of these are emerging from medication errors.[6] There

*Correspondence: eczhasanmemis@gmail.com, Phone: +90 4223411216 , ORCID-ID: orcid.org/0000-0001-7158-1795
Received: 28.05.2023, Accepted: 07.08.2023

are studies that include the interventions of pharmacists in order to identify and solve the DRPs seen in ICUs.[7-9] In a study, the interventions of clinical pharmacists decreased DRP rates in geriatric patients.[9] Clinical pharmacists can help determine and solve DRPs early.[10] The integration of clinical pharmacists into the existing healthcare system, it will be possible to better detect and tackle DRPs.

The study aimed to identify DRPs and risk factors associated with the emergence of DRPs in ICU patients.

MATERIALS AND METHODS

Study design and setting

The current retrospective study was conducted in the reanimation ICU with a 26-bed capacity of a university-affiliated tertiary care hospital in Malatya, Türkiye between May 2022 and December 2022. In the ICU, the physicians in charge consist of two professors, an assistant professor, and four physicians. Specialists and resident physicians also work alternate shifts. The working hours are between 8 a.m. and 5 p.m. in the ICU. Two clinical pharmacy residents participated in weekday rounds with ICU and infectious diseases physicians, nurses, and technicians. The recommendations for DRPs made by the clinical pharmacy residents were recorded. The classification of DRPs according to the PCNE classification system was performed by reaching a consensus among clinical pharmacy residents.

Ethics approval

This study was conducted in line with the principles of the Declaration of Helsinki. Approval was granted by the İnönü University Scientific Research and Publication Ethics Committee (approval number: 4521, date: 11.04.2023). Participant consent was obtained from all patients included in the study.

Participants

All patients hospitalized for at least 24 hours in the ICU were included in the study. Patients whose hospitalization and discharge occurred on the same weekend or when the clinical pharmacy residents were absent from the ICU, or patients whose data were missing, were excluded from the study.

Data collection

The hospital's electronic database was used to obtain information about the patients' demographics, diagnoses, laboratory results, Glasgow Coma Scale (GCS) scores, Acute Physiology and Chronic Health Evaluation (APACHE) II scores at admission, duration of hospitalization, the status of mechanical ventilation support at admission, and types of admission. Daily medication charts were obtained from patient files. Admission diagnoses and drugs associated with DRPs were classified using the International Classification of Diseases, 10th revision (ICD-10) and the Anatomical Therapeutic Chemical (ATC) Classification System, respectively. The UpToDate®, Micromedex®, Lexicomp®, Sanford Antimicrobial Guide®, CredibleMeds®, and LiverTox® databases were used to identify DRPs. The identified DRPs were classified using the PCNE Classification for DRPs, version 9.1.

Outcomes

The primary outcomes of this study were determining the DRPs, the acceptance rates of the interventions, and the resolution rates of the DRPs administered by clinical pharmacists in the ICU. The secondary outcomes of this study are determining the most frequent DRPs and the association between DRPs and various patient-related factors. DRPs were classified using the National Coordinating Council for Medication Error Reporting and Prevention (NCC MERP), revised in October 2022 Index revised in October 2022 to determine the extent to which patients were harmed.

Statistical analysis

Statistical analysis was performed using the Statistical Package for the Social Sciences (SPSS) v27.0. The normality of the continuous data was tested using the Kolmogorov-Smirnov test, and it was observed that none of the data was distributed normally; thus, non-parametric tests were applied. Continuous and categorical data were presented as median (25th percentile-75th percentile) and number (percentage), respectively. All the data in this study were present. The continuous data between the two groups were compared using the Mann-Whitney U test, whereas the categorical data were compared using Fisher's exact test. The presence of a correlation between the two continuous variables was explored using Spearman's correlation test. The correlation coefficient value was interpreted as follows: Correlation coefficient < 0.3 was interpreted as poor; correlation coefficient 0.3 to 0.5 was interpreted as fair; correlation coefficient 0.6 up to 0.8 was interpreted as moderately strong; and correlation coefficient ≥ 0.8 was interpreted as very strong linear relationship.[11] Binary logistic regression analysis was performed to examine the extent to which various patient-related factors affect the emergence of DRP. A p value of 0.05 was considered statistically significant.

RESULTS

During the study period, 418 patients were admitted to the ICU. Of the 196 patients, 196 were excluded from the study because of admission/discharge on the same weekend or because the clinical pharmacy residents were absent from the ICU, or whose data were missing. Finally, the study included 222 patients, of whom 57.7% were men. One or more DRPs were identified in 135 patients, for a total of 388 DRPs (1.75 ± 2.47 DRPs per patient). The total number of patient days was 4,868 (79.7 DRPs per 1000 patient days). The characteristics of the patients are summarized in Table 1.

The top 4 admission diagnoses classified according to the ICD-10 are given in Table 2.

The number of DRPs were compared according to the presence of mechanical ventilation support, mortality, and surgery and are presented in Table 3.

The correlations between DRP count, duration of hospitalization, age, GCS score at admission, and APACHE II score at admission are given in Table 4.

Table 1. Characteristics of the patients

Characteristic	Total	DRPs identified	No DRPs were identified	*p* value
Patients (n, %)	222 (100.0)	135 (60.8)	87 (39.2)	
Sex (n, %)				
Male Female	128 (57.7) 94 (42.3)	80 (59.3) 55 (40.7)	48 (55.2) 39 (44.8)	0.580[a]
Age, years (median, (25th percentile-75th percentile)]	66.50 (50.00-79.00)	69.00 (55.00-78.00)	61.00 (41.00-79.00)	0.053[b]
Duration of hospitalization, days [median, (25th percentile-75th percentile)]	10.00 (5.00-26.25)	15.00 (7.00-36.00)	6.00 (4.00-13.00)	<0.001[b]
Presence of surgery (n, %)	94 (42.3)	58 (43.0)	36 (41.4)	0.890[a]
Presence of mechanical ventilation support at admission (n, %)	89 (40.1)	64 (47.4)	25 (28.7)	0.008[a]
Mortality (n, %)	85 (38.3)	64 (47.4)	21 (24.1)	<0.001[a]
Total GCS at admission [median, (25th percentile-75th percentile)]	11.00 (3.00-15.00)	9.00 (3.00-14.00)	14.00 (3.00-15.00)	<0.001[b]
Total APACHE II Score upon admission [median, (25th percentile-75th percentile)]	15.00 (8.00-24.00)	18.00 (10.00-26.00)	10.00 (5.00-18.00)	<0.001[b]
Admitted from (n, %)				
Emergency Another ward/hospital	90 (40.5) 132 (59.5)	44 (32.6) 91 (67.4)	46 (52.9) 41 (47.1)	0.003[a]
CRP level upon admission (upper limit of normal* is 0.351 mg/dL) (n, %)				
Normal High	41 (18.5) 181 (81.5)	22 (16.3) 113 (83.7)	19 (21.8) 68 (78.2)	0.376[a]
PCT at admission (upper limit of normal* is 0.5 ng/mL) (n, %)				
Normal High	98 (44.1) 124 (55.9)	53 (39.3) 82 (60.7)	45 (51.7) 42 (48.3)	0.073[a]
SCr level upon admission (upper limit of normal* is 1.25 mg/dL) (n, %)				
Normal High	118 (53.2) 104 (46.9)	66 (48.9) 69 (51.1)	52 (59.8) 35 (40.2)	0.130[a]

[a]Fisher's exact test, [b]Mann-Whitney U test, *The upper limit of normal values was obtained from the hospital's laboratory results.
APACHE II: Acute Physiology and Chronic Health Evaluation II, CRP: C-reactive protein, GCS: Glasgow Coma Scale, PCT: Procalcitonin, SCr: Serum creatinine, DRP: Drug-related problem

Table 2. The top 4 diagnoses classified according to the ICD-10

Diagnosis	n (%)
Subarachnoid hemorrhage	15 (6.8)
Sepsis	13 (5.9)
Bacterial pneumonia	12 (5.4)
Car occupant (any) injured in unspecified traffic accident	12 (5.4)

ICD: International Classification of Diseases

Table 3. Comparison of mean DRP counts according to various patient-related factors

Factor	Total (mean ± SD)	Yes (mean ± SD)	No (mean ± SD)	*p* value
Presence of mechanical ventilation support	1.75 ± 2.47	2.20 ± 2.50	1.44 ± 2.42	< 0.001[a]
Mortality		2.52 ± 2.81	1.27 ± 2.12	< 0.001[a]
Presence of surgery		2.11 ± 2.97	1.48 ± 2.01	0.254[a]

[a]Mann-Whitney U test, DRP: Drug-related problem, SD: Standard deviation

On the basis of binary logistic regression analysis, the effects of age, GCS score at admission, APACHE II score at admission, duration of hospitalization, and presence of mechanical ventilation support at admission on the likelihood of DRP were determined. The logistic regression model was significant, $\chi^2(5) = 42.132$, $p < 0.001$. The Hosmer-Lemeshow test showed that the data fit the model well, $\chi^2(8) = 12.579$, $p = 0.127$. The model accurately identified 73.9% of the cases and explained 23.4% (Nagelkerke R^2) of the variance in DRP emergence. An increase of 1 unit in the APACHE II score at admission and the duration of hospitalization increased the likelihood of the emergence of DRP by 1.042 (95% CI 1.000-1.086) and 1.032 (95% CI 1.012-1.051), respectively. However; age, GCS score at admission, and the presence of mechanical ventilation support at admission did not have a statistically significant effect on the risk of the emergence of DRP.

The DRPs were classified according to the NCC MERP Index in an attempt to visualize the harm status, and the results are given in Table 5.

The DRPs were classified according to PCNE v9.1, of which 205 (52.8%) were potential DRPs and 183 (47.2%) were actual DRPs. Among the actual DRPs, 168 (91.80%) of them were accepted and 153 (83.61%) of them were solved. The related results are presented in Table 6.

According to the ATC classification system, the three classes most closely related to DRPs were as follows: antibacterials for systemic use (n= 104; 26.8%), general nutrients (n= 45; 11.6%), and IV solution additives (n= 25; 6.4%). Meropenem (24, 23.1%), colistin (20, 19.2%), and piperacillin/tazobactam (13, 12.5%) were the top three antibacterial medications most closely associated with DRPs. In total, 116 DRPs associated with possible ADEs were identified. The first three drugs for which interventions were made to assess possible ADEs were meropenem (14, 12.1%), colistin (13, 11.2%), and piperacillin-tazobactam (9, 7.8%). The examples of clinical pharmacist interventions are presented in Table 7.

Table 4. Correlations between various patient characteristics and DRP count

Patient characteristics	Spearman's rho	Orientation and degree of association	*p* value
Duration of hospitalization	0.446	Positive-oriented fair	< 0.001
Age	0.133	Positive-oriented poor	0.048
GCS upon admission	-0.302	Negatively oriented fair	< 0.001
APACHE II score upon admission	0.308	Positive-oriented fair	< 0.001

APACHE II: Acute physiology and chronic health evaluation, GCS: Glasgow Coma Scale, DRP: Drug-related problem

Table 5. Distribution of DRPs according to NCC MERP index

Category	Explanation	n (%)	Harm status, n (%)
A	Circumstances or events that have the capacity to cause errors	205 (52.8)	No error, 205 (52.8)
B	An error occurred, but it did not reach the patient	2 (0.5)	Error, no harm, 142 (36.6)
D	An error occurred that reached the patient and required monitoring to confirm that it resulted in no harm to the patient and/or intervention to preclude harm	140 (36.1)	
E	An error that may have contributed to or resulted in temporary harm to the patient	20 (5.2)	Error, harm, 41 (10.6)
F	An error that may have contributed to or resulted in temporary harm to the patient and required initial or prolonged hospitalization	21 (5.4)	

DRP: Drug-related problem, NCC MERP: National Coordinating Council for Medication Error Reporting and Prevention

Table 6. Classification of DRPs according to PCNE classification system v9.1

Domains	Code	Subdomains	n (%)
Problems			388 (100.0)
	Treatment effectiveness		186 (47.9)
	P1.3	Untreated symptoms or indications	95 (24.5)
	P1.2	Effect of drug treatment not optimal	90 (23.2)
	P1.1	No effect of drug therapy despite correct use	1 (0.3)

Table 6. Continued

Domains	Code	Subdomains	n (%)
	Treatment safety		116 (29.9)
	P2.1	Adverse drug event (possibly) is occurring	116 (29.9)
	Other		86 (22.2)
	P3.1	Unnecessary drug-treatment	65 (16.8)
	P3.2	Unclear problem/complaint	21 (5.4)
Causes			418 (100.0)
	Dose selection		184 (44.0)
	C3.2	Drug dose of a single active ingredient	59 (14.1)
	C3.1	Drug dose too low	55 (13.2)
	C3.4	Too frequent dosage regimen	46 (11.0)
	C3.3	Dosage regimen not frequent enough	22 (5.3)
	C3.5	Dose timing instructions are incorrect, unclear, or missing	2 (0.5)
	Drug selection		154 (36.8)
	C1.5	No or incomplete drug treatment in spite of existing indication	96 (23.0)
	C1.2	No indication for the drug	26 (6.2)
	C1.3	Inappropriate combination of drugs, herbal medications, and dietary supplements	15 (3.6)
	C1.4	Inappropriate duplication of therapeutic groups or active ingredients	11 (2.6)
	C1.1	Inappropriate drug according to the guidelines/formularies	3 (0.7)
	C1.6	Too many different drugs and active ingredients prescribed for indication	3 (0.7)
	Other		38 (9.1)
	C9.2	Other cause	17 (4.1)
	C9.3	No obvious cause	16 (3.8)
	C9.1	No or inappropriate outcome monitoring	5 (1.2)
	Treatment duration		34 (8.1)
	C4.2	Too long treatment duration	34 (8.1)
	Patient transfer-related		4 (1.0)
	C8.1	Medication reconciliation	4 (1.0)
	Drug form		2 (0.5)
	C2.1	Inappropriate drug form/formulation (for this patient)	2 (0.5)
	The drug use process		2 (0.5)
	C6.1	Inappropriate timing of administration or dosing intervals by a health professional	1 (0.2)
	C6.6	Drug administration *via* the wrong route by a health professional	1 (0.2)
Planned interventions			388 (100.0)
	At the drug level		377 (97.2)
	I3.2	Dosage changed to	171 (44.1)
	I3.6	Drug started	101 (26.0)
	I3.5	Paused or stopped drug	77 (19.9)
	I3.1	Drug changed to	19 (4.9)
	I3.4	Instructions for use changed to	7 (1.8)
	I3.3	The formula was changed to	2 (0.5)

Table 6. Continued

Domains	Code	Subdomains	n (%)
	The prescriber level		11 (2.8)
	I1.3	Intervention proposed to the prescriber	9 (2.3)
	I1.1	The prescriber is informed only	2 (0.5)
Intervention acceptance			388 (100.0)
	Intervention accepted		363 (93.6)
	A1.1	Intervention accepted and fully implemented	346 (89.2)
	A1.2	Intervention accepted, partially implemented	11 (2.8)
	A1.3	Intervention accepted but not implemented	4 (1.0)
	A1.4	Intervention accepted, implementation unknown	2 (0.5)
	Intervention not accepted		24 (6.2)
	A2.2	Intervention not accepted, no agreement	20 (5.2)
	A2.1	Intervention not accepted, not feasible	4 (1.0)
	Other		1 (0.3)
	A3.2	Intervention not proposed	1 (0.3)
DRP status			388 (100.0)
	Solved		330 (85.1)
	O1.1	Problem totally solved	330 (85.1)
	Not solved		32 (8.3)
	O3.2	Problem not solved, lack of physician cooperation	21 (5.4)
	O3.4	No need or possibility to solve the problem	7 (1.8)
	O3.3	Problem not solved, intervention not effective	4 (1.0)
	Not known		22 (5.7)
	O0.1	Problem status is unknown	22 (5.7)
	Partially solved		4 (1.0)
	O2.1	Problem partially solved	4 (1.0)

DRP: Drug-related problem, PCNE: Pharmaceutical Care Network Europe Association

Table 7. The sample pharmacist interventions at the drug and DRP levels

Cause	Drug	Pharmacist intervention
Dose selection		
C3.2 High drug dose of a single active ingredient	Piperacillin-tazobactam	The patient was administered 4.5 g q6h piperacillin-tazobactam in spite of hemodialysis therapy. The pharmacist recommended changing the drug dosage to 2.25 g every 6 hours
C3.1 Too low a drug dose	Valproic acid	The patient was administered 500 mg of valproic acid q12h and the serum valproic acid level was 29 mg/L. The pharmacist recommended changing the drug dosage to 500 mg every 8 hours
C3.4. Dosage regimen too frequent	Pantoprazole	The patient was administered intravenous pantoprazole 40 mg every 12 hours despite the absence of gastrointestinal bleeding signs. The pharmacist recommended changing the drug dosage to 40 mg every 24 hours
C3.3 Dosage regimen not frequent enough	Meropenem	The patient was administered 1 g of meropenem every 12 hours despite the absence of renal impairment. The pharmacist recommended changing the drug dosage to 1 g every 8 hours
C3.5 Dose timing instructions that are incorrect, unclear, or missing	Meropenem	The patient was administered 30 min of meropenem infusion therapy despite the presence of microorganism resistance. The pharmacist recommended increasing the infusion duration to 3 hours

Table 7. Continued

Cause	Drug	Pharmacist intervention
Drug selection		
C1.5 No or incomplete drug treatment despite an existing indication	Levetiracetam	The patient admitted with subdural hemorrhage did not receive prophylactic antiseizure medication. The pharmacist recommended 1 g of levetiracetam every 12 hours for a duration of 7 days
C1.2. No indication for drugs	Cefazoline	The patient admitted for postoperative thyroidectomy was administered antibacterial prophylaxis. The pharmacist recommended discontinuing cefazolin therapy because clean procedures do not require antibacterial prophylaxis
C1.3 Inappropriate combination of drugs, herbal medications, and dietary supplements	Clarithromycin	Clarithromycin and phenytoin therapy were concomitantly administered. The pharmacist recommended replacing clarithromycin with azithromycin, which does not interact with phenytoin
C1.4 Inappropriate duplication of therapeutic groups or active ingredients	Furosemide	The patient with decompensated heart failure was administered intravenous and oral furosemide therapy concomitantly. The pharmacist recommended discontinuing oral furosemide
C1.1 Inappropriate drug according to the guidelines/formularies	Dexamethasone	A patient admitted with a brain tumor was administered dexamethasone therapy in an attempt to reduce the cerebral edema. The pharmacist recommended stopping dexamethasone therapy because it was of no use in this case
C1.6 Too many different drugs and active ingredients prescribed for indication	Tramadol	The patient was administered fentanyl and tramadol concomitantly as part of analgosedation therapy. The pharmacist recommended stopping tramadol therapy
Other		
C9.2 Other causes	Normal saline	The patient was administered normal saline despite the serum sodium level of 161 mmol/L. The pharmacist recommended replacing normal saline with 1/2 normal saline therapy
C9.3 No obvious cause	Rivaroxaban	The patient was administered rivaroxaban. The pharmacist recommended that the drug be withheld for 24 hours before surgery
C9.1 No or inappropriate outcome monitoring	Valproic acid	The patient was administered valproic acid and meropenem therapy concomitantly; however, the valproic acid level was not monitored. The pharmacist recommended therapeutic drug monitoring of valproic acid
Treatment duration		
C4.2 Too long treatment duration	Hydrocortisone	The patient was administered 50 mg q6h hydrocortisone therapy because of septic shock; however, the duration of therapy was > 7 days. The pharmacist recommended discontinuation of hydrocortisone therapy with a taper
Patient transfer-related		
C8.1 Medication reconciliation problem	Valsartan-hydrochlorothiazide	For hypertensive patients, the pharmacist recommended the administration of home antihypertensive medication
Drug form		
C2.1 Inappropriate drug form/formulation (for this patient)	Levodopa-benserazide	Being fed via a nasogastric tube, the patient is prescribed levodopa-benserazide capsules. The pharmacist recommended replacing the capsule form with the tablet form because capsules should not be opened while tablets are crushed
The drug use process		
C6.1 Inappropriate timing of administration or dosing interval by a health professional	Pyridostigmine	The patient with diarrhea was administered pyridostigmine and continuous feeding. The pharmacist recommended replacing continuous feeding with bolus feeding and administering pyridostigmine in combination with bolus feeding
C6.6 Drug administration via the wrong route by a health professional	Tamsulosin	For patients who could not take the tamsulosin capsule orally, it was administered by opening the capsule. The pharmacist recommended replacing tamsulosin with doxazosin, which can be crushed and administered via a nasogastric tube

DISCUSSION

To the best of our knowledge, this is the first DRP study to have been performed in the anesthesiology and reanimation ICU of a tertiary care hospital in Türkiye that included clinical pharmacist interventions for DRP resolution.

Since clinical pharmacy specialization is a new healthcare profession in Türkiye, this study is important to enlighten pharmacists who are considering specializing in critical care pharmacy in the future.

This study has a number of strengths, one of which is that the PCNE classification was determined by reaching a consensus between two clinical pharmacists, which helped reduce the possibility of bias. Another strength of this study is that it classifies DRPs that occur in ICUs, provides recommendations for the management of DRPs, and classifies the severity of medication errors using the NCC MERP. Besides, this study provides a sample pharmacist intervention table classified according to the causes of specific DRPs, which may be especially useful for those who would like to increase their expertise in the critical care pharmacy field.

Interpretation

In this study, at least one DRP was identified in 60.8% of patients, with an average of 1.75 DRPs per patient. In an ICU study conducted in 2022, at least one DRP was detected in 71.5% of patients, and 1.36 DRPs were found in each patient.[12] In another study, 69.8% of patients had at least one DRP, and the average DRP count per patient was 1.36.[13] However, in another study conducted in the cardiology service in 2022, at least 1 DRP was detected in 54.3% of patients, and the DRP count per patient was found to be 1.84.[14] This difference may be due to the fact that the rate of patients with at least 1 DRP was higher due to the inability of critically ill patients in the ICU to continue their medications at home. At the same time, the fact that the intensive care team in which the study was conducted was not familiar with the clinical pharmacist recommendations was one of the factors affecting the detected DRP numbers.[15]

In our study, the mean DRP counts were significantly higher in the group receiving mechanical ventilation support than in the group not receiving mechanical ventilation support (p = 0.008). In a study conducted in Türkiye in 2022, it was found that receiving mechanical ventilation support increased the incidence of DRP by 3,435 times ($p < 0.001$).[16] Since mechanical ventilation support requires additional drug therapy (stress ulcer prophylaxis, analgosedation, *etc.*), it is expected to increase the incidence of DRP.

A high APACHE II score and a low GCS score indicate that the patient's condition is critical. Given the complexity of pharmacotherapy in such patients, extra attention is required regarding DRPs. According to our findings, the mean APACHE II score and GCS score were higher in the group in which DRP was identified than in the group in which DRP was not identified.

Due to alterations in drug pharmacokinetics and organ function, critically ill patients are at increased risk of ADEs.[17] At the same time, critically ill patients experience many physiological changes that can affect drug metabolism and excretion. Organ dysfunction, particularly renal failure, may lead to increased ADEs.[18] Given these changes, the incidence of DRP may be higher in critically ill patients than in the general population. In a study examining the causes of DRPs, C1 drug selection (41.3%) and C3 drug selection were the most common causes (29.0%).[19] In another study, DRPs were categorized according to their causes, and C3-dose selection (39.7%) and C5-drug use process (32.7%) were determined to be the most prominent causes.[20] In our study, C3-drug selection (44.0%) and C1-drug selection (36.8%) associated DRPs were the most prevalent. These differences may be due to differences in countries, populations, and healthcare providers.

With the intervention of clinical pharmacists, potential medication errors and adverse drug reactions can be effectively prevented, and patients' drug safety can be further improved.[21] Implementation of interventions with pharmacists participating in a multidisciplinary team can play a crucial role in executing drug protocols and preventing drug-related issues.[22] Among the pharmacist interventions for DRPs in studies conducted on geriatric[23] and neurological[24] patients, I1-at prescriber level interventions had the highest rate. In our study, most interventions were performed at the I3 level (97.1%). We believe that the biggest reason for the difference is that physicians in the service area, especially infectious disease specialists, allow clinical pharmacists to make changes in drug dose adjustments.

It has been observed that the acceptance rate of recommendations in previous studies exceeds 90%.[23,25-27] In another study, the acceptance rate of recommendations for DRPs was 100.0%, and 78.4% of DRPs were completely resolved.[28] The acceptance rate of interventions in our study was 93.6%, and 85.1% of the DRPs were completely resolved, which is in line with the literature.

In a study, antibiotics were found to be the drug group that caused the most DRP, followed by antiplatelet drugs and PPIs.[29] In another study, the most common drug groups causing DRP were antihypertensive drugs, antithrombotic drugs, and statins.[30] In our study, the most common drug groups causing DRP were systemic antibacterials (26.8%), general nutrients (11.6%), and IV solution additives (6.4%).

In a study conducted in 2020, it was determined that due to drug dosing error, sulfamethoxazole/trimethoprim caused the most DRP,[31] and in our study, meropenem (23.1%), colistin (19.2%), and piperacillin/tazobactam (12.5%) were found to be the drugs that caused the most DRP. The main reason why, especially meropenem and colistin, have been identified as drugs that cause a lot of DRP is the high frequency of acinetobacter-induced infections in the ICU and the use of these drugs in the treatment of these infections. In addition, colistin requires frequent renal dose adjustment.

In many studies, each DRP was graded using the NCC MERP, which is an index that categorizes medication errors to determine their severity.[32] In a study conducted with medical ward patients, DRPs defined according to the NCC MERP Index

were classified according to their severity rates, with 45.9% in category B, 41.5% in category C, and 12.7% in category D.[33] In our study, the distribution of DRPs according to the NCC MERP was 52.8% in category A, 36.1% in category D, 5.3% in category E, and 5.4% in category F. Temporary harms were detected early, and necessary interventions were made by clinical pharmacists so that these harms could not be converted to permanent harm. This difference across studies may stem from the nature of the place where healthcare is provided and the diversity of patient profiles.

In a study conducted in the internal medicine ward in Türkiye, a positive fair (r = 0.411) correlation was found between DRP counts and age, and a positive-oriented fair (r = 0.302) relationship was found between DRP counts and the length of stay in the hospital.[34] In this study, the DRP counts had a positive poor (r = 0.133) correlation with age and a positive fair (r = 0.446) correlation with the duration of hospitalization. Changes in pharmacokinetics and pharmacodynamics associated with aging can be noticed in geriatric patients, which explains the higher incidence of DRPs in this patient population. On the other hand, the patient's risk of acquiring DRP may increase if they are hospitalized for a longer duration.

In a study conducted in 2018 in which 474 older patients were included, the multivariate analysis showed that the length of stay increased the presence of DRP by 1,086 times ($p < 0.05$).[23] However, in a study published in 2019 in which 162 ICU patients were included, according to the multinomial logistic regression analysis, the length of stay had no significant effect on the presence of DRP ($p > 0.05$).[13] However, in our study, the duration of hospitalization increased the presence of DRP by 1.042 times ($p < 0.05$). This difference across the aforementioned studies may have arisen from the diversity of sample sizes. Martins et al.[13] may have made a type 2 error in detecting the effect of length of stay on the presence of DRP due to their relatively small sample size.

Further research

Further studies should be conducted to obtain more generalizable results in which a larger number of patients are included and more than one center is included. More advanced research on the risk factors associated with the emergence of DRPs should be conducted to inform healthcare providers. In addition, more studies are needed to demonstrate the impact of clinical pharmacy services in different areas of the health system, particularly in ICUs.

Study limitations

One of the limitations of the study was that it was conducted in a single center with a relatively small number of patients; so, the generalizability of the study results is limited. The identified DRP counts may be lower than the actual counts because clinical pharmacists were absent from the ward on weekends and holidays.

CONCLUSION

DRPs are adverse conditions that can cause significant changes in the treatment courses of patients. Clinical pharmacists play a key role in the timely detection and resolution of DRPs. Clinical pharmacists can offer the most appropriate solutions by providing suggestions for DRPs in line with the current literature. Our study showed that clinical pharmacy services are necessary in wards, such as ICUs, where the rate of DRPs may be high.

Acknowledgments

We would like to convey our deepest gratitude to the healthcare team of the reanimation ICU.

Ethics

Ethics Committee Approval: This study was conducted in line with the principles of the Declaration of Helsinki. Approval was granted by the İnönü University Scientific Research and Publication Ethics Committee (approval number: 4521, date: 11.04.2023).

Informed Consent: Participant consent was obtained from all patients included in the study.

Authorship Contributions

Surgical and Medical Practices: M.B., Concept: Z.Ü.G., M.B., Design: Z.Ü.G., M.B., Data Collection or Processing: A.Ç., H.M., Analysis or Interpretation: A.Ç., H.M., Literature Search: A.Ç., H.M., Writing: A.Ç., H.M., Z.Ü.G.,

Conflict of Interest: No conflict of interest was declared by the authors.

Financial Disclosure: The authors declared that this study received no financial support.

REFERENCES

1. Mil JWFv, Horvat N, Westerlund T, Richling I. PCNE classification for drug-related problems V9.1. Available from: https://www.pcne.org/upload/files/417_PCNE_classification_V9-1_final.pdf
2. Maslub MG, Radwan MA, Mikhail MS, Abdalla ZA, Youssef YL, Abdal Hafiz AI, Zain Eldien KM, Sha'aban A. Assessment of the latest prescribed drug-related problems. Eur Rev Med Pharmacol Sci. 2022;26:2373-2387.
3. Rothschild JM, Landrigan CP, Cronin JW, Kaushal R, Lockley SW, Burdick E, Stone PH, Lilly CM, Katz JT, Czeisler CA, Bates DW. The critical care safety study: the incidence and nature of adverse events and serious medical errors in intensive care. Crit Care Med. 2005;33:1694-1700.
4. Bell CM, Brener SS, Gunraj N, Huo C, Bierman AS, Scales DC, Bajcar J, Zwarenstein M, Urbach DR. Association of ICU or hospital admission with unintentional discontinuation of medications for chronic diseases. JAMA. 2011;306:840-847.
5. Leendertse AJ, Egberts AC, Stoker LJ, van den Bemt PM; HARM Study Group. Frequency of and risk factors for preventable medication-related hospital admissions in the Netherlands. Arch Intern Med. 2008;168:1890-1896.

6. Krähenbühl-Melcher A, Schlienger R, Lampert M, Haschke M, Drewe J, Krähenbühl S. Drug-related problems in hospitals: a review of the recent literature. Drug Saf. 2007;30:379-407.
7. Tharanon V, Putthipokin K, Sakthong P. Drug-related problems identified during pharmaceutical care interventions in an intensive care unit at a tertiary university hospital. SAGE Open Med. 2022;10:20503121221090881.
8. Howle LM, Kirkpatrick CMJ, Trethewy CE. Clinical pharmacy in a regional Australian intensive care unit. J Pharm Pract Res. 2018;48:36-43.
9. Chiang LH, Huang YL, Tsai TC. Clinical pharmacy interventions in intensive care unit patients. J Clin Pharm Ther. 2021;46:128-133.
10. Bremer S, Henjum S, Sæther EM, Hovland R. Drug-related problems and satisfaction among patients receiving pharmacist-led consultations at the initiation of cardiovascular drugs. Res Social Adm Pharm. 2022;18:3939-3947.
11. Chan YH. Biostatistics 104: correlational analysis. Singapore Med J. 2003;44:614-619.
12. Albayrak A, Başgut B, Bıkmaz GA, Karahalil B. Clinical pharmacist assessment of drug-related problems among intensive care unit patients in a Turkish university hospital. BMC Health Serv Res. 2022;22:79.
13. Martins RR, Silva LT, Lopes FM. Impact of medication therapy management on pharmacotherapy safety in an intensive care unit. Int J Clin Pharm. 2019;41:179-188.
14. Amankwa Harrison M, Marfo AFA, Buabeng KO, Nkansah FA, Boateng DP, Ankrah DNA. Drug-related problems among hospitalized hypertensive and heart failure patients and physician acceptance of pharmacists' interventions at a teaching hospital in Ghana. Health Sci Rep. 2022;5:e786.
15. Jiang SP, Chen J, Zhang XG, Lu XY, Zhao QW. Implementation of pharmacists' interventions and assessment of medication errors in an intensive care unit of a Chinese tertiary hospital. Ther Clin Risk Manag. 2014;10:861-866.
16. Ayhan YE, Karakurt S, Sancar M. The effect of the clinical pharmacist in minimizing drug-related problems and related costs in the intensive care unit in Turkey: A non-randomized controlled study. J Clin Pharm Ther. 2022;47:1867-1874.
17. Kane-Gill SL, Kowiatek JG, Weber RJ. A comparison of voluntarily reported medication errors in intensive care and general care units. Qual Saf Health Care. 2010;19:55-59.
18. Kane-Gill SL, Kirisci L, Verrico MM, Rothschild JM. Analysis of risk factors for adverse drug events in critically ill patients. Crit Care Med. 2012;40:823-828.
19. Li XX, Zheng SQ, Gu JH, Huang T, Liu F, Ge QG, Liu B, Li C, Yi M, Qin YF, Zhao RS, Shi LW. Drug-related problems identified during pharmacy intervention and consultation: implementation of an intensive care unit pharmaceutical care model. Front Pharmacol. 2020;11:571906.
20. Leopoldino RD, Santos MT, Costa TX, Martins RR, Oliveira AG. Drug-related problems in the neonatal intensive care unit: incidence, characterization and clinical relevance. BMC Pediatr. 2019;19:134.
21. Liu XX, Wang HX, Hu YY, Zhu XT, Tan X, Yang Y, Hang YF, Zhu JG. Drug-related problems identified by clinical pharmacists in nephrology department of a tertiary hospital in China-a single center study. Ann Palliat Med. 2021;10:8701-8708.
22. Agnol RD, Dos Santos MT, Michalowski MB, Einsfeld L. Pharmacists' interventions on 2 years of drug monitoring in an oncology pediatric inpatient ward. J Oncol Pharm Pract. 2022;28:1754-1762.
23. Ma Z, Sun S, Zhang C, Yuan X, Chen Q, Wu J, Wang X, Liu L. Characteristics of drug-related problems and pharmacists' interventions in a geriatric unit in China. Int J Clin Pharm. 2021;43:270-274.
24. Ali MAS, Khedr EMH, Ahmed FAH, Mohamed NNE. Clinical pharmacist interventions in managing drug-related problems in hospitalized patients with neurological diseases. Int J Clin Pharm. 2018;40:1257-1264.
25. Hailu BY, Berhe DF, Gudina EK, Gidey K, Getachew M. Drug related problems in admitted geriatric patients: the impact of clinical pharmacist interventions. BMC Geriatr. 2020;20:13.
26. Iqbal MJ, Mohammad Ishaq G, Assiri AA. Connecting Pharmacists and Other Health Care Providers (HCPs) towards drug therapy optimization: a pharmaceutical care approach. Int J Clin Pract. 2023;2023:3336736.
27. Tan BK, Chua SS, Chen LC, Chang KM, Balashanker S, Bee PC. Acceptability of pharmacist-led interventions to resolve drug-related problems in patients with chronic myeloid leukaemia. J Oncol Pharm Pract. 2021;27:1644-1656.
28. Boşnak AS, Birand N, Diker Ö, Abdi A, Başgut B. The role of the pharmacist in the multidisciplinary approach to the prevention and resolution of drug-related problems in cancer chemotherapy. J Oncol Pharm Pract. 2019;25:1312-1320.
29. Babelghaith SD, Wajid S, Alrabiah Z, Othiq MAM, Alghadeer S, Alhossan A, Al-Arifi M, Attafi IM. Drug-related problems and pharmacist intervention at a general hospital in the Jazan Region, Saudi Arabia. Risk Manag Healthc Policy. 2020;13:373-378.
30. Semcharoen K, Supornpun S, Nathisuwan S, Kongwatcharapong J. Characteristic of drug-related problems and pharmacists' interventions in a stroke unit in Thailand. Int J Clin Pharm. 2019;41:880-887.
31. Belaiche S, Goulois S, DeBerranger E, Odou P, Balagny S, Décaudin B. Clinical pharmacist and pharmaceutical interventions in HBH unit: a French observational study. Acta Clin Belg. 2021;76:258-263.
32. Hartwig SC, Denger SD, Schneider PJ. Severity-indexed, incident report-based medication error-reporting program. Am J Hosp Pharm. 1991;48:2611-2616.
33. Deawjaroen K, Sillabutra J, Poolsup N, Stewart D, Suksomboon N. Characteristics of drug-related problems and pharmacist's interventions in hospitalized patients in Thailand: a prospective observational study. Sci Rep. 2022;12:17107.
34. Abunahlah N, Elawaisi A, Velibeyoglu FM, Sancar M. Drug related problems identified by clinical pharmacist at the Internal Medicine Ward in Turkey. Int J Clin Pharm. 2018;40:360-367.

Turk J Pharm Sci 2024;21(4):284-296
DOI: 10.4274/tjps.galenos.2023.01379

ORIGINAL ARTICLE

Use of Cosmetics and Adverse Cosmetic Events Among Female Nurses: Need for a Cosmetovigilance System

Zakir KHAN[1,2*], Yusuf KARATAŞ[1], Gönül PEKKAN[3], Ayşe Nur ÇAKIR GÜNGÖR[4], Hazir RAHMAN[5], Faiz Ullah KHAN[6], Olcay KIROĞLU[1]

[1]Çukurova University Faculty of Medicine, Department of Medical Pharmacology, Adana, Türkiye
[2]Riphah International University Faculty of Pharmaceutical Sciences, Gulberg Green Campus, Islamabad, Pakistan
[3]Çukurova University Faculty of Medicine, Department of Child Health and Diseases, Adana, Türkiye
[4]Çukurova University Faculty of Medicine, Department of Gynecology and Obstetrics, Adana, Türkiye
[5]Abdul Wali Khan University Mardan (AWKUM) Faculty of Chemical and Life Sciences, Department of Microbiology, Mardan, Pakistan
[6]Xi'an Jiaotong University Faculty of Pharmacy, Department of Pharmacy Administration and Clinical Pharmacy, Xi'an, China

ABSTRACT

Objectives: Cosmetics are known to cause adverse events in users, and there is limited information on this topic both globally and in Türkiye. This study was conducted to assess the use of cosmetics, patterns, and characteristics of adverse cosmetic events (ACEs) among female nurses.

Materials and Methods: This cross-sectional study was conducted from February to April 2022 among registered female nurses with at least 1 year of work experience in a tertiary care hospital in Adana, Türkiye. A validated questionnaire was used for data collection, which included 13 questions with three main sections. The first part comprised demographic variables and cosmetic uses, the second part addressed ACE, and the final section consisted of consultation types and reporting methods for adverse events adopted after experiencing ACE.

Results: Of the total 158 participants, 144 were included in this study, resulting in a response rate of 91.1%. All female nurses reported using cosmetics, and 26.4% (n= 38) reported experiencing one or more cosmetic ACEs. Itching, burning, and eczema were the most frequently observed ACEs. A higher proportion of ACEs were associated with face care products (18.4%) and deodorants (13.1%). More than half (57.9%) of the nurses did not consult with healthcare professionals after experiencing ACE. Moreover, most participants (47.4%) did not report ACE to healthcare authorities.

Conclusion: A considerable proportion of the participants reported ACEs. The underreporting of ACE was also highlighted in this study. The results also emphasize the need for a robust cosmetovigilance system.

Keywords: Cosmetics, adverse event, cosmetovigilance, safety

INTRODUCTION

Cosmetics are major components of daily life for people of all ages and are used for a variety of purposes.[1] The United States Food and Drug Administration defines a cosmetic as "a substance that is applied to the body of a person with the intention of cleansing, beautifying, enhancing attractiveness, or changing appearance".[2] However, in terms of the legal definitions of drugs and cosmetics, the use of color additives and other ingredient restrictions as well as registration procedures are different for cosmetics in the United States and other countries.[3] According to the Turkish Medicines and Medical Devices Agency and the European Union (EU), a cosmetic is any substance or mixture that is applied to the skin, hair, external genital organs, lips, teeth, and mucous membranes of the oral cavity with the sole or primary intention of cleaning, perfuming, altering appearance, protecting, maintaining good condition, or removing body odors.[4]

According to the World Health Organization, an adverse cosmetic drug reaction is an unintended and harmful reaction

*Correspondence: zakirkhan300@gmail.com, Phone: +90 531 592 11 09, ORCID-ID: orcid.org/0000-0003-1365-548X
Received: 03.05.2023, Accepted: 07.08.2023

to a cosmetic that normally occurs following a proper application of a cosmetic, whereas an adverse cosmetic event (ACE) is a hypothetically anticipated noxious injury linked to the use of cosmetics.[5,6] The global cosmetic market has grown in recent years, which is driven by consumer demands that are increasingly concerned about their appearance.[6] Most cosmetic users are more concerned regarding the immediate effects on appearance than the long-term effects on the entire body.[1,5] Cosmetic products are thought to be reasonably safe and tolerable.[1,3] However, It is well known that cosmetic use can sometimes cause adverse reactions.[3,5,6] Numerous studies have documented severe ACEs, including eczema, blistering, breathing difficulties, hair loss, unconsciousness, dizziness, skin burns, nausea, and vomiting.[5] Similarly, the most frequently reported adverse effects linked to prolonged exposure to heavy makeup were headache, fatigue, dizziness, and nausea.[7] Previous studies reported a range of reactions to cosmetics, from mild hypersensitivity to severe anaphylactic reactions or even lethal intoxication. These reactions may occur immediately or after the use of cosmetics for an extended period.[1,8,9] It is suggested that more emphasis should be placed on testing and monitoring the potentially harmful effects of cosmetics.[8,9] Cosmetovigilance is a term used to describe the processes involved in gathering, analyzing, and monitoring spontaneous reports related to unfavorable events noticed during, or after usual or reasonably anticipated usage of cosmetics.[3,10] Cosmetovigilance is crucial for better health surveillance of cosmetic products.[10] The French health products safety agency established cosmetovigilance as a component of the pharmacovigilance system for cosmetics.[11] Nowadays, the safety of cosmetic products is considered as public health issue at a global level. Türkiye started a cosmetovigilance regulation system in 2012.[12,13] These guidelines recommend reporting undesirable effects related to cosmetics.[14] In Türkiye, although implementation may be poor, but regulations are harmonized with the EU regulations. Consumers may still experience ACE with cosmetic products.[1,3,14] The number of reported ACEs is relatively low due to self-diagnosis, self-medication, and lack of consultation by the consumers.[1,5,7] Moreover, ACEs are still underreported and miscalculated.[5]

Nurses fulfill many important roles in the provision of cosmetic services.[15] They play a critical role in pharmacovigilance activities and adverse drug events reporting.[16] Cosmetic use and its adverse effects may vary and depend on an employee's background characteristics, including income level, education, informational access, and other factors.[6] Additionally, females are more likely affected due to more use of cosmetics than males.[17,18] It is important to understand the patterns and characteristics of ACEs among all stakeholders, including health professionals. Only one review article highlighted cosmetic safety in the context of the Turkish cosmetovigilance regulation.[14] However, no research on cosmetic use and ACEs has been conducted among the Turkish population or among any group of healthcare professionals (HCPs). Therefore, this study was conducted to assess the use of cosmetics, patterns, and characteristics of ACEs among female nurses in Türkiye.

MATERIALS AND METHODS

Study design and population

A cross-sectional descriptive study was conducted among registered female nurses working in a tertiary care hospital in the Adana Province of Türkiye between February and April 2022. Full-time registered female nurses with at least 1 year of work experience were included in this study. Nursing students on a traineeship and part-time registered nurses who had less than < 1 year of work experience and were unwilling to participate were excluded.

Sample size

According to hospital data, 326 nurses (both male and female) worked in a selected healthcare setting, and 218 of them were female nurses. To determine the appropriate sample size for a proportional or descriptive study, we entered this data into Epi Info™ software (Centers for Disease Control and Prevention, Epi Info™). A minimum of 140 participants were required, taking into account a 50% predicted frequency of the outcome factor ACE in the population, a 95% confidence interval, and a design effect of 1 [*https://www.openepi.com/SampleSize/SSPropor.htm*]. A convenient sampling technique was used, and the sample size was increased to 158 participants to ensure reliability and compensate for any missing data or non-response rate.

Data collection methods and tools

The authors chose some sections of a previously used questionnaire among the general public by Malaysian researchers with their permission.[5] The questionnaire was also adapted and modified from earlier studies on cosmetic usage patterns and adverse events.[1,6,7] The developed questionnaire was translated from English into Turkish (Türkiye's official language) using one-way direct translation rather than back-translation. This approach was used because it reduces time and cost.[5,19] The translations were performed by two competent and experienced researchers who were fluent in both Turkish and English. Minor changes were suggested after the instrument underwent face and content validity testing. The final instrument was then modified as recommended by the experts. A pilot study was conducted with a sample of 20 nurses. The purpose of the pilot study was to assess the study tool's applicability and clarity as well as detect potential issues that might arise during data collection. Minor modifications were made. Following the pilot, the reliability coefficient (Cronbach alpha value: 0.800 and Cronbach alpha based on standardized items: 0.896) was also determined. The pilot sample was excluded from the final study sample. Respondents were able to finish the questionnaire on an average of 5 minutes.

The final questionnaire had 13 questions and three main sections (Supplementary File 1): the first section asked about general demographic data and cosmetic use; the second section addressed ACEs. The final section outlines the consultation types and reporting methods adopted after experiencing ACE. The first section consisted of 5 questions and the

participants' age, working experience, cosmetic use (yes/no), factors considered while purchasing/using cosmetics, and recommendations/advice sources were collected. The second part included 6 questions regarding ACEs (yes/no), frequency, types, symptoms, affected body area, and type of cosmetic product. The final section consisted of 2 questions about the type of consultation adopted (such as medical specialists, pharmacists, general practitioners, beauticians, and others) and the reporting method for ACE. Two trained researchers collected the data prospectively by distributing a Turkish version of the questionnaire. The respondents were informed about the purpose of the study and data confidentiality and informed consent (oral and written) was obtained.

Ethical consideration

The study was approved by the Çukurova University Non-Invasive Clinical Research Ethics Committee (approval number: 119, date: 04.02.2022).

Statistical analysis

The Statistical Package for the Social Sciences (SPSS) version 25 was used to tabulate and analyze the data gathered for this study. Descriptive statistics were used to determine the frequency and percentage of all sections.

RESULTS

In the current study, a total of 158 female nurses were invited to participate. Sixteen (n= 14; 8.8%) were excluded due to less than 1 year of working experience (n= 9; 5.7%) and lack of time (n= 5; 3.1%). A total of 144 nurses were included (response rate of 91.1%). The mean age of nurses was 33.99 years (range 20-64 years), with a standard deviation of 7,870. We found that most younger age participants (20-30 years) reported using cosmetics. Most participants had working experience of 1-5 years (n= 56; 38.9%) followed by 11-15 years (n= 15; 35.4%) (Table 1).

All female nurses reported their use of cosmetics. Most of the participants considered safety and quality (27.1%), expiry date (11.8%), and manufacturer/brand (11.1%) before purchasing or applying cosmetics. Thirty-one (21.5%) respondents also reported a combination of factors, whereas 17.4% of the participants considered nothing before purchasing or using cosmetics. The participants reported that they give importance to advice from friends/relatives (31.3%), cosmetologists (26.4%), and pharmacists (11.8%) when selecting cosmetics (Table 1).

Of the 144 respondents, 26.4% (n= 38) reported having experienced one or more ACEs. Most ACEs were cutaneous (n= 35; 92.1%), followed by systemic and cutaneous (n= 2; 5.3%) and systemic (n= 1: 2.6%). Itching, burning, and eczema were the most frequently observed cutaneous adverse drug reactions (ADRs). Headache was the most common systemic ACE (Table 2).

In this study, messy faces, armpits, hands, neck, scalp, and eye (ocular mucosa) were the most commonly affected body sites by ACEs (Figure 1).

A higher proportion of ACEs were associated with face care products (18.4%), deodorants (13.1%), body care products (10.5%), eye makeup (7.9%), and face makeup (5.2%) (Table 3).

In the current study, more than half (n= 22; 57.9%) of the nurses did not consult with a medical specialist, pharmacist, general practitioner, or beautician. However, 42.1% (n= 16) consulted with professionals regarding ACEs. Medical specialists (15.8%) followed by the pharmacist (7.9%), general practitioners (5.2%), and beauticians (2.6%), were the commonly chosen consultations by participants. A combination of medical specialists and general practitioners (7.9%) and medical specialists and general practitioners and beauticians (2.6%) were also sought for consultation by the participants (Figure 2).

Of them, 38 participants, nearly half (n= 18; 47.4%) did not report the ACEs to the concerned authority. However, 28.9% (n= 11) reported ADR to a hospital, and only 10.5% and 7.9% forwarded the ACE report to the Turkish Pharmacovigilance Centre (TUFAM) and beauty center, respectively (Figure 3).

DISCUSSION

Cosmetovigilance is a developing pharmacovigilance field both globally and in Türkiye. This is the first study in Türkiye to use a self-reported survey to analyze cosmetic use patterns and associated ACEs among female nurses. In this study, all participants reported their cosmetic use (100%). A study conducted in Ethiopia reported that a higher proportion (80.1%) of participants utilized at least one cosmetic item.[6] Additionally, we found that most younger participants reported using cosmetics, which could be attributed to the younger age group's high consumption rate. A similar pattern has also been reported in previous studies.[1,6]

In our study, more than one-fourth of the patients (26.4%) reported the occurrence of ACEs. The proportion was higher than that in a study conducted in Ethiopia (19%).[6] However, a higher rate of ACEs was reported in Malaysia (29.0%),[5] Brazil (38%),[20] and Saudi Arabia (50.6%).[1] The variation may result from differences in the frequency, cosmetic type, duration of the study, and sample, as well as cultural and methodological differences between the study population.

The findings revealed that the skin was the most affected region due to ACEs. These findings were consistent with those of previously published studies conducted in different countries.[3,5,21] In the current study, itching followed by burning, eczema, and redness were the most commonly observed cutaneous ACEs. A similar finding was reported by Lucca et al.[1] and Hadi et al.[5] However, the frequency of redness and eczema were frequently reported in the studies by Lucca et al.[1] and Hadi et al.[5] studies, respectively. Similarly, headache, dizziness, and dyspnea were also observed in our study. These findings also align with previous studies.[1,5] Therefore, climatic differences did not play a role in this matter, as the manifestations of similarities in Türkiye were nearly identical to those found in previous studies conducted in various countries.

The face was the body site most affected by ACEs in this study. Previous studies have documented similar findings.[5,6]

Table 1. Socio-demographic characteristics, cosmetic use, factors, and advice considered by the participants (n= 144)

Variables	Frequency	Percentage
Age		
20-30	60	41.7
31-40	51	35.4
41-50	31	21.5
51-60	1	0.7
More than 61 years	1	0.7
Experience		
1-5 years	56	38.9
6-10 years	13	9
11-15 years	51	35.4
16-20 years	7	4.9
More than 20 years	17	11.8
Cosmetic use		
Yes	144	100
No	0	0
Factors to be considered when purchasing/applying cosmetics		
Safety and quality	39	27.1
Expiration date	17	11.8
Manufacturer/brand	16	11.1
Price	15	10.4
Packaging	1	0.7
Expiration date + manufacturer/ brand	4	2.8
Expiration date + safety and quality	3	2.1
Expiration date + price	3	2.1
Manufacturer/brand + packaging	2	1.4
Expiration date + safety and quality + manufacturer/brand	5	3.5
Safety and quality + manufacturer/ brand + price	1	0.7
Expiration date + safety and quality + price	1	0.7
Expiration date + safety and quality + manufacturer/brand + price + packaging	12	8.3
None	25	17.4
To whom do you give importance when selecting cosmetics?		
Friends/relatives	45	31.3
Cosmetologist	38	26.4
Pharmacist	17	11.8
Beauty center/beautician	16	11.1
Doctor	14	9.7
Pharmacy/pharmacist + doctor	2	1.4

Table 1. Continued

Variables	Frequency	Percentage
To whom do you give importance when selecting cosmetics?		
Cosmetologist + pharmacist	2	1.4
Cosmetologist + doctor	1	0.7
Cosmetologist + beauty center/ beautician	1	0.7
Pharmacist + friends/relatives	1	0.7
Pharmacist + friends/relatives + beauty center/beautician	1	0.7
Cosmetologist + pharmacist + doctor	1	0.7
Cosmetologist + pharmacist + friends/relatives + beauty center/ beautician + doctor	1	0.7
None	4	2.8

Table 2. ACEs and types (n= 38)

Questions	Frequency	Percentage
ACEs experienced		
Yes	38	26.4
No	106	73.6
Number of ACEs (n= 38)		
1	20	52.6
2	14	36.8
3	3	7.9
4	0	0
More than 4	1	2.6
ACE types		
Cutaneous (skin)		
Itching	8	21
Burning	7	18.4
Eczema	2	5.2
Redness	2	5.2
Itching + eczema	6	15.8
Itching + burning	8	21
Itching + burning + eczema	2	5.2
Systemics		
Headache	1	2.6
Cutaneous + systemics		
Itching + burning + nausea + dizziness + shortness of breath	1	2.6
Itching + burning + headache	1	2.6
Total	**38**	**100**

ACEs: Adverse cosmetic events

Table 3. ACEs observed in the cosmetic class (n= 38)

Cosmetic class	Number of observed ACEs	Percentage
Face care products	7	18.4
Deodorants	5	13.1
Body care products	4	10.5
Eye makeup	3	7.9
Face makeup	2	5.2
Hair care products	2	5.2
Cleaning product	2	5.2
Depilatory (hair removal) product	2	5.2
Face care products + face makeup	2	5.2
Face care products + body care products	1	2.6
Face care products + cleaning products	1	2.6
Eye makeup + cleaning product	1	2.6
Hair care products + eye care products	1	2.6
Cleaning product + depilatory (hair removal) product	1	2.6
Body care products + eye makeup + face makeup	1	2.6
Body care products + cleaning products + eye care products	1	2.6
Eye makeup + face makeup depilatory (hair removal) product + after sun products	1	2.6
Face care products + body care products + eye makeup + face makeup + hair care products + cleaning products	1	2.6
Total	**38**	**100**

ACEs: Adverse cosmetic events

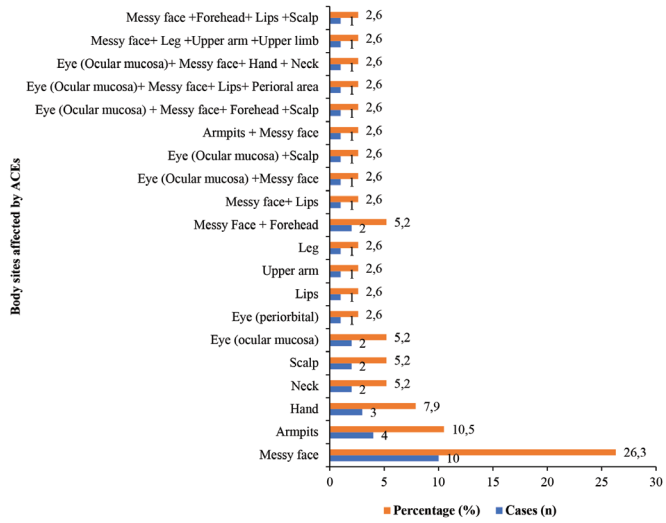

Figure 1. Body sites affected by ACEs (n= 38)
ACEs: Adverse cosmetic events

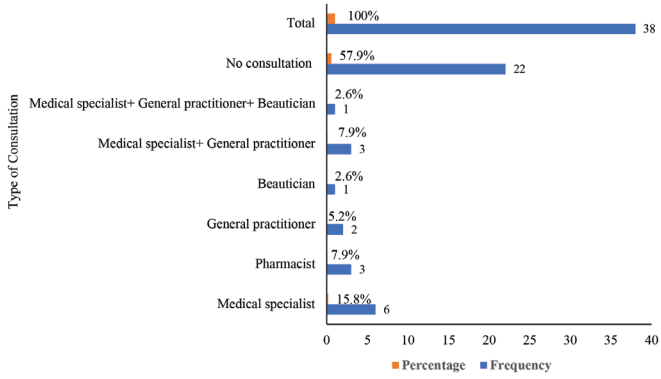

Figure 2. Type of consultation adopted after experiencing ACEs (n= 38)
ACEs: Adverse cosmetic events

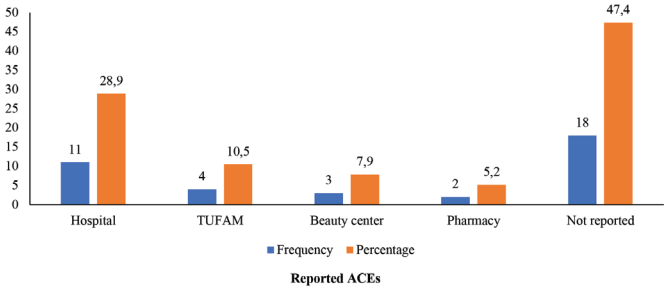

Figure 3. Reporting of ACEs (n= 38)
ACEs: Adverse cosmetic events, TUFAM: Turkish Pharmacovigilance Centre

Furthermore, the findings of this study revealed that a higher proportion of ACEs were related to face care products and deodorants. Similarly, previous studies also reported that the majority of ACEs occur as a result of products intended for use on the face.[1,3,5] According to a Brazilian study, the most common cause of ACEs was soap, shampoo, and deodorants.[20] Another study found that face lotion and hair cosmetics were the most commonly reported causes of ACEs.[6] Additionally, the type of cosmetic product may also have an impact on the adjacent site.[5] It is widely known that these products contain a variety of chemical additives to enhance the functionality, potency, and sustainability of cosmetics.[1,8,22] Exposure to the different chemicals found in cosmetics poses a health risk that can range from a mild hypersensitivity reaction to a lethal intoxication.[23] Moreover, misbranded and spurious cosmetics are common.[1,23]

In the current study, > 50% (57.9%) of the respondents did not receive any consultation after experiencing ACEs. A similar finding was also reported in a Malaysian study.[5] The number of nurses who attempted to consult HCPs: medical

practitioners, pharmacists, and general practitioners) was 29.9% in our study. The small number of respondents who sought consultation indicated that they were misjudging the occurrence of ACEs. Studies have revealed that consumers underreported ACEs even though they may have suffered severe harm in some cases.[3,5,21,24] Prior studies have highlighted the possibility of more serious reactions involving internal body systems, such as cancer.[25,26] Previous studies have also recommended the identification of cosmetics' harmful ingredients to avoid harmful effects and protect consumers.[26,27] Therefore, it is suggested that manufacturers conduct a safety evaluation of their products before they are marketed.[3,5,28,29] Furthermore, dermatologists and primary care physicians are reported to be the first points of contact for the general public with skin complaints.[1] A pharmacist's role in public engagement is well documented.[30] Therefore, there is a need for effective communication, counseling sessions, and education among cosmetic consumers and HCPs to avoid the potential risk of ACEs.

In this study, we also observed that despite experiencing ACEs due to cosmetic use, most participants (47.4%) did not report such events to the healthcare authority. Globally, the reported number of ACEs is extremely low.[31,32] The under-reporting of ACEs has also been highlighted in the literature.[3,5,33,34] Additionally, the absence of formal and trustworthy monitoring systems (referred to as "cosmetovigilance") may also contribute to the underestimation of such harmful effects and under-reporting.[34] The US Food and Drug Administration launched a "MedWatch Online Voluntary Reporting Form" for cosmetic-related complaints and adverse reactions.[35] Türkiye initiated the cosmetovigilance program under the pharmacovigilance system in 2012.[12,13] The Turkish Medicines and Medical Devices Agency developed an online form for consumers, patients, and HCPs to report cosmetic-related undesirable effects.[36] However, our study reported low reporting rates of cosmetic ADRs in Türkiye as well as previously reported in a global context.[3,10,25,34] Therefore, to address a lower reporting rate, awareness-raising campaigns and the promotion of cosmetovigilance among cosmetic users, retailers, HCPs, and other stakeholders are needed.

Study limitations

This study has some limitations. First, the current study utilized a self-reported questionnaire to gather information on cosmetic use and associated ACEs. As a result, there is a chance of recall bias, which may lead to underestimation. Second, this study did not include participants' medical illness or medication history. Similarly, some of the ACEs reported by the participants may not have been caused by cosmetics. It could have been evaluated using proper further causality analysis studies, which were not possible in our study scope. Third, the current findings may not be generalizable, especially because our study was based on a sample of female nurses recruited from a single hospital in Türkiye. Further research with larger samples and validated scales is required to confirm our findings, as the findings among female nurses may not be representative of all practices across the country.

Despite these limitations, this study has some strengths. This is the first study to assess the cosmetic use, pattern, and characteristics of ACEs among female nurses in our healthcare setting as well as in Türkiye. Socio-cultural factors also have a significant impact, which varies from country to country. Furthermore, this study provides baseline local data, and the findings may be useful for cosmetic users, clinical practitioners, HCPs, and policymakers.

CONCLUSION

A considerable proportion of the participants reported ACEs. The most commonly affected skin area was the face, and itching, followed by burning, and eczema were frequently reported ACEs. Most respondents did not receive any consultation from qualified HCPs after experiencing ACEs. The underreporting of ACEs was also highlighted in this study. Cosmetovigilance is a new model of cosmetic safety monitoring that can be considered a major component of public health activities. Therefore, some measures to strengthen the implementation of cosmetovigilance include the distribution of informational leaflets, awareness sessions, media campaigns, and the offering of direct information facilities to consumers and HCPs. Similarly, prompt detection and management of ACEs may enhance the financial aspects of therapeutic efficacy. Furthermore, in the future, a nationwide prospective prevalence study based on causality analyses should be conducted in different populations to further validate existing data and strengthen the cosmetovigilance system in Türkiye as well as globally.

Ethics

Ethics Committee Approval: The study was approved by the Çukurova University Non-Invasive Clinical Research Ethics Committee (approval number: 119, date: 04.02.2022).

Informed Consent: The respondents were informed about the purpose of the study and data confidentiality, and informed consent (oral and written) on their willingness to participate in the study was obtained.

Authorship Contributions

Concept: Z.K., Y.K., G.P., Design: Z.K., Y.K., G.P., Data Collection or Processing: Z.K., Y.K., G.P., Analysis or Interpretation: Z.K., Y.K., G.P., A.N.Ç.G., H.R., F.U.K., O.K., Literature Search: Z.K., Y.K., G.P., A.N.Ç.G., H.R., F.U.K., O.K., Writing: Z.K., Y.K., G.P.

Conflict of Interest: No conflict of interest was declared by the authors.

Financial Disclosure: The authors declared that this study received no financial support.

REFERENCES

1. Lucca JM, Joseph R, Hussain Al Kubaish Z, Mohammad Al-Maskeen S, Ali Alokaili Z. An observational study on adverse reactions of cosmetics: The need of practice the Cosmetovigilance system. Saudi Pharm J. 2020;28:746-753.

2. United States Food and Drug Administration (FDA). What is a cosmetic? 2021 [cited on December 10, 2022]. Available from: https://www.fda.gov/industry/importing-fda-regulated-products/importing-cosmetics#cosmetic
3. Toklu HZ, Antigua A, Lewis V, Reynolds M, Jones J. Cosmetovigilance: A review of the current literature. J Family Med Prim Care. 2019;8:1540-1545.
4. Turkish Medicines and Medical Devices Agency. Cosmetics law. 2005 [cited on December 10, 2022]. Available from: https://www.resmigazete.gov.tr/eskiler/2005/03/20050330-1.htm
5. Hadi H, Ai N, Zamli M, Awadh AI, Zafar MZ, Jamshed S. Cosmetic use-related adverse events: findings from lay public in Malaysia. Cosmetics. 2020;7:41.
6. Getachew M, Tewelde T. Cosmetic use and its adverse events among female employees of Jimma University, Southwest Ethiopia. Ethiop J Health Sci. 2018;28:717-724.
7. Husain K. A survey on usage of personal care products especially cosmetics among university students in Saudi Arabia. J Cosmet Dermatol. 2019;18:271-277.
8. Alani JI, Davis MD, Yiannias JA. Allergy to cosmetics: a literature review. Dermatitis. 2013;24:283-290.
9. Draelos ZD. Cosmetics: the medicine of beauty. J Cosmet Dermatol. 2015;14:91.
10. Vigan M, Castelain F. Cosmetovigilance: Definition, regulation and use "in practice". Eur J Dermatol. 2014;24:643-649.
11. Tissier MH, Lepagnol F. Cosmetovigilance: a French pharmacovigilance system for cosmetics developed by the French health products safety agency. A proposal for the future. Therapie. 2002;57:273-282.
12. Köse Ö, Sabuncuoğlu S, Erkekoğlu P, Koçer-Gümüşel B. Cosmetovigilance: Current status in Europe and Türkiye, its practices and cosmetovigilance surveys. FABAD J Pharm Sci. 2018;43:79-90.
13. Guidelines for notification of the undesirable effects/serious undesirable effects of cosmetic products to the institution. 2012 [cited on December 25, 2022]. Available from: https://www.titck.gov.tr/PortalAdmin/Uploads/UnitPageAttachment/U7mT8sjY.pdf
14. Altıokka İ, Üner M. Safety in cosmetics and cosmetovigilance, current regulations in Türkiye. Turk J Pharm Sci. 2022;19:610-617.
15. The dermatology nurses' association. The nurse's role in the provision of cosmetic services. J Dermatol Nurses' Assoc. 2013;5:288.
16. Salehi T, Seyedfatemi N, Mirzaee MS, Maleki M, Mardani A. Nurses' knowledge, attitudes, and practice in relation to pharmacovigilance and adverse drug reaction reporting: a systematic review. Biomed Res Int. 2021;2021:6630404.
17. Mafra AL, Silva CSA, Varella MAC, Valentova JV. The contrasting effects of body image and self-esteem in the makeup usage. PLoS One. 2022;17:e0265197.
18. Stefania C, Luca P, Rosa D, Rosanna M. Cosmetics, chemical exposure and gender differences. Ital J Gender-Specific Med. 2018;4:21-26.
19. Sportiello L, Cammarota S, de Portu S, Sautebin L. Notification of undesirable effects of cosmetics and toiletries. Pharmacol Res. 2009;59:101-106.
20. Huf G, Rito Pda N, Presgrave Rde F, Boas MH. Adverse reactions to cosmetic products and the Notification System in Health Surveillance: a survey. Rev Bras Epidemiol. 2013;16:1017-1020.
21. Salverda JG, Bragt PJ, de Wit-Bos L, Rustemeyer T, Coenraads PJ, Tupker RA, Kunkeler LC, Laheij-de Boer AM, Stenveld HJ, van Ginkel CJ, Kooi MW, Bourgeois FC, van Gorcum TF, van Engelen JG, van Dijk R, de Graaf J, Donker GA, de Heer C, Bruynzeel D. Results of a cosmetovigilance survey in The Netherlands. Contact Dermatitis. 2013;68:139-148.
22. Juhász ML, Marmur ES. A review of selected chemical additives in cosmetic products. Dermatol Ther. 2014;27:317-322.
23. Bilal M, Iqbal HMN. An insight into toxicity and human-health-related adverse consequences of cosmeceuticals-a review. Sci Total Environ. 2019;670:555-568.
24. Nayak M, Ligade VS, Prabhu SS. Awareness level regarding adverse reactions caused by cosmetic products among female patients: A cross-sectional study. J Cosmet Dermatol. 2023;22:2512-2519.
25. Sautebin L. Understanding the adverse effects of cosmetics: a pilot project in cosmetovigilance. Drug Saf. 2008;31:433-436.
26. Jacob SL, Cornell E, Kwa M, Funk WE, Xu S. Cosmetics and cancer: adverse event reports submitted to the Food and Drug Administration. JNCI Cancer Spectr. 2018;2:pky012.
27. Franken L, de Groot A, Laheij-de Boer AM. Allergic contact dermatitis caused by menthoxypropanediol in a lip cosmetic. Contact Dermatitis. 2013;69:377-378.
28. Ross G. A perspective on the safety of cosmetic products: a position paper of the American Council on Science and Health. Int J Toxicol. 2006;25:269-277.
29. Pauwels M, Rogiers V. Safety evaluation of cosmetics in the EU. Reality and challenges for the toxicologist. Toxicol Lett. 2004;151:7-17.
30. Ashique KT, Chandrasekhar D. Role of clinical pharmacist in cosmeto-vigilance of misuse and abuse of topical corticosteroids. Indian J Dermatol. 2017;62:213.
31. Di Giovanni C, Arcoraci V, Gambardella L, Sautebin L. Cosmetovigilance survey: are cosmetics considered safe by consumers? Pharmacol Res. 2006;53:16-21.
32. Nayak M, Sreedhar D, Prabhu SS, Ligade VS. Global trends in cosmetics use-related adverse effects: a bibliometric analysis of literature published during 1957-2021. Cosmetics. 2021;8:75.
33. Kwa M, Welty LJ, Xu S. Adverse events reported to the US Food and Drug Administration for cosmetics and personal care products. JAMA Intern Med. 2017;177:1202-1204.
34. Bilal AI, Tilahun Z, Osman ED, Mulugeta A, Shekabdulahi M, Berhe DF. Cosmetics use-related adverse events and determinants among Jigjiga Town Residents, Eastern Ethiopia. Dermatol Ther (Heidelb). 2017;7:143-153.
35. The United States Food and Drug administration (FDA). How to report a cosmetic related complaint. 2022. Available from: https://www.fda.gov/cosmetics/cosmetics-compliance-enforcement/how-report-cosmetic-related-complaint
36. Turkish Medicines and Medical Devices Agency. Cosmetic undesirable effect. Available from: https://utsuygulama.saglik.gov.tr/UTS/

Supplementary File 1. English and Turkish version questionnaires

The usage of cosmetics and adverse drug reactions among female nurses in a tertiary care hospital

We want to conduct a survey to evaluate female nurses' knowledge of the adverse effects of cosmetics. Identity information of the participants of the study is not required. The results will only be used in the scientific field.

Do you want to participate in the study?

☐ Yes
☐ No

Section 1: General demographic information and cosmetic use.

Age: .....

Work experience

☐ 1-5 years
☐ 6-10 years
☐ 11-15 years
☐ 15-20 years
☐ 20+

Have you used cosmetics?

☐ Yes
☐ No

What factors do you consider when purchasing/applying cosmetics?

☐ Safety and Quality
☐ Expiration date
☐ Packaging
☐ Manufacturer/brand
☐ Price
☐ None
☐ Others: .....

Whose advice do you give importance when selecting a cosmetic product?

☐ Cosmetologist
☐ Friend-relative
☐ Pharmacy/Pharmacist
☐ Beauty Center/Beautician
☐ Doctor
☐ None
☐ Others: .....

Section 2: Adverse cosmetic reactions.

Have you experienced adverse effects due to cosmetics use?

☐ Yes
☐ No

If the answer is yes, how many cosmetic adverse events have you experienced?

☐ 1
☐ 2
☐ 3
☐ 4
☐ 4+

What type of cosmetic adverse events have you encountered?

☐ Skin
☐ Systemic
☐ Others: .....

What were the symptoms of the adverse cosmetic events you experienced?

☐ Itching
☐ Burning
☐ Eczema
☐ Headache
☐ Nausea
☐ Dizziness
☐ Shortness of breath
☐ Others: .....

Which body area was affected by adverse cosmetic events?

☐ Armpits
☐ Eye (ocular mucosa)
☐ Eye (periorbital)
☐ Messy face
☐ The front part of the arm
☐ Forehead
☐ Groin
☐ Hand
☐ Heart
☐ Leg
☐ Lips
☐ Mammary gland
☐ Neck
☐ Perioral area
☐ Scalp diffuse

☐ Thigh
☐ Thorax
☐ Upper arm
☐ Upper limb
☐ Others: .....

Section 3: Type of consultation and reporting method adopted after experiencing adverse drug reaction.

What type of counseling did you receive after adverse cosmetic events?
☐ Medical specialist
☐ General practitioner
☐ Pharmacist
☐ General practitioner and medical specialist
☐ Pharmacist and medical specialist
☐ Beautician
☐ None
☐ Other: .....

Where do you report the cosmetic adverse event?
☐ TUFAM (Turkish Pharmacovigilance Centre)
☐ Hospital
☐ Pharmacy
☐ Beauty center
☐ Not reported
☐ Others: .....

Thank you so much for your time and participation.

Üçüncü basamak bir hastanede kadın hemşirelerin kozmetik kullanımı ve advers ilaç reaksiyonları

Kadın hemşirelerin, kozmetiklerin advers etkileri konusunda bilgilerini değerlendirmek amacıyla bir anket yapıyoruz. Çalışmaya katılanların kimlik bilgisi istenmemektedir. Sonuçlar sadece bilimsel alanda kullanılacaktır.

Çalışmaya katılmak istiyor musunuz?

☐ Evet
☐ Hayır

Bölüm 1: Genel demografik bilgiler ve kozmetik kullanımı.

Yaşınız: .....

Çalışma deneyimi

☐ 1-5 yıl
☐ 6-10 yıl
☐ 11-15 yıl
☐ 15-20 yıl
☐ 20+

Kozmetik kullandınız mı?

☐ Evet
☐ Hayır

Kozmetik alırken/yaptırırken hangi faktörlere dikkat edersiniz?

☐ Güvenlik ve Kalite
☐ Son kullanma tarihi
☐ Ambalaj
☐ Üretici/marka
☐ Fiyat
☐ Hiçbiri
☐ Diğer: .....

Kozmetik ürün seçerken kimin tavsiyesine önem verirsiniz?

☐ Kozmetik Uzmanı
☐ Arkadaş-akraba
☐ Eczane/Eczacı
☐ Güzellik Merkezi/Güzellik Uzmanı
☐ Doktor
☐ Hiçbiri
☐ Diğer: .....

Bölüm 2: Advers kozmetik reaksiyonlar.

Kozmetik kullanırken advers etkiye maruz kaldınız mı?

☐ Evet
☐ Hayır

Cevap evet ise, kaç tane kozmetik advers olay yaşadınız?

☐ 1
☐ 2
☐ 3
☐ 4
☐ 4›

Hangi tip kozmetik advers olayla karşılaştınız?

☐ Deri
☐ Sistemik
☐ Diğer: .....

Yaşadığınız Adverse kozmetik olayların belirtileri nelerdi?

☐ Kaşıntı
☐ Yanma
☐ Egzema
☐ Baş ağrısı
☐ Mide bulantısı
☐ Baş dönmesi
☐ Nefes darlığı
☐ Diğer: .....

Advers kozmetik olaylardan hangi vücut bölgesi etkilendi?

☐ Koltuk altı
☐ Göz (oküler mukoza)
☐ Göz (periorbital)
☐ Yüz dağınık
☐ Kolun ön kısmı
☐ Alın
☐ Kasık
☐ El
☐ Kalp
☐ Bacak
☐ Dudaklar
☐ Meme bezi
☐ Boyun
☐ Perioral alan
☐ Saç derisi diffüz

☐ Uyluk
☐ Toraks
☐ Üst kol
☐ Üst uzuv
☐ Diğer: .....

Advers kozmetik olaylara hangi kozmetik sınıfı neden olmuştur?

☐ Güneş sonrası ürünler
☐ Vücut bakım ürünleri
☐ Temizlik ürünleri
☐ Deodorantlar
☐ Tüy dökücü ürünler
☐ Göz bakım ürünleri (göz çevresi krem)
☐ Göz makyajı
☐ Yüz bakım ürünleri
☐ Yüz makyajı
☐ Saç bakım ürünleri
☐ Parfüm ve kokular
☐ Güneş kremleri
☐ Diş macunları
☐ Diğer: .....

Bölüm 3: Advers kozmetik olaylar deneyiminden sonra danışma türü ve raporlama yöntemi.

Advers kozmetik olaylardan sonra kime danışırsınız?

☐ Tıbbi uzman
☐ Pratisyen
☐ Eczacı
☐ Genel pratisyen ve Tıbbi uzman
☐ Eczacı ve tıp uzmanı
☐ Güzellik uzmanı
☐ Hiçbiri
☐ Diğer: .....

Advers kozmetik olayı nereye bildirirsiniz?

☐ TUFAM (Türk Farmakovijilans Merkezi)
☐ Hastane
☐ Eczane
☐ Güzellik merkezi
☐ Bildirmem
☐ Diğer: .....

İlginize teşekkür ederiz.

Turk J Pharm Sci 2024;21(4):297-302
DOI: 10.4274/tjps.galenos.2023.92645

ORIGINAL ARTICLE

A High-Dose Corticosteroid Treatment Increases Coronavirus Disease of 2019 Mortality in Intensive Care Units

İsmail DEMİR[1]*, İsmail YILMAZ[2], Hüseyin YILMAZ[2], Hüseyin ÖZKARAKAŞ[3], Şebnem ÇALIK[4]

[1]University of Health Sciences Türkiye, Bozyaka Training and Research Hospital, Clinic of Internal Medicine, İzmir, Türkiye
[2]İzmir Kâtip Çelebi University Faculty of Medicine, Department of Pharmacology and Toxicology, İzmir, Türkiye
[3]University of Health Sciences Türkiye, Bozyaka Training and Research Hospital, Department of Anesthesiology, İzmir, Türkiye
[4]University of Health Sciences Türkiye, Bozyaka Training and Research Hospital, Clinic of Infectious Diseases and Clinical Microbiology, İzmir, Türkiye

ABSTRACT

Objectives: The study is aimed to investigate the association between different corticosteroid treatment regimens and clinical status, complications, mechanical ventilation requirement, and intensive care unit (ICU) mortality in individuals diagnosed with Coronavirus Disease of 2019 (COVID-19).

Materials and Methods: This is a descriptive retrospective study. Patients admitted to the ICU for COVID-19 and treated with low- or medium-dose corticosteroid therapy (methylprednisolone at a dose of 0.5-1 mg/kg for 7-10 days) were compared with patients treated with high-dose pulse corticosteroid therapy (methylprednisolone at varying doses of 250 mg, 500 mg or 1000 mg for 3-7 days) in addition to standard therapy because of increased pulmonary infiltrate and elevated inflammatory markers during clinical monitoring. All demographic and clinical data, including age, sex, clinical course, laboratory findings, discharge status, 28-day mortality, intubation status, acute physiological assessment and chronic health evaluation II score, Charlson Comorbidity Index, and sequential organ failure assessment score, were recorded.

Results: Corticosteroid treatment was administered to 689 (88.3%) of 780 COVID-19 ICU patients between April 2020 and October 2021. The overall mortality rate was 45.1% (n= 352). When the mortality rates of patients were compared according to the corticosteroid dose, the mortality rate in the low-to-medium-dose group (40%) was significantly lower than that in the high-dose group (76%). In addition, significant deterioration in laboratory and clinical parameters was observed in the high-dose corticosteroid group.

Conclusion: High mortality, adverse effects, and complications were significantly increased when high-dose corticosteroids were administered. Corticosteroid therapy should be used cautiously according to the patient's clinical condition, disease stage, comorbidities, and systemic or organ reserves.

Keywords: COVID-19, intensive care unit, corticosteroid treatment, mortality

INTRODUCTION

Severe Acute Respiratory Syndrome Coronavirus 2 (SARS-CoV-2) was declared a pandemic by the World Health Organization (WHO) on January 11, 2020, because of its rapid global spread following the identification of acute respiratory distress syndrome (ARDS) and pneumonia in China. Approximately 80-85% of patients are asymptomatic or present with mild upper respiratory symptoms, whereas approximately 20% present with severe clinical symptoms.[1] In addition, severe pneumonia and respiratory failure may occur in 2-5% of patients. Elevated laboratory parameters, such as D-dimer, fibrinogen, and C-reactive protein (CRP), suggest that the thrombo-inflammatory mechanism plays an active role. An intense cytokine storm with immunological and pathological mechanisms is observed in patients with a severe clinical course. The intense inflammatory process in the clinic leads to pneumonia, ARDS, respiratory failure, and hospitalization in

*Correspondence: driyilmaz@yahoo.com, Phone: +90 532 285 95 82, ORCID-ID: orcid.org/0000-0001-7787-1443
Received: 12.06.2023, Accepted: 18.08.2023

about 2-9% of cases and may even require intensive care unit (ICU) and mechanical ventilation.[2]

However, aspects of the immunopathology and management of SARS-CoV-2 infection remain unresolved. Many treatment protocols are in the research phase due to uncertainty regarding the treatment of severe respiratory failure. Molnupiravir, hydroxychloroquine, favipiravir, anticoagulant therapy, and antibiotic treatment are used in the initial treatment of the disease. As the clinical course worsens, plasma, immunoglobulin, immunomodulator, tocilizumab, interleukin antibody, and steroid treatments are used as advanced treatments. Despite the intensive use of hydroxychloroquine, favipiravir, lopinavir, redeliver, ritonavir, and interferon-beta, there are many controversial studies on the effectiveness of these drugs in mortality and even the efficacy of treatment.[3] Although molnupravir reduces mortality, more clinical studies are needed to prove that.[4]

Regarding the use of steroids in patients with Coronavirus Disease of 2019 (COVID-19) and SARS-CoV-2 infection, steroid treatment is not recommended if the patient does not have hypoxemia.[5] However, if hypoxemia is present, steroids are used extensively to prevent thrombo-inflammation and to reduce and suppress the severity of the cytokine storm in pneumonia and ARDS. Three stages of SARS-CoV-2 disease have been defined based on clinical and laboratory findings. In stage-1, there is no lung or specific organ involvement in the viral response phase, in stage-2, there are pulmonary infiltrates in the lung in the pulmonary phase (in stage 2A, there is no hypoxemia, while in stage 2B, the oxygen saturation is below 96 and hypoxemia is observed), and in Stage-3, there is a hyperinflammatory stage where the lung involvement is intense (> 50%). Although antiviral treatment is recommended in Stage-1 and Stage-2A, it is thought that anti-inflammatory treatments (such as corticosteroids, interleukin antibody treatments, and cytokine adsorption therapy) may be more effective because of the hyperinflammation in Stage-2B and Stage-3.[6] Corticosteroids have both stimulatory and suppressive effects on the immune system, especially at high doses, depending on the duration of use and blood levels.[7] These drugs suppress inflammation and limit the effects of inflammatory cytokines and chemokine when a hyperinflammatory state develops in COVID-19.[8] The corticosteroid treatment protocols used in the trials are quite different. It still needs to be determined the appropriate dose for the therapeutic efficacy of corticosteroids in patients with COVID-19, and the use of different steroid molecules may produce different results. In patients with respiratory distress, severe lung involvement, and life-threatening organ failure, low doses of 1 mg/kg and high doses of 250 mg, 500 mg, or 1000 mg of methylprednisolone are recommended, depending on the patient's clinical assessment.[9] In the COVID-19 treatment guideline from the Turkish health authority, it was emphasized that low-to-medium-dose methylprednisolone could be started at 0.5-1 mg/kg in Stage-2B and Stage-3 patients, and then the dose can be gradually reduced over 7-10 days. In addition, the section in the guideline focusing on the treatment of severe pneumonia, ARDS, septic shock, and sepsis, recommends considering pulse methylprednisolone administration at a dosage of at least 250 mg per day for a period of 3-7 days. This treatment option may be considered for patients who experience a deterioration in their clinical status within 24 to 48 hours or demonstrate an increase in oxygen requirements despite receiving low-dose corticosteroid therapy. It has been suggested that after high-dose corticosteroid therapy, the dose may be tapered in patients with clinical worsening or high acute phase reactants.[10]

The aim of this study was to evaluate the relationship between the corticosteroid treatment protocols used in the COVID-19 ICU and the patient's clinical status, corticosteroid dose, complications, need for mechanical ventilation, and mortality.

MATERIALS AND METHODS

This clinical study is a descriptive retrospective study. The study population consisted of individuals diagnosed with COVID-19 who were admitted to our tertiary care hospital's COVID-19 ICU. The principles of the Declaration of Helsinki were followed in all the study phases. This study was approved by the Clinical Research Ethics Committee of University of Health Sciences Türkiye, Bozyaka Training and Research Hospital after obtaining permission from the Ministry of Health COVID-19 Scientific Research and Evaluation Commission (protocol number: 21.05.2020-222). The data were collected from April 2020 to October 2021 and included patients receiving corticosteroid treatment.

In the COVID-19 ICU, patients were treated with corticosteroids according to ethical treatment principles, considering vital signs, laboratory values, comorbidities, resorptive organ capacity, and the adverse effects of corticosteroids. In patients with ARDS, diffuse lung infiltrates, elevated clinical and imaging lung infiltrates, and elevated inflammatory markers, pulmonary steroid therapy was incorporated as an adjunct to the standard treatment protocol. According to the COVID-19 treatment guideline prepared by the health authority of our country, low-to-medium-dose methylprednisolone was started at 0.5-1 mg/kg and gradually decreased over 7-10 days. High-dose methylprednisolone was administered at 250 mg, 500 mg, or 1000 mg/day for 3-7 days to patients whose clinical condition worsened within 24-48 hours or whose oxygen requirements increased despite low-dose corticosteroid therapy. The dose was then tapered over 3-7 days.

The data collected for these patients encompassed a wide range of parameters (including age, sex, oxygen saturation levels, intubation status, clinical recovery, discharge status, length of stay, mortality, hemogram values, and selected laboratory values, such as glucose, urea, creatinine, alanine transaminase, aspartate aminotransferase, total bilirubin, creatine kinase, lactate dehydrogenase, D-dimer, and fibrinogen). Additionally, prothrombin time, activated prothrombin time, activated partial thromboplastin time, international normalized ratio, CRP, ferritin, procalcitonin (PCT), arterial blood gas values, sequential organ failure assessment (SOFA), acute physiological assessment and

chronic health evaluation (APACHE) II scores were included in the data collection process.

Statistical analysis

The normality of data distribution was determined using the Kolmogorov-Smirnov test or the Shapiro-Wilk test. Normally distributed variables are expressed as means ± standard deviations, whereas categorical variables are expressed as frequencies (n) and percentages. Variables that were not normally distributed were defined using median and interquartile range. Two group comparisons were performed by using independent Student's t-test or Mann-Whitney U test, where appropriate. Fisher's exact chi-square test or Pearson's chi-square test was used to compare categorical variables. *p* values below 0.05 were considered indicative of statistical significance.

RESULTS

After 18 months of clinical observation in the COVID-19 ICU between April 2020 and October 2021, data from 780 patients were analyzed. Of the 780 patients, 91 did not receive steroid therapy due to contraindications (gastrointestinal bleeding, hyperglycemic coma, severe acid-base electrolyte disturbances, and those receiving corticosteroid immunosuppressive therapy). Patients were 429 (55%) male and 351 (45%) female. The number of patients who received corticosteroid therapy was 689 (88.3%). The mortality rate was 45.1% (n= 352). The mortality rate was 64.9% in men (n= 229) and 35.1% in females (n= 123). The number of patients younger than 65 years was 359 (46.0%), and the number of patients 65 years and older was 421 (54.0%). Among patients younger than 65 years old, the mortality rate was 52.7% (n= 185), whereas for patients 65 years and older, the mortality rate was 47.3% (n= 167).

The mean age was 63 ± 9 years in the low-medium-dose corticosteroid group and 64 ± 12 years in the high-dose corticosteroid group. The male/female was 285 (50.6%)/278 (49.4%) in the low-medium-dose group and 53 (42.1%)/73 (59.9%) in the high-dose group. The Charlson Comorbidity Index of the groups was 10 ± 3 in the low-to-medium-dose group and 11 ± 4 in the high-dose group. There are no statistically significant differences between the two groups regarding these parameters ($p > 0.05$).

The effect of the corticosteroid treatment dose (high and low-medium-doses) given to patients with COVID-19 in the ICU on mortality and intubation of the patients is shown in Table 1.

The effects of the dose (high and low-medium-doses) on laboratory parameters, SOFA score, APACHE II score, and length of stay in COVID-19 patients receiving corticosteorid therapy in the ICU are presented in Table 2.

DISCUSSION

The aim of using corticosteroids in SARS-CoV-2 infection was to reduce pulmonary inflammation, suppress destructive inflammation, and reduce fibrosis. However, factors such as corticosteroid-related adverse effects, reversible metabolic and organ failure, complications such as hyperglycemia and gastrointestinal bleeding, and the fact that the real benefit of corticosteroids on survival is controversial limit the use of corticosteroids.[11] The WHO Rapid Evidence Appraisal for COVID-19 Therapies trial found that systemic steroids reduced 28-day mortality from all causes compared with standard care or placebo in COVID-19 disease.[12] Many studies have compared their effectiveness against COVID-19. A retrospective analysis was conducted on 200 patients diagnosed with ARDS to compare the effectiveness of different treatments for COVID-19. The study found that patients receiving methylprednisolone had a lower mortality rate than those receiving other treatments.[13] In a study conducted in Pakistan, there was no difference in ICU and ventilator use and mortality between the two groups of patients receiving dexamethasone (n= 35) or methylprednisolone (n= 65) in the intermediate ICU. Simultaneously, no statistically significant difference was observed in adverse effects.[14] The literature on corticosteroid treatment has revealed no difference in efficacy after administering equivalent doses of corticosteroid. Our study used methylprednisolone, which is readily available in our hospital. Low-dose (0.5 mg/kg) or medium-dose (1 mg/kg) methylprednisolone was administered

Table 1. Effect of dose on mortality and intubation among patients with COVID-19 receiving corticosteroid treatment in the ICU

	Corticosteroid therapy dose		Total (n%)	*p* value	χ^2
	Low-medium dose (n%)	High dose (n%)			
Mortality					
Yes	225 (40)	96 (76)	321 (46.6)	< 0.0001	54.2
No	338 (60)	30 (24)	368 (53.4)		
Total	563 (81.7)	126 (18.3)	689		
Intubation					
Yes	304 (54)	98 (78)	402 (64.4)	< 0.0001	24.0
No	259 (46)	28 (22)	287 (35.6)		
Total	563 (81.7)	126 (18.3)	689		

Pearson's chi-squared analysis was used and $p < 0.05$ was considered significant, ICU: Intensive care unit, COVID-19: Coronavirus disease 2019

Table 2. Effect of dose on laboratory parameters, SOFA score, APACHE II score and length of stay among patients with COVID-19 receiving corticosteroid treatment in the ICU

	Corticosteroid therapy dose		
Parameters	**High dose**	**Low-medium dose**	***p* value**
Hemoglobin	9.7 ± 2.2	11.7 ± 1.7	$p < 0.0001$
Leukocyte*	9550 ± 5900	8600 ± 5300	$p = 0.075$
Thrombocyte*	211000 ± 153000	209000 ± 140000	$p = 0.887$
Glucose*	109.2 ± 79.2	82.2 ± 33.6	$p < 0.0001$
Urea*	41.4 ± 33.9	37.3 ± 22.1	$p = 0.092$
Creatinine*	3.2 ± 0.9	1.6 ± 0.7	$p < 0.0001$
ALT*	44.6 ± 36.4	42.2 ± 25.5	$p = 0.369$
AST*	70.4 ± 20.5	67.7 ± 21.0	$p = 0.177$
Bilirubin-total*	4.0 ± 3.9	1.6 ± 1.2	$p < 0.0001$
CK*	641.0 ± 766.1	185.5 ± 32.1	$p < 0.0001$
LDH*	111.9 ± 48.8	108.2 ± 51.1	$p = 0.459$
D-dimer*	1425.5 ± 658.2	616.2 ± 582.2	$p < 0.0001$
Fibrinogen	990.2 ± 298.3	602.3 ± 198.7	$p < 0.0001$
PT*	13.6 ± 15.4	9.9 ± 10.1	$p < 0.0002$
aPTT	38.6 ± 15.2	29.7 ± 4.3	$p < 0.0001$
INR*	2.4 ± 2.7	1.6 ± 3.2	$p = 0.048$
CRP**	410.2 ± 111.3	291.1 ± 12.3	$p < 0.0001$
Ferritin*	446.5 ± 389.7	212.4 ± 297.7	$p < 0.0001$
PCT*	41.3 ± 9.2	32.9 ± 4.5	$p < 0.0001$
SOFA score	13.2 ± 2.6	8.5 ± 1.6	$p < 0.0001$
APACHE II score	21.2 ± 3.3	16.1 ± 2.3	$p < 0.0001$
Length of stay*	11.4 ± 6.0	7.7 ± 5.9	$p < 0.0001$

Independent t-test was used and $p < 0.05$ was considered significant. *Mann-Whitney U test was used, ** Pearson's chi-square test was used, SOFA: Sequential organ failure assessment, APACHE: Acute physiological assessment and chronic health evaluation, COVID-19: Coronavirus disease 2019, ALT: Alanine transaminase, AST: Aspartate aminotransferase, CK: Creatine kinase, LDH: Lactate dehydrogenase, PT: Prothrombin time, aPTT: Activated partial thromboplastin time, INR: International normalized ratio, CRP: C-reactive protein, PCT: Procalcitonin

to patients in the mild and moderate clinics. During clinical observation, the weekly dose was reduced in patients who received corticosteroids for 7 or 10 days and showed clinical improvement. High-dose methylprednisolone (250, 500, and 1000 mg/day was given for 3-7 days, after which the weekly dose was gradually reduced in patients with clinical worsening within 24 or 48 hours.

The randomized evaluation of COVID-19 therapies trial, a significant multicenter randomized controlled trial, was conducted in the United Kingdom to assess the efficacy of corticosteroids in patients diagnosed with COVID-19. This trial was designed to compare mortality rates between the corticosteroid-treated groups and the standard care groups and to evaluate the effectiveness of other potential treatments, such as hydroxychloroquine, favipiravir, and lopinavir/ritonavir, in patients hospitalized for COVID-19. In the corticosteroid group, patients received oral or intravenous dexamethasone at a dose of 6 mg daily until discharge after 10 days of clinical observation. The primary outcomes examined in this study were 28-day mortality, clinical improvement, and the need for mechanical ventilation. Results from the study revealed a mortality rate of 22.9% in the group receiving dexamethasone (n= 2104) compared with 25.7% in the standard care group (n= 4321).[15] A single-center retrospective study by Fernández-Cruz et al.[16] no significant difference in survival and mortality was observed between patients with COVID-19 pneumonia treated with steroids and those treated with high-dose pulse steroids or 1 mg/kg/day steroids. In patients receiving corticosteroids (n= 126), the mortality rate was 76%, whereas the ICU mortality

rate was 45.1% for all patients (n= 780) and 40% for those receiving low-to-medium-dose corticosteroids (n= 563). Higher mortality rates were observed in patients receiving high-dose corticosteroids. However, limited information is available on the use of high-dose corticosteroids. In a study by So et al.[17] involving seven patients, a 3-day pulse steroid treatment (500-1000 mg/day methylprednisolone) was administered and gradually discontinued, successfully weaning off mechanical ventilation within 1 week. In contrast to other studies, our study showed that patients receiving high-dose corticosteroids had more extended stays in the ICU and higher rates of mechanical ventilation and intubation. Specifically, the intubation rates were 54% and 78% in the low- and medium-dose groups, respectively.

In a prospective randomized controlled trial of pulse steroid therapy in Iran, standard care and treatment (n= 34) were compared with 250 mg intravenous methylprednisolone for three days in addition to this treatment (n= 34) in terms of cure and death rates. The study findings showed a notable favorable difference associated with the use of methylprednisolone. However, these results need to be interpreted, taking into account several limitations in the study design and the relatively small sample size.[18] In the study by Monreal et al.,[19] an observational study retrospectively compared high-dose (≥ 250 mg/day) (n= 177) and standard-dose (≤ 1.5 mg/kg/day) (n= 396) methylprednisolone treatments in patients with severe COVID-19. The study revealed a statistically significant increase in mortality in patients receiving high-dose corticosteroids compared with those receiving standard-dose therapy (18.6% vs. 39%). This difference could be attributed to the greater disease severity observed in the high-dose corticosteroid group. However, it is worth noting that similar mortality rates were observed in younger individuals, suggesting that factors other than age may contribute to the outcomes. It has been emphasized that it is necessary to be very careful when administering pulse steroid therapy, especially in patients over 70. Our study was consistent with the patient characteristics and findings of Monreal et al.[19] One of the similarities in our study was that the patients who received high-dose corticosteroids had clinically worsening symptoms. The mortality rates were 76% and 40% in the high- and low-dose corticosteroid groups, respectively. In addition to higher mortality rates in patients receiving high-dose corticosteroids, high APACHE, SOFA, fibrinogen, D-dimer, hemoglobin, urea, creatinine, hyperglycemia due to adverse effects, and serious complications, such as gastrointestinal bleeding and renal failure, were more common. In a study conducted in our country, patients with ARDS and COVID-19 were treated with methylprednisolone at different doses (low or high) and durations. This study aimed to compare various factors, such as lactate levels, PCT levels, neutrophil-to-lymphocyte ratio, intubation time, weaning time, need for hemoperfusion, length of stay, and prognosis among the treatment groups. It has been reported that different doses and durations of methylprednisolone. The study's limited number of patients and some data collection limitations have been emphasized.[20]

CONCLUSION

In conclusion, when using corticosteroids for COVID-19, the treatment strategy should be determined after considering the adverse effects of steroids and systemic complications. Corticosteroid treatment should be carefully applied according to the patient's clinical situation, disease stage, comorbidities, and systemic or organ reserves.

The mortality rate was lower with low- and medium-dose steroid use in corticosteroid treatments for COVID-19. In addition to high mortality rates, high-dose steroids are associated with increased adverse effects and complications. The evidence on steroid treatment for COVID-19 is insufficient, and more evidence-based systematic clinical trials are needed to establish an appropriate corticosteroid protocol.

Ethics

Ethics Committee Approval: This study was approved by the Clinical Research Ethics Committee of University of Health Sciences Türkiye, Bozyaka Training and Research Hospital after obtaining permission from the Ministry of Health COVID-19 Scientific Research and Evaluation Commission (protocol number: 21.05.2020-222).

Authorship Contributions

Surgical and Medical Practices: İ.D., H.Ö., Ş.Ç., Concept: İ.D., İ.Y., H.Ö., Ş.Ç., Design: İ.D., İ.Y., H.Y., Data Collection or Processing: İ.D., İ.Y., H.Ö., Ş.Ç., Analysis or Interpretation: İ.D., İ.Y., H.Y., Literature Search: İ.Y., H.Y., Writing: İ.D., İ.Y., H.Y.

Conflict of Interest: No conflict of interest was declared by the authors.

Financial Disclosure: The authors declared that this study received no financial support.

REFERENCES

1. Qian GQ, Yang NB, Ding F, Ma AHY, Wang ZY, Shen YF, Shi CW, Lian X, Chu JG, Chen L, Wang ZY, Ren DW, Li GX, Chen XQ, Shen HJ, Chen XM. Epidemiologic and clinical characteristics of 91 hospitalized patients with COVID-19 in Zhejiang, China: a retrospective, multi-centre case series. QJM. 2020;113:474-481.
2. Huang C, Wang Y, Li X, Ren L, Zhao J, Hu Y, Zhang L, Fan G, Xu J, Gu X, Cheng Z, Yu T, Xia J, Wei Y, Wu W, Xie X, Yin W, Li H, Liu M, Xiao Y, Gao H, Guo L, Xie J, Wang G, Jiang R, Gao Z, Jin Q, Wang J, Cao B. Clinical features of patients infected with 2019 novel coronavirus in Wuhan, China. Lancet. 2020;395:497-506.
3. Collaborative Group. Lopinavir-ritonavir in patients admitted to hospital with COVID-19 (RECOVERY): a randomised, controlled, open-label, platform trial. Lancet. 2020;396:1345-1352.
4. Singh AK, Singh A, Singh R, Misra A. An updated practical guideline on use of molnupiravir and comparison with agents having emergency use authorization for treatment of COVID-19. Diabetes Metab Syndr. 2022;16:102396.
5. Bhimraj A, Morgan RL, Shumaker AH, Lavergne V, Baden L, Cheng VC, Edwards KM, Gandhi R, Muller WJ, O'Horo JC, Shoham S, Murad MH, Mustafa RA, Sultan S, Falck-Ytter Y. Infectious diseases society of

America guidelines on the treatment and management of patients with COVID-19. Clin Infect Dis. 2020:ciaa478.

6. Siddiqi HK, Mehra MR. COVID-19 illness in native and immunosuppressed states: a clinical-therapeutic staging proposal. J Heart Lung Transplant. 2020;39:405-407.
7. Chrousos GP. The hypothalamic-pituitary-adrenal axis and immune-mediated inflammation. N Engl J Med. 1995;332:1351-1362.
8. Villar J, Ferrando C, Martínez D, Ambrós A, Muñoz T, Soler JA, Aguilar G, Alba F, González-Higueras E, Conesa LA, Martín-Rodríguez C, Díaz-Domínguez FJ, Serna-Grande P, Rivas R, Ferreres J, Belda J, Capilla L, Tallet A, Añón JM, Fernández RL, González-Martín JM; dexamethasone in ARDS network. Dexamethasone treatment for the acute respiratory distress syndrome: a multicentre, randomised controlled trial. Lancet Respir Med. 2020;8:267-276.
9. Myall KJ, Mukherjee B, Castanheira AM, Lam JL, Benedetti G, Mak SM, Preston R, Thillai M, Dewar A, Molyneaux PL, West AG. Persistent post-COVID-19 interstitial lung disease. An observational study of corticosteroid treatment. Ann Am Thorac Soc. 2021;18:799-806.
10. Ministry of Health, General Directorate of Public Health. COVID-19 (SARS-CoV-2 Infection) management of severe pneumonia, ARDS, sepsis and septic shock. Available from: https://covid19.saglik.gov.tr/Eklenti/40781/0/covid19rehberiagirpnomoniardssepsisveseptiksokyontemipdf.pdf (Accessed May 27, 2021)
11. Ruan SY, Lin HH, Huang CT, Kuo PH, Wu HD, Yu CJ. Exploring the heterogeneity of effects of corticosteroids on acute respiratory distress syndrome: a systematic review and meta-analysis. Crit Care. 2014;18:R63.
12. WHO rapid evidence appraisal for COVID-19 therapies (REACT) working group; Sterne JAC, Murthy S, Diaz JV, Slutsky AS, Villar J, Angus DC, Annane D, Azevedo LCP, Berwanger O, Cavalcanti AB, Dequin PF, Du B, Emberson J, Fisher D, Giraudeau B, Gordon AC, Granholm A, Green C, Haynes R, Heming N, Higgins JPT, Horby P, Jüni P, Landray MJ, Le Gouge A, Leclerc M, Lim WS, Machado FR, McArthur C, Meziani F, Møller MH, Perner A, Petersen MW, Savovic J, Tomazini B, Veiga VC, Webb S, Marshall JC. Association between administration of systemic corticosteroids and mortality among critically Ill patients with COVID-19: a meta-analysis. JAMA. 2020;324:1330-1341.
13. Wu C, Chen X, Cai Y, Xia J, Zhou X, Xu S, Huang H, Zhang L, Zhou X, Du C, Zhang Y, Song J, Wang S, Chao Y, Yang Z, Xu J, Zhou X, Chen D, Xiong W, Xu L, Zhou F, Jiang J, Bai C, Zheng J, Song Y. Risk factors associated with acute respiratory distress syndrome and death in patients with coronavirus disease 2019 Pneumonia in Wuhan, China. JAMA Intern Med. 2020;180:934-943.
14. Fatima SA, Asif M, Khan KA, Siddique N, Khan AZ. Comparison of efficacy of dexamethasone and methylprednisolone in moderate to severe covid 19 disease. Ann Med Surg (Lond). 2020;60:413-416.
15. RECOVERY Collaborative Group; Horby P, Lim WS, Emberson JR, Mafham M, Bell JL, Linsell L, Staplin N, Brightling C, Ustianowski A, Elmahi E, Prudon B, Green C, Felton T, Chadwick D, Rege K, Fegan C, Chappell LC, Faust SN, Jaki T, Jeffery K, Montgomery A, Rowan K, Juszczak E, Baillie JK, Haynes R, Landray MJ. Dexamethasone in hospitalized patients with Covid-19. N Engl J Med. 2021;384:693-704.
16. Fernández-Cruz A, Ruiz-Antorán B, Muñoz-Gómez A, Sancho-López A, Mills-Sánchez P, Centeno-Soto GA, Blanco-Alonso S, Javaloyes-Garachana L, Galán-Gómez A, Valencia-Alijo Á, Gómez-Irusta J, Payares-Herrera C, Morrás-Torre I, Sánchez-Chica E, Delgado-Téllez-de-Cepeda L, Callejas-Díaz A, Ramos-Martínez A, Múñez-Rubio E, Avendaño-Solá C. A retrospective controlled cohort study of the impact of glucocorticoid treatment in SARS-CoV-2 infection mortality. Antimicrob Agents Chemother. 2020;64:10-20.
17. So C, Ro S, Murakami M, Imai R, Jinta T. High-dose, short-term corticosteroids for ARDS caused by COVID-19: a case series. Respirol Case Rep. 2020;8:e00596.
18. Edalatifard M, Akhtari M, Salehi M, Naderi Z, Jamshidi A, Mostafaei S, Najafizadeh SR, Farhadi E, Jalili N, Esfahani M, Rahimi B, Kazemzadeh H, Mahmoodi Aliabadi M, Ghazanfari T, Sattarian M, Ebrahimi Louyeh H, Raeeskarami SR, Jamalimoghadamsiahkali S, Khajavirad N, Mahmoudi M, Rostamian A. Intravenous methylprednisolone pulse as a treatment for hospitalised severe COVID-19 patients: results from a randomised controlled clinical trial. Eur Respir J. 2020;56:2002808.
19. Monreal E, Sainz de la Maza S, Natera-Villalba E, Beltrán-Corbellini Á, Rodríguez-Jorge F, Fernández-Velasco JI, Walo-Delgado P, Muriel A, Zamora J, Alonso-Canovas A, Fortún J, Manzano L, Montero-Errasquín B, Costa-Frossard L, Masjuan J, Villar LM; COVID-HRC group. High versus standard doses of corticosteroids in severe COVID-19: a retrospective cohort study. Eur J Clin Microbiol Infect Dis. 2021;40:761-769.
20. Koc S, Kupeli Ilke. Comparison of high-dose, short-term steroid and low-dose long-term steroid use in ARDS caused by COVID-19: Retrospective cohort study. J Surg Med. 2022;6:360-363.

Turk J Pharm Sci 2024;21(4):303-312
DOI: 10.4274/tjps.galenos.2023.46735

ORIGINAL ARTICLE

Formulation and Evaluation of a Transferosomal Gel of Famciclovir for Transdermal Use

Sayani BHATTACHARYYA[1]*, Kalai Tamilselvi Lakshmanan[1], Andhuvan MUTHUKUMAR[2]

[1]Krupanidhi College of Pharmacy, Department Of Pharmaceutics, Bengaluru, India
[2]Al Ameen College of Pharmacy, Department of Pharmacology, Bengaluru, India

ABSTRACT

Objectives: Famciclovir, the drug of choice for cold sores and recurrent genital herpes, has poor oral bioavailability and is associated with numerous side effects. The study aimed to explore the possibility of transdermal application of famciclovir through a transferosome-loaded gelling system to localize the drug at the site of application with improved penetrability, therapeutic effects, and comfort.

Materials and Methods: Transferosomes of famciclovir were prepared using tween 80, phospholipid, and cholesterol. To optimize drug entrapment and the vesicular size of the transferosomes, a central composite design was employed. The optimized formulation was evaluated for physicochemical characteristics, surface morphology, and degree of deformability. The optimized product was included in the Carbopol 940 gelling system. The gel was evaluated for *ex vivo* permeation, skin irritation, drug deposition at various skin layers, and histopathological analysis.

Results: The design optimization yielded an optimized product (FAMOPT) of nanosized (339 nm) stable vesicles of the transferosome of famciclovir. The surface morphology analysis revealed the formation of nanovesicles without aggregation. Compatibility between the drug and excipients was established. The elasticity of the vesicles demonstrated resistance to leakage. The permeation of the drug was enhanced by 2.8 times. The gel was found to be non-irritating and non-sensitizing to the animal skin. The drug deposition at various skin layers was remarkably improved, indicating effective drug penetration. The histopathological examination further demonstrated the penetration of nano-vesiculate drugs through deeper layers of the skin.

Conclusion: Hence, nano-vesicular famciclovir delivery is a promising alternative to conventional famciclovir delivery with enhanced local and systemic action for herpes treatment.

Keywords: Famciclovir, transferosome, deformable vesicle, transdermal penetration, skin deposition

INTRODUCTION

The era of nanotechnology offers novel therapeutic avenues for antivirals to treat viral diseases successfully. Generally, the side effects associated with these small molecules need attention. The novel delivery of drugs in nanocarriers attempts to lower viral loads in a more efficient manner than conventional dosage forms.

Famciclovir is a guanine analog used to treat herpes virus infections of the skin, which are expressed through cold sores around the mouth, sores around the anus, and genital herpes.[1] The drug has poor oral bioavailability but suffers from many side effects when administered orally.[2] The dose of the drug is relatively high, and the treatment lasts for more than 7 days. Hence, a new mode of delivery of famciclovir through the transdermal route could be beneficial for the efficacy of the therapy.

Transdermal delivery of drugs through the stratum corneum is a challenge. One of the most important factors to consider for a successful transdermal formulation is the penetration of the drug through the skin, which is mostly dependent on the physicochemical properties of the drug. Drugs with optimal lipophilicity are best suited for transdermal delivery. Hence, a hydrophilic drug must penetrate the skin to elicit a systemic effect. As a result, in the last decade, lipid-based vesicles or carriers have been routinely studied for topical drug delivery.[3] Niosome, ethosomes, liposomes, and transferosomes have

*Correspondence: sayanibh@gmail.com, Phone: +9845561865, ORCID-ID: orcid.org/0000-0002-4013-4316
Received: 12.05.2023, Accepted: 18.08.2023

been investigated as promising vesicular carriers for enhancing transdermal drug delivery of drugs.[4,5]

Transferosomes are vesicles of phospholipids with edge activators and are one of the superior drug delivery systems for topical application.[6] They are elastic in nature, which enables them to squeeze themselves as intact vesicles through the narrow pores of the skin. The presence of edge activators is responsible for the deformable properties of the transfersomes.[7] The elastic transport is propelled by the trans-epidermal osmotic gradient between the surface of the skin and interior of the skin. Their flexibility facilitates their passage through pores that are smaller than themselves.[8]

Famciclovir has a log *p* value of 0.6, which does not support transdermal permeation. Hence, a novel carrier system is necessary for famciclovir to cross the stratum corneum and localize at the site of action.[9] The composition of transferosomes allows the vesicles to self-optimize to cross dermal barriers efficiently.[10] Therefore, the present study focused on the development and characterization of ultra-deformable vesicles of famciclovir for transdermal delivery in the treatment of herpes. [11]

MATERIALS AND METHODS

Materials

Famciclovir was obtained from Strides Pvt. Ltd., (Bangalore). Acetonitrile, methanol, cholesterol, and carbopol-940 were purchased from SD Fine Chemicals Ltd. (Mumbai, India). Tween 80, soya lecithin was supplied by Central Drug House Pvt, Ltd. (Delhi). All other chemicals were of analytical grade, and distilled water was used throughout the study.

Methods

Design of experiments

Considering the vesicle size, polydispersity index (PDI), and entrapment of sparingly soluble famciclovir as dependent variables, the transfersomes of famciclovir were prepared by optimizing three prime independent factors of the formulations, namely the phospholipid (SPC) and cholesterol ratio (CH), surfactant concentration (tween 80) (*w/v*%), and phase volume ratio. The central composite design was performed using the Design Expert V11 software. The correlation between independent and dependent factors was analyzed using the response surface methodology. The design generated 13 experimental runs with three center points. Two-level [low (-1) and high level (+1)] testing of each independent variable was performed to estimate the effect of composition on the responses, as listed in Table 1.[12] Table 2 explains the formulation table as per the design.

Transferosome preparation

A thin-film hydration technique was employed to form transferosomes.[13,14] To optimize the composition of transfersomes, various formulations were prepared using the central composite design. Specific amounts of lipids were dissolved in a mixture of organic solvents consisting of methanol and chloroform (1:3) in a dry round-bottom flask. The evaporation of organic solvents was performed under vacuum using a rota evaporator at 100 rpm, at 48-50 °C. The thin lipid film thus obtained was then hydrated using water containing surfactant and drug (1.5% *w/v*) by rotation for 1 hour at 50 °C. Each formulation was placed in an ultrasonicator bath at 150 W for 20 seconds. A dialysis bag was used to remove the free drug, and the final formulation was stored at 4 °C for further use. Blank transfersomes were prepared using the same method for each formulation.

Evaluation of transfersomes

Vesicle size

The vesicle sizes of the prepared formulations were measured using Horiba SZ100 (Dynamic light scattering technique) at 25 °C. Samples were diluted with Millipore water as a dispersant. The measurements were performed in triplicate.[15]

Zeta potential

Zeta potential was measured using a Horiba SZ100 spectrophotometer. The formulations were diluted with Millipore water before being subjected to measurements, and each measurement was performed in triplicate.[16]

Table 1. List of independent factors

Factors	Low level (-1)	High level (+1)
SPC:CH	1:1	2:1
Surfactant concentration (*w/v*%)	5	20
Phase volume ratio	0.4	0.6

SPC: Phospholipid, CH: Cholesterol

Table 2. Central composite design for transferosome formulation

Runs	Factor 1 SPC:CH	Factor 2 Non-ionic surfactant %	Factor 3 Phase volume ratio
1	1	1	-1
2	0	0	0
3	-1	1	1
4	0	1.41421	0
5	0	0	0
6	0	-1.41421	0
7	-1	-1	-1
8	1	-1	1
9	-1.41421	0	0
10	0	0	0
11	0	0	-1.41421
12	1.41421	0	0
13	0	0	1.41421

SPC: Phospholipid, CH: Cholesterol

Entrapment efficiency

The prepared dispersion was centrifuged at 3000 rpm at 4 °C for 30 minutes. The transfersomes were settled into pellets, and the supernatant layer was collected to determine the amount of unentrapped drug. The pellet was disrupted with an equal volume of methanol in a vortex mixture for 5 minutes. The sample was diluted and analyzed spectrophotometrically using 0.02 M potassium dihydrogen orthophosphate and acetonitrile (80:20) at 307 nm to determine the entrapped drug. The unentrapped drug was determined by analyzing the supernatant layer. Entrapment efficiency was calculated for all formulations in triplicate. The percentage entrapment efficiency is computed using the formula.[17]

$$\% \text{ Entrapment efficiency} = \frac{\text{Entrapped drug}}{\text{Entrapped drug} + \text{Free drug}} * 100$$

Blank transfersomes of each formulation were used as blanks to terminate the effect of the excipients. All studies were performed in triplicate.

Statistical analysis

A central composite design was employed in the study to investigate the experimental variables at five different levels on the responses with a minimum number of experiments. The results were subjected to regression analysis using the Design Expert software V13 to determine the relationship between factors and responses. The use of center points in the design increased the confidence level and helped minimize experimental errors

The 13 formulations thus prepared were evaluated for vesicle size, PDI, and % drug entrapment, and the model validation was established through ANOVA analysis at a significance level of $p < 0.05$. Design optimization was carried out to acieve maximum drug entrapment, minimum vesicle size, andPDI. The optimized formulation (FAMOPT) was adopted for further evaluation.

Fourier transform infrared spectroscopy (FTIR)

FTIR spectrophotometric analysis was performed to investigate the compatibility between the drug and excipients. The Bruker attenuated total reflection alpha technique was used for the analysis. The spectra of the pure drug, the physical mixture of the optimized blank, and FAMOPT were recorded at a temperature of 25.0 ± 0.5 °C by placing the samples on a zinc solenoid crystal plate over the wavenumber 4000 to 400 cm^{-1}.[18]

Transmission electron microscopy (TEM)

The morphology of FAMOPT was examined using a TEM [TEM; FEI Tecnai T20 (North America)]. Transferosome dispersion was placed on paraffin sheets on which carbon-coated grids were placed to allow the samples to adhere. The excess sample was removed by adsorption onto a small piece of filter paper. A drop of phosphotungstate (1%) was added to the grid. The samples were air-dried and imaged.[19]

Degree of deformability

The elasticity of the FAMOPT vesicles was determined by the extrusion method. The transfersomes were extruded at a pressure of 2.5 bar through a polycarbonate membrane (pore diameter, 0.2 microns), (Merck, India). Vesicle size was noted before and after passing through the membrane using Horiba SZ100. The degree of deformability was calculated by estimating the ratio of vesicle size before and after the extrusion process.[20] The entrapment efficiency was also determined after the extrusion method to estimate leakage, if any.

Transferosomal gel preparation of famciclovir

The transferosomal gel of famciclovir was formulated by incorporating FAMOPT (5% *v/v*) in an aqueous dispersion of carbopol 940. Carbopol 940 (0.5% *w/w*) was accurately weighed and dispersed into distilled water in a beaker. Propylene glycol (7% *w/w*) was added to the solution. Stirring was continued at 500 rpm for 2 hours, and the final pH of the gel base was adjusted to 5.5 using sodium hydroxide.[21] A gel of pure drug gel of equivalent strength to the optimized product was prepared using the same composition and used for comparative evaluation for drug release studies.

Evaluation of gel

Physicochemical characterization of the transferosomal gel of FAMOPT

The transferosomal gel of FAMOPT was tested for appearance, feel, odor, clarity, and homogeneity.[22]

The pH of the gel was determined using a digital pH meter. Viscosity measurements of the prepared transferosomal gel were performed using a Brookfield viscometer with a spindle T-D at an optimum speed of 10 rpm at 25 °C. The measurements were performed in triplicate.[23]

Ex vivo diffusion studies of transfersome-loaded gel and skin deposition

Ex vivo diffusion studies of the transferosomal gel of FAMOPT were conducted using Wistar albino rat skin. The animals were euthanized with excess carbon dioxide, and the abdominal skin was surgically removed. The excised skin was cleaned with saline water and placed in the receptor compartment. The receptor compartment was filled with a freshly prepared buffer solution (pH 5.5). The diffusion medium was stirred at 100 rpm, at 37.0 ± 0.5 °C. The transfersome-loaded gel (500 µL) was placed in the donor compartment, and samples of diffusion medium (1 mL) were collected at different time intervals for 24 hours. The samples were withdrawn at intervals of a specific time, and donor cells were replenished with an equal volume of fresh medium. The samples were analyzed spectrophotometrically. A gel of pure drug of equivalent strength and an optimized drug-loaded transferosomal formulation (FAMOPT) were subjected to a comparative drug diffusion study using the same procedure.

The drug release kinetics was studied by plotting diffusion into different rate kinetics models.

For all selected formulations, the amount of permeated drug (mg/cm^2) over time was also calculated. The flux and permeation constant are calculated using the following formula.[24]

Jss = dq/dt

p = dq/dt.1/AC_D

In which A- diffusion area (4,512)

dq/dt slope of the linear region of the *ex vivo* diffusion curve

C_D-is the donor concentration

At the end of the *ex vivo* permeation study, the skin was removed from the diffusion flask, the remaining gel was swabbed, and the skin was washed repeatedly with 0.02 M potassium dihydrogen orthophosphate and acetonitrile (80:20) solution to remove the excess drug.[25]

The skin was carefully sectioned into the dermis and epidermis layers using a tweezer.[20] The separated layers were homogenized with phosphate buffer and centrifuged at 10000 rpm for 5 minutes, and the supernatant was analyzed by ultraviolet spectrophotometry using spiking (known concentration 10 µg/mL) experiments to estimate drug deposition in various layers of skin.

Skin irritation study

The skin irritation study was conducted using albino Wistar rats. The back of the animal was shaved carefully. The animals were divided into three groups, each containing 6 animals-control, test, and placebo. The optimized formulation was applied on the backside of the animal for 7 days for an irritation study. Changes in skin color, morphology, and the development of erythema and edema were observed daily for 7 days of the study.[26]

Histopathological studies

The skin from the animals of Group I and Group II was taken for histopathological studies. The excised skin was dipped in 10% formalin solution and subjected to histopathological examination. The sections were observed using a light microscope equipped with a digital camera using hematoxylin and eosin stains.[27]

Ethical Aproval

This study approved by Krupanidhi College of Pharmacy Institutional Animal Ethics Committee (approval number: KCP/IAEC-407/2021-22, date: 11.06.022)

RESULTS

Evaluation of experimental design

The experimental runs of the thirteen trials are listed in Table 3. The response surface graphs show the most statistically significant variables for the evaluated responses, as shown in Figure 1. The model was established for all dependent variables at a significance level of $p < 0.05$ as shown in Table 4. The effects of the main factors on the formulation responses are listed below. It was found that the lipid ratio (SPC:CH) had a significant effect on drug entrapment, whereas the non-ionic surfactant had a remarkable impact on particle size. PDI was greatly affected by both the phase volume ratio and surfactant concentration, as indicated in Table 4.

The model optimization was carried out at a desirability of 0.77, and an optimized condition was predicted at an SPC:CH ratio of 1.44:1, surfactant concentration of 6.65 *w/v* %, and phase volume of 0.42 to produce drug-loaded transfersomes with high entrapment efficiency, low vesicle size, and polydispersity. The optimized formulation (FAMOPT) was prepared and exhibited the properties predicted by the design with a bias within 10%, as shown in Table 5. The zeta potential of the optimized formulation was determined to be 9.7 mV. The zeta potentials and vesicle sizes of the optimized formulations are shown in Figure 2.

Table 3. Experimental evaluation of transferosomes according to the central composite design

Formulation code	Entrapment efficiency %	Particle size (nm)	PDI
F1	70.9 ± 0.001	452.9 ± 20.1	0.553 ± 2.32
F2	71.6 ± 0.096	483.0 ± 31.2	0.73 ± 1.45
F3	94.3 ± 0.007	440.7 ± 33.4	0.604 ± 0.95
F4	49.2 ± 0.014	508.5 ± 11.5	0.951 ± 1.02
F5	76.0 ± 0.011	519.0 ± 26.8	0.77 ± 2.01
F6	71.0 ± 0.172	314.2 ± 30.4	0.196 ± 0.95
F7	55.2 ± 0.036	213.7 ± 16.9	0.434 ± 1.48
F8	62.9 ± 0.037	415.8 ± 25.9	0.337 ± 1.21
F9	53.7 ± 0.006	493.5 ± 39.7	0.317 ± 2.13
F10	68.9 ± 0.007	456.0 ± 24.4	0.750 ± 1.06
F11	66.3 ± 0.060	416.8 ± 36.1	0.361 ± 0.78
F12	86.3 ± 0.023	344.9 ± 19.2	0.381 ± 1.71
F13	61.3 ± 0.012	278.6 ± 28.5	0.769 ± 1.82

All values are mean (n= 3) ± standard deviation, PDI: Polydispersity index

Table 4. Model validation statistics

Response	Suggested fit summary	*p* value	R^2	Model equation
Entrapment efficiency	2FI	0.0243*	0.855	Entrapment efficiency = +68.33+11.51A 7.69B 1.78C 9.54AB 19.43AC+15.43BC
	A-SPC:CH	0.0147*		
	B-% non-ionic surfactant	0.0643		
	C-Phase volume ratio	0.6194		
Particle size	Quadratics	0.0456*	0.966	Particle size = +477.85-52.54A+68.70B-48.86C-96.34AB+2.67AC-106.11BC-23.21A^2-27.13B^2-58.96C^2
	A-SPC:CH	0.0579		
	B-% non-ionic surfactant	0.0296*		
	C-Phase volume ratio	0.0687		
PDI	Quadratics	0.0374*	0.970	PDI = +0.723353+0.022627A+0.0266933B+0.14425C+0.15575AB +0.170433AC+0.059627BC-0.16719A^2-0.05494B^2-0.051919C^2
	A-SPC:CH	0.6085		
	B-% Non-ionic surfactant	0.0067*		
	C-Phase volume ratio	0.0359*		

*Denotes significant, PDI: Polydispersity index, SPC: Phospholipid, CH: Cholesterol

Table 5. Model prediction vs. observed responses for optimized product (FAMOPT)

Responses	Predicted	Observed	Bias %
Entrapment efficiency (%)	84.89	81.78 ± 0.02	3.65
Particle size (nm)	335	340.5 ± 23.7	1.64
PDI	0.383	0.419 ± 1.16	9.39

All values are mean (n= 3) ± standard deviation, FAMOPT: Optimized product

FTIR

The characteristic peaks of $COOCH_3$ stretching, C=C, C=N, and C-0 stretching, and C-N bending of the pure drug were observed at 1745, 1653, 1614, 1211, and 1249 cm^{-1} respectively (Figure 3A). The spectra of the blank formulation (Figure 3B) and FAMOPT (Figure 3C) were analyzed for compatibility.

TEM

The nanovesicles of FAMOPT were observed by TEM as shown in Figure 4.

Degree of deformability

The ratio of the change in the size of the FAMOPT vesicles was found to be less than 1, as listed in Table 6, The % of leakage was calculated to be 3.46%.

Evaluation of the transferosomal gel of famciclovir

The optimized formulation (FAMOPT) was dispersed in a carbopol 940 gel matrix. The gel was found to be translucent; pH was found to be 5.5, with a viscosity of 88.6 centimpoise. The drug content in the gel was estimated at 69.5%.

Ex vivo diffusion studies of transfer some-loaded gels

Ex vivo drug release studies were conducted for FAMOPT, transferosomal gel of FAMOPT, and pure drug gel of famciclovir. The FAMOPT formulation and FAMOPT gel exhibited sustained drug release. The pure drug gel release reached a steady state at 6 hours as shown in Figure 5.

The permeation of the drug from the transferosomal gel and FAMOPT was approximately 2.8 and 3 times higher, respectively, than that from the pure drug gel, as listed in Table 7. The drug deposition in the various skin layers is presented in Figure 6, and permeation of the drug from the transferosomal formulations was remarkably higher compared to the pure drug.

Skin irritation study

The skin irritation test was performed for the animals such that the first group received control, the second group received placebo, and the third group received test formulation (transferosomal gel of FAMOPT). All animals in the test groups showed no signs of erythema or edema.

Histopathology study

The histopathology of the rat skin is presented in Figure 7.

DISCUSSION

The response surface diagrams showed significant effects of lipid composition, surfactant concentration, and phase

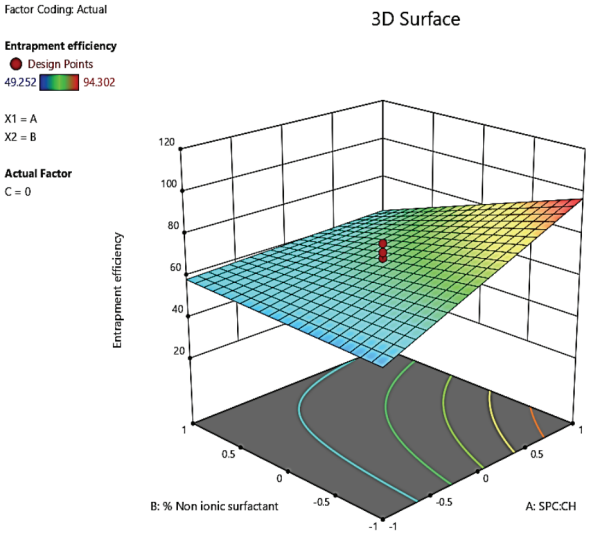

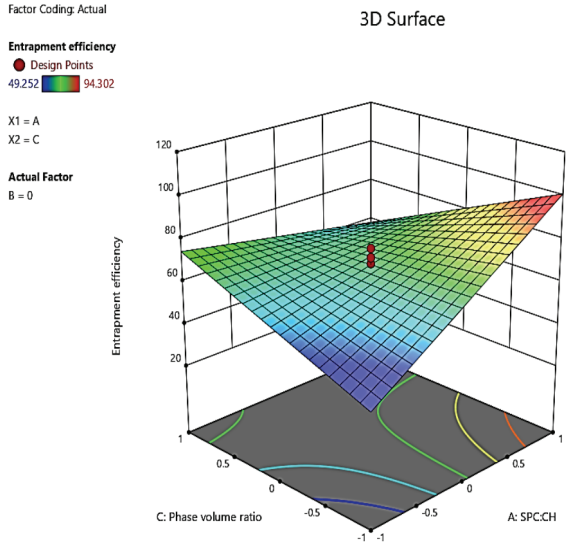

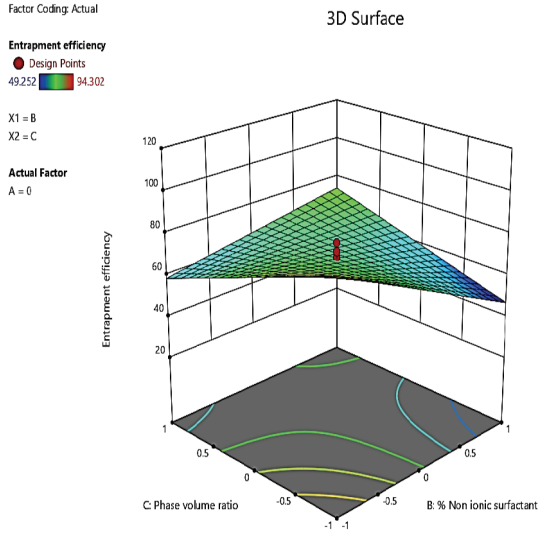

Figure 1A. Response surface diagram for entrapment efficiency

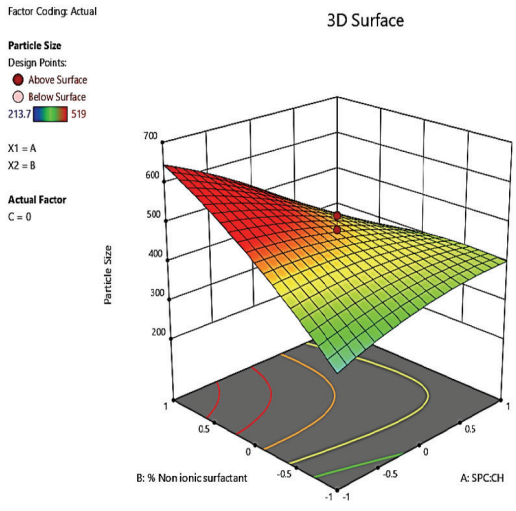

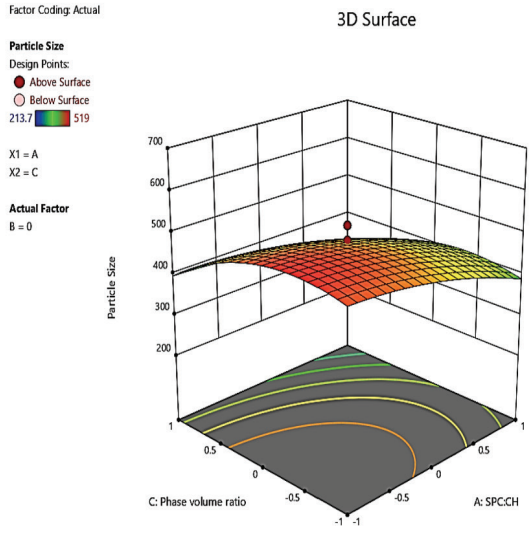

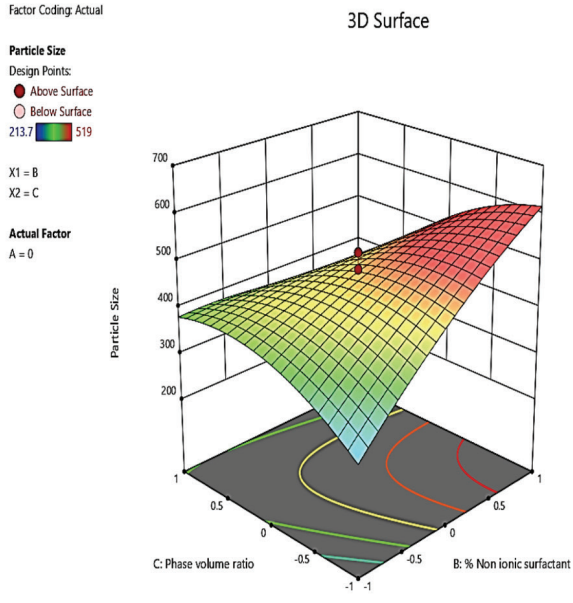

Figure 1B. Surface response for particle size

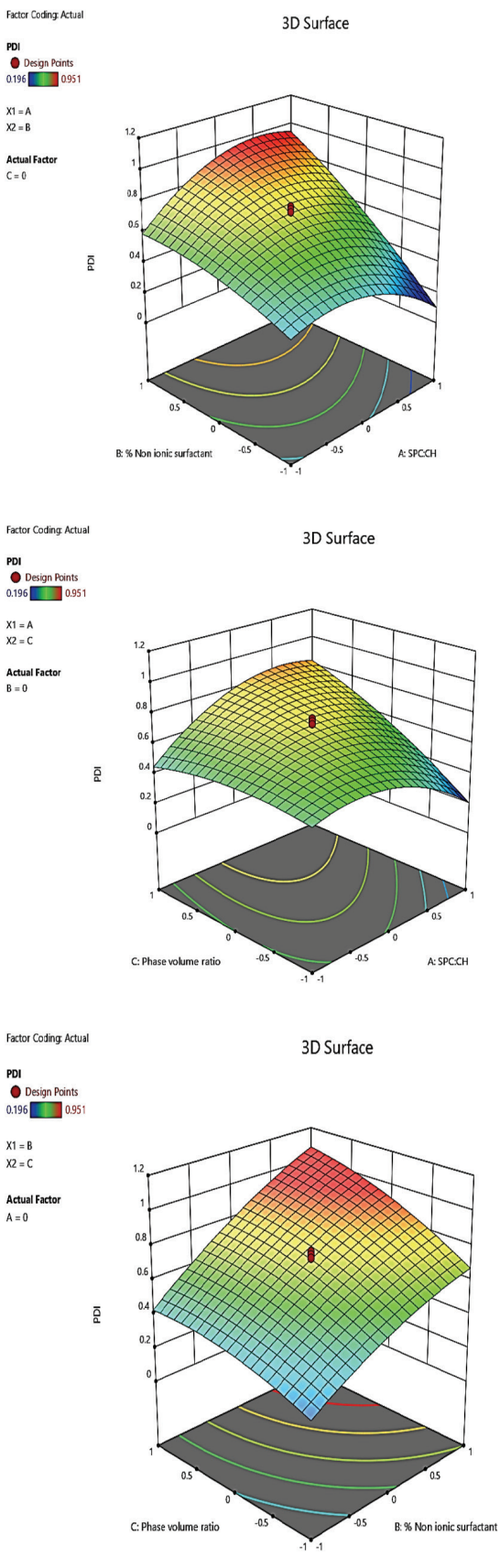

Figure 1C. PDI response surface of
PDI: Polydispersity index

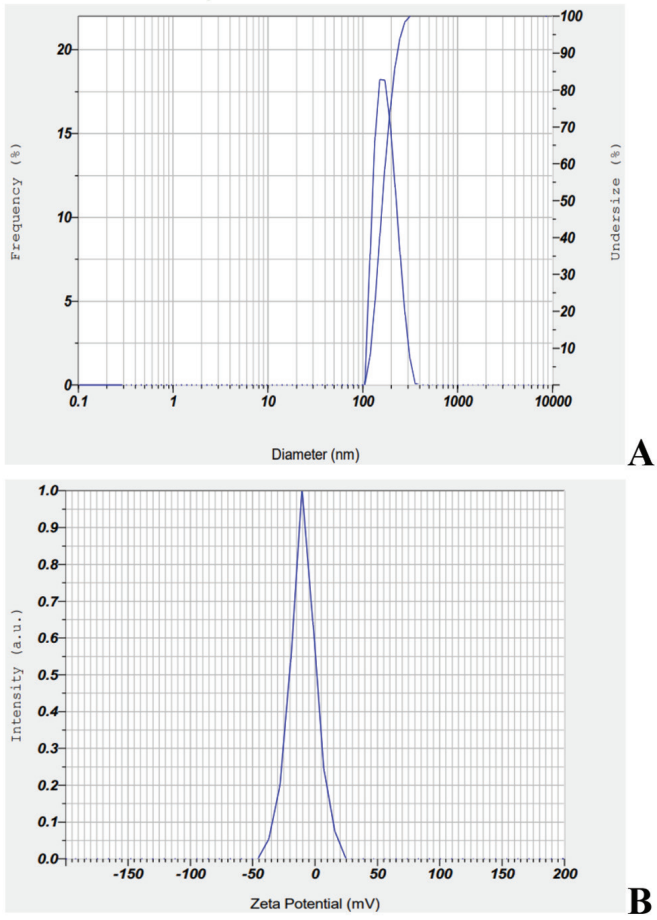

Figure 2. Particle size (A) and zeta potential (B) of FAMOPT
FAMOPT: Optimized product

Table 6. Degree of deformability of the optimized product (FAMOPT)

	Vesicle size (nm)	Entrapment of the drug %
Before extrusion	340.5 ± 0.02	84.15 ± 0.02
After extrusion	320.33 ± 5.05	81.23 ± 0.05
Deformability	0.94	-
%Leakage	-	3.46

All values are mean (n= 3) ± standard deviation, FAMOPT: Optimized product

volume ratio on entrapment efficiency. The vesicle size of the transfersomes was greatly affected by the surfactant concentration and phase volume ratio, as indicated by the extent of curvature in the response surface diagram. The drug has good water solubility; hence, entrapment of the drug in the core of the bilayer vesicle was a challenge. The presence of cholesterol made the bilayer sufficiently stable to prevent drug leakage. The non-ionic surfactant contributed to the elasticity of the vesicles.[28] The effect of the main factors on the properties of the transferosomes was remarkable as evidenced from the model validation.

The model equation provides a fit summary of the factors with the responses. The positive sign in the equation indicates the critical parameters' significant contribution to the responses. The analysis of the variance test showed that the model was significant for approximating the effects of the variables on entrapment efficiency, vesicle size, and PDI. The optimization of the model was carried out considering the high entrapment efficiency of the drug, minimizing the particle size and PDI at high desirability. The vesicle size of FAMOPT after experimentation was found to be within the predicted range, and the surface charge indicated the stability of the vesicles with less aggregation and flocculation.[29]

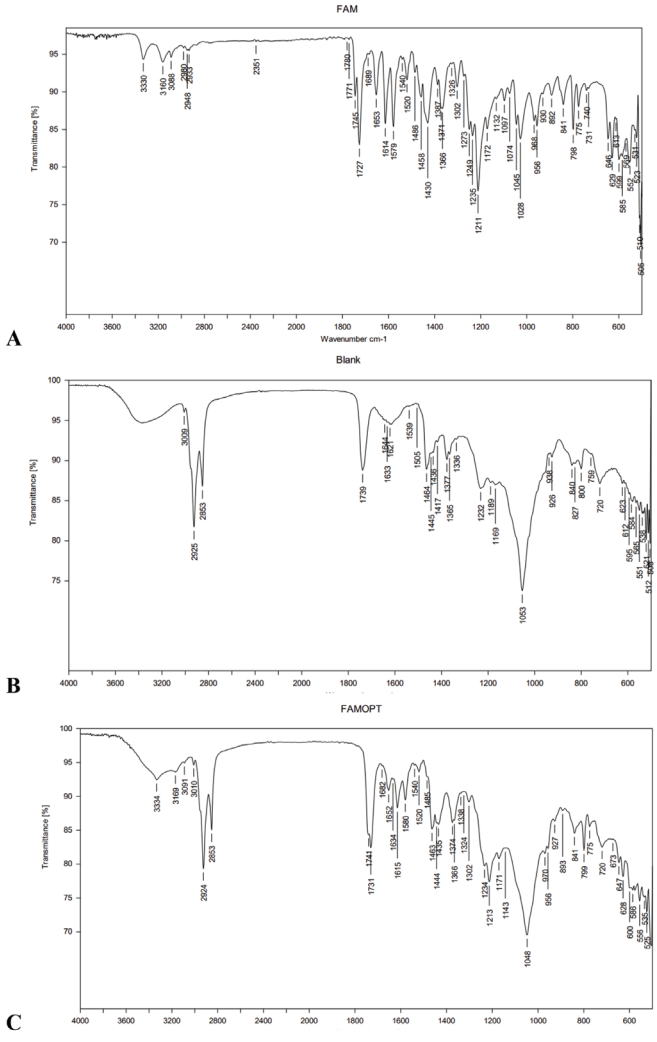

Figure 3. FTIR Spectra of pure drug (A), blank FAMOPT (B), and FAMOPT (C)

FTIR: Fourier transform infrared spectroscopy, FAMOPT: Optimized product

The compatibility of the pure drug with excipients was confirmed by the retention of specific peaks in the fingerprint region of the formulation. The optimized formulation could retain the major peaks of the pure drug and excipients. Hence, it establishes compatibility between the drug and excipients.

The TEM analysis revealed that the vesicles were spherical and did not aggregate. The size range of the vesicles of the optimized product was found to be within the predicted range as per the design.

The degree of deformability of the optimized formulation was calculated by estimating the vesicle size of the formulation before and after extrusion through a polymeric membrane with a lower aperture size. The obtained deformability index (< 1) of the optimized formulation indicates the retention of the vesicle size and proves the minimum leakage of the vesicles.[30] The elasticity of the prepared nanovesicles was determined.

The physicochemical properties of the hydrogel of the optimized formulation in Carbopol 940 were found to be suitable for spreading and application over the skin.

The *ex vivo* diffusion study revealed that drug release from the transferosomal gel of the optimized formulation was very high compared with that from the gel containing the pure drug. The diffusion of the drug from the nanocarriers was much higher and more sustained than that from the gel containing the pure drug. The transferosomal gel of FAMOPT was almost comparable to that of FAMOPT, and a slight reduction in drug release from the gel was attributed to its viscosity. The release of famciclovir from the transferosomal gel was evaluated using first-order kinetics. The exponent of the Korsmeyer-Peppas model (n) is 0.96, which indicates non-fickian anomalous diffusion of the drug from the gel.

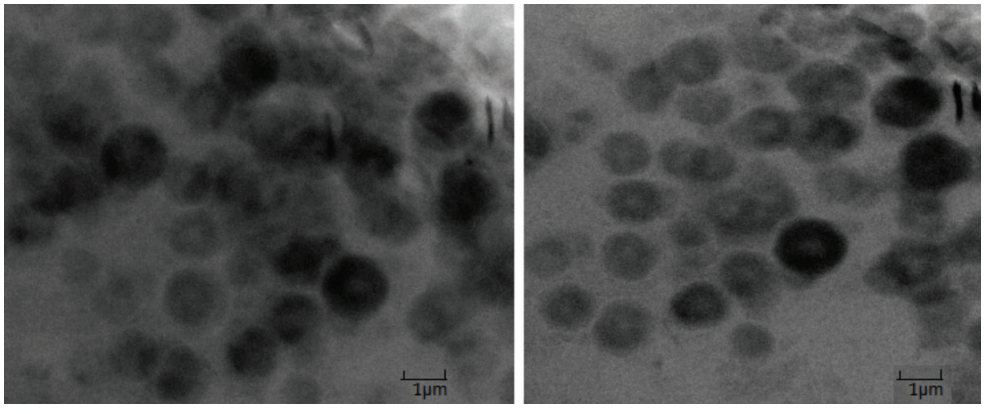

Figure 4. TEM images of transferosomes of famciclovir

TEM: Transmission electron microscope

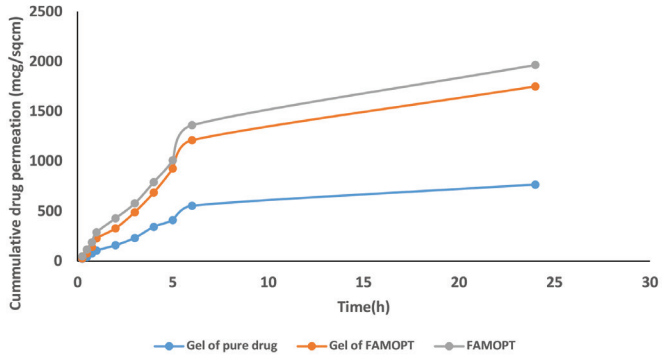

Figure 5. *Ex vivo* diffusion curve of famciclovir
FAMOPT: Optimized product

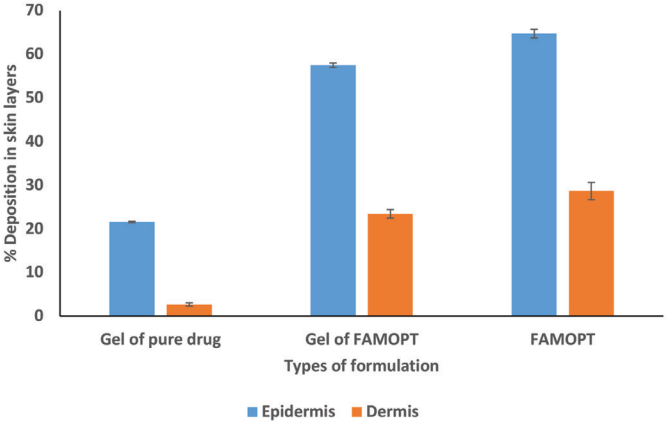

Figure 6. Estimation of famciclovir deposition in skin
FAMOPT: Optimized product

Skin permeation studies showed significantly higher permeation of the drug from the nanocarriers; hence, the penetrability of famciclovir was significantly improved.[30]

The drug deposition in various layers represents a high deposition of the drug in the layers of the skin from the gel of the nanovesicles compared with the gel of the pure drug, and the result was in conformation with the *ex vivo* permeation study. This further confirmed the efficient permeation of the drug into different layers of the skin from the nanovesicles.[29]

The gel was found to be non-sensitive to the skin. Histopathology revealed that there were no sensitization or irritation on the different layers of skin following the application of the nano gel, and a near-normal morphology was observed, similar to the control group. Focal inflammation in the dermal layers upon transferosomal gel application provides evidence of nanovesiculate drug penetration.

CONCLUSION

In this study, novel deformable famciclovir vesicles was developed and evaluated as a nanocarrier for transdermal delivery. These nanosized vesicles exhibit deformable properties. These properties of the vesicles allow drug delivery into deeper layers of the skin. Moreover, the incorporation of the drug into the carbopol 940 gel enhanced the penetration and deposition of the drug into the dermis layer. The permeation of famciclovir was significantly enhanced by the transferosomal gel compared with that of the pure drug. The transferosomal gel was non-sensitive and did not irritate the animal skin. Hence, it can be concluded that transdermal application of transferosomal gel of famciclovir could be an alternative for conventional delivery to reduce virus

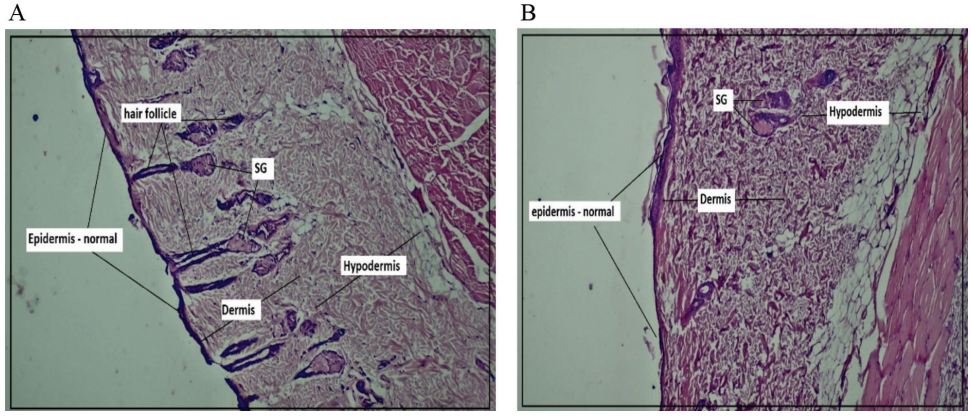

Figure 7. Histopathological examination of rat skin (A) control and (B) after application of transferosomal gel

Table 7. Permeation data of famciclovir after 24 hours

Formulation	Permeated amount of drug at 24 h (μg/cm²)	Drug flux (μg/cm²/h)	Permeability coefficient (Kp) (cm/h)	Permeation of pure drug gel enhanced
FAMOPT	1977	46.32	579	3
Gel of FAMOPT	1751	42.7	534	2.77
Gel containing pure drug	767	19.26	192	-

FAMOPT: Optimized product, Kp: Permeability coefficient

load and could be a non-invasively promising technique for the treatment of cold sores and genital herpes.

Ethics

Ethics Committee Approval: This study approved by Krupanidhi College of Pharmacy Institutional Animal Ethics Committee (approval number: KCP/IAEC-407/2021-22, date: 11.06.022).

Informed Consent: Not applicable.

Authorship Contributions

Concept: S.B., Design: S.B., K.T.L., A.M., Data Collection or Processing: S.B., K.T.L., A.M., Analysis or Interpretation: S.B., K.T.L., Literature Search: S.B., K.T.L., A.M., Writing: S.B., K.T.L.

Conflict of Interest: No conflict of interest was declared by the authors.

Financial Disclosure: The authors declared that this study received no financial support.

REFERENCES

1. Famciclovir oral: uses, side effects, interactions, pictures, warnings and dosing. WebMD. Available from: https://www.webmd.com
2. Side effects of famvir (famciclovir), warnings, uses. RxList. Available from: https://www.rxlist.com
3. Paliwal SR, Paliwal R, Vyas SP. A review of mechanistic insight and application of pH-sensitive liposomes in drug delivery. Drug Deliv. 2015;22:231-242.
4. Gupta M, Goyal AK, Paliwal SR, Paliwal R, Mishra N, Vaidya B, Dube D, Jain SK, Vyas SP. Development and characterization of effective topical liposomal system for localized treatment of cutaneous candidiasis. J Liposome Res. 2010;20:341-350.
5. Paliwal SR, Paliwal R, Agrawal GP, Vyas SP. Liposomal nanomedicine for breast cancer therapy. Nanomedicine (Lond). 2011;6:1085-1100.
6. Omar MM, Hasan OA, El Sisi AM. Preparation and optimization of lidocaine transferosomal gel containing permeation enhancers: a promising approach for enhancement of skin permeation. Int J Nanomedicine. 2019;14:1551-1562.
7. Opatha SAT, Titapiwatanakun V, Chutoprapat R. Transfersomes: a promising nanoencapsulation technique for transdermal drug delivery. Pharmaceutics. 2020;12:855.
8. Cevc G, Schätzlein A, Blume G. Transdermal drug carriers: Basic properties, optimization and transfer efficiency in the case of epicutaneously applied peptides. J Control Release. 1995;36:3-16.
9. DrugBank Online. Available from: https://www.drugbank.com
10. Jangdey MS, Gupta A, Saraf S, Saraf S. Development and optimization of apigenin-loaded transfersomal system for skin cancer delivery: *in vitro* evaluation. Artif Cells Nanomed Biotechnol. 2017;45:1452-1462.
11. Kassem MA, Aboul-Einien MH, El Taweel MM. Dry gel containing optimized felodipine-loaded transferosomes: a promising transdermal delivery system to enhance drug bioavailability. AAPS PharmSciTech. 2018;19:2155-2173.
12. Setyawati DR, Surini S, Mardliyati E. Optimization of luteolin-loaded transfersome using response surface methodology. Int J Appl Pharm. 2017;9:107-111.
13. El Zaafarany GM, Awad GA, Holayel SM, Mortada ND. Role of edge activators and surface charge in developing ultradeformable vesicles with enhanced skin delivery. Int J Pharm. 2010;397:164-172.
14. Maji R, Omolo CA, Jaglal Y, Singh S, Devnarain N, Mocktar C, Govender T. A transferosome-loaded bigel for enhanced transdermal delivery and antibacterial activity of vancomycin hydrochloride. Int J Pharm. 2021;607:120990.
15. Qushawy M, Nasr A, Abd-Alhaseeb M, Swidan S. Design, optimization and characterization of a transfersomal gel using miconazole nitrate for the treatment of candida skin infections. Pharmaceutics. 2018;10:26.
16. Arafa MG, Ayoub BM. DOE optimization of nano-based carrier of pregabalin as hydrogel: new therapeutic and chemometric approaches for controlled drug delivery systems. Sci Rep. 2017;7:41503.
17. Bhattacharyya S, Sudheer P, Das K, Ray S. Experimental design supported liposomal aztreonam delivery: *in vitro* studies. Adv Pharm Bull. 2021;11:651-662.
18. Kanugo A, Deshpande A, Sharma R. Formulation optimization and evaluation of nanocochleate gel of famciclovir for the treatment of herpes zoster. Recent Pat Nanotechnol. 2023;17:259-269.
19. Alvi IA, Madan J, Kaushik D, Sardana S, Pandey RS, Ali A. Comparative study of transfersomes, liposomes, and niosomes for topical delivery of 5-fluorouracil to skin cancer cells: preparation, characterization, *in vitro* release, and cytotoxicity analysis. Anticancer Drugs. 2011;22:774-782.
20. Zhang ZJ, Michniak-Kohn B. Flavosomes, novel deformable liposomes for the co-delivery of anti-inflammatory compounds to skin. Int J Pharm. 2020;585:119500.
21. Bhattacharyya S. Statistical optimization amalgamated approach on formulation development of nano lipid carrier loaded hydrophilic gel of fluticasone propionate. Indian J Pharm Educ Res. 2021;55:418-427.
22. Thakur N, Jain P, Jain V. Formulation development and evaluation of transferosomal gel. J Drug Deliv Ther. 2018;8:168-177.
23. Rajan R, Vasudevan DT. Effect of permeation enhancers on the penetration mechanism of transfersomal gel of ketoconazole. J Adv Pharm Technol Res. 2012;3:112-116.
24. Abdellatif AAH, Tawfeek HM. Transfersomal nanoparticles for enhanced transdermal delivery of clindamycin. AAPS PharmSciTech. 2016;17:1067-1074.
25. Ghanbarzadeh S, Arami S. Formulation and evaluation of piroxicam transferosomal gel: an approach for penetration enhancement. J Drug Deliv Sci Technol. 2013;23:587-590.
26. Dudhipala N, Gorre T. Neuroprotective effect of ropinirole lipid nanoparticles enriched hydrogel for Parkinson's disease: *in vitro*, *ex vivo*, pharmacokinetic and pharmacodynamic evaluation. Pharmaceutics. 2020;12:1-24.
27. Yuan M, Niu J, Xiao Q, Ya H, Zhang Y, Fan Y, Li L, Li X. Hyaluronan-modified transfersomes based hydrogel for enhanced transdermal delivery of indomethacin. Drug Deliv. 2022;29:1232-1242.
28. Ramakanth S, Anith P, Gayathri R, Mohan S, Babu D. Formulation and design optimization of nanotransferosomes using pioglitazone and eprosartan mesylate for concomitant therapy against diabetes and hypertension. Eur J Pharm Sci. 2021;16:105811.
29. Danaei M, Dehghankhold M, Ataei S, Hasanzadeh Davarani F, Javanmard R, Dokhani A, Khorasani S, Mozafari MR. Impact of particle size and polydispersity index on the clinical applications of lipidic nanocarrier systems. Pharmaceutics. 2018;10:57.
30. Johl S, Bhattacharyya S. Novel deformable vesicle for the transdermal delivery of terbinafine hydrochloride-formulation and cytotoxic evaluation. Ind J Pharm Edu Res. 2024; 58:460-469.

Turk J Pharm Sci 2024;21(4):313-326
DOI: 10.4274/tjps.galenos.2023.80799

ORIGINAL ARTICLE

Formulation and Evaluation of Butenafine Hydrochloride-Incorporated Solid Lipid Nanoparticles as Novel Excipients for the Treatment of Superficial Fungal Infections

Anagha BAVISKAR[1], Vivekanand KASHID[1], Sapana AHIRRAO[2]*, Deepak BHAMBERE[2], Manoj AKUL[3]

[1]Dr. Kolpe Institute of Pharmacy, Department of Pharmaceutics, Maharashtra, India
[2]MET Bhujbal Knowledge City, Institute of Pharmacy, Maharashtra, India
[3]Glenmark Pharmaceuticals Limited, Maharashtra, India

ABSTRACT

Objectives: The objective of the present study was to develop natural excipient-based solid lipid nanoparticles (SLN) of butenafine hydrochloride (BUTE) using a modified solvent emulsification technique and to evaluate the competence of *aloe vera* nanolipidgel in enhancing the penetration of BUTE.

Materials and Methods: BUTE-SLNs were prepared using a 2^3 factorial design to correlate the effect of formulation components on the BUTE-SLN. Particle size, polydispersity index (PDI), zeta potential, entrapment performance, and drug loading were assessed in the formed SLNs. The fabricated BUTE-SLN was evaluated for transmission electron microscopy, fourier transform infrared spectroscopy, differential scanning calorimetry, and X-ray diffraction study studies and revealed the encapsulation of BUTE in lipid in the amorphous state. BUTE-SLN-based *aloe vera* gel was formulated and evaluated compared with the marketed product with respect to primary skin irritation, hydration, skin permeation, and antifungal activity.

Results: The BUTE-SLN *aloe vera* gel, optimized for its formulation, features excellent slip properties and controlled drug release. DSC and XRD studies confirm its amorphous nature with effective drug entrapment. The gel provides enhanced skin deposition, improved antifungal activity, and reduced irritation. This makes it a cost-effective and innovative alternative to traditional dosage forms. BUTE-SLN promisingly showed no irritation, higher hydrating potential, slow and sustained release, and enhanced antifungal activity. With an aim to target deeper skin strata, minimize the side effects of drugs and symptomatic impact of fungal infection, and shorten the duration of therapy, BUTE-SLN was successfully prepared. The mean particle size and PDI were 261.25 ± 2.38 nm and 0.268 ± 0.01, respectively.

Conclusion: BUTE-SLN gel offers improved topical delivery of BUTE with significantly higher compatibility and antifungal activity than the marketed formulation.

Keywords: Modified solvent emulsification technique, factorial design, butenafine, *aloe vera* gel, natural origin lipid, surfactant, *in vitro* antifungal activity.

INTRODUCTION

Fungal infections are one of the most common skin diseases in the global population. According to an unpublished survey by the International Foundation of Dermatology, superficial mycosis was usually reported as one of the three most common diseases among the community patterns of skin diseases in nine different countries across the world.[1] Human skin has favorable conditions forthe growth of dermatophytes[1]. Dermatophyte fungi

*Correspondence: sapana.58ahirrao@gmail.com, Phone: +919623854577, ORCID-ID: orcid.org/0000-0002-2532-5392
Received: 19.06.2023, Accepted: 28.08.2023

invade the stratum corneum. Dermatophytes areenriched with keratinolytic, proteolytic and lipolytic activity.[2] Dermatophytes also contain serine proteinases that play a major role in breaching the skin barrier. Invasion of the skin involves two basic mechanisms-Colonization and Host-parasite interaction. During the colonization phase, the host begins to respond immunologically, and the first detectable immune response is cell-mediated immunity (CMI), which is characterized in colonized skin by an intense inflammatory process. During the host-parasite interaction phase, CMI produces most of the pathology as an acute inflammatory type of dermatophytosis, which results in erythema and edema of the dermis and epidermis leadingto breaching epidermal integrity.[3]

Current medications for superficial fungal infections include various antifungal agents. Oral toxicity of antifungal drugs and the treatment of fungal infections in the stratum corneumfocus on topical delivery of antifungal agents. Topical treatment has several advantages over oral and systemic delivery. Still, it has some pitfalls, such as side effects, diffusion of the drug across biological tissues, drug and biological cell interactions, and residence time of conventional dosage forms. Novel colloidal drug delivery systems have been developed to overcome the limitations of the conventional route. Among the various colloidal carriers solid lipid nanoparticles (SLN) have shown promising healing abilities against skin infections.

Butenafine hydrochloride (BUTE) is a synthetic allylamine antifungal agent. The suggested mode of action is that inhibits the enzyme squalene monooxygenase, which is responsible for converting squalene to 2,3-oxide squalene. Hence, it interferes with the biosynthesis of ergosterol, resulting in increased cellular permeability and leakage of cellular contents. Blockage of squalene monooxygenase causes squalene accumulation and leads to a fungicidal effect.[4,5] The observed side effects of BUTE include contact dermatitis, erythema, irritation, burning, and itching at the site of application.[6] To mitigate the side effects of BUTE and the symptomatic effects of fungal infection, such as inflammation, stinging, and itching, a possible combination of BUTE and agents with anti-inflammatory activity can be applied. Topical steroids provide rapid symptomatic relief but are associated with many steroid-related complications like atrophy, purpura, and rosacea.[7] Hence, to provide better therapeutic and pharmacological effects for fungal infection, the present workaimed to formulate BUTE-SLN having natural lipid and surfactant incorporatedinto *aloe vera* gel, which has in-built anti-inflammatory, antioxidant, and healing properties that showed synergistic effects. The present research work can be used to develop natural excipient-based SLN of BUTE using a modified solvent emulsification technique and to evaluate the competence of *aloe vera* nanolipidgels for the enhancement of the penetration of BUTE.

MATERIALS AND METHODS

Materials

Butenafine was a kind gift from Cipla Pvt. Ltd., Mumbai (India). Olivem 1000 as a lipid and Olivem 300 as a surfactant were generous gifts from Chemhouse Marketing, Mumbai. D-α tocopheryl polyethylene glycol succinate (TPGS) was purchased from BASF India Ltd., Mumbai. Stearyl amine was purchased from Sigma-Aldrich GmbH (St. Louis, MO) and other chemicals, such as stearic acid, glyceryl monostearate, tween 80, acetone, dimethyl sulfoxide, and poloxamer 188, were of analytical grade and purchased from Merck Chemical Company (Mumbai, India).

Optimization of surfactant, solid lipid, and organic solvent concentrations/effects of variables

To determine the influence of the concentration of different ingredients on the properties of butenafine-loaded solid lipid nanoparticles (BUTE-SLN), 3-factor 2-level factorial experimental design was employed using Design Expert software 8.0.1 (Stat-Ease, Inc., Minneapolis, MN, USA). On the basis of the solubility study and pre-optimization study, various variables at different levels were selected. The effects of three independent variables concentration of surfactant Olivem 300 (X_1), concentration of lipid Olivem 1000 (X_2), and concentration of organic solvent (X_3), were determined on the formulation of nanoparticle dispersions in terms of five responses: particle size (Y_1), polydispersity index (PDI) (Y_2), zeta potential (ZP) (Y_3), percent entrapment efficiency (EE) (Y_4), and percent drug loading (DL) (Y_5). All eight possible combinations of the three factors at two different levels were evaluated for each response. All nine experimental runs, different independent variables with two levels [*i.e.*, low (-1) and high (+1)], and obtained responses are presented in Table 1. Using the Design Expert software, response surface plots were generated to identify the influence of significant variables.

Preparation of BUTE-SLN

A Simple and easily accessible method was adopted to prepare BUTE-SLN. A modified solvent emulsification technique was used, and a BUTE-SLN dispersion was prepared for the solubility and compatibility studies of lipids, drugs, and excipients. BUTE-SLN is composed of the natural excipients from the natural stearin fraction of olive as lipid Olivem 1000 and surfactant Olivem 300. BUTE-SLN was prepared by dissolving butenafine in acetone and dimethyl sulfoxide (DMSO) (1:1) and then mixing it with stearyl amine and lipid Olivem 1000 at 80 °C. The water phase containing TPGS and surfactant Olivem 300 was maintained at 80 °C, similar to the lipid phase. The lipid phase was added to the aqueous phase with constant stirring at 2000 rpm for 1 hour followed by sudden cooling of the dispersion.

Table 1. Independent variables and their levels of 23 factorial design for formulation of BUTE-SLN

Factors	Levels	
	Low (-1)	High (+1)
Surfactant concentration % (X1)	2	4
Concentration of lipid % (X2)	3	5
Concentration of organic solvent % (X3)	0.5	1.5

BUTE-SLN: Butenafine hydrochloride-solid lipid nanoparticles

Physicochemical characterization of BUTE-SLN dispersion

Particle size analysis (PS) and PDI

The particle size in the nanometric range can be determined by the concept of dynamic lightscattering. The particle size and PDI of the optimized BUTE-SLN were determined by photon correlation spectroscopy (PCS) using a Zeta sizer (Nano ZS 90, Malvern Instruments, UK) at 20 °C using 900 scattering optics.[8,9]

ZP

The ZP of the SLN dispersion was determined using a Zetasizer (Nano ZS 90, Malvern Instruments, UK) at 2 °C with an electric field strength of 23 V/m 10, 11, 12. The BUTE-SLN samples were diluted with double-distilled water.

EE and DL

EE% of butenafine in BUTE-SLN can be calculated by determining the concentration of butenafine in the supernatant of the SLN dispersion. An ultracentrifuge was used to determine the concentration of un-entrapped butenafine in an aqueous BUTE-SLN dispersion. 1.5 mL of BUTE-SLN dispersion was filled in Eppendorf tubes, and the speed of cooling ultracentrifuge (Remi Instruments Ltd., Mumbai, India) was maintained at 60,000 rpm for 45 minutes at 4 °C. An ultraviolet (UV)-visible spectrophotometer (UV 1700, Shimadzu, Japan) was used to measure the concentration of butenafine in the aqueous phase at a wavelength of 224 nm. Equations (Eq.). (1) and (2) were used to measure the EE and DL percent values, respectively.[10-13]

$$\% EE = \frac{\text{Total mass of Bute} - \text{Total mass of Bute in Supernatant}}{Total\ mass\ of\ Drug} \times 100 \quad \text{Eq. 1}$$

$$\% DL = \frac{\text{Total mass of Bute} - \text{Total mass of Bute in Supernatant}}{Total\ mass\ of\ Lipid} \times 100 \quad \text{Eq. 2}$$

Transmission electron microscopy study (TEM)

Particle size, shape, and morphology were studied using TEM. In this study, the BUTE-SLN dispersion was mixed with water, and a drop of it was mounted on a copper grid coated with a thin film of carbon, which was then dried for 45 minute. A transmission electron microscope Philips CM200 (Philips, Netherlands) was used for scanning.

Screening of cryoprotectant

BUTE-SLN dispersion was freeze-dried by using mannitol as a cryoprotectant. The frozen (-25 °C) dispersions containing 5, 7.5 and 10% mannitol were lyophilized at 0.25 barfor 24 hours, and the temperature was increased from 15 °C to 0 °C. In the final step, drying was carried out for 2 hours at +15 °C and 0.01 bar and then stored at 4 °C. BUTE-SLN was further characterized for differential scanning calorimetry (DSC), X-ray diffraction (XRD) study, and fourier transform infrared spectroscopy (FTIR) studies.[14,15]

Characterization of lyophilized BUTE-SLN

DSC

The thermal behavior and interaction between the drug and its additives were studied using DSC. In a differential scanning calorimeter (DSC 1 STARe System, Mettler-Toledo, Switzerland), an empty standard aluminum pan was used as a reference, and scans wererecorded at a heating rate of 10 °C/minute in the range of 30 °C-300 °C. DSC studies were carried out on Butenafine pure drug, bulk lipid Olivem 1000, and lyophilized BUTE-SLNs of the optimized batch.

XRD study

XRD analysis was performed to study the spacing of the lattice planes in the crystals. The crystal structures of butenafine, pure lipid, and butenafine in SLN were determined by XRD analysis. A Philips PAN analytical expert PRO X-ray diffractometer (1780) was used for the study. A Cu-Ka radiation source was used, and the scanning rate was 2°/minute. XRD measurements were performed on butenafine pure drug, bulk lipid Olivem 1000, and lyophilized BUTE-SLNs from the optimized batch.

FTIR study

A Jasco FTIR spectrophotometer (Perkin Elmer Jasco FTIR-401, Japan) was used to determine the compatibility between excipients. FTIR studies were carried out on pure lipid Olivem 1000, butenafine, and SLN loaded with butenafine. The samples were examined in transmission mode over awavenumber range of 4000 to 400 cm^{-1}, using about 1-2 mg of sample mixed with dry potassium bromide.

Preparation of BUTE-SLN into semisolid formulation

BUTE-SLNs were formulated using *aloe vera* gel as a semisolid base. *Aloe vera* gel was formulated with the *aloe vera* extract of *Aloe barbadensis* along with highly pure and GRASS-grade stabilizers, antioxidants, and preservatives. After centrifugation of the dispersion, drug contentwas determined, and a BUTE-SLN dispersion equivalent to 0.1 g butenafine was added to *aloe vera* gel to prepare 1% gel.

Evaluation of BUTE-SLN gel

Rheological measurement

Viscosity

The rheological behavior and characteristic flow properties of formulated *aloe vera* gels incorporated with SLN dispersion were studied. A cone and plate rheometer (Brookfield viscometer AP 2000+2) was used to determine the effects of shear stress and shear rate on the SLN gels. To determinethe influence of storage temperature and the nature of the lipid matrix on the rheological behavior of BUTE-SLN-based *aloe vera* gel was investigated by recording the variation in shear stress at a pre-defined shear rate from 0 s-1 to 1000 s-1 as an up curve and 1000 s-1 to 0 s-1 as a down curve at three different temperatures (5 °C, 25 °C and 40 °C).

Spreadability

The BUTE-SLN-enriched gel was evaluated on the basis of its rheological pattern, film-forming ability, degree of consistency, and spreadability. Spreadability is an important parameter for assessing topical dosage forms because it represents the stability and particle-particle interaction. This study includes the use of a wooden block and a glass slide apparatus in which one rectangular wooden block is fixed with a glass slide. In the same apparatus, another movable glass slide was attached with a thread to pan through a pulley. The time was noted to separate the upper movable slide from the fixed slide was noted when a BUTE-SLN gel was placed between the slides. Spreadability was quantitatively determined as the ratio of time required to completely separate two glass slides according to the weight of the sample. Spreadability was computed using formulas.[16,17]

$$S = \frac{M \times L}{T}$$

Where,

S = spreadability

M = weight of the upper glass slide

L = glass slide length

T = time taken to separate the slides from each other

Occlusive study

An *in vitro* occlusion study was performed to determine the efficiency of BUTE-SLN gel in preventing water loss from the surface of the test assembly, which simulates transepidermal water loss from the skin. In this study, pre-weighed beakers of approximately the exact dimensions with 50 mL capacity were filled with 25 mL purified water and covered with Whatman Microfiber Filters 9.0 cm. For a comparative study, one beaker surface was spread with 0.25 g of BUTE-SLN gel, the other with plain gel without BUTE-SLN, and one beaker without any application was kept as a reference. All beakers were stored at 32 °C and 60 ± 5% relative humidity for 72 hours. The occlusion factor, F, was calculated for the formulation according to formula.[18]

$$F = 100 \times \frac{A - B}{A}$$

Where,

Here, A represents water loss in the absence of a sample

B represents water loss in the presence of the sample

Ex vivo skin hydration study

The *ex vivo* skin hydrating effect of BUTE-SLN was studied and compared with the conventional cream. The BUTE-SLN *aloe vera* gel and the marketed cream were applied to the prepared human cadaver skin. The skin samples were isolated after 24 hours of gel and cream application. The skin was vertically sliced using a microtome, stained with carbol fuchsin, and observed under an optical microscope to determine stratum corneum. An optical microscope equipped with an image analyzer was used to obtain the photomicrographs (Magnus MLX).[19]

In vitro drug diffusion study

In vitro drug release of BUTE-SLN was studied in Franz diffusion cells using a cellulose acetate membrane. Phosphate buffer (pH 7.4) and methanol (60:40) were used as the diffusion medium, andthe membrane was soaked in the diffusion medium for 30 minutes before placing the sample. Phosphate buffer (pH 7.4) and methanol (60:40) (10 mL) were placed in the receptor compartment of Franz diffusioncells. The diffusion medium in the receptor compartment was continuously stirred using a magnetic bar while maintaining the temperature at 37 °C. The experiment was started with the application of 0.5 g of BUTE-SLN gel on the surface of the cellulose acetate membrane from the donor compartment side. Sampling was performed after 0, 1, 2, 5, 7, 9, 12, and 24 hours, and a fresh diffusion medium was addedwith each withdrawal of the sample. The samples were diluted and analyzed by UV spectrophotometry at 224 nm.

Drug permeation

In vitro skin penetration and permeation experiments were performed using Franz diffusion cellson pig ear skin. Among rodents, the most relevant animal model for human skin is the pig. Pig ear skin has been proven thave similar histological and biochemical properties, vascular anatomy, and stratum corneum contents to human skin, thereby giving comparable results to human skin. Fresh pig ears were obtained from a local slaughter house. Pig ears were washed with distilled water, and subcutaneous adipose tissue was removed. The skin was placed between the donor and receptor compartments of Franz diffusion cells, exposing the dermal side to the receptor compartment and stratum corneum in contact with the donor compartment. Sink conditions were maintained in the receptor compartment using diffusion fluid. The cell temperature was maintained at 37.0 ± 0.1 °C. The BUTE-SLN gel equivalent to 1% of the drug was applied on the membrane in the donor compartment, ensuring close contact with the skin. Sampling was performed at 0, 1, 2, 5, 7, 9, 12, and 24 hours. At each point, 1 mL aliquots were drawn from the receiver compartment, and an equivalent volume of the receptor fluid was simultaneously replaced. The amount of butenafine in the diffusion medium was determined by UV irradiation. A graph of cumulative percent drug release vs. time and another graph of the amount of BUTE diffused per unit area (Q/A) vs. time (h) were plotted. Excess BUTE amount found on the surfaceof the skin and in the entire dosing area was determined. The amount of unabsorbed drug on the skin was also quantified.[20,21]

In vivo skin retention study

BUTE-SLN gel (0.25 g) was applied to the shaved skin of albino rats. After 24 hours, the animals were humanely sacrificed, and their skin was collected. The applied formulation was removed, the stratum corneum layer was stripped away with adhesive tape, and the epidermis layer was differentiated using the heat separation technique. The presence of butenafine in different skin stratawas extracted and quantitatively determined.[22]

Skin irritation study

The primary skin irritation of the SLN-based butenafine gel was evaluated using an acute skin irritation test according to OECD

guidelines #404. The protocol for the study was approved by the Pravara Rural College of Pharmacy (approval number: 2013714-543, date: 07.01.2014). 2.5-3.0 kg healthy male New Zealand white rabbits were used in the study. Animals were categorized into four groups: positive control (formalin), plain butenafine gel, marketed formulation, and BUTE-SLN gel. 0.5 g of each test sample was applied to the hair-free shaved area of the skin, *i.e.*, right side of the trunk (approximately 6 cm^2), and covered with a gauze patch. The left side of the trunk was kept as an untreated skin area to serve as a control. After 1 hour of exposure to the test sample, the rabbits were observed for signs of erythema, edema, and irritation. The degree of irritation, erythema, and edema were assessed and scored according to the Grading of skin reactions according to the OECD guidelines. Data were recorded at interval of 24 hours, 48 hours and 72 hours after patch removal.[23]

Antifungal activity

An in vitro antifungal activity study was conducted against *Candida albicans* using a modified agar diffusion method. Fresh *C. albicans* cultures were prepared and then incubated in the dark at 37 ± 2 °C for 48 hours. The *in vitro* antifungal activity of blank gel, BUTE-SLN gel, plain butenafine gel, and the marketed formulations was studied. The formulations were mixed with potato dextrose agar and poured into a spherical ditch made using a sterile borer on an agar plate under sterile conditions. The plates were dried and incubated for 48 hours at 37 ± 2 °C. At the end of the incubation, the inhibition zone was measured.[23-26]

Statistical analysis

The effect of various independant variables on dependant variables of BUTE-SLN formulations was optimized using 23 factorial design and analyzed statistically using Design-Expert software (Version 8.0.1., Stat-Ease Inc., and Minneapolis, MN). The multiple linear regression analysis was used to generate polynomial models including interaction and regression equations for all response variable. Statistical significance of the suitable model selected by software were analyzed by analysis of variance (ANOVA) based on p value and regression analysis. The 3D response graphs were constructed using Design-Expert software. The model was validated using numerical optimization. The observed responses were coincided well with the predicted values given by optimization technique.

RESULTS

Effects of different variables on the preparation of BUTE-SLN and the optimization of the surfactant, solid lipid, and organic solvent concentrations.

A 2^3 factorial design was used to determine the effects of various variables on the optimization of the BUTE-SLN. The

Table 2. 2^3 factorial design for formulation of BUTE-SLN

Run code	Concentration of lipid % (X1)	Concentration of surfactant % (X2)	Concentration of organic solvent % (X4)
1	2	5	1.5
2	4	5	0.5
3	4	3	0.5
4	2	3	1.5
5	2	3	0.5
6	4	5	1.5
7	4	3	1.5
8	2	5	0.5

BUTE-SLN: Butenafine hydrochloride-solid lipid nanoparticles

Table 3. Observed responses of eight experimental formulations (2^3 factorial design)

Run code	Particle size nm	PDI*	ZP (mV)	% EE*	% DL*
1	271 ± 2.74	0.368 ± 0.014	20.2 ± 0.32	91.2 ± 1.82	18.33 ± 0.79
2	258 ± 3.61	0.267 ± 0.009	24.9 ± 0.41	91.65 ± 1.69	18.24 ± 0.86
3	231 ± 2.79	0.254 ± 0.012	17.8 ± 0.43	88.95 ± 2.17	21.05 ± 0.35
4	250 ± 3.65	0.324 ± 0.009	12.3 ± 0.22	88.29 ± 1.73	22.86 ± 0.46
5	245 ± 4.12	0.241 ± 0.005	11.7 ± 0.16	87.45 ± 2.26	21.33 ± 0.78
6	278 ± 3.19	0.369 ± 0.01	22.4 ± 0.26	89.25 ± 1.58	15.2 ± 0.31
7	239 ± 2.37	0.33 ± 0.009	17.23 ± 0.39	88.41 ± 1.42	22.16 ± 0.91
8	269 ± 4.26	0.264 ± 0.009	21.5 ± 0.31	90.46 ± 2.36	15.05 ± 0.58

*Each value represents as mean ± standard deviation
PDI: Polydispersity index, ZP: Zeta potential, EE: Entrapment efficiency, DL: Drug loading

eight formulations were obtained with a possible combination of surfactant concentration X_1, concentration of lipid X2 and concentration of organic solvent X3 as independent variables with low and high levels, as shown in Tables 1, 2. The responses Y1, Y2, Y3, Y4, and Y5 were found to be in the range of 231-278 nm, 0.241-0.369, 11.7-24.9 mV, 87.45-91.65% and 15.05-22.86% respectively as shown in Table 3. The observed responses were fitted to various models using the Design Expert software. The dependent variables show that the models were important for all measured responses, as determined by the negligible lack of fit ($p < 0.05$) ANOVA results. It was observed that independent variables X_1, X_2, and X_3 had positive as well as negative influences on selected dependent variables such as particle size, PDI, ZP, EE, and DL (see Eq. 3 to 7).

$$\text{Particle size}=+255.625-3.125*X_1+14.375*X_2+3.875*X_3+3.125*X_1X_2+2.125*X_1X_3 \quad \text{Eq. 3}$$

$$\text{Polydispersity index}=+0.302125+0.002875*X_1+0.014875*X_2+0.045625*X_3-0.001125*X_1X_3+0.005875*X_2X_3 \quad \text{Eq. 4}$$

$$\text{Zeta Potential}=+18.5038+2.07875*X_1+3.74625*X_2-0.47125*X_3-0.67875*X_1X_2+0.47875*X_2X_3 \quad \text{Eq. 5}$$

$$\text{Entrapment Efficiency}=+89.7075-0.17*X_1+1.1825*X_2+0.3575*X_3-0.565*X_1X_3-0.2975*X_2X_3 \quad \text{Eq. 6}$$

$$\text{Drug Loading}=+18.8625-0.21*X_1-1.7075*X_2-1.585*X_3+0.175*X_1X_2 \quad \text{Eq. 7}$$

As per the ANOVA analysis, near-100% desirability was found to be at predicted values of 264 nm for Y_1, 0.270 for Y_2, 24.60 mV for Y_3, 91.225% for Y_4, and 18.705% for Y_5 with a surfactant concentration of 4%, concentration of lipid 5% and concentration of organic solvent 0.5%. To confirm and reproduce the predicted model, the optimized values of the independent variables were applied, and the observed responses were measured, as shown in Table 4. The observed values of Y_1, Y_2, Y_3, Y_4, and Y_5 were 261.25 nm, 0.268, 23.98 mV, 91.35%, and 19.692%, respectively, which were in close agreement with the predicted values, demonstrating the reliability and reproducibility of this method. The effects of various independent variables on the dependent variables were expressed using the 3D graphical presentation shown in Figure 1.

Physicochemical characterization of BUTE-SLN dispersion

PS and size distribution

The effects of various formulation components and process variables on the preparation of SLN can be observed from the particle size and PDI of BUTE-SLN gel, as depicted in Table 3. The particle size and PDI of BUTE-SLN increased with increasing lipid content. The range of particle size and PDI of the BUTE-SLN were observed to be 231 ± 2.79 nm to 278 ± 3.19 nm and 0.241 to 0.369, respectively. The particle size and PDI of optimized batch was found to be 261.25 ± 2.38 nm and 0.268 ± 0.01 respectively.

ZP

ZPs indicate the stability of the nanoparticles in SLN dispersion. The ZPs of all nine batches were found to be 11.7 ± 0.16 mV and 24.9 ± 0.41 mV, and for the optimized batch, it was observed to be 23.98 ± 0.27 mV.

EE and DL

Different concentrations of lipid and organic solvent showed significant effects on the EE and DL of butenafine loading in lipid nanospheres. The EE of BUTE was found to be higher in the selected formulation. The EE of eight formulations from run 1 to run 8 were found to be in between 87.45 ± 2.26% to 91.65 ± 1.69% with the DL in between 15.05 ± 0.58% to 22.86 ± 0.46%. The EE and DL of the optimized formulation were found to be 91.35 ± 2.35% and 19.692 ± 0.95%, respectively.[10,13]

TEM Imaging

With similar results to those obtained for PS, the TEM image of BUTE-SLN (Figure 2) revealed the presence of spherical nanometric-range particles.

Screening of the cryoprotectant

The cryoprotectant concentration was optimized on the basis of SLN aggregation, time of reconstitution, and particle size distribution upon reconstitution. From the different concentrations of cryoprotectant screened for lyophilization, mannitol at 5% *w/w* resulted in good lyophilized product upon reconstitution with quick reconstitution, no aggregation, and less difference in particle size distribution (PDI).[14,15]

Characterization of lyophilized BUTE-SLN

DSC

The thermal profiles of bulk lipid, pure butenafine, and lyophilized drug-loaded SLN formulation are given in Figure

Table 4. Observed and predicted responses for optimized formulation parameters

Reponses	Constraints	Set observed values*	Predicted values	Error %
Particle size (nm)	Minimize	261.250±2.38	264	1.041
PDI	Minimize	0.268±0.01	0.27	0.7407
ZP (mV)	Minimize	23.98±0.27	24.60	2.5203
EE %	Maximize	91.35±2.35	91.225	1.370
DL %	Maximize	19.692±0.95	18.705	5.2766

*Each value represents as mean ± standard deviation, PDI: Polydispersity index, ZP: Zeta potential, EE: Entrapment efficiency, DL: Drug loading

3[1]. The melting point of bulk lipid Olivem 1000 was determined using a DSC thermogram that showed a high endothermic peak at 63.20 °C (curve A). A sharp endothermic peak at 217.35 °C was observed on the second thermogram of pure butenafine. The endothermic peak wasobserved for BUTE-SLN at 46.91 °C, indicating the transformation of crystalline lipids and drugs into amorphous forms with numerous lattice defects in which the drug is encapsulated.[14]

X-ray Diffraction (XRD) analysis

The XRD patterns of the drug butenafine (a), lipid Olivem 1000 (b), and BUTE-SLN (c) areshown in Figure 3.[2] Pure butenafine showed a sharp peak, which is indicative of its crystalline nature. Lipid Olivem 1000 also showed a sharp peak revealing the crystalline nature of the lipid crystals. BUTE-SLN showed broad peaks instead of sharp ones, indicating an amorphous nature. All the major characteristicpeaks of butenafine and lipid

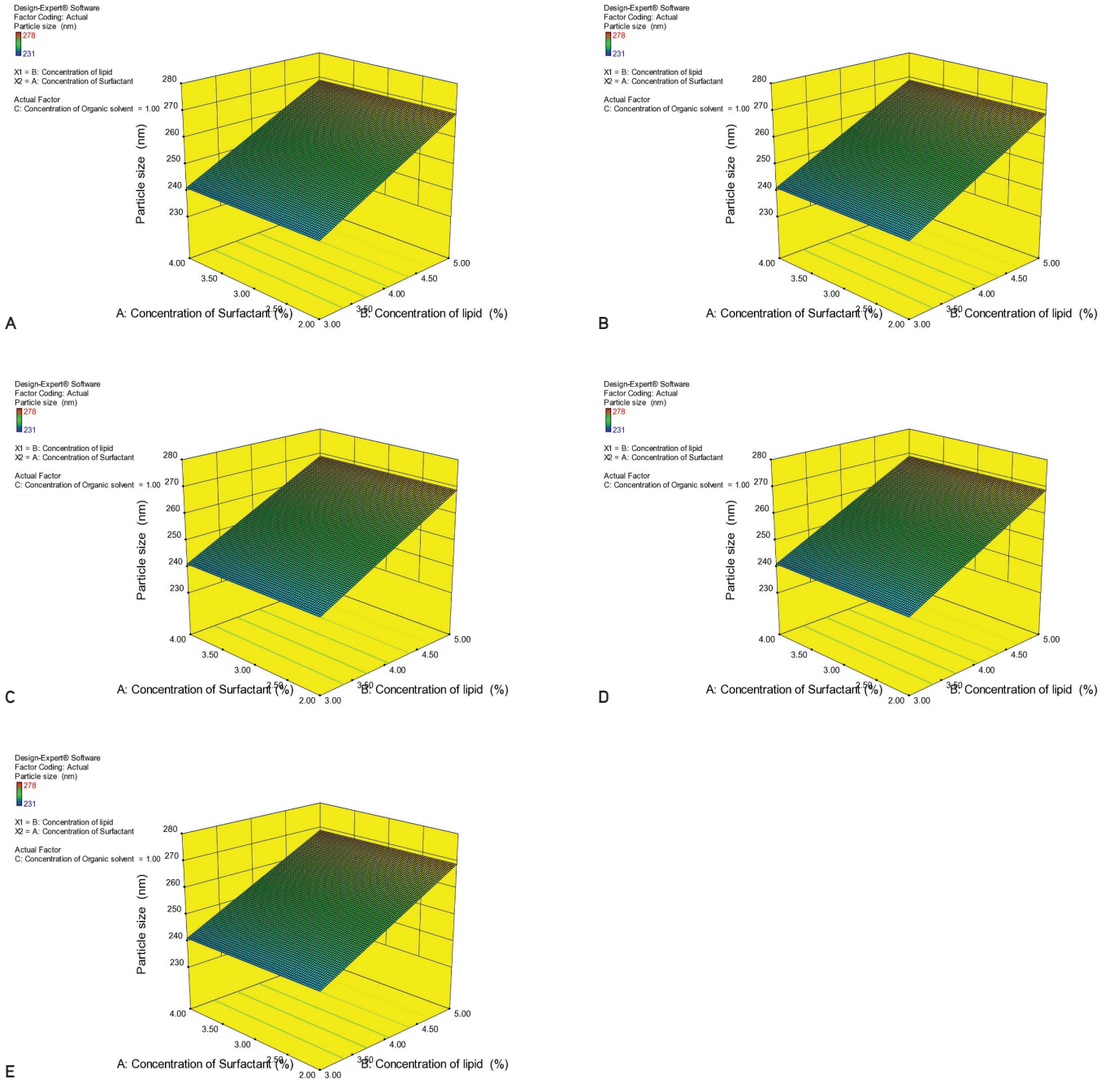

Figure 1. 3D response surface plot of BUTE-SLN showing. A) Effect of lipid Olivem 1000 and surfactant Olivem 300 on the particle size, B) Effect of lipid Olivem 1000 and organic solvent on the polydispersity index, C) Effect of lipid Olivem 1000 and surfactant Olivem 300 on the zeta potential, D) Effect of surfactant Olivem 300 and lipid Olivem 1000 on the percent entrapment efficiency and E) Effect of organic solvent and surfactant Olivem 300 on the percent drug loading

BUTE-SLN: Butenafine hydrochloride-solid lipid nanoparticles

Olivem 1000 were absent in BUTE-SLN. The presence of broad and small XRD peaks reveals the existence of butenafine and lipid Olivem 1000 in BUTE-SLN in the amorphous state.

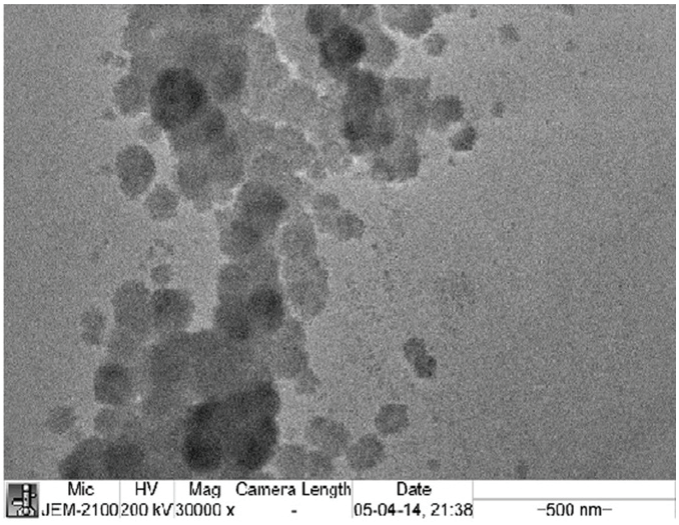

Figure 2. TEM image of BUTE-SLN

TEM: Transmission electron microscopy, BUTE-SLN: Butenafine hydrochloride-solid lipid nanoparticles

FTIR

The FTIR spectra of butenafine, pure lipid Olivem 1000, and BUTE-SLN are compared in Figure 4. The FTIR spectra indicated amorphization of the drug and lipid in the formulation.

BUTE-SLN showed no new peaks, revealing that there was no interaction between the formulation ingredients and no structural or functional changes in the formulation.

Preparation of BUTE-SLN into semisolid formulation

Instead of a conventional semisolid dosage form, we have formulated BUTE-SLN for incorporation into *aloe vera* gel. *Aloe vera* gel has been used for the external treatment of mild wounds as well as inflammatory skin diseases for a long time, with the aim of speeding up the healing process and reducing inflammation and tissue scarring. Mild skin irritation can be treated with this gel. Here, an attempt has been made to formulate a semisolid product that will have synergetic antifungal effects as well as anti-inflammatory, wound healing, and skin irritation effects by aloe *vera gel.*[24-26]

Evaluation of BUTE-SLN gel

Rheological measurement

Viscosity

The viscosity of any semisolid formulation depends on its adhesion, ease of application, and spreadability. The results

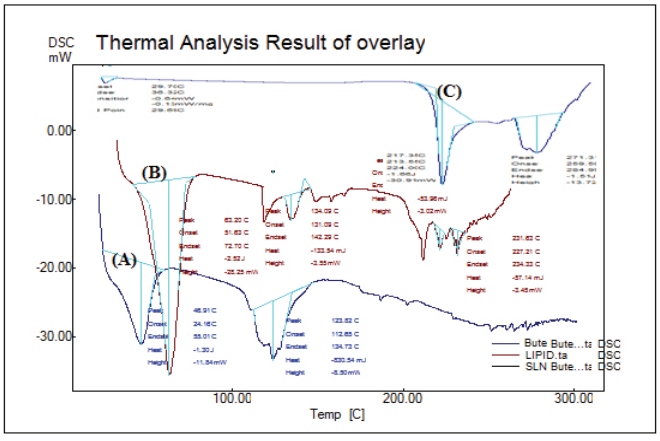

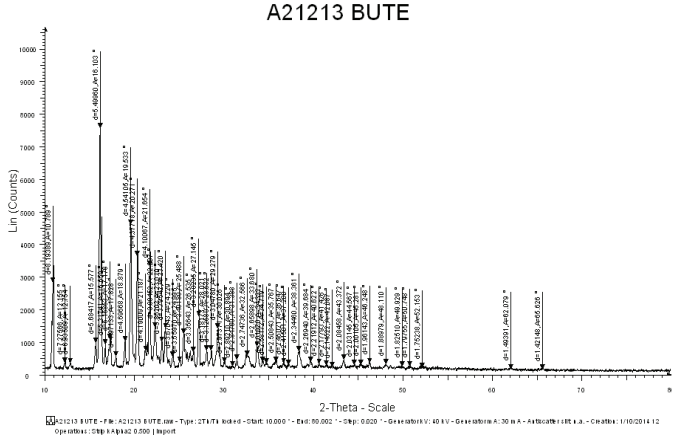

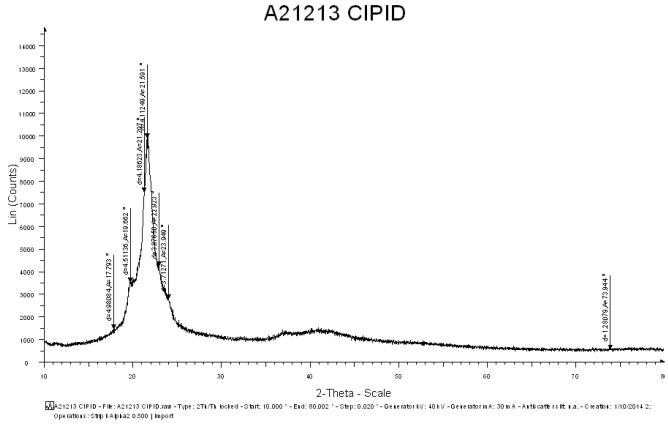

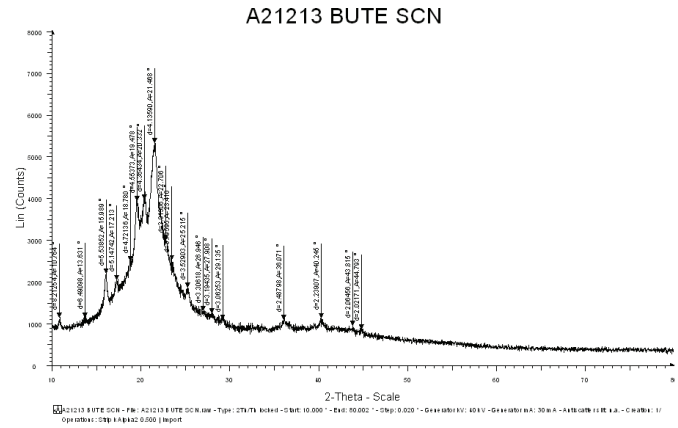

Figure 3. (1) DSC thermogram of sample, A) Butenafine, B) Pure lipid Olivem 1000, C) BUTE-SLN; (2) Comparison of XRD patterns: I. Butenafine, II. Lipid Olivem 1000; III. BUTE-SLN

DSC: Differential scanning calorimetry, BUTE-SLN: Butenafine hydrochloride-solid lipid nanoparticles, XRD: X-ray diffraction

were recorded for the BUTE-SLN *aloe vera* gel at 5 °C, 25 °C and at 40 °C after the storage of one week to check the consistency and compatibility of the gel with pharmaceutical excipients. A slight increase in the viscosity of the BUTE-SLN gel was observed compared to plain *aloe vera* gel due to existence of nanometric particle size of SLN and the polysaccharide crosslinking with the lipid component of SLN. The increase in total lipid content and particle size increases the viscosity of the gel. when a BUTE-SLN gel was placed between the slides. The spreadability of the BUTE-SLN gel was evaluated by placing it between two slides. The results showed that its spreadability was superior to that of pure aloe vera gel.

Spreadability

The potential application of semisolid topical dosage forms with desired consistency and adhesion onto skin was studied according to the spreadability values. Nanometric and uniform particle sizes lead to good spreadability, forming a uniform layer on skin. The presence of BUTE-SLN did not cause any changes in spreadability. The spreadability value of BUTE-SLN was found tobe 4.6 ± 0.37 s/g, and that for the plain gel base was 4.06 ± 0.41 s/g. A slight increase in the spreadability value indicates that SLN forms a 3D structure with a polysaccharide group, which leads to an increase in the viscosityand spreadability.

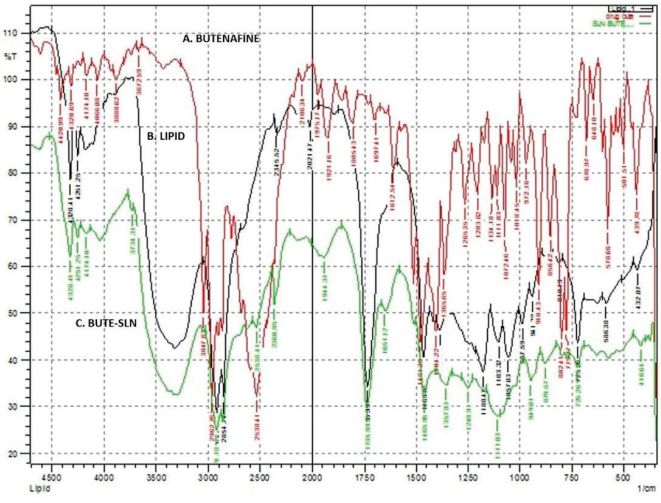

Figure 4. Comparative FTIR spectra of A) Butenafine, B) Lipid Olivem 1000 and C) BUTE-SLN

FTIR: Fourier transform infrared radiation, BUTE-SLN: Butenafine hydrochloride-solid lipid nanoparticles

Occlusive study

Successful topical drug delivery is based on the occlusive and skin hydration ability of semisolid formulations. Figure 6A shows a comparison of BUTE-SLN versus plain gel effects. After the 6 hours, 24 hours, 48 hours, and 72 hours study, occlusion factor F were found to be 31.362 ± 0.65%, 41.1372 ± 0.47%, 43.2659 ± 0.28%, and 45.7 ± 0.44%, respectively, as shown in Figure 6A. Whilst that of plain gel F were found to be 18.2795 ± 0.55%, 23.0020 ± 0.59%, 31.2094 ± 0.21% and 31.5209 ± 0.29% when compared to the control. BUTE-SLN showed higher occlusion factor *f* values in comparison to the plain gel owing to its high lipid content, which forms an impermeable layer on the surface of the skin.

Ex vivo skin hydration study

Using an optical microscope and image analyzer, the skin hydrating response of the SLN formulation was investigated in human cadaver skin and compared with that of the marketed cream Fintop® (Magnus MLX). This data analysis aimed to compare the effects of SLN gel and the marketed cream Fintop® on the stratum corneum, which is associated with skin moisturization and drug penetration. Figure 6B I shows a photomicrograph of untreated human cadaver skin. The photomicrograph's dark brown left side layer reflects the skin's top layer (*i.e.*, stratum corneum). The thickness of the stratum corneum changed significantly after the application of the marketed cream Fintop®, as seen in Figure 6B II. In contrast, the application of the gel enriched with SLN resulted in a substantial improvement in the thickness of the stratum corneum, nearly 3-fold when compared with the marketed

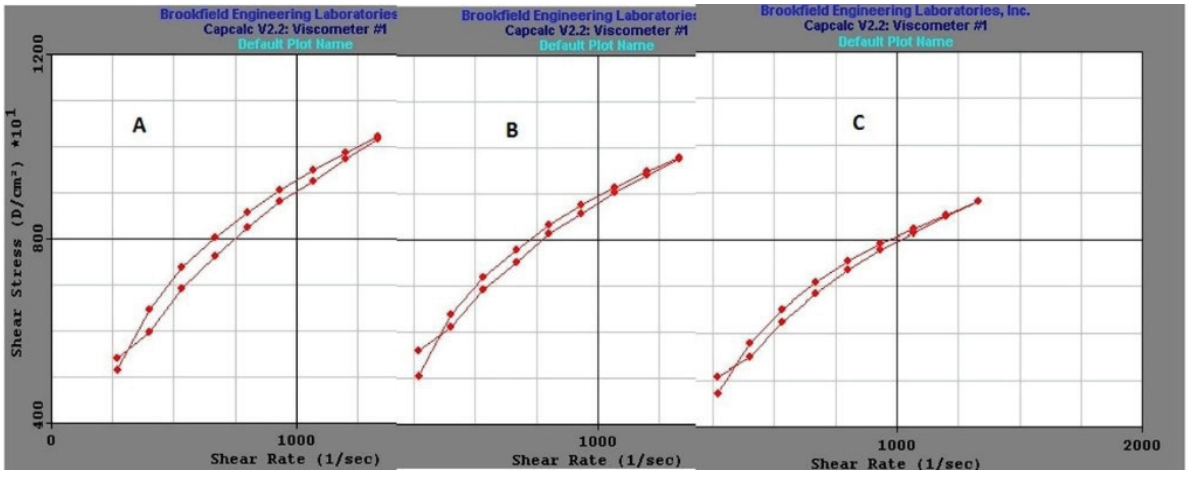

Figure 5. Effect of temperature on the viscosity of BUTE-SLN-enriched gel at A) 5°C, B) 25°C, and C) 40°C

BUTE-SLN: Butenafine hydrochloride-solid lipid nanoparticles

cream and 3.5-fold when compared with the untreated skin (Figure 6B).

In vitro drug diffusion study

BUTE-SLN was evaluated against Fintop® cream in an *in vitro drug release* study.The release pattern of butenafine from SLN was initially faster and was sustained after 2 hours. Sustained drug release from gels is further useful for maintaining drug release depots[27]. The marketed cream exhibited a more controlled release than the SLN gel (Figure 7A).

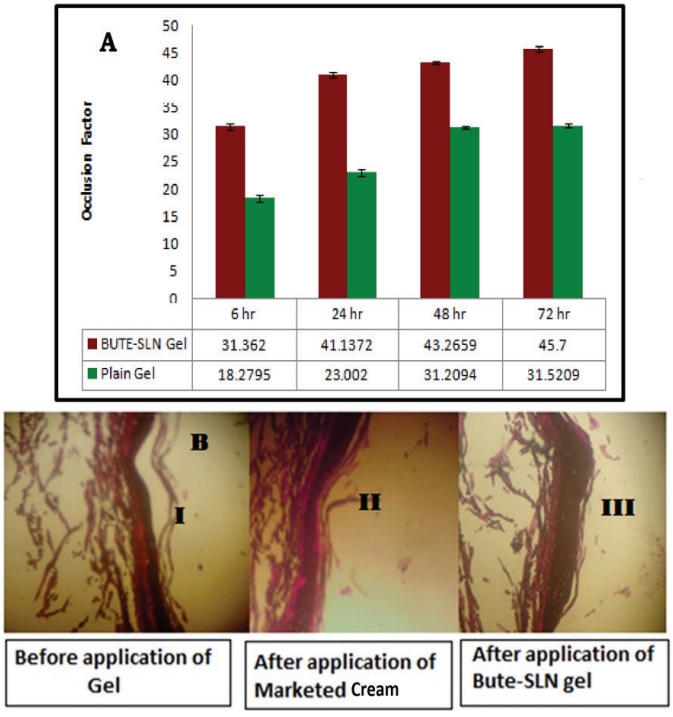

Figure 6. Comparison of the occlusion factor of BUTE-SLN-enriched gel and plain gel, B) Photomicrograph showing the skin hydrating potential of BUTE-SLN gel compared with a marketed cream and untreated human cadaver skin

BUTE-SLN: Butenafine hydrochloride-solid lipid nanoparticles

Drug permeation

The ability of BUTE-SLN to permeate pig ear skin was studied. The plot of the cumulative amount of drug permeated showed a 5.42-fold higher drug release for the BUTE-SLN gel compared with the reference cream. The flux value calculated from the linear portion of graph Q/A vs. time (Figure 7B) from SLN gel was found to be 1666.7 ± 0.198 ng $cm^{-2}h^{-1}$ and 818.181 ± 0.392 ng $cm^{-2}h^{-1}$ for reference cream.[27] Results of quantification of butenafine after 24 hours were expressed in percentage of the undiffused, deposited, and permeated drug through the skin, as depicted in Figure 8.

In vivo skin retention studies

The drug content in various epidermal layers was quantitatively estimated according to procedures or methods described in the literature. Butenafine was extracted into methanol from the stratum corneum by the tape stripping method. The epidermis was separated using the heat-separation technique for drug content. Using the UV spectrophotometer as an analytical method, the amount of butenafine present in different skin strata was depicted in the percent of the skin, as shown in Figure 8.

Skin irritation study

In a rabbit skin irritation analysis, the formulation did not display any signs of skin irritation, such as redness or inflammation, at the application site (erythema). As a result, it can be assumed that all the tested formulations are safe for topical use.

In vitro antifungal activity

The antifungal activity of butenafine was measured *in vitro* against *C. albicans* NCIM 3471 with the goal of evaluating the effect of process parameters on the intensity (potency) of butenafine and studying its antifungal activity in terms of the inhibition zone. In this study, the extract of BUTE-SLN equivalent to 500 µg/mL was compared with a marketed cream dilution equivalent to 500 µg/mL and different standard drug dilutions. From the present investigation, the test sample with a strength equivalent to 500 µg/mL showed a greater zone of inhibition (32 mm) comparedwith the standard 500 µg/mL butenafine solution (30 mm), as shown in Figure 9.

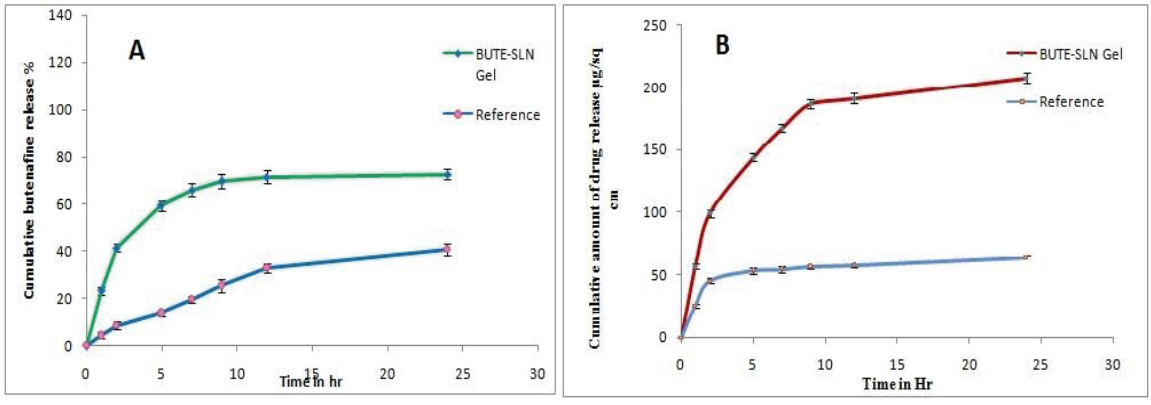

Figure 7. A) *In vitro* drug release profile of BUTE-SLN gel and its reference, B) *In vitro* skin permeation profile of BUTE from SLN gel and reference

BUTE-SLN: Butenafine hydrochloride-solid lipid nanoparticles

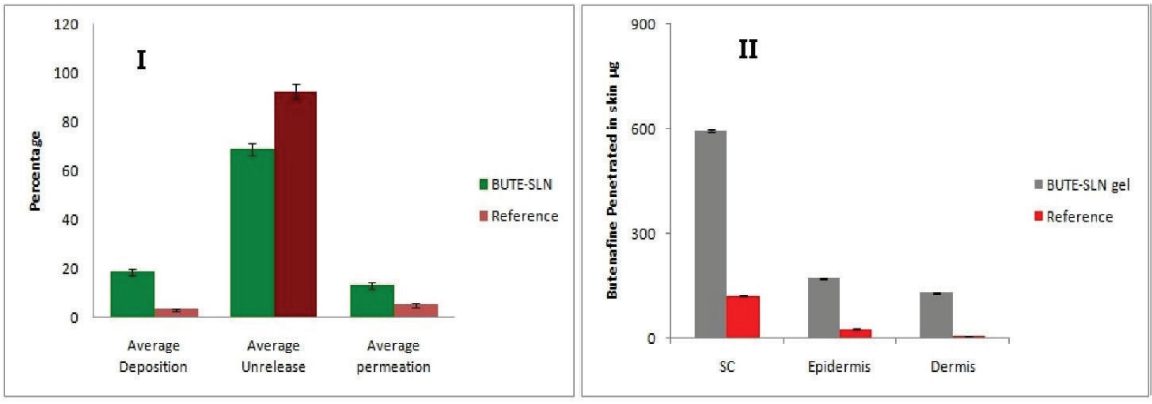

Figure 8. I) Percentage of drug permeated, deposited, and remaining unabsorbed in the skin, II) *In vivo* drug retention in different skin strata
BUTE-SLN: Butenafine hydrochloride-solid lipid nanoparticles

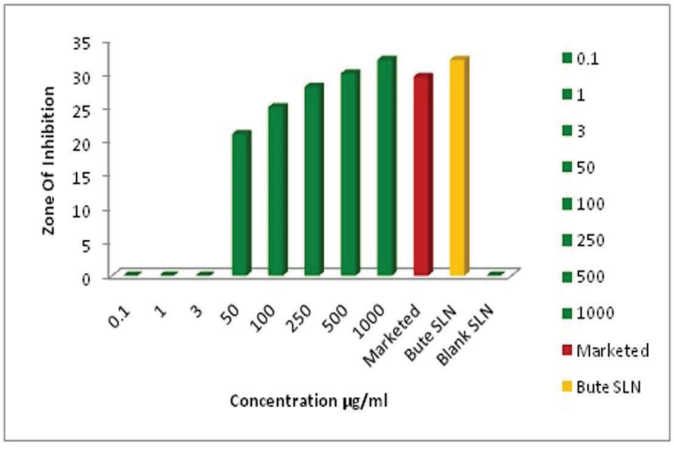

Figure 9. Comparative antifungal activity of different butenafine dilutions with marketed and BUTE-SLN formulation
BUTE-SLN: Butenafine hydrochloride-solid lipid nanoparticles

DISCUSSION

The objective of this study was to develop and evaluate antifungal drug BUTE-SLNs for treating topical fungal infections. The novelty of this work is the use of novel excipients such as natural surfactants and lipids, the use of organic solvents in the fabrication of SLN, and the very simple and novel modified solvent emulsification method of preparation.

The particle size model revealed that the concentrations of lipids, surfactants, and organic solvents and their interactions significantly affect the formation of nanometric particles. The response surface plot for the effect of factor X_1 and factor X_2 on particle size (Y_1) of BUTE-SLN is shown in Figure 1A. Changes in lipid concentration, in particular, resulted in increased particle size, whereas increases in surfactant concentration had negligible effects on particle size. The increase in particle size is attributed to an increase in lipid concentration, which allows the primary emulsion's globule size to increase. The smaller droplets enter the emulsion and redeposit onto the surface of nanoparticles to reach a more thermodynamically stable state. An insufficient surfactant concentration could not cover the formed new interfaces, resulting in an increase in particle size. The involvement of organic solvents in the BUTE-SLN formulation was a possible explanation for the increase in surfactant concentration, which contributed to a small increase in particle size. The surfactant present in the SLN formulation is in equilibrium with the organic solvent; hence, the surfactant covers the SLN at the interface and reduces the interfacial tension so that nano-lipid particles are formed, but the additional rise in surfactant concentration goes into organic solvent; hence, the rise in surfactant slightly increases the particle size.[28]

The regression equation no.4, generated for the PDI was significant, with an *f* value of 240.33 ($p < 0.0001$). The PDI model revealed that the percent concentration of lipids and organic solvents and their interactions have a significant impact on the PDI. The response surface plots (Figure 1B) illustrate that the PDI increases as organic solvent and lipid concentration (%) increase. An increase in organic solvent concentration causes non-uniform precipitation of SLN (heterogeneous SLN dispersion), leading to the deposition of smaller particles on larger particles as per the phenomenon of Ostwald ripening. This resulted in variable particles with bi-or tri-modal size distributions; hence, PDI increased.

The regression equation no.5, generated for the ZP was significant, with an *f* value of 87.80 ($p < 0.0001$). The model generated for ZP revealed that only the lipid concentration had a significant impact on ZP. The response surface plot in Figure 1C shows that increasing the lipid concentration lowers the ZP while increasing the surfactant concentration has less of an impact on particle charge. The charge on the nanolipid dispersion is the most important factor for the stability of the formulation of any colloidal system. Generally, particles with a ZP of ± 30 mV could be considered stable due to the electric repulsion between the particles.[11] The individual ZPs of the BUTE-SLN ingredients were -16.9 mV for butenafine, -4.81 mV for surfactant, and 20.5 for lipid Olivem 1000. From the given data, we can predict that lipids have a greater influence on ZP. The surfactant reduces the negative charge on the ZP of

particles. The surface-covered butenafine, surfactant, TPGS, and organic solvent collectively induce negative charges.

The regression equations no. 6 and 7 generated for EE and DL were significant with *f* values of 848.75 and 12.22, respectively ($p < 0.0001$). Figure 1D and Figure 1E demonstrate the response surface plots of the effect of surfactant and lipid concentrations on EE and the effect of organic solvent and surfactant concentrations on DL, respectively. The increase in the concentration of lipid showeda remarkable increase in EE as the solubility profile of the drug showed higher solubility in the selected lipid. Due to drug distribution into aqueous and lipid phases, an increase in surfactant concentration resulted in a slight increase in EE. An increase in the surfactant concentration causes the formation of micelles, which have the property to dissolve lipophilic drugs, hence reducing the solubility in the lipid phase.[29] Cosurfactant also helps to dissolve drugs into SLN as it tends to support the emulsifying property of surfactant and additionally improves drug solubilization.

Organic solvent and surfactant concentrations positively influenced DL. The organic solvent used here dissolves more drugs, and at the time of cooling of the SLN dispersion, the lipid core encapsulates DMSO between the imperfect crystal lattice structures of the lipid. Solidified SLN exhibited a nanostructured lipid carrier-like structure composed of solid lipids inamorphous form with various lattice defects in which the drug dissolved in organic solvent is presented as pockets. Along with independent variables, some practical experimentation work has been done forthe fabrication of modified SLN, such as sudden cooling of hot SLN dispersion leading to sudden precipitation of lipid and drug, which forms lipid in α form containing maximum amount of drug andorganic solvent.

The nanometric size of BUTE-SLN was determined by TEM analysis of the particle structure and surface morphology. Figure 2 illustrates that the BUTE-SLN formulated appeared to be spherical in shape with a narrow particle size distribution, which is in goodagreement with PCS and PDI analysis.

DSC is a powerful investigational tool used to determine the physical properties of compounds, such as the crystalline or amorphous nature of samples, which can be drawn on the basis of the fact that different lipid modifications exhibit different melting points and physicochemical properties. Figure 3A shows the thermal analysis results of pure butenafine, Lipid Olivem 1000 and BUTE-SLN. A sharp endothermic peak at the melting point was observed on a DSC thermogram of pure drug at 217.35 °C. The thermogram of pure lipid Olivem 1000 showed a sharp endothermic peak at 63.20 °C indicating lipid is present in pure crystalline form. Further small peaks are attributed to the decomposition of the formed liquid droplets. The curve for BUTE-SLN shows a small but broad peak at 46.91 °C. The result shows that crystalline lipids are converted into amorphous states as heat flow through larger and perfectly ordered crystals requires greater energy, resulting in large and sharp peaks, while heat flow through small and less ordered particles requires less energy to melt the particle. Our solid lipid nanoparticle formulation showed small and broad peaks with a difference of 16.29 °C with pure lipid, indicating the presence of nanostructure in amorphous form along with surfactant and pockets of organic solvent inside it.[30,31]

From the XRD data, we can clearly observe sharp diffraction peaks of butenafine at a 2 θ value of 16.0768 with a *d* value of 5.4996 and pure lipid 2 θ at 21.664 with a *d* value of 4.1124, which indicates a high crystalline nature of the compound, as shown in Figure 3B. Whereas BUTE-SLN formulation showed a broader and shorter peak with no specific diffraction peak for butenafine, revealing encapsulation of the drug within the lipid matrix, which existed in amorphous form.[32] The comparative FT-IR spectra of butenafine, pure lipid Olivem 1000 and BUTE-SLN shown in Figure 4. The FTIR spectra for butenafine gave a typical specific absorption character at 3047.63, 1365.65 and 1072.46 cm^{-1} corresponding to -C-H stretch, -C-C and -C-N vibrations, respectively, but the BUTE-SLN spectra showed the absence of these peaks. The FTIR results revealed that there was no strong interaction and no incompatibility, and butenafine was successfully encapsulated into the lipid structure.

For effective topical delivery, some constraints should be considered, including the physicochemical parameters of the drug, such as log *p* and *pKa* values, rheological study of gel-enriched SLN, occlusive and hydrating potential of formulation, and disease state. Natural *aloe vera* gel with many additive effects, such as excellent anti-inflammatory activity, natural healing ability, and moisturizing effect, is beneficial for skin conditions. *Aloe vera* gel contains the building blocks of glucomannan, C-glucosyl chromone, lupeol and 8 enzymes, *Aloe vera* gel is useful and comfortable for treating exaggerated skin conditions.[33] In the evaluation of semisolid formulation viscosity and spreadability parameters, we gave more attention because the ultimate formulation was going to be used on inflamed skin. BUTE-SLN *aloe vera* gel showed pseudoplastic rheological flow, which is expected for skin conditions. Small nanosized particles showed excellent slip properties required for gel spreading onto inflamed skin. The entrapment of SLN into the gel network slightly increased the rheology of the gel due to an increase in amphiphilic surfaces upon which water could bind and become immobile.

The process of SLN permeation starts with occlusion and skin hydration. Because SLN is composed of solid lipids and the stratum corneum also contains intercellular lipids such as cholesterol, phospholipids, and ceramide, SLN has a strong affinity toward the stratum corneum. Hence, they form an impermeable occlusive layer on the skin surface, preventing transepidermal water loss. Due to water pore dynamics, pores that exist in uniform spreading of the SLN gel attract permeated vapor, which condenses at the pores of the SLN. Hence, due to the negative pressure, they attract water rather than lose it. This particular mechanism is very useful in the treatment of superficial fungal infections, which cause scaling, dry skin, and irritation.[34,35] The stratum corneum comprises compactly packed corneocyte and intercellular lipids. Occlusive film formation and reduction in trans epidermal water loss result in hydration of the stratum corneum, which reduces the compact packing between

corneocyte and increases the pore size. This is the possible mechanism for the transport of SLN through the skin.

Drug release and permeation showed a biphasic release pattern of drugs from the SLN matrix. This can be due to the use of novel excipients such as surfactants such as lipid Olivem 1000, DMSO, and TPGS, which entrap the drug, forming nanosized mini pockets in SLNs. The process of fabrication provokedthe α state lipid transformation; hence, it could include more excipients. The formation of α state lipid structure slowly convert into β' form and then most stable β form then slowly expel the drug from the lipid matrix, which accounts for sustained release.

The possible mechanism for the diffusion of drug from the lipid matrix can start with possible events like distribution of drug between lipid and DMSO, lipid Olivem 1000, and TPGS, diffusion of drug through lipid, transformation of lipid from α state to most stable β form, distribution of drug between lipid and dissolution medium, and release of drug to dissolution medium. The incorporation of TPGS facilitates burst release from SLN matrix. This can occur at the time of sudden cooling of the dispersion. The saturated emulsion when cooled suddenly leads to solidification of the drug and lipids and forms the drug lipid matrix, whereas the presence of TPGS and DMSO partially solubilizes the drug in the aqueous phase from which it precipitates at the time of cooling. This forms a uniform coat around the SLN particles when applied to skin, resulting in initial burst release. The efficacy of the formulation also depends on the skin condition, such as the diseased state, type of infection, inflammation, edema, and dry skin. All these factors pose the problem of permeation of drugs intothe superficial layer of skin. In the disease state, the superficial layer of the skin is disturbed, exposing the epidermal cell along with the existence of various metabolites of fungal cells, enzymes secreted by fungal cells and the body's immune system (cytokines) degenerate the drug into inactive fragments. Marketed cream showed reduced diffusion of the drug into the skin layer compared to SLN, which forms a depotby concentrating in the SC and releasing the drug slowly. Skin retention studies revealed that BUTE-SLN dominantly concentrates in the stratum corneum, which forms a reservoir for further drug release,and natural surfactant Olivem 300 aids in the partitioning of drugs into epidermal cells.[35]

The skin irritation study revealed the non-irritant nature of BUTE-SLN gel, which explains its usefulness in treating fungal infections. An in vitro antifungal analysis was conducted to examine the comparative efficacy of butenafine with marketed cream and to establish the effects of different method parameters on the formulation of BUTE-SLN. The zone of inhibition of the marketed preparation was found to be 30 mm and that of BUTE-SLN was found to be 32 mm, which is greater than that of the marketed formulation proving the therapeutic efficacy of the SLN formulation.

CONCLUSION

Various formulation ingredients like lipid, surfactant and DMSO have an influence on the fabrication of SLN dispersions, which directly affects the particle size, EE, and ZP of SLN. The DSC and XRD studies indicated that the optimized formulation was amorphous in nature and contained the drug, DMSO, and surfactant entrapped inside the SLN. Rheological and spreadability study of BUTE-SLN *aloe vera* gel revealed excellent slip properties beneficial for inflamed skin application. Along with its excellent rheological and spreadability, the BUTE-SLN gel possesses good occlusive properties and hydrating potential. For long-term drug delivery through the stratum corneum, BUTE-SLN showed accumulation of the SLN in the stratum corneum with controlled drug release. BUTE -SLN demonstrated increased skin deposition, improved *in vitro* antifungal action, and a topical formulation that was less irritating. As a result, the BUTE-SLN *aloe vera* gel formulation is a cost-effective, novel, and reproducible alternative to the currently available traditional dosage method.

Acknowledgments

The authors would like to express their gratitude to Chem House Marketing, Mumbai for offering a gift sample of lipids and surfactants, as well as his advice on SLN fabrication. For the XRD report, the authors are grateful to Niksha Laboratories, Hyderabad.

Ethics

Ethics Committee Approval: The protocol for the study was approved by the Pravara Rural College of Pharmacy (approval number: 2013714-543, date: 07.01.2014).

Informed Consent: Not required.

Authorship Contributions

Concept: A.B., V.K., S.A., Design: A.B., S.A., Data Collection or Processing: A.B., S.A., D.B., M.A., Analysis or Interpretation: A.B., V.K., S.A., D.B., M.A., Literature Search: A.B., S.A., D.B., M.A., Writing: S.A., D.B., M.A.

Conflict of Interest: No conflict of interest was declared by the authors.

Financial Disclosure: The authors declared that this study received no financial support.

REFERENCES

1. Hay R, Bendeck SE, Chen S, Estrada R, Haddix A, McLeod T, Mahé A. Skin Diseases (2006). In: Jamison, D.T. 2nd ed. Disease Control Priorities in Developing Countries. Washington (DC): World Bank, 5173-5193.
2. Richardson MD, Aljabre SHM. Pathogenesis of dermatophytosis. In: Borgers, M, Hay R, Rinaldi MG. Eds Current Topics in Medical Mycology, Vol 5. Prous Science, Barcelona, 1993;49-77.
3. Akaki Tsereteli State University Kutaisi. Available from: https://www.atsu.edu/faculty/chamberlain/website/lectures/tritzid/supermy.htm (Accessed: 02.02.2023)
4. DRUGBANK Online. Available from: https://go.drugbank.com/drugs/DB01091 (Accessed: 02.02.2023)
5. Wikipedia. Available from: https://wikipedia.org/wiki/Butenafine (Accessed: 02.02.2023)
6. MedicineNet. Available from: https://www.medicinenet.com/butenafine-topical_cream/article.htm (Accessed: 02.02.2023)

7. Weinstein A, Berman B. Topical treatment of common superficial tinea infections. Am Fam Physician. 2002;65:2095-2102.
8. Tan SW, Billa N, Roberts CR, Berley JC. Surfactant effects on the physical characteristics of Amphotericin B-containing nanostructured lipid carriers. Colloids and surfaces a: physicochemical and engineering aspects. 2010;372:73-79.
9. Zhang X, Liu J, Qiao H, Liu H, Ni J, Zhang W, Shi Y. Formulation optimization of dihydroartemisinin nanostructured lipid carrier using response surface methodology. Powder Technology. 2010;197:120-128.
10. Yang HC, Hon MH. The effect of the degree of deacetylation of chitosan nanoparticles and its characterization and encapsulation efficiency on drug delivery. Polymer Plastics Technology and Engineering. 2010;49:1292-1296.
11. Khan F, Dahman Y. A novel approach for the utilization of biocellulose nanofibres in polyurethane nanocomposites for potential applications in bone tissue implants. Designed Monomers and Polymers. 2012;15:1-29.
12. Baboota S, Shah FM, Javed A, Ahuja A. Effect of poloxamer 188 on lymphatic uptake of carvedilol-loaded solid lipid nanoparticles for bioavailability enhancement. J Drug Target. 2009;17:249-256.
13. Kollipara S, Bende G, Movva S, Saha R. Application of rotatable central composite design in the preparation and optimization of poly (lactic-co-glycolic acid) nanoparticles for controlled delivery of paclitaxel. Drug Dev Ind Pharm. 2010;36:1377-1387.
14. Pardeshi CV, Rajput PV, Belgamwar VS, Tekade AR, Surana SJ. Novel surface modified polymer-lipid hybrid nanoparticles as intranasal carriers for ropinirole hydrochloride: *In vitro*, *ex vivo* and *in vivo* pharmacodynamic evaluation. Journal of Materials Science: Materials in Medicines. 2013;24:2101-2115.
15. Pardeshi CV, Rajput PV, Belgamwar VS, Tekade AR, Surana SJ. Novel surface modified solid lipid nanoparticles as intranasal carriers for ropinirole hydrochloride: application of factorial design approach. Drug Delivery. 2013;20:47-56.
16. Kumar L, Verma R. *In vitro* evaluation of topical gel prepared using natural polymer. International Journal of Drug Delivery. 2010;2:58-63.
17. Patel H, Panchal MS, Shah S, Vadalia KR. Formulation and evaluation of transdermal gel of sildenafil citrate. International journal of pharmaceutical research and allied sciences. 2012;1:103-118.
18. Wissing SA, Muller RH. The influence of the crystallinity of lipid nanoparticles on their occlusive properties. Int J Pharm. 2002;242:377-379.
19. Sainini GS. *API* Textbook of medicine, association of physician of India, 6th ed. New York: McGraw Hill, 1999;1178-1180.
20. Godin B, Touitou E. Transdermal skin delivery: predictions for humans from *in vivo*, *ex vivo* and animal models. Adv Drug Deliv Rev. 2007;59:1152-1161.
21. Liu J, Hu H, Ni Q, Xu H, Yang X. Isotretinoin loaded solid lipid nanoparticles with skin targeting for topical delivery. Int J Pharm. 2007;328:191-195.
22. Pople PV, Singh KK. Targeting tacrolimus to deeper layers of skin with improved safety for treatment of atopic dermatitis. Int J Pharm. 2010;398:165-178.
23. Wavikar P, Vavia P. Nanolipidgel for enhanced skin deposition and improved antifungal activity. AAPS PharmSciTech. 2013;14:222-233.
24. Hekmatpou D, Mehrabi F, Rahzani K, Aminiyan A. The effect of *Aloe vera* clinical trials on prevention and healing of skin wound: a systematic review. Iran J Basic Med Sci. 2019;44:1-9.
25. Davis RH, Donato JJ, Hartman GM, Haas RC. Anti-inflammatory and wound healing of growth substance in *Aloe vera*. JAMA Pediatr. 1994;84:77-81.
26. Shelton RM. *Aloe vera*, its chemical and therapeutic properties. Int J Dermatol. 1991;30:679-683.
27. Shah KA, Date AA, Joshi MD, Patravale VB. Solid lipid nanoparticles (SLN) of tretinoin: Potential in topical delivery Int J Pharm. 2007;345:163–171.
28. Trotta M, Debernardi F, Caputo O. Preparation of solid lipid nanoparticles by solvent emulsification-diffusion technique, Int J Pharm. 2003;257:153-160.
29. Jain SA, Chauk DS, Mahajan HS, Tekade AR, Gattani SG. Formulation and evaluation of nasal mucoadhesive microspheres of Sumatriptan succinate. Journal of Microencapsulation. 2009;26:711–721.
30. Freitas C, Muller RH. Correlation between long-term stability of solid lipid nanoparticles (SLN) and crystallinity of the lipid phase. Eur J Pharm Biopharm. 1999;47:125–132.
31. Hou D, Xie C, Huang K, Zhu C. The production and characteristics of solid lipid nanoparticles (SLNs). Biomaterials. 2003;24:1781–1785.
32. Agrawal Y, Petkar K, Sawant K. Development, evaluation and clinical studies of Acitretin loaded nanostructured lipid carriers for topical treatment of psoriasis. Int J Pharm. 2010;401:93–102.
33. Surjushe A, Vasani R, Saple DG. *Aloe Vera*: A Short Review. Indian Journal of Dermatology. 2008;53:163-166.
34. https://medicalguidelines.msf.org/viewport/CG/english/superficial-fungal-infections-16689659.html [Accessed 2 Feb 2023].
35. Desai P, Patlolla RR, Singh M. Interaction of nanoparticles and cell-penetrating peptides withskin for transdermal drug delivery. Mol Membr Biol .2010;27:247-259.

Turk J Pharm Sci 2024;21(4):327-339
DOI: 10.4274/tjps.galenos.2023.71242

ORIGINAL ARTICLE

Development and Evaluation of Methotrexate and Baicalin-Loaded Nanolipid Carriers for Psoriasis Treatment

Sundus SOHAIL[1], Saloma ARSHAD[1], Sidra KHALID[2], Muhammad Junaid DAR[1], Kashif IQBAL[1,3]*, Hassan SOHAIL[1]

[1]University of Lahore (Islamabad Campus) Faculty of Pharmacy, Department of Pharmacy, Islamabad, Pakistan
[2]Drug Regulatory Authority of Pakistan, Islamabad, Pakistan
[3]IBADAT International University Faculty of Pharmacy, Department of Pharmacy, Islamabad, Pakistan

ABSTRACT

Objectives: Psoriasis is a chronic inflammatory, T-lymphocyte immune-mediated skin disease. In this study, skin-permeating nanolipid carriers (NLCs) of Methotrexate (MTX) and Baicalin (BL) were formulated. This further gave formulation of nano-lipid encapsulated carriers for dual-drug delivery of the hydrophilic and hydrophobic drugs through the liposomal gel.

Materials and Methods: Optimization of the formulation of NLCs was performed and characterized by determining their particle size, drug permeation, skin irritation, drug loading capacity, stability, *in vitro* drug release behavior, and *in vitro* cellular viability. *Ex vivo* skin permeation and *in vivo* psoriatic efficiency were also evaluated and compared.

Results: Results revealed that the amount of MTX permeating the skin was 2.4 to 4.4 fold greater for dual-drug s than for single NLCs. The optimized dual-drug loaded NLCs had an average particle size (150.20 ± 3.57 nm) and polydispersity index (0.301 ± 0.01) and high entrapment (86.32 ± 2.78% *w/w*). The MTX nanoparticles exhibit a positive Zeta potential of 38.6 mV. The psoriasis area and severity index scoring showed the lowest skin erythema, skin thickness and scaling. MTX-BL NLCs were inhibited the expression of inflammatory cytokines (tumor necrosis factor-alpha, and interleukin-17) .

Conclusion: It can be concluded that newer targeting strategies for NLCs for dual-drug delivery of nano-lipid carriers could be administered topically for the treatment of psoriasis.

Keywords: Psoriasis, Baicalin, Methotrexate, nano structured lipid carriers, topical delivery

INTRODUCTION

Psoriasis is a chronic inflammatory, T-lymphocyte immune-mediated skin disease characterized by the deregulated multiplication of skin cells, which increases skin cell thickness, causing the appearance of salmon-red plaques with a silver scaly surface. The etiology of psoriasis remains unknown. Several biochemical factors lead to the maturation and proliferation of epidermal cells.[1] Red and white/scaly patches are formed on the epidermis, which is caused by the immune system. The pathogens increase the epidermal growth and multiplication of epidermal cells.[2] Psoriasis is treated according to disease severity. Mild to moderate psoriasis symptoms are treated topically, whereas systemic therapy and phototherapy are used for severe disease. Systemic therapies have been of significant concern throughout history. They have been continuously developed and modified for the treatment of psoriasis.[3] The first-line treatment of psoriasis is Methotrexate (MTX) (cytotoxic drug), which is usually administered orally and parenterally. Therefore, transdermal and topical delivery of MTX with improved local and systemic delivery is

*Correspondence: kashifiqbal321@yahoo.com, Phone: +03356951284, ORCID-ID: orcid.org/0000-0003-2758-7094
Received: 09.04.2023, Accepted: 28.08.2023

preferred to reduce gastrointestinal side effects.[4] Different methods for topically delivering MTX to psoriasis lesions have been developed.[2] A traditional anti-psoriatic medicinal product, MTX is most effective when used as a single active ingredient or in combination with biologics.[5] MTX belongs to Dihydro-folate reductase enzyme inhibitor.[6] This drug shows good therapeutic activity in tumor necrosis factor (TNF), skin tumor, and rheumatoid arthritis. Due to its high molecular weight of MTX which is 454.56 D, water solubility, and ionized form, MTX will not diffuse passively through the Stratum Corneum.[7] Various types of MTX-based drug delivery systems, including nano-carriers solid lipid nanoparticles (SLNs), self-emulsifying nano-systems, transferosomes, liposomes, carbon nanotubes, polymeric nanoparticles, dendrimer, metallic nanoparticles, nanolipid carriers, and niosome formulated for the topical delivery of MTX.[7] Baicalin (BL) is extracted from the roots *Scutellaria baicalensis* is a traditional Chinese herb.[8] *S. baicalensis* has pharmacological activity against psoriasis.[9] Baicalin reduced the proliferation of keratinocytes and increased antitumor activity.[10] The liposomes were introduced to develop MTX-entrapped liposomes. The lipid carrier released the drug before permeation into the target area.[11] These deformable liposomes are composed of lipid content and a surfactant, an inner aqueous compartment surrounded by a lipid bilayer formulated to increase MTX skin penetration. The advantage of conventional liposomes over transfersomes is the characteristic of flexibility.[2] A topical formulation of MTX and etanercept for the treatment of psoriasis has previously been reported, and it provides a new pathway for combination formulations that noticeably increase bioavailability and better skin permeation compared with plain MTX gel. Dual-drug therapy is the most frequent approach to treat psoriasis, as it lowers the systemic toxic effects, improves patient compliance and increase the efficacy of the drug.[3] Topical preparation of co-loaded lipid nano-carrier lipid-soluble and water soluble drug formulated.[12] Dual-drug s with different polarities are formulated with the aid of an edge activator (EA) through the film hydration method (TFH).[13]

To achieve the treatment goal, MTX-entrapped transferomal formulations with improved permeability. Deformable transfersomes, elastic vesicles made of lipid materials and a surfactant with at least one inner aqueous compartment surrounded by a lipid bilayer, known as transfersomes were introduced previously.[2] Transfersomes are formulated from phosphatidylcholine (PC), EA sodium cholate (SC), and surfactant KG Dipotassium Glycyrrhizinate for the entrapment of MTX. By using KG as a surfactant, the amount of MTX permeated across the skin is 3-4 fold higher as compared to conventional liposomes.[14] Natural ingredient-based transfersomes are the choice because of the increased permeation of drugs into the skin.[2]

No previous study on MTX-BL transfersomes (TRs) gel co-loaded nano-lipid carriers has been reported. Both drugs have anti-psoriasis activity and have been used as single drug carriers. This study aimed to establish a nano-lipid carrier containing two drugs and evaluate their topical delivery for the topical treatment of psoriasis.

MATERIALS AND METHODS

Materials

MTX was gifted from Werrick Pharmaceutical (Islamabad, Pakistan). Tween 80 (Polysorbate 80) was purchased from Bio-Labs from the source of Hangzhou Zhongbao Imp. and Exp Corp. Ltd., China. Carboxy methyl cellulose purchased by bio-labs from the source of Qingdao Icd Biochemistry Co. Ltd. China. Sodium lauryl sulfate was purchased by bio-labs from the source of Emery Chemicals Malaysia. Soyabean PC was purchased from Bio-Labs from the source of Vigilant Tenent Laboratories. Carbopol 940 was purchased from Bio-Labs from the source of Lubrizol Advanced Materials INC. Brecksville USA. Carbopol 934 bio-labs were obtained from the source of Lubrizol Advanced Materials INC., Brecksville, USA. BL and SC were purchased from Sigma-Aldrich, USA. Phospholipon 90G was received as a gift sample from Lipoid AG, Switzerland. PBS (pH 7.4) and Alamar Blue reagent were obtained from Thermo Fisher Scientific, USA. Cytokine standards interleukin (IL)-17 and tumor necrosis factor-alpha (TNF-α) were purchased from BD Biosciences (Case, USA). All other used reagents were of pure analytical grade.

Preparation of MTX-BL-co-loaded TRs

Single MTX-TRs (Methotrexate and Transfersomes) and dual-drug-loaded MTX/BL TRs were prepared by the thin-TFH with some modifications.[15] Phospholipon 90G, tween 80, or SC as an EA, and MTX were dissolved in chloroform, methanol, and HCl 1:1:0 at pH 3 mixture and evaporated at 50 °C by using rotary evaporator under vacuum at 90 rpm for 20 minute. The thin film was evaporated under a vacuum to remove a few traces of the organic solvent. The dried film was hydrated with 100 mg of MTX solution in 20 mL PBS (pH 7.4) for 1 hour at 60 ± 1°. The transfersomes were extruded 5 times for 2 minutes through 450-and 200-nm filters. Dialysis was used to purify the formulation from the unbound drug. The vesicles were stored at 4 °C in glass vials.[16]

Encapsulation of BL

A mixture of Baicalin with cholesterol, chloroform, and Tween 80 or SC was formed. MTX loading was performed using Baicalin-loaded nano-lipid carriers in the MTX solution. Continue to stir in 1 mg/mL solution for 30 minutes. The excess drug present in the supernatant was removed by washing with water. The prepared MTX/BL TRs at 4 °C in a dark place. Dual-drug-loaded MTX/BL TRs were optimized in terms of entrapment efficiency (EE), vesicle size (VS), and elasticity by varying the percentage of Phospholipid or Sodum Cholate.[17]

Experimental design for the optimization of TRs

Nano-lipid carriers were prepared using the thin-TFH in a rotary vacuum evaporator. Phospholipon 90G, surfactant tween 80, sodium calcium, and cholesterol were added to a methanol: chloroform (1:9) mixture of 10 mL. In the rotary vacuum evaporator film, the film was allowed for 20 minutes at 50 °C temp and RPM 90. The quantity of phospholipon 90G and SC (PL:SC) ratio was varied as 90:10, 80:20, 70:30, 60:40, 80:20, and 80:20, and cholesterol was varied as 25 and 50 mg for preparation of trial batches of nano-lipid carriers formulations.

The formulations were kept in desiccators overnight for the removal of trace amounts of organic solvents by evaporation. The dried film was hydrated with 100 mg of the MTX solution in 20 mL PBS (pH 7.4) for 1 hour at 60 ± 1°. The batches were referred to as MTX/BL TRs 1, MTX/BL TRs 2, MTX/BL TRs 3, MTX/BL TRs 4, MTX-TRs, and blank TRs. Surfactants are selected according to the drug EE percentage and the VS of the nano-lipid carriers formed. SC lipid nanocarrier formulation has a higher flux value.[18]

Physicochemical characterization of co-loaded TRs

VS, polydispersity index (PDI), and zeta potential of the prepared co-loaded TRs were measured using a Zetasizer Nano ZS-90 instrument (Malvern instruments, Worcestershire, UK). All batches were diluted with millipore water at a 1:10 dilution and analyzed in triplicate using 90° scattering angle at 25 °C. Zeta potential was determined for drug-loaded nano-lipid carriers by Smoluchowski equation.[1] The EE of MTX was determined by direct method. Pellets were obtained by centrifugation of nano-lipid carriers for 15 mints at 15000 rpm. Then, it was treated with Triton X-100. Then 0.5 mL methanol was added to the disrupted nano-lipid carriers to make the drug more soluble. The samples were centrifuged at 10,000 rpm for 5 minutes. Prepared the dilution of 10 mL of TRs and diluted up to 5 mL with double-distilled water. Un-entrapped MTX was determined by direct method. The MTXs were unentrapped and separated from NLCs by exhaustive dialysis at 4 °C.[3] Then, MTX-TRs were added to the dialysis bag containing Molecular Weight cut off 12-24 kDa containing PBS (pH 7.4) and stirred with a magnetic stirrer. PBS was changed every 2 hours and its MTX content was determined using the atomic absorption spectrophotometer (AAS). The sample was dissolved with nitric acid, heated, and dried.[19]

Preparation of the gel

The optimized TRs were loaded with 100 mg of Carbopol 940 for topical preparation. Carbopol powder was added in 10 mL of distilled water and placed in a dark place for 24 hours. It swelled completely.[20] Drug-loaded MTX/BL TR gel was formulated by adding 50% *(w/w)* of MTX-TRs and BL/TRs slowly in carbopol gel. In contrast, constant stirring, while simple MTX-TR gel was prepared by adding 10% *(w/w)* of a single drug in the gel.[21] The formulation was adjusted by neutralizing with triethanolamine dropwise, resulting in a transparent gel was formed.[22]

Nano-lipid carriers stability

The optimized transfersomal preparations were stored at 4 °C for 3 months. The evaluation parameters were VS, PDI, EE, and zeta potential with different formulation's concentrations.[23]

Deformability index

To determine the deformability index, the developed TRs were formed using the extrusion technique. The VS of TRs were determined earlier and later of extrusion technique.[24]

Physicochemical and rheological evaluation of the MTX/BL TR gel

The MTX/BL TRs, MTX-TRs, and plain MTX gels were evaluated for pH, steady flow behavior, thixotropy, visco elastic behavior, and water-holding capacity.

Evaluation of pH

In 20 mL of distilled water add 1 gm of each gel; the pH of the gel was determined using a digital pH meter. A calibrated pH meter's electrode was dipped in the dispersion medium to determine the pH of the gel.

Homogeneity

To improve patient compliance, it is necessary to evaluate the homogeneity of topically applied transfersomal gels. The consistency of the gel was measured by applying a small amount of gel to the thumb and index finger and rubbing them over each other. The homogeneity was measured by its consistency.

Spreadability

A 0.5 g gel sample was placed between two transparent circular glass slides. Rest the gel over the glass for 5 minutes. The diameter was the indicator of spreadability. Measured the diameter of the gel circle.

Drug content determination

The MTX content was determined using an analytical method of MTX content (equivalent to 10 mg) in a 100 mL volumetric flask. Stirred the dilution and remained for 24 hours. The samples were filtered and analyzed using AAS.[19]

Rheological studies

The gel's viscosity was assessed using a Brookfield viscometer. Spindle no. 96 was used in the viscometer to measure the gel flow behavior. The sample was placed in the holder, a spindle was attached to it, and it was allowed to rotate at a speed of 5 rpm for a 10 s run time at 37 °C to attain the minimum turning force of 10%. Various rotational speeds were used to determine the viscosity of gels.

In vitro drug release and release kinetic study

Franz diffusion cell and dialysis membrane were used for *in vitro* drug release for transferomal dispersion. For activation of the dialysis membrane, soak it for 1 hour. PBS (pH 7.4) with sodium lauryl sulfate solution was used as the release medium. Filled the dialysis bag with 1 mL of transpersonal formulation while the the release medium was added to a separate vial of 10 mL. Place in a shaker bath with a shaking speed of 100 rpm at 37 °C. A sample of 5 mL was collected at a time interval of 0.5, 1, 3, 6, 24, 48, 96, and 120 hours and replaced with 5 mL fresh PBS medium. The MTX contents were analyzed using an AAS until no MTX appeared. Nitric acid was added after dialysis, followed by heat for complete drying. HCl:water (1:1) was added. Then it was boiled. Then, the best-fit model was used for regression co-efficient.[25] The permeation flux study was conducted for optimized transferomal and plain gels. The slope of the percentage of drug release vs. time is expressed for permeation flux.[10]

In vivo screening model, CFA, and formaldehyde

To induce psoriasis, a mixture of CFA and formaldehyde (1:10 ratio) was prepared. [26] Removed hair from the dorsal side of rats approximately 2 x 2 cm. A volume of 0.1 mL of the prepared

mixture was applied topically to the shaved area (n= 5 animals per group) on days 1, 2, and 3. The psoriatic lesions were observed daily for 7 days.[27]

Anti-psoriatic activity of the MTX/BL TR gel

Psoriasis was induced using the CFA and formaldehyde method. Animals were divided into 5 groups: 1) disease untreated, 2) plain drug MTX (water soluble), 3) single-loading MT 4. dual-drug-loaded MTX/BL TRs. The all groups treated every 24 hours for 21 days with MTX/BL TR gel (20 mg/kg) and MTX/BL TR gel (20 mg/kg) while the control group was left untreated. Drug efficacy was measured using the PASI. The intensity of psoriasis was found by stain smears through microscopic examination.[28]

Ex vivo permeation and drug deposition studies

Ex vivo skin penetration studies were performed for all trial batches using dialysis membrane and franz diffusion cell. The permeation fluxes of trial batches of transferomal gel and plain drug were determined MTX 20 mg/kg[2] and BL 5 mg/kg.[15] The outcomes of applying MTX 20 mg/kg and Baicalin 5 mg/kg formulation on normal mice skin showed no MTX and BL in the acceptor compartment within 24 hours, but the same dosage of MTX and BL applied on psoriatic skin, and 50% penetration was detected in the acceptor compartment. First, the abdominal hair of BALB/c mice was removed using an animal hair clipper. Mice were then sacrificed. The skin samples and abdominal fat tissues were excised. The excised skin was organized on the donor and receptor compartment with the SC side in the direction of the donor and dermis layers toward the receptor of the Franz diffusion cell apparatus. 7 mL of PBS (pH 7.4) was filled into the receptor compartment with a constant stirring rate of 300 rpm at 32 °C. 1 gm of the simple MTX gel, single MT/TRs, or MTX/BL TRs gel (equivalent to 20 mg/kg and 5 mg/kg of both drugs (MTX-BL) was placed on the skin surface. The cumulative amounts of MTX and BL permeated were assessed by the AAS method per unit area plotted against time.[16] Skin samples from the *ex vivo* permeation study were saved and blot-dried. Using the tape stripping method, the skin pieces were stripped into 20 parts. The entire tape was collected and placed in a beaker. MTX was extracted when the tape was added to a mixture of HCL:water (1:1). The remaining skin was chopped, meshed and homogenized.[22,29]

Evaluation of skin structure after MTX/BL TR gel treatment

In vivo skin irritation and histopathological study

In the histopathological study, epidermal changes and irritation potential in psoriatic mice were examined. The animals were divided into 5 groups with 5 animals in each group: group I had normal mice with epidermis psoriasis not induced to them, group II acted as an untreated control group, group III received plain drug MTX, group IV received single-loaded MTX, and group V received dual-drug-loaded MTX/BL TRs. Respectively, which were applied topically for 1 week. Histopathological examination was performed to determine pathological changes during topical application of gels. Striped skin samples were prepared from sacrificed mice in different treatment groups. Stained the skin samples with Hematoxylin and Eosin and a cryostat microtome on slide and observe under electric light microscope.[4]

Macrophage cytotoxic assay

Several cytokines are involved in the regulation of immunity against psoriasis. IL-17 is mainly produced by Th-17 cells. IL-17 plays an important role in the production of chemokines and secretions of neutrophils and antimicrobial proteins at the site of inflammation. In psoriatic skin samples, the cytokine levels (TNF-α and IL-17) were determined by enzyme-linked immunosorbent assay (ELISA).[30] Skin tissues of induced psoriasis were treated with PBS, and then the mixture was properly homogenized in a tissue homogenizer at 3000 rpm for 5 minutes. After centrifugation at 10,000 rpm for 15 minutes at 4 °C, the levels of TNF-α and IL-17 were determined by ELISA according to manufacturer's protocol.[14]

In vivo efficacy of the formulation in a BALB/c infection model of psoriasis

Clinical severity was expressed by the psoriasis-affected area and severity index (PASI). It was developed on the basis of the PASI. Redness, scales, and erythema were scored independently on a scale from 0 to 4: 0: none, 1: slight, 2: moderate, 3: marked, and 4: marked. PASI was calculated based on redness, erythema, and the scale scores. Anesthesia was administered at the end, and skin samples were collected. Preserved in 10% formalin solution for histological examination. Stained the rat skin specimen in hematoxylin and eosin dye for histological examination.[10,31]

Statistical analysis

The analysis of trial batches of MTX/BL TRs gel was performed using the response surface methodology. Assessment responses were analyzed using surface and contour plots to observe the design space and determine suitable quantities of excipients for maximum responses. The optimization plots explain the formulation factors and levels that produced the desired target responses. One-way analysis of variance (ANOVA) was applied for comparisons between groups. For significant *p* values, multiple Tukey's tests were used to compare the means of different groups. The significance level of this study was set at 0.05. SPSS V23 software was used. Kruskal-Wallis test for non-parametric statistical differences was used.[19]

RESULTS

The optimized dual-drug formulations were characterized on the basis of physiological parameters, including the varying concentrations of surfactant and EA, VS, polydispersity index, EE, and *in vitro* and *ex vivo* drug permeation study.

Selection of the surfactant and EA

For the flexibility of MTX/BL TRs, various EAs, such as SC, tween 80, phospholipon 90G, sorbitan monolaurate, sorbitan monopalmitate, sorbitan stearate, and sorbitan monolaurate.[2] SC was selected on the basis of observations seen in the dispersion; it increased the flexibility of the vesicles while with other surfactants, frothing was seen in the dispersion.

Formulation of nano-lipid carriers

Six formulations were prepared with different concentrations of phospholipon 90G and SC. The Transfersomal preparations were prepared using thin-TFH.[16] After the formulation of dual-drug-loaded carbopol gel TRs, they were evaluated on the basis of key parameters, *i.e.* VS, PDI, deformability Index and EE. Optimized formulation codes with MTX/BL TRs 4 were selected for further study.

Physicochemical characterization of NLCs

MTX/BL TRs were prepared by thin-TFH, SC is used as an EA. Co-delivery of MTX/BL TRs allows targeted delivery of nanoparticles to the immune system involved in the pathology of psoriasis. The main results of the physicochemical properties are shown in Table 1. These results show that mean VS decreases with increasing SC, with a quick reduction in VS as SC reaches 10%. It was established that the VS of single MTTRs was considerably higher ($p < 0.01$) at 10% SC than that of MTX/BL TRs. In Table 1 the PDI value is < 0.3 of formulations containing 5% or 10%. This results in homogenous dispersion. When SC% increases from 10% to 20%, PDI exhibits an increase in value. MTX/BL TRs incorporation did not affect the average TR size. TRs had a PDI in the range of 0.116 (blank TRs) to 0.359 (MTX/BL TRs). The PDI values suggest that the transferredomal preparation was homogenous with a low tendency toward aggregation. The average VS of the MTX/BL TRs was 170.1 ± 3.7 nm, with a PDI value of 0.138 and a ZP value of -38.6 Figure 1. The PDI values of MT/TRs and MTX/BL TRs ranged from 0.15 to 0.359, indicating better uniformity and homogeneity of the formulations.

The deformability index is the major parameter of NLCs for topical drug delivery because it allows drug molecules to easily permeate into the skin with the help of EA.[24]

Moreover, the effect of SC on the deformability index increased with each other to the extent of 10% ($p < 0.01$), and the deformability index decreased. The values of the deformability index of blank TRs, single MTX TRs, and MTX/BL TRs were 59.7 ± 3.7, 56.1 ± 3.3 and 52.8 ± 2.4, respectively. This explains that the addition Baicalin created a detrimental influence on the deformability of elastic vesicles, whereas the addition of MTX had an optimistic effect. It was observed that lipid content increased the particle size of nano-lipid carriers.

Effect of independent variables on vessel size

The VS of the optimized co-loaded nano-lipid carriers were evaluated using a Zetasizer nano ZS-90 instrument (Malvern Instruments, Worcestershire, UK). Various concentrations of PL:SC had significant effects on dual-drug-loaded transferomal preparations. The VS of formulations is shown in Table 1. There was no considerable difference in VS at 70:30 or above concentrations, but at 60:40 the rapid reduction of dual-drug-

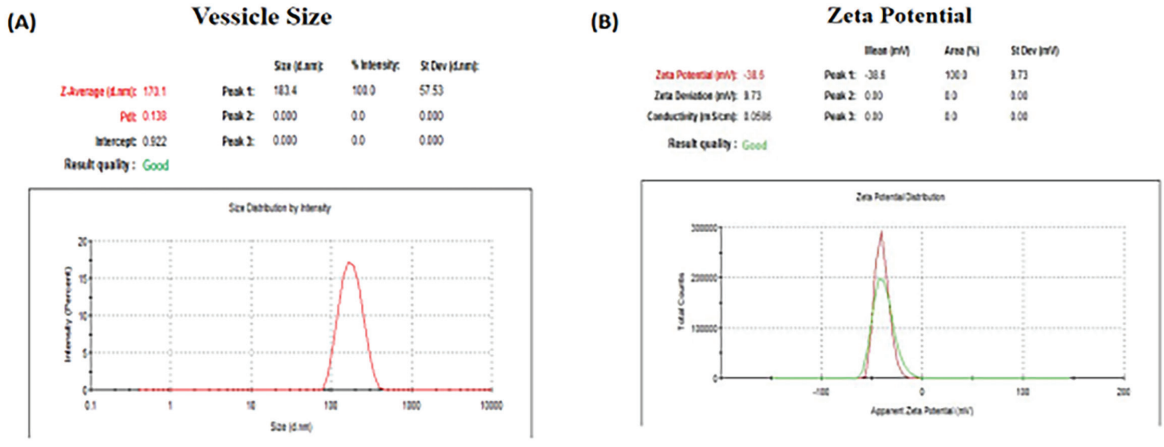

Figure 1. Independent variables, (A) vesicle size, (B) zeta potential

Table 1. Physicochemical characterization

Formulation code	PL:SC	Vesicle size (nm)	PDI	Deformability index	EE% ± SD (PT/CR)
MTX/BL TRs 1	90:10	241.5 ± 7.4	0.154	45.3 ± 2.7	71.9 ± 5.2/86.8 ± 5.7
MTX/BL TRs 2	80:20	170.1 ± 3.7	0.138	52.8 ± 2.4	69.5 ± 4.7/81.9 ± 4.4
MTX/BL TRs 3	70:30	111.3 ± 4.1	0.272	49.7 ± 2.9	47.0 ± 4.1/59.7 ± 4.8
MTX/BL TRs 4	60:40	56.4 ± 3.5	0.359	33.5 ± 2.6	37.8 ± 5.0/44.1 ± 4.9
MTX TRs	80:20	152.5 ± 5.0	0.131	56.1 ± 3.3	33.7 ± 4.1
Blank TRs	80:20	141.2 ± 3.5	0.116	59.5 ± 3.7	-

PL: Phospholipon 90G, SC: Sodium cholate, PDI: Polydispersity index, MTX/BL TRs: Methotrexate-baicalin dual loaded transfersomes, MTX TRs: Single Methotrexate loaded transfersomes, EE: Entrapment efficiency, SD: Standard deviation

loaded MTX/BL TRs was observed. The preferred VS was obtained by sonication for 10 minutes.

Effect of the independent variable on zeta potential

Vesicle's charge is evaluated by the Zeta potential. The zeta potentials of single MTX-TRs and MTX/BL TRs are described in Table 1. The zeta potential was approximately 38.6 mV, which is considered as a stable colloidal dispersion. MTX/BL TR incorporation did not have significant interference in the zeta potential values and consequently in the stability of the formulations. Neutral charged or slightly negative nano-lipid carriers with a zeta potential ranging from 10 to and 10 mV are acceptable.

Effect of the independent variable on the percentage EE

The EE of TRs were evaluated. It was observed that EE gradually decreased with increasing PL:SC until 10%. Increased PL:SC resulted in an immediate decrease in EE. Single MTX-TRs have lower EEs than dual-drug-loaded MTX/BL TRs. After consideration of all the important factors, MTX-co-loaded nano-lipid carriers with a PL:SC of 60:40 and VS 56.4 ± 3.5 nm were selected for the rest of the studies because they showed high EE. Dual-drug-loaded TRs showed an increase in EE compared to single-loaded hydrophilic drugs.

The EE percentage of MTX TRs was approximately 37.8% and that of blanks was 33.7%, which indicates that the further incorporation of the drug was not affected by the functionalization process. The EE% values of the results were relatively high, which shows that the transferomal preparation has better stability and good drug entrapment.

Physicochemical and rheological evaluation of TR gels

Spreadabilty

MTX/BL TRs were formulated with a carbopol 940 gel base, which retained the concentration of the drug for the prolong period of time into the stratum corneum. The spreadability factor of the TR gel was evaluated for the characteristics of topical gel formulations of the MTX/BL TR gel, MTX-TRs, and blank TRs. No significant difference in the physicochemical properties of the transferredomal carbopol gels was observed. At the initial stages, the spreadability profiles of all transfersomal gels were similar.

The MTX/BL TRs gel was evaluated for rheological behavior. The rheological properties of the transferredomal gel were analyzed for topical application. The results were compared with those of the blank drug gel. The viscosities of the gels were analyzed using a Brookfield viscometer spindle no 96.

The dual-loaded drug-incorporated gel showed shear thinning characteristics after the application of the slightest shear stress, which explained the pseudoplastic behavior. This assumption assumes physical stability of the formulations under several conditions during manufacturing and transportation.

Ex vivo skin penetration

The total amount permeated per unit area from simple MTX gel, single MTX-TR gel 31.42 µg/mL was released with standard deviation (SD) ± 9.4 µg/cm^2, single BLTRs gel 73.2 µg/mL was released with SD ± 12.4 µg/cm^2. In combination drug delivery, the MTX/BL TRs the MTX was 218.6 µg/mL permeated with SD ±19.5 µg/cm^2 and the BL was 237.61 µg/mL permeated with SD ± 25.5 µg/cm^2, respectively. When drugs were applied with co-loaded MTX/BL TRs, the skin permeation of the drugs was significantly improved ($p < 0.01$). Co-loaded MTX/BL TRs were more efficiently deposited in the skin than simple MTX and single MTX gels.

VS and lipid content of nano-lipid carriers (liposomal formulations) affected the release pattern of TRs. Additionally, the deposition of MTX/BL TRs in the skin was much higher than that of the single drug-loaded MTX gel. It has a longer retained period of time at the site of psoriasis due to more skin deposition than less skin permeation (Figure 2).[21]

Evaluation of skin structure after MTX/BL TRs treatment

Histopathological examinations compared the normal skin of healthy mice with the typical epidermis and dermis with that of psoriatic-induced treated or untreated mice. The results obtained from group I (normal mice epidermis) Figure 3A, group II (untreated control) Figure 3B, group III (plain drug MTX) Figure 3C, group IV (single loaded MTX) Figure 3D and group V (dual-drug loaded MTX/BL TRs) Figure 3E, respectively.

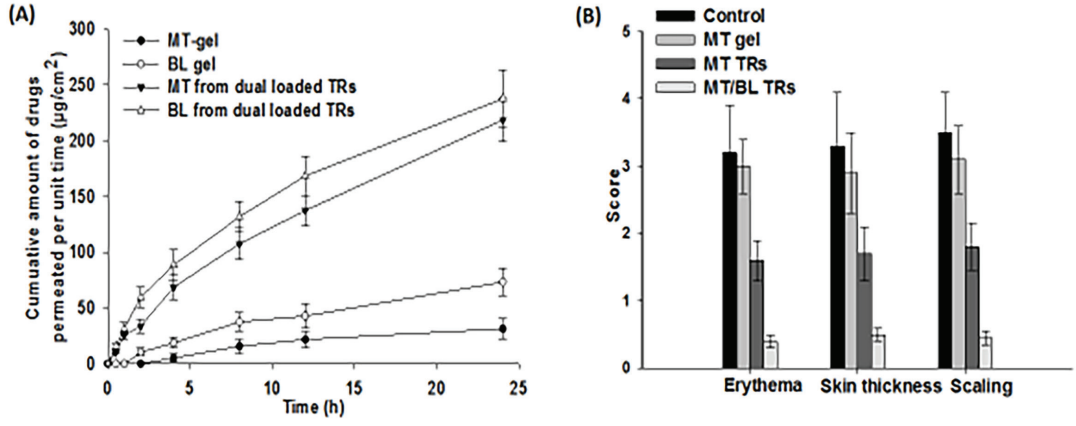

Figure 2. A, B) Drug's permeation and skin penetration studies

MT: Methotrexate, BL: Baicalin, TRs: Transfersomes

Group I included normal skin with well-defined epidermis, dermis, subcutaneous tissue, and muscles. The epidermis shows stratified squamous keratinized epithelium supported by a dermis layer of dense fibro elastic connective tissue that is devoid of inflammatory cells. Histopathological changes in the treatment group were highly dependent on formulation type. The thickness index varies among the groups. During the treatment the thickness was reduced. After treatment with MTX gel, psoriatic skin showed no significant reduction in epidermal thickness. This result indicated that the anti-psoriatic activity of the single MTX gel was relatively partial. Single MTX/TRs showed better anti-psoriatic activity by reducing epidermal thickness, which indicates that nano-lipid carriers of MTX within nano-lipid carriers have better anti-psoriatic activity, but MTX/BL TRs, a dual-drug delivery gel, showed similar histopathological characteristics as compared to the normal epidermis of mice, where the epidermis of the skin was almost normalized. This confirms that single MTX/TRs and MTX-BL nano-lipid carriers have significant ($p < 0.05$) reduced thickness in all groups. Relatively acceptable safety profile and does not cause irritation in clinical trials when applied topically. This was based on the absence of apparent signs of skin irritation in the *in vivo* study (Figure 2).

Scoring of skin inflammation

For 30 consecutive days, the PASI scores for skin erythema and skin thickening in the psoriasis-affected area were observed. All formulations of simple MTX drug, single MTX TRs, and MTX/BL TRs exhibited clear PASI scores on day 10, which were later more improved on day 15. Compared with these formulations, the dual-drug-loaded MTX-BL/TR gel showed reduction in both skin erythema and skin thickening and had the best anti-psoriatic activity. The PASI score ranged from 0 to 6, and the scoring parameters were 1. Erythema, 2. skin thickness, 3. scaling. The formulations for PASI scoring were the control, simple MTX, MTX-TR, and MTX/BL TRs gels. The control group had a score of 3 in erythema, skin thickness, and scaling. The control group had the highest score in all the parameters, which indicates severe erythema, skin thickness, and scaling. Simple MTX gel: showed less score of 3 compared to the control group for all the parameters of erythema, skin thickness, and scaling. Simple MTX gel showed a score of 2.5 for all the parameters, which indicates that the severity of erythema, skin thickness, and scaling decreased. MTX-TRs gel: The PASI scoring scale decreased by up to 1.5. The TR gel preparation has more efficacy and permeation into the skin than the plain MTX gel. MTX/BL TR gel: The combination dual-drug delivery has shown the scaling of zero or above for all parameters, which shows that the dual-drug combination of MTX/BL TRs gel has the lowest erythema, skin thickness, and scaling, which leads to improving the improve the condition of psoriasis.

Cytotoxicity assay

Increased levels of cytokines characterize psoriatic skin is characterized. TNF-α and IL-17.[32] ELISA was performed to find the level of TNF-α and IL-17, as shown in Figure 4A and Figure 4B. The TNF-α and IL-17 levels were analyzed in 5 groups. Each group consisted of 5 members. The optimized topical transferomal gel for psoriasis decreased the level of cytokines TNF-α, IL-22 and IL-17.[22]

TNF-α

Figure 4A shows the results of the relative % of TNF-α at a scale of 0-120 at the Y-axis and different group formulations of control, untreated, MTX solution, MTX TRs, and MTX/BL TRs. The results show major differences between the control and untreated groups. The percentage of TNF-α increased up to 90%, simple MT sol:showed 65% TNF-α. The relative percentage of TNF-α decreased as compared to the untreated

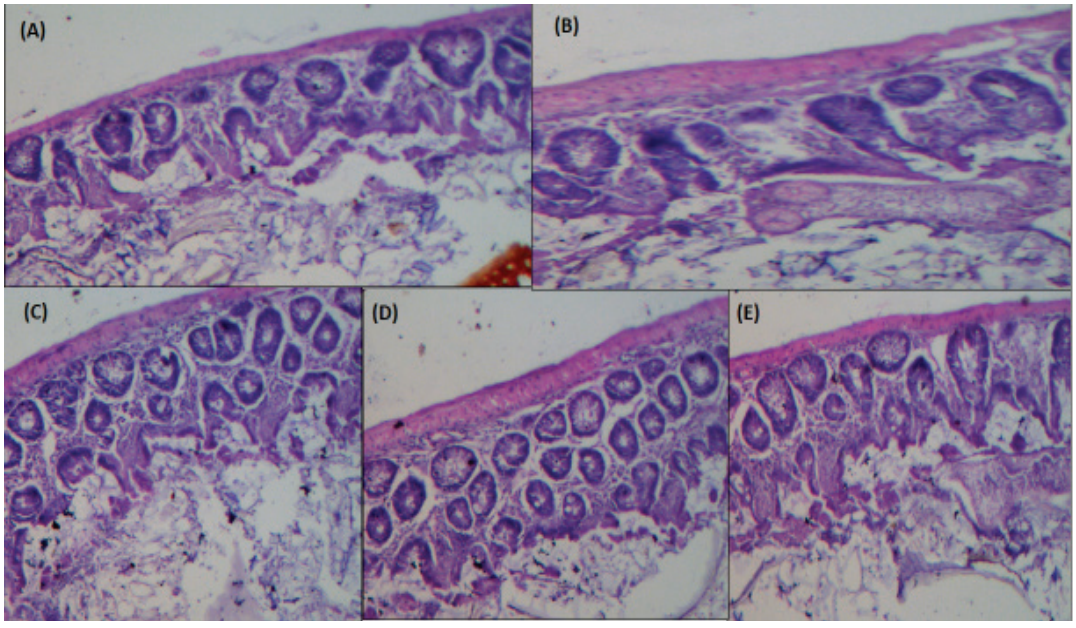

Figure 3. Histopathological studies. A) Normal, B) Psoriasis, C) Single Methotrexate drug, D) Single Methotrexate transfersomes, E) Dual-loaded Methotrexate-Baicalin transfersomes

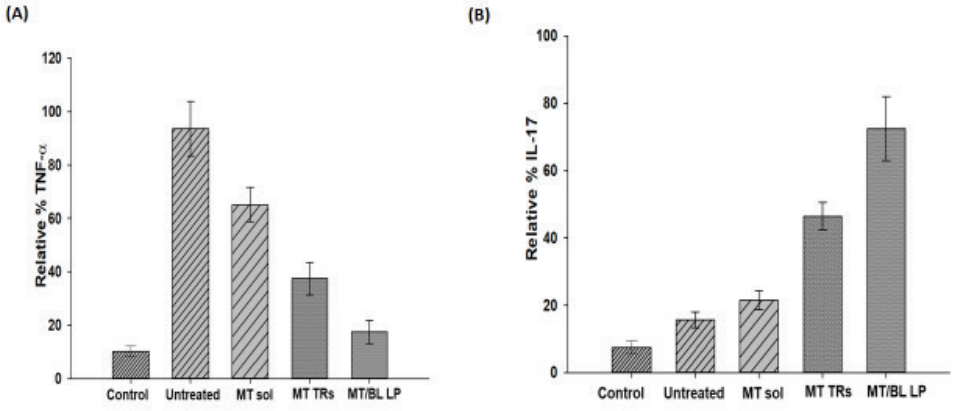

Figure 4. Cytotoxicity sssay A: TNF- α, B: IL-17

MT: Methotrexate, BL: Baicalin, TRs: Transfersomes, LP: Liposomes, TNF- α: Tumor necrosis factor-alpha, IL-17: Interleukin-17

group. MTX is effective in psoriasis as the results showed a decrease value. The MTX TR gel was incorporated with MTX. The gel showed more penetration permeation than the plain MTX solutionl. The TNF-α was decreased up to 35%. The MTX/BL TR gel percentage relative of TNF-α has been 10%, which was near 5% of the control group. The results were interpreted as indicating that nano-lipid carriers have more permeation and penetration than plain gel. Transfersomal gels have greater efficacy than plain single-dose drug delivery. The results are similar to those of the control group, indicating a better choice of nano-lipid carriers for topical drug delivery. The results of the control group are much more concise than those of the other groups. The control group was used as a standard, and the relative percentage of TNF-α was 5%. Other groups had high relative percentage of TNF-α, the untreated group had the highest percentage of TNF-α.

IL-17

The relative percentage of IL-17 was significantly higher in patients with psoriasis than in the control group. Because it was treated with different formulations, the relative percentage of IL-17 was twice that of other formulations. Figure 4B shows the results of the relative % of TNF-α at a scale of 0-120 at Y-axis and different group formulations of control, untreated, MTX solution, MTX-TRs, and MTX/BL TRs. The results show major differences between the control and untreated groups. The percentage of IL-17 increased up to 65%, and the Simple MTX solution produced 20% IL-17. The relative percentage of IL-17 was increased compared with the untreated group. MTX is effective against psoriasis as evidenced by the increased value. The MTX-TR gel was incorporated with MTX. The gel showed more penetration permeation than the plain MTX sol. The IL-17 was increased up to 40%. The MTX/BL TR gel percentage relative of IL-17 was 65%, which is significantly different from the control group. The results were interpreted as indicating that nano-lipid carriers have more permeation and penetration than plain gel. Transfersomal gels have greater efficacy than plain single-dose drug delivery. The results are similar to those of the control group, indicating a better choice of nano-lipid carriers for topical drug delivery. The results of the control group are quite more concise than those of the other groups. The control group was used as a standard, and the relative percentage of IL-17 was 20%. Other groups had a high relative percentage of IL-17, whereas the untreated group had the lowest percent of IL-17. The comparison between TNF-α and IL-17. In comparison with the control group the TNF-α and IL-17 levels were relative of 20. In untreated group the level of TNF-α were increased up to 90% in psoriatic-induced untreated skin, respectively. After treatment with MTX- solution, MTX-TRs, and MTX/BL TRs the level of TNF-α was decreased by 65%, 25%, and 20%, respectively. Similarly, in the untreated group, the level of IL-17 was raised compared with the control group, indicating the induction of psoriasis (Figure 4). After the application of MTX- solution, MTX-TRs, and MTX/BL LP, the level of IL-17 was increased by 20%, 40% and 65%. The present data showed that an increased serum concentration of IL-17 was present. The role of IL-17 in neutrophil production at the site of inflammation and chemokine production. The TNF-α cytokine assay data shows that in the psoriasis-affected group (untreated) the serum level was increased, which was later on decreasing when treated with MTX nano-lipid carriers. The IL-17 cytokine assay data showed that in the psoriasis-affected group (un treated) the serum level was decreased, which was later on increasing when treated with MTX nano-lipid carriers. Both cytokines assays showed the activity of nano-lipid carriers of MTX solution, MTX-TRs, and MTX/BL TRs. TNF-α interacts with inflammatory cells to trigger cytolysis.

DISCUSSION

In this study, dual-drug nanocarrier physiological and *in vitro* and *in vivo* characteristics were examined. The topical treatment of psoriasis is preferred over systemic drug delivery because of fewer adverse effects.[33] Topical formulations have greater bioavailability with fewer side effects. Dual-drug delivery shows a significant therapeutic approach at a very low dose for complicated and single therapy resistant diseases.[16] Adverse drug reactions were reported with systemic MTX

therapy in patients with psoriasis, but there was no significant effect on liver and serum enzyme level.[8] To improve the efficacy of treatment of various pathological diseases, dual-drug therapy is required. The limitations of the dual-drug delivery method are the entrapment of different charged molecules, physicochemical incompatibility, solubility, selection of surfactants, stability, and various drug concentrations.[11] Co-loaded nano-lipid carriers penetrated and permeated into the deeper layer of dermis, slowly releasing a dual-drug into the subcutaneous.[34] Previously, many studies have described the MTX nano-carrier skin penetration results for the topical application for the treatment of psoriasis.[35] It was concluded that the VS of single MTX-TRs was considerably higher ($p < 0.01$) at 10% SC as an EA compared to MTX/BL TRs.

EAs act as stabilizers to increase the drug permeation of lipid-nano carriers.[7] The VS decreases with increasing SC concentration from 10% to 20%, and the PDI shows an increase in its value. The PDI value of MTX-TRs and MTX/BL TRs ranges from 0.15 to 0.359, which shows better uniformity and homogeneity of formulations.[36] The hydrophobic drugs have a higher membrane flux and have direct interaction with the lipid bilayer of the skin. Phospholipon 90G increased the permeation flux ($p < 0.05$) of the MTX formulation because of its high lipid content. The effect of SC on the deformability index increased with each other at the extent of 10% ($p < 0.01$). The amount of EE significantly decreased when the amount of surfactant increased.[37] The nano-lipid carriers prepared by SC have a concise particle size and an EE% higher than that of tween 80. SC provides better EE compared to other surfactants. The formulation of MTX, phospholipon 90G, sodium calcium, and cholesterol has the most concise particle size and better EE. In TR vesicles, the greater the lipid content, the greater is the EE. The effect of cholesterol in formulations is the least effective, but its effect on EE is greater due to its high lipid content. Phospholipon 90G had a greater influence on EE%. This explained that the addition of Baicalin created a detrimental influence on the deformability of elastic vesicles, whereas the addition of MTX had an optimistic effect. To increase the deformability of ultra-deformable liposomes, the EA is of vital importance. The effect of SC as an EA is concentration-dependent.[38] Advanced rigid molecular structures have more skin permeation, rigid VS and more bioavailability.[39] In the present study, single MTX-TRs had lower EEs than dual-drug loaded MTX/BL TRs. Decreased concentrations of EA and Phospholipon 90G decrease the rapid reduction of dual-drug loaded TRs vs. more increase in phospholipon 90G and SC resulted in immediate decrease in EE. Single MTX-TRs had lower EE compared with dual-drug loaded MTX/BL TRs. Dual-drug loaded TRs showed an increase in EE compared to single-loaded hydrophilic drugs. Transfersomal preparations have better stability and good entrapment of a drug. VS of nano-lipid carriers plays an important role in topical delivery. To achieve advanced targeted drug delivery and deeper penetration of the drug, the formulation should be optimum and characterized on the basis of particle size. These formulations varying from different (phospholipon 90G and SC) concentrations were prepared by thin-film hydration. Polar and high-molecular-weight molecules diffuse through the stratum corneum by encapsulation with a non-ionic surfactant of particle size.[29] To increase the stability of the formulation, the vesicle should have a highly negative zeta potential charge due to electrostatic repulsion. Highly positively charged nanoparticles are more cytotoxic because they cause protein aggregation in the blood. To determine the stability, cellular uptake, and cytotoxicity of transferomal preparation, the Zeta potential is required.[1] The stable colloidal dispersion exhibited a Zeta potential of approximately 38.6 mV. Highly positively charged nanoparticles are more cytotoxic because they cause protein aggregation in the blood. The surface charge of nano-lipid carriers maintains its stability.[22] The Ideal pH for carbopol gel is 5.0-8.0 which does not affect its rheological properties, so it can be used as a topical formulations.[40] The formulations of carbopol gel having different concentrations showed a non-Newtonian, higher shear-thinning, which increased the drug's retention time, bioavailability, and therapeutic efficacy.[16] Nano-carrier emulsion gels are more beneficial in topical preparations hence they covered the maximum coverage area.[41] The dual-drug delivery of MTX and Baicalin into the nano-carrier molecule improves the therapeutic activity as compared to single drug delivery. The previous studies has been reported.[34] The thin film was formed at 50 °C temperature and 90 RPM at 20 minutes in a rotary vacuum evaporateator. Nano-lipid carriers have 5 fold more penetration of drug into the Stratum Corneum.[22] Lipid nano-carrier is the advanced Drug Delivery System in Cosmeceuticals. The Novel Drug Delivery system termed as nano-safe carriers due to their safety profile.[42] The components were selected based on the characteristics of skin permeation, molecular compatibility, and GRAS condition.[41] In a previous study, the dual-drug delivery of MTX lipid ultra-deformable liposomes formed by a carbopol gel showed increased skin drug bioavailability.[3] For the Topical route of drug administration, spreadability is an important characteristic for the development and formulation of appropriate drugs in the target area. The PSRAL gel and PSRCL gel showed that the rheological properties of gels result in a reduction of viscosity due to shear stress.[43] Drug loaded incorporated gel showed shear thinning characteristics by applying the slightest shear stress, which explained the pseudoplastic behavior. This shows the stability of the formulations. *In vitro* and *ex vivo* permeation studies of all the transferomal batches were conducted to determine drug release and permeation studies. The MTX/BL TRs improved the skin permeation of drugs was much improved ($p < 0.01$) However co-loaded MTX/BL TRs were more efficiently deposited when applied into the skin compared to a simple MTX and single MTX gel. The VS and lipid content behavior of TRs affected the release pattern of TRs. It has a longer retained period of time at the site of psoriasis due to more skin deposition. *In vitro* results of MTX SLNs showed a 8 hour sustained release.[3] The dual-drug MTX-loaded TRs decreased the PASI score, and the formulation was developed for treating psoriasis topically.[1] *In vitro* results explained the lipid nano-carrier anti-psoriatic activity, decreased the IL-17

and TNF-α. Cell lines explain the decreased levels of NO, IL-2, IL-6 and IL 1β.[31]

MTX with Baicalin transferomal gel showed significant penetration and permeation parameters in psoriasis affected skin. Psoriasis is a chronic inflammatory, T-lymphocyte immune-mediated skin disease. The etiology of psoriasis is unknown, but the risk factors are drugs, IBD, lifestyle, environmental, and genetic factors, which lead to the proliferation of keratinocytes.[13] As a result, silver scales, papules, and plaques are formed due to epidermal thickening. Scaly skin lesions are usually observed at the elbows, knee joints, palms, soles, and extensor surfaces, and erythrodermic psoriasis diffuses in areas covering > 90% of the body surface. Psoriasis treatment focuses on relieving symptoms and improving skin function. Depending upon the type and severity of psoriasis, the treatment should be planned, which may include phototherapy, systemic treatments, Monoclonal antibodies, or topical treatments.[44] Application of Drug Directly at Topical Affected Psoriasis Sites with a narrow Therapeutic Window Reduced Systemic Absorption.[45] MTX (orally as well as systematically) is the gold standard drug for the treatment of psoriasis. MTX is a dihydro-folate reductase enzyme inhibitor. This drug shows good therapeutic activity in TNF, skin tumor, and rheumatoid arthritis. Due to the high molecular weight of MTX (454.56 D, water solubility, and its ionized form, it will not diffuse passively through the Stratum Corneum.[46] Various types of MTX-based drug delivery systems, including nano-carriers, SLNs (solid lipid nanoparticles), self-emulsifying nano-systems, nano-lipid carriers, liposomes, carbon nanotubes, polymeric nanoparticles, dendrimer, metallic nanoparticles, nanolipid carriers, and niosome, have been formulated for the Topical Delivery of MTX.[47]

MTX-entrapped nano-lipid carriers are elastic vesicles made of lipid materials and a surfactant with at least one inner aqueous compartment surrounded by a lipid bilayer.[48] By using KG as a surfactant, the amount of MTX permeated across the skin is 3-4 fold higher as compared to conventional liposomes. Natural ingredient-based nano-lipid carriers are the better choice because of increased permeation of drugs into the skin. Formulations were analyzed and optimized by thin-film rehydration using phospholipon 90G, tween 80, and cholesterol. Optimization and characterization of drug carriers based on particle size, zeta potential, and drug EE. Evaluation of pH, homogeneity, spreadability, rheological studies, and drug content determination for all formulations showed that drug-loaded TRs (MTX/BL TRs) have better physicochemical properties than plain drugs.

The result of VS at 70:30 or higher concentrations but at 60:40 the rapid reduction of dual-drug-loaded MTX/BL TRs was observed. The zeta potential was approximately 38.6 mV, which is considered stable colloidal dispersion. The incorporation of MTX/BL TR did not have significant interference in the zeta potential values and consequently in the stability of the formulations. Neutral charged or slightly negative nano-lipid carriers with zeta potentials ranging from 10 mV to and 10 mV are acceptable. Highly positively charged nanoparticles are more cytotoxic because they cause protein aggregation in the blood. The EE percentage of MTX-TRs was approximately 37.8% and that of blanks was 33.7%, which indicates that the further incorporation of drug was not affected by the functionalization process. The EE% values of the results were relatively high, which shows that the transferomal preparation has better stability and good drug entrapment. The dual-loaded drug-incorporated gel showed shear thinning characteristics after the application of the slightest shear stress, which explained the pseudoplastic behavior. This assumption assumes physical stability of the formulations under several conditions during manufacturing and transportation.

Characterization by *in vitro* release and membrane diffusion studies of transferomal gel formulations revealed that the VS and lipid content of nano-lipid carriers (liposomal formulations) affected TR release patterns.[49] Additionally, the deposition of MTX/BL TRs in the skin was much higher than that of the single drug-loaded MTX gel. It has a longer retained period of time at the site of psoriasis due to more skin deposition than less skin permeation.

The effects of the formulations on anti-psoriatic efficacy were evaluated by PASI scoring of skin severity and thickening. The scoring parameters were set to 1. erythema, 2. skin thickness, 3. scaling. The combination dual-drug delivery has shown the scaling of zero or above for all parameters, which shows that the dual-drug combination of MTX/BL TRs gel has the lowest erythema, skin thickness, and scaling, which leads to improving the improve the condition of psoriasis.[50]

Histopathological examinations compared the normal skin of healthy mice with the typical epidermis and dermis with that of psoriatic-induced treated or untreated mice. The epidermis is characterized by stratified squamous keratinized epithelium supported by a dermis layer of dense fibroelastic connective tissue that is devoid of inflammatory cells. Histopathological changes in the treatment group were highly dependent on formulation type. The thickness index varies among the groups. During the treatment the thickness was reduced. After treatment with MTX gel, psoriatic skin showed no significant reduction in epidermal thickness. This result indicated that the anti-psoriatic activity of the single MTX gel was relatively partial. In contrast, single MTX-TRs showed better anti-psoriatic activity by reducing epidermal thickness, which indicates that nano-lipid carriers of MTX within nano-lipid carriers have better anti-psoriatic activity, but MTX/BL TRs, a dual-drug delivery gel, showed similar histopathological characteristics as compared to the normal epidermis of mice; the epidermis of the skin was almost normalized.[51]

Increased levels of cytokines characterize psoriatic skin is characterized. TNF-α and IL-17.[49] ELISA assay was performed to find the level of TNF-α and IL-17. The increased levels of the pro-inflammatory cytokines IL-17, IL-23, TNF-α and IL-27 due to the activation of Th1 and Th 17 cells (CD4+T cells and CD8+T cells) enhance the inflammatory response.

Stable MTX/TR-based transferomal gel with advanced efficiency for the psoriasis model in BALB/c mice was investigated for the liposomal targeted drug delivery of MTX/BL TRs. The results

establish that MTX/BL TRs were more potent and exhibited better penetration and permeation than single-loaded drugs.

Study limitations

The sample size in this study was small, 25 animals in 5 groups because of limited Research and Development facilities. To study more effectively ELISAs and more cytokines assays should be applied, More variables of surfactants and EAs should be studied.

Future perspective

This study will create new opportunities for the release of the profile of topical dual delivery of anti-psoriasis drugs. Further evaluation of the synergistic mechanism and cytotoxicity of novel co-loaded nano-lipid carriers for the treatment of psoriasis.

CONCLUSION

It can be concluded that newer targeting strategies for NLCs for dual-drug delivery of nanolipid carriers MTX/BL TRs gel that could be administered topically for the treatment of psoriasis. Furthermore, this approach opens new avenues for continued and sustained research in pharmaceuticals with much more effective outcomes.

Acknowledgements

The authors acknowledge Bio Labs (Pvt. Ltd.) and the National Institute of Health Islamabad for providing samples, *in vitro* and *in vivo* anti-psoriasis assays. The authors are thankful to the COMSTECH the Ministerial Standing Committee on Scientific and Technological Cooperation of the OIC (Organization of Islamic Cooperation for awarded the fellowship in International Centre for Chemical and Biological Sciences (ICCBS), Karachi-Pakistan.

Ethics

Ethics Committee Approval: *In vitro* and *ex vivo* permeation studies were conducted as per the experimental protocol approved by the IBADAT International University, Islamabad Faculty of Allied Health Sciences Bioethics Committee (approval number: #BEC/0525, date: 23.02.2023).

Informed Consent: Not required.

Authorship Contributions

Surgical and Medical Practices: S.S., S.A., Concept: M.J.D., Design: K.I., Data Collection or Processing: S.S., S.K., Analysis or Interpretation: M.J.D., K.I., Literature Search: S.S., H.S., Writing: M.J.D., S.A.

Conflict of Interest: No conflict of interest was declared by the authors.

Financial Disclosure: The authors declared that this study received no financial support.

REFERENCES

1. Abdelbary AA, AbouGhaly MH. Design and optimization of topical Methotrexate loaded niosomes for enhanced management of psoriasis: application of Box-Behnken design, *in vitro* evaluation and *in vivo* skin deposition study. Int J Pharm. 2015;485:235-243.
2. Al-Mahallawi AM, Fares AR, Abd-Elsalam WH. Enhanced permeation of Methotrexate *via* loading into ultra-permeable niosomal vesicles: fabrication, statistical optimization, *ex vivo* studies, and *in vivo* skin deposition and tolerability. AAPS PharmSciTech. 2019;20:171.
3. Babaloo Z, Oskoei MR, Kohansal MH, Barac A, Ahmadpour E. Serum profile of IL-1β and IL-17 cytokines in patients with visceral leishmaniasis. Comp Immunol Microbiol Infect Dis. 2020;69:101431.
4. Batool S, Zahid F, Ud-Din F, Naz SS, Dar MJ, Khan MW, Zeb A, Khan GM. Macrophage targeting with the novel carbopol-based miltefosine-loaded transfersomal gel for the treatment of cutaneous leishmaniasis: *in vitro* and *in vivo* analyses. Drug Dev Ind Pharm. 2021;47:440-453.
5. Chandra A, Aggarwal G, Manchanda S, Narula A. Development of topical gel of Methotrexate incorporated ethosomes and salicylic acid for the treatment of psoriasis. Pharm Nanotechnol. 2019;7:362-374.
6. Chaudhary H, Kohli K, Kumar V. Nano-transfersomes as a novel carrier for transdermal delivery. Int J Pharm. 2013;454:367-380.
7. Chen M, Shamim MA, Shahid A, Yeung S, Andresen BT, Wang J, Nekkanti V, Meyskens FL Jr, Kelly KM, Huang Y. Topical delivery of carvedilol loaded nano-transfersomes for skin cancer chemoprevention. Pharmaceutics. 2020;12:1151.
8. Cosco D, Paolino D, Maiuolo J, Marzio LD, Carafa M, Ventura CA, Fresta M. Ultradeformable liposomes as multidrug carrier of resveratrol and 5-fluorouracil for their topical delivery. Int J Pharm. 2015;489:1-10.
9. Dar MJ, Din FU, Khan GM. Sodium stibogluconate loaded nano-deformable liposomes for topical treatment of leishmaniasis: macrophage as a target cell. Drug Deliv. 2018;25:1595-1606.
10. Dar MJ, Khalid S, McElroy CA, Satoskar AR, Khan GM. Topical treatment of cutaneous leishmaniasis with novel amphotericin B-miltefosine co-incorporated second generation ultra-deformable liposomes. Int J Pharm. 2020;573:118900.
11. Dar MJ, Khalid S, Varikuti S, Satoskar AR, Khan GM. Nano-elastic liposomes as multidrug carrier of sodium stibogluconate and ketoconazole: A potential new approach for the topical treatment of cutaneous Leishmaniasis. Eur J Pharm Sci. 2020;145:105256.
12. Dar MJ, McElroy CA, Khan MI, Satoskar AR, Khan GM. Development and evaluation of novel miltefosine-polyphenol co-loaded second generation nano-transfersomes for the topical treatment of cutaneous leishmaniasis. Expert Opin Drug Deliv. 2020;17:97-110.
13. Doppalapudi S, Jain A, Chopra DK, Khan W. Psoralen loaded liposomal nanocarriers for improved skin penetration and efficacy of topical PUVA in psoriasis. Eur J Pharm Sci. 2017;96:515-529.
14. Ferreira M, Barreiros L, Segundo MA, Torres T, Selores M, Costa Lima SA, Reis S. Topical co-delivery of Methotrexate and etanercept using lipid nanoparticles: A targeted approach for psoriasis management. Colloids Surf B Biointerfaces. 2017;159:23-29.
15. García-Manrique P, Machado ND, Fernández MA, Blanco-López MC, Matos M, Gutiérrez G. Effect of drug molecular weight on niosomes size and encapsulation efficiency. Colloids Surf B Biointerfaces. 2020;186:110711.
16. Goyal G, Garg T, Malik B, Chauhan G, Rath G, Goyal AK. Development and characterization of niosomal gel for topical delivery of benzoyl peroxide. Drug Deliv. 2015;22:1027-1042.

17. How KN, Yap WH, Lim CLH, Goh BH, Lai ZW. Hyaluronic acid-mediated drug delivery system targeting for inflammatory skin diseases: a mini review. Front Pharmacol. 2020;11:1105.

18. Hsieh WC, Fang CW, Suhail M, Lam Vu Q, Chuang CH, Wu PC. Improved skin permeability and whitening effect of catechin-loaded transfersomes through topical delivery. Int J Pharm. 2021;607:121030.

19. Hung CH, Wang CN, Cheng HH, Liao JW, Chen YT, Chao YW, Jiang JL, Lee CC. Baicalin ameliorates imiquimod-induced psoriasis-like inflammation in mice. Planta Med. 2018;84:1110-1117.

20. Ita KB, Du Preez J, Lane ME, Hadgraft J, du Plessis J. Dermal delivery of selected hydrophilic drugs from elastic liposomes: effect of phospholipid formulation and surfactants. J Pharm Pharmacol. 2007;59:1215-1222.

21. Jain A, Pooladanda V, Bulbake U, Doppalapudi S, Rafeeqi TA, Godugu C, Khan W. Liposphere mediated topical delivery of thymoquinone in the treatment of psoriasis. Nanomedicine. 2017;13:2251-2262.

22. Kaur L, Jain SK, Singh K. Vitamin E TPGS based nanogel for the skin targeting of high molecular weight anti-fungal drug: development and *in vitro* and *in vivo* assessment. RSC advances. 2015;5:53671-53686.

23. Khan MA, Pandit J, Sultana Y, Sultana S, Ali A, Aqil M, Chauhan M. Novel carbopol-based transfersomal gel of 5-fluorouracil for skin cancer treatment: *in vitro* characterization and *in vivo* study. Drug Deliv. 2015;22:795-802.

24. Lin YK, Huang ZR, Zhuo RZ, Fang JY. Combination of calcipotriol and Methotrexate in nanostructured lipid carriers for topical delivery. Int J Nanomedicine. 2010;5:117-128.

25. Malekar SA. Liposomes for the controlled delivery of multiple drugs: University of Rhode Island (2004).

26. Otero ME, van Geel MJ, Hendriks JC, van de Kerkhof PC, Seyger MM, de Jong EM. A pilot study on the Psoriasis Area and Severity Index (PASI) for small areas: Presentation and implications of the Low PASI score. J Dermatolog Treat. 2015;26:314-317.

27. Pietrzak AT, Zalewska A, Chodorowska G, Krasowska D, Michalak-Stoma A, Nockowski P, Osemlak P, Paszkowski T, Roliński JM. Cytokines and anticytokines in psoriasis. Clin Chim Acta. 2008;394:7-21.

28. Pradhan M, Alexander A, Singh MR, Singh D, Saraf S, Saraf S, Ajazuddin. Understanding the prospective of nano-formulations towards the treatment of psoriasis. Biomed Pharmacother. 2018;107:447-463.

29. Puglia C, Bonina F. Lipid nanoparticles as novel delivery systems for cosmetics and dermal pharmaceuticals. Expert Opin Drug Deliv. 2012;9:429-441.

30. Qushawy M, Nasr A, Abd-Alhaseeb M, Swidan S. Design, optimization and characterization of a transfersomal gel using miconazole nitrate for the treatment of candida skin infections. Pharmaceutics. 2018;10:26.

31. Rabia S, Khaleeq N, Batool S, Dar MJ, Kim DW, Din FU, Khan GM. Rifampicin-loaded nanotransferosomal gel for treatment of cutaneous leishmaniasis: passive targeting *via* topical route. Nanomedicine (Lond). 2020;15:183-203.

32. Rahman M, Alam K, Ahmad MZ, Gupta G, Afzal M, Akhter S, Kazmi I, Jyoti, Ahmad FJ, Anwar F. Classical to current approach for treatment of psoriasis: a review. Endocr Metab Immune Disord Drug Targets. 2012;12:287-302.

33. Rai S, Pandey V, Rai G. Transfersomes as versatile and flexible nano-vesicular carriers in skin cancer Chen therapy: the state of the art. Nano Rev Exp. 2017;8:1325708.

34. Rashid SA, Bashir S, Ullah H, Shah KU, Khan DH, Shah PA, Danish MZ, Khan MH, Mahmood S, Sohaib M, Irfan MM, Amin A. Development, characterization and optimization of Methotrexate-olive oil nano-emulsion for topical application. Pak J Pharm Sci. 2021;34:205-215.

35. Roh NK, Han SH, Youn HJ, Kim YR, Lee YW, Choe YB, Ahn KJ. Tissue and serum inflammatory cytokine levels in Korean psoriasis patients: a comparison between plaque and guttate psoriasis. Ann Dermatol. 2015;27:738-743.

36. Sala M, Elaissari A, Fessi H. Advances in psoriasis physiopathology and treatments: Up to date of mechanistic insights and perspectives of novel therapies based on innovative skin drug delivery systems (ISDDS). J Control Release. 2016;239:182-202.

37. Sharma V, Anandhakumar S, Sasidharan M. Self-degrading niosomes for encapsulation of hydrophilic and hydrophobic drugs: An efficient carrier for cancer multi-drug delivery. Mater Sci Eng C Mater Biol Appl. 2015;56:393-400.

38. Singh S, Vardhan H, Kotla NG, Maddiboyina B, Sharma D, Webster TJ. The role of surfactants in the formulation of elastic liposomal gels containing a synthetic opioid analgesic. Int J Nanomedicine. 2016;11:1475-1482.

39. Singh Y, Meher JG, Raval K, Khan FA, Chaurasia M, Jain NK, Chourasia MK. Nanoemulsion: Concepts, development and applications in drug delivery. J Control Release. 2017;252:28-49.

40. Srisuk P, Thongnopnua P, Raktanonchai U, Kanokpanont S. Physico-chemical characteristics of Methotrexate-entrapped oleic acid-containing deformable liposomes for in vitro transepidermal delivery targeting psoriasis treatment. Int J Pharm. 2012;427:426-434.

41. Srivastava AK, Nagar HK, Chandel HS, Ranawat MS. Antipsoriatic activity of ethanolic extract of *Woodfordia fruticosa* (L.) Kurz flowers in a novel *in vivo* screening model. Indian J Pharmacol. 2016;48:531-536.

42. Tamayo I, Gamazo C, de Souza Reboucas J, Irache JM. (2017). Topical immunization using a nanoemulsion containing bacterial membrane antigens. Journal of Drug Delivery Science and Technology. 2017;42:207-214.

43. Tan Q, Liu W, Guo C, Zhai G. Preparation and evaluation of quercetin-loaded lecithin-chitosan nanoparticles for topical delivery. Int J Nanomedicine. 2011;6:1621-1630.

44. Trotta M, Peira E, Carlotti ME, Gallarate M. Deformable liposomes for dermal administration of Methotrexate. Int J Pharm. 2004;270:119-125.

45. Walunj M, Doppalapudi S, Bulbake U, Khan W. Preparation, characterization, and in vivo evaluation of cyclosporine cationic liposomes for the treatment of psoriasis. J Liposome Res. 2020;30:68-79.

46. Wang J, Zhang H, Liu T, Wu M, Cao Y, Wu L, He S. [Baicalin inhibits the activity of keratinocytes in psoriasis by activating Notch signaling pathway]. Xi Bao Yu Fen Zi Mian Yi Xue Za Zhi. 2019;35:441-446.

47. Warren RB, Weatherhead SC, Smith CH, Exton LS, Mohd Mustapa MF, Kirby B, Yesudian PD. British Association of Dermatologists' guidelines for the safe and effective prescribing of Methotrexate for skin disease 2016. Br J Dermatol. 2016;175:23-44.

48. Wollina, U, Ständer K, Barta U. Toxicity of Methotrexate treatment in psoriasis and psoriatic arthritis–short-and long-term toxicity in 104 patients. Clin Rheumatol. 2001;20:406-410.

49. Wollina, U., Tirant, M, Vojvodic A, Lotti T. Treatment of psoriasis: Novel approaches to topical delivery. Access Maced J Med Sci. 2019;7:3018-3025.

50. Wu X, Deng X, Wang J, Li Q. Baicalin inhibits cell proliferation and inflammatory cytokines induced by tumor necrosis factor α (TNF-α) in human immortalized keratinocytes (HaCaT) human keratinocytes by inhibiting the STAT3/nuclear factor kappa B (NF-κB) signaling pathway. Med Sci Monit. 2020;26:e919392.

51. Yang C, Dai X, Yang S, Ma L, Chen L, Gao R, Wu X, Shi X. Coarse-grained molecular dynamics simulations of the effect of edge activators on the skin permeation behavior of transfersomes. Colloids Surf B Biointerfaces. 2019;183:110462.

Turk J Pharm Sci 2024;21(4):340-347
DOI: 10.4274/tjps.galenos.2023.28092

ORIGINAL ARTICLE

Phytochemical and Toxicological Analyses of Herbal Mixtures Containing *Hypericum perforatum* and *Melissa officinalis*

Faezeh FATEMI[1]*, Mehran ZAMANY[2], Somayeh FARAHMAND[2], Salome DINI[3]

[1]Nuclear Science and Technology Research Institute, Nuclear Fuel Cycle Research School, Tehran, Iran
[2]Payame Noor University (PNU) Faculty of Basic Science, Department of Biology, Tehran, Iran
[3]University of Otago, Department of Food Science, Dunedin, New Zealand

ABSTRACT

Objectives: This study aimed to formulate a novel herbal mixture of *Hypericum perforatum* (H) and *Melissa officinalis* (M) and evaluate its toxicity, microbial load, and phytochemical content.

Materials and Methods: Total flavonoids were measured using the $AlCl_3/NaNO_2$ complex formation method and colorimetric assay. The quercetin content of the herbal mixture was determined by reverse-phase high-performance liquid chromatography. The *in vitro* and *in vivo* safety of the herbal formulations were analyzed using the 3-(4,5-dimethylthiazol-2-yl)-2,5-diphenyltetrazolium bromide (MTT) assay and acute oral toxicity analysis in the rat model, respectively.

Results: The formulated extract (HM), compared with the standard rutin extract, had a total flavonoid content of 15.29 ± 0.64 mg rutin per mL sample. Reverse-phase high-performance liquid chromatography revealed a quercetin content of 0.187 mg/mL. Microbial tests for *Escherichia coli, Pseudomonas aeruginosa, Staphylococcus aureus,* and *Salmonella* spp. were negative. Colony counts for total aerobic microbial and yeast and mold counts were 10 in each case. The MTT assay (with up to about 5% *v/v* HM extract) using the NIH/3T3 cell line revealed no cell toxicity in the range of concentrations tested. Acute oral toxicity was tested in the Wistar rat model, and the LD_{50} was 695.2 ± 7.5 mg/kg. The dry weight of the HM extract was 38.1 mg/mL.

Conclusion: Preliminary results proved the safety of the HM herbal mixture, with its toxicity and microbial load within the limits of accepted guidelines allowable for use in clinical trials.

Keywords: *Melissa officinalis*, *Hypericum perforatum*, combined hydroethanolic extract, cell toxicity, animal toxicity

INTRODUCTION

In the course of history, humans have always looked toward nature for food, nutrients, and natural substances to treat various illnesses. Traditional medicine was founded on the relationship between man and nature thousands of years ago.[1] To date, only a small percentage of the total number of plant species on earth has been analyzed phytochemically, and even a smaller percentage has been screened for potential pharmacological use. Despite recent advances in our fundamental understanding of many disease mechanisms, such as cancer, chronic inflammation, diabetes, and neurodegenerative disorders, there is a great need for more effective pharmaceutical solutions. Plant extracts containing many secondary metabolites with various biological/pharmacological activities can affect many targets and potentially fill this gap. Previous studies have shown that essential oils and extracts isolated from different plant species exhibit powerful antimicrobial and antioxidant activities, as well as anti-inflammatory, anti-cancer, and

*Correspondence: fatemi81@yahoo.com, Phone: +989124186349, ORCID-ID: orcid.org/0000-0002-1092-9038
Received: 10.06.2023, Accepted: 28.08.2023

hepatoprotective activities.[2-6] A significant proportion of all drugs produced worldwide are either plant products or derived from them and phytopharmaceutical research has played an important role in the discovery and development of many more synthetic drugs.[7] At the same time, mixed herbal extracts can be used as multi-target drugs that act synergistically, have fewer side effects, and in the process lower treatment costs.[8]

Lemon balm, with the scientific name *Melissa officinalis* (M), is a well-known perennial herbaceous plant belonging to the Lamiaceae family that has been studied extensively for its medicinal properties. It is native to Asia, North America, the Mediterranean, and Southern Europe, and is extensively cultivated in these regions.[9] The leaves of M have been used to treat a number of ailments, including digestive and inflammatory diseases and microbial infections.[10] The presence of phenolics, terpenoids, and flavonoids, such as quercetin, rutin, and quercetin, in the M extract is believed to be responsible for their ability to treat various diseases.[11] Essential oils contain important secondary metabolites, such as geranial, cineol, and caffeic acid, which are capable of reducing serum cholesterol and triacylglyceride. Flavonoids are known for their powerful antioxidant activities, and they are also present in M extract.[12] *Hypericum perforatum* (H), also known as St. John's wort, is another medicinal plant of great importance that has been used for thousands of years. This perennial herb belongs to the Hypericacea family and is native to temperate regions of the world. It has been studied extensively because of its importance as a powerful medicinal plant that can treat various illnesses.[13] Leaves of plants are known to contain active metabolites such as flavonoids, naphthodianthrone, and phloroglucinol. The antidepressant effects of H extract are comparable to those of common synthetic antidepressants in mild to moderate cases.[14] Many studies have focused on the antiviral activity of H, and the results appear promising.[15,16]

Each of these plants contains a multitude of secondary metabolites that can exert a positive influence on the treatment of various diseases. A question that comes to mind is whether a combined extract of these two plants could be formulated for clinical use and maximize their therapeutic efficacy. Previous studies have confirmed that the combination of herbal formulations is generally associated with increased functional properties and biological activities of mixed extracts.[17,18] However, scientific data on the phytochemical analysis of the combined extract of M and H, particularly in, the determination of cell and animal toxicities, are scarce. In the current study, a new formulation of the combined ethanolic herbal extracts of H and M was prepared to perform preliminary safety and phytochemical analyses in preparation for future clinical testing.

MATERIALS AND METHODS

Plant acquisition and extraction

Both H and M herbal extracts were obtained from a medicinal plant farm in Ardabil, Iran. The samples were carefully cleaned of debris and air-dried in the laboratory. Herbarium samples of the plants were sent to the Institute of Pharmacology, Tehran University of Medical Sciences for identification. After proper identification, samples were registered and code numbers were assigned (PMP-2310 and 14001 for H and M, respectively). After weighing the plants, they were ground together in a pharmaceutical grinding mill to an adequate size for extraction (coarse ground). An Accelerated Solvent Extraction system (ASE) was used to perform extraction using 70% pharmaceutical-grade ethanol in water. Preliminary test trials indicated that extraction temperatures of 10 MPa were not required and the extraction was performed. The mixed ground plant tissue was loaded into extraction vessels and allowed to fill with the extraction solvent. The system was allowed to stand for static extraction for 24 hours, after which dynamic extraction was resumed. The extraction solvent was fluxed through the ASE system twice (*i.e.*, a total of three times). The final product (HM extract) was used for subsequent analysis. To determine the dry weight, 10 mL of the HM extract was dried in triplicate at 35-40 °C in a drying oven until no further weight change was noted. The total extraction volume and final percentage of ethanol in the extract were also measured and recorded.

Phytochemical analysis

Total flavonoid content

The aluminum chloride/sodium nitrite method was used to determine the total flavonoid content of the HM extract.[19] In this method, the o-nitroso derivatives of flavonoids form a complex with Al III, which absorbs maximally at or near 510 nm. Rutin (Sigma-Aldrich, USA) was used as the standard to determine the total flavonoid content of HM as µg rutin/mL. Sodium hydroxide (4%), sodium nitrite (5%), and 10% aluminum chloride in deionized water were used for the procedure. Samples were prepared by adding 25 µL (1:10 dilution) of HM extract to 100 µL water and 7.5 µL sodium nitrite solution into a 96-well Enzyme-Linked Immunosorbent Assay (ELISA) plate in 8 replicates. After six minutes, 7.5 µL aluminum chloride, 100 µL sodium hydroxide, and 110 µL of deionized water were added to each well, and the wells were covered with aluminum foil for 15 minutes. Absorption at 510 nm was read and recorded using an ELISA reader (Synergy, BioTek Instruments Inc., Germany). The same procedure was repeated for different rutin standard concentrations. The 6 best results were selected for total flavonoid determination.

Quercetin concentrations determined by reversed-phase high-performance liquid chromatography (RP-HPLC)

Quercetin, a key marker and constituent of both H and M, was analyzed using HPLC. RP-HPLC is routinely used for the optimal separation of flavonoids due to their hydrophobicity and low solubility in aqueous solutions.[20] All HPLC-grade solutions and equipment were obtained from the Alborz Academic Institute, Iran. To prepare the standard solution (Figure 1), 10 mg of quercetin dihydrate (Sigma-Aldrich, USA) was dissolved in 20 mL methanol, 15 mL dilute hydrochloric acid, and 5 mL water, and the final volume was adjusted to 50 mL with methanol. To prepare the sample solution, 15 mL of the HM extract was first dried. The dry extract was then added to the same series

of solutions as the standard with a final volume of 50 mL, as described above. A 25 cm C18 column (Phenomenex, USA) with a 4 mm diameter and 5 µm particle size was used for HPLC on an Alliance E2695 (Waters, USA). Gradient elution was performed with a mobile phase consisting of 0.3 g/L phosphoric acid (solution A) and pure methanol (solution B). The gradient started with 60% solution A and 40% solution B and ended with 0% A and 100% B. The injection volume was 10 µL and the running time was 25 minutes at 25 °C. The detector was set at a wavelength of 370 nm with a flow rate of 1 mL/min. Quercetin was identified by comparing the retention times of the sample peaks with the quercetin peak in the standard (Figure 2).

Cell culture and toxicity

3-(4,5-dimethylthiazol-2-yl)-2,5-diphenyltetrazolium bromide (MTT) assay was used to assess the toxicity of the HM hydroethanolic extract in the NIH/3T3 cell line based on the general protocols described in ISO-10993-5 and Danihelová et al.[21] The NIH/3T3 cell line was obtained from The Iranian National Center for Genetics and Biological Resources. The cell culture medium consisted of complete Dulbecco's Modified Eagle's Medium (DMEM) supplemented with 10% fetal bovine serum (FBS), 10 IU/mL penicillin, and 100 IU/mL streptomycin (Capricorn, Germany). Standard growing conditions included 5% CO_2 and 95% humidity at 37 °C. After three passages, cells were grown in T175 cell culture flasks until reaching confluence. The samples were then trypsinized and centrifuged at 1200 rpm for 5 min. After suspending the cells in the cell culture medium, viable cells were counted using a hemocytometer aided by trypan blue to identify non-viable cells. An average number of 2×10^4 cells were incubated (24 hours at 37 °C) in the wells of a flat-bottom ELISA plate and used to perform the MTT assay. The culture medium was replaced with various concentrations of HM extract (0.5 to 50% *v/v*), which was added to NIH/3T3 cells and incubated at 37 °C for 24 hours. The control wells received media containing complete DMEM supplemented with FBS and antibiotics, but no HM extract. To perform the MTT assay, the culture medium was removed from each well, and the cells were washed with 100 µL of fresh DMEM. To each well, 50 µL of cell culture medium and 50 µL 5 mg/mL MTT reagent (Sigma-Aldrich, USA) were added, and the flasks were incubated for 4 hours at 37 °C. MTT is a yellow solution converted to formazan crystals by mitochondrial nicotinamide adenine dinucleotide phosphate-dependent oxidoreductases in metabolically active cells. To dissolve the formazan crystals, 150 µL dimethyl sulfoxide (DMSO) was added to each well and shaken for 15 min. A blank containing MTT reagent and DMSO was used to adjust baseline absorption. Absorbance was measured at 570 nm using an ELISA reader (Synergy, BioTek Instruments Inc., Germany). Results are expressed as percentage control ± standard error of the mean (SEM).

Acute oral toxicity, LD_{50} in Wistar rats

The acute oral toxicity of HM was studied in Wistar rats obtained from the Institute of Pharmacological Sciences, Tehran University of Medical Sciences (Iran). Procedural and ethical considerations were based on OECD UDP Procedure 425 (2020). Animal procedures were approved by the Payame

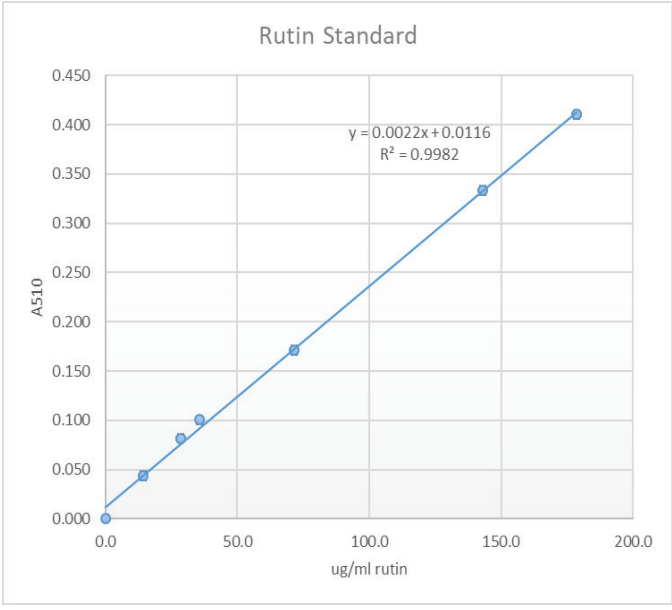

Figure 1. Standard calibration curve of rutin. The total flavonoid content of HM was determined by linear regression analysis

HM: *Melissa officinalis-Hypericum perforatum*

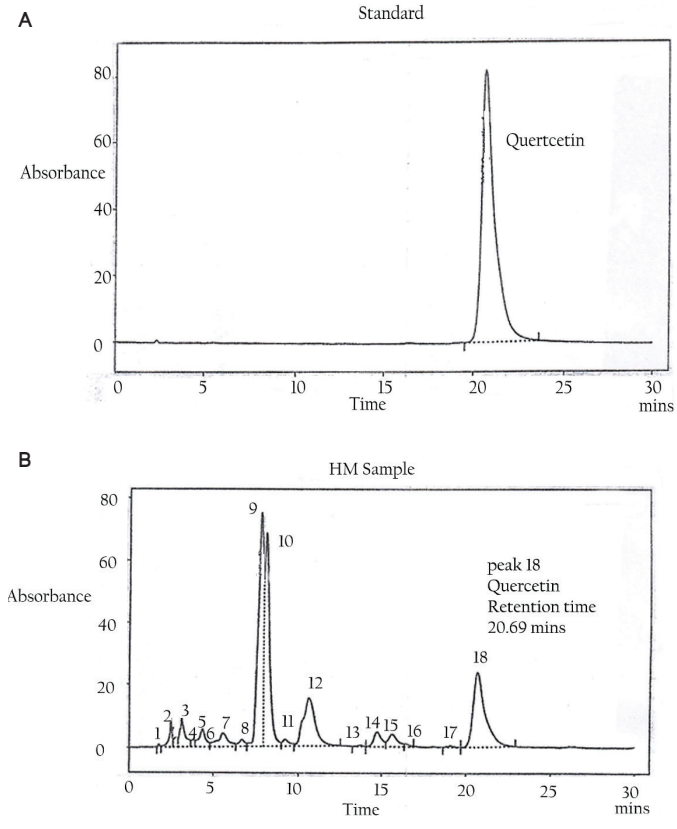

Figure 2. A) Chromatograph of standard quercetin at a concentration of 200 mg/mL, B) Chromatograph of the HM extract. An arrow indicates the Quercetin peak

HM: *Melissa officinalis-Hypericum perforatum*

Noor University Research Ethics Committee (approval number: IR.PNU.REC.1401.082, date: 15.05.2022). Animals were housed under standard conditions of a 12-hours/12-hours light/dark cycle with no food or water restrictions at 25 °C. All animals were acclimated to standard conditions for 10 days prior to dosing. The average weight of the animals was 200-250 grams, and all doses were calculated according to body weight. Animals were singly dosed in the test stage using the default doses recommended by the OECD guidelines (50, 100, 500, 1000 mg/kg) to find a suitable range of doses/response for the main stage of the experiment. After the initial dosing, the animals were monitored for 72 hours for signs of toxicity. The HM doses selected for the main stage of the experiment were 381.0 mg/kg, 571.5 mg/kg, 685.8 mg/kg, and 762.0 mg/kg administered by oral gavage. The main stage consisted of 1 control and 4 treatment groups with 10 rats in each group (n= 10). Clinical manifestations of toxicity as well as mortality were monitored and recorded for 14 days. LD_{50} was calculated.

Microbial content analysis

In order to analyze the microbial load of the HM extract, the USP-40 general protocol for the analysis of non-sterile products was used. Serial dilutions of 1:10, 1:100, and 1:1000 HM extract were prepared in peptone water buffer, and the total aerobic microbial count (TAMC) was performed by adding 1 mL of each dilution to 15 mL plate count agar in 9 cm Petri dishes in duplicates. The incubation period was 5 days at 30 °C. The same procedure was used to obtain total yeast and mold counts (TYMCs) on casein-soybean digest agar. The presence of the four main groups of food pathogens, *i.e.*, *Escherichia coli, Salmonella* spp., *Staphylococcus aureus,* and *Pseudomonas aeruginosa*) in HM extract was explored on MacConkey, bismuth sulfite, mannitol salt, and cetrimide agars. Uninoculated negative control plates were run in parallel, and the results were recorded as colony-forming units per mL (colony-forming units/mL).

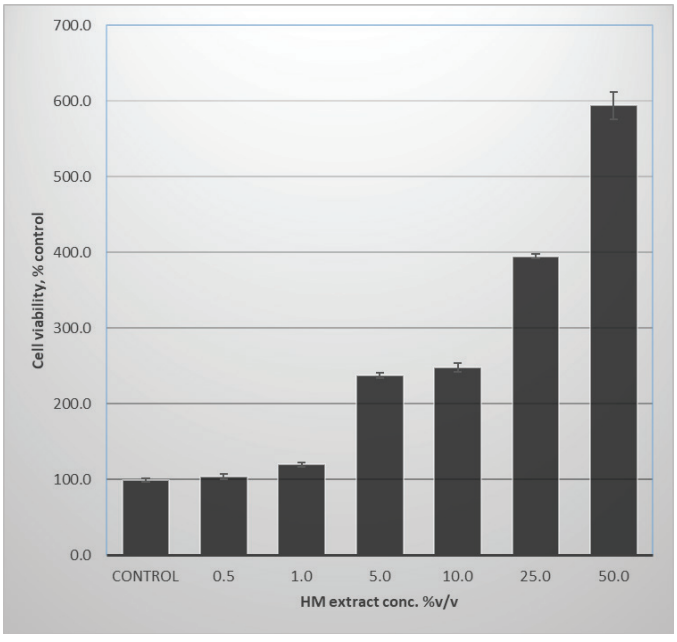

Figure 3. Graphical results of the MTT viability test of the NIH/3T3 cell line in response to various concentrations of the HM extract, expressed as a percentage of the control

MTT: 3-(4,5-dimethylthiazol-2-yl)-2,5-diphenyltetrazolium bromide, HM: *Melissa officinalis-Hypericum perforatum*

Statistical analysis

One-Way analysis of variance and Probit analysis of LD_{50} were performed using SPSS 26 software. The Dunnett test was performed as a post hoc analysis method where $p < 0.05$ was statistically significant. The final results are presented as mean ± standard error of the mean (SEM).

RESULTS

Phytochemical analysis

The total extraction volume, percent ethanol, and dry mass of the HM extract are presented in Table 1. Total flavonoid content was determined using the aluminum chloride/sodium nitrite method by measuring A_{510}. Comparing the A_{510} of the HM sample (Table 2) with the rutin standard curve revealed a total flavonoid content of 15.29 ± 0.64 mg rutin/mL (Table 3) HM extract (*$p < 0.05$).

Eighteen peaks were detected in the reverse-phase HPLC chromatogram of HM. The quercetin peak in the HM sample (peak number 18, chromatograph b) was identified by comparing peak retention times with those of the quercetin standard (chromatograph a). The areas under the peaks were compared, and quercetin concentration per mL of HM extract was calculated relative to the standard. These numbers were corrected for dilutions to determine quercetin concentrations in the HM samples. The quercetin concentration was 0.187 mg/mL.

Microbial content

The presence of four main pathogenic contaminants in food and non-sterile products, *i.e. E. coli*, *P. aeruginosa*, *Salmonella* spp.,

Table 1. Percent alcohol content, volume, and mass of dried extract per mL HM extract

Total volume extracted	Alcohol (%)	Dried extract
1320 mL	58	38.1 mg/mL

HM: *Melissa officinalis-Hypericum perforatum*

Table 2. The absorbance of different rutin concentrations (at 510 nm) used to construct the standard curve

Rutin standard (µg/mL)	A510 ± SEM
0.0	0.000 ± 0.001
14.2	0.044 ± 0.001
28.6	0.082 ± 0.001
35.7	0.100 ± 0.001
71.4	0.171 ± 0.001
142.9	0.333 ± 0.001
178.6	0.410 ± 0.001

SEM: Standard error of mean

and *S. aureus,* was tested, and growth was negative in all cases. The TAMC and TYMC yielded negative results. The results of the microbial load tests are summarized in Table 4. According to USP-40 guidelines for microbial testing of non-sterile pharmaceutical products, HM extract meets the requirements for human consumption.

Toxicity assays

Cellular toxicity: The MTT assay was used to determine HM toxicity in the NIH/3T3 cell line. Results are summarized in Figure 2 and Table 5. Cellular toxicity was measured by colorimetric assay of formazan crystals produced by viable cells. No toxicity was noted in the range of tested concentrations. However, a significant concentration-dependent increase in apparent cell viability was observed above 5% v/v for HM, which may indicate interference with the assay. Such effects are commonly observed with electron transport chain uncouplers or molecules that directly reduce the MTT reagent to form formazan crystals independent of mitochondrial oxidoreductases. Examples include NADH, ascorbic acid, glutathione, and flavonoids, which are powerful antioxidants present at significant levels in HM extract. This would explain the dose-dependent increase in absorption at HM concentrations above 5% *v/v*.

Animal toxicity: The results for acute oral toxicity (LD_{50}) in Wistar rats are summarized in Table 6. Animals were monitored for 14 days for the visual clinical manifestations of toxicity (Table 7) following the administration of HM extract by gavage. The data indicate an LD_{50} of 685.8 mg/Kg. SPSS software was used to perform non-linear regression analysis (PROBIT analysis) of the LD_{50}. The software calculated an LD_{50} of 695.2 ± 7.5* mg/kg ($p < 0.05$) with a 95% confidence interval of 599.4-913.3 mg/kg. The only clinical signs noted were abdominal distension and diarrhea in the dose range of 571.5-685.8 mg/kg, as shown in Table 6. Therefore, the maximum dose without signs of toxicity was 381.0 mg/kg of the HM extract.

DISCUSSION

Previous studies have reported that the extracts obtained from several natural sources, such as *Zataria multiflora*[22], *Carum carvi*[23], *Rosa damascenes*[24], and *Mentha piperita*[25] possessed

Table 3. Total flavonoid expressed as mg standard rutin (*$p < 0.05$)

Total flavonoids in HM, corrected for 1:140 dilution SEM ± mg/mL	Total flavonoids as mg standard rutin SEM ± µg/mL	A510 ± SEM
15.29 ± 0.64*	109.2 ± 4.6*	0.259 ± 0.001

Significant differences were assessed by *$p < 0.05$. SEM: Standard error of mean, HM: *Melissa officinalis-Hypericum perforatum*

Table 4. Summarized results of microbiological tests

Test	Results	Acceptable range	Standard	unit
Pseudomonas aeroginosa	-	-	USP 40	CFU/mL
Staphylococcus aureus	-	-	USP 40	CFU/mL
Salmonella spp.	-	-	USP 40	CFU/mL
Escherichia coli	-	-	USP 40	CFU/mL
TYMC	*10›	Max 10^2	USP 40	CFU/mL
TAMC	*10›	Max 10^3	USP 40	CFU/mL

Significant differences were assessed by *$p < 0.05$. TYMC: Total yeast and mold, TAMC: Total aerobic microbial count, CFU: Colony-forming units

Table 5. MTT assay results for cell toxicity in NIH/3T3 cell line

Concentration (v/v %)	0	0.5	1	5	10	25	50
Mean (control %) ± SEM	99.20 ± 2.11	103.55 ± 3.17	119.52 ± 3.31	237.10 ± 3.67*	248.07 ± 5.65*	395.00 ± 2.69*	594.20 ± 18.4*

Significant differences were assessed by *$p < 0.05$. Results are expressed as % control. MTT: 3-(4,5-dimethylthiazol-2-yl)-2,5-diphenyltetrazolium bromide, SEM: Standard error of mean

Table 6. Raw data for acute oral toxicity (mortality for 14 days) with single dose of HM extract in Wistar rats

Dose (mg/kg)	0	381.0	571.5	685.8	762.0
Mortality	0	0	3	5	6
Mortality (%)	0	0	30	50	60

HM: *Melissa officinalis-Hypericum perforatum*

Table 7. Visible clinical manifestations of toxicity with HM treatment in Wistar rats

Visible clinical manifestations	0 mg/kg (control)	381.0 mg/kg	571.5 mg/kg	685.8 mg/kg	762.0 mg/kg
Skin	-	-	-	-	-
Eyes	-	-	-	-	-
Abdominal distention	-	-	+	-	-
Diarrhea	-	-	+	+	-
Respiratory	-	-	-	-	-
Arrhythmias	-	-	-	-	-
Hair	-	-	-	-	-
Mobility	-	-	-	-	-
Paralysis	-	-	-	-	-
Pain	-	-	-	-	-

Animals were monitored for 14 days and results were recorded. HM: *Melissa officinalis-Hypericum perforatum*

considerable functional properties, including chemopreventive, antioxidant, and anti-inflammatory potential. These beneficial effects may be associated with the antioxidant compounds, particularly flavonoids, present in the tested plant species. Therefore, in the current study, the flavonoid content of the herbal mixtures (HM) has been measured spectrophotometrically, and the results revealed that these herbal mixtures contained a significant amount of flavonoid (40.1% of total dry weight), which is comparable with the findings reported by Arceusz et al.[26] and Germ et al.[27]. However, multiple factors, such as habitat and environmental conditions during plant growth, sample preparation, extraction methods, and analytical techniques, can affect secondary metabolite concentrations.[28] The HPLC analysis confirmed that the major flavonoid present in HM extracts was Quercetin (Figure 2). These findings are in line with Aghakarim et al.[29] and Mohagheghzadeh et al.[30].

Moreover, microbiological testing is typically used to assess the presence of harmful microbes in herbal medication products before commercialization. This testing involves measuring the total number of microorganisms, checking for the presence of specific pathogenic species, and verifying the absence of certain indicator organisms. Common test methods include microbial plate counting, as well as tests for *E. coli, Salmonella* spp., and *S. aureus*[31]. The present study confirmed the absence of harmful microorganisms such as *E. coli* and *S. aureus* in the herbal mixture (Table 4), thereby ensuring the quality and safety of the studied herbal products.

Furthermore, although there has been a growing interest in using plant-based medicines, it is necessary to assure consumers about the safety of herbal treatments. Diverse essential oils have been recognized by the United States Food and Drug Administration as Generally Recognized as Safe, underscoring their potential safety and eco-friendly nature. However, before use, their toxicity should be thoroughly tested. Hence, the current was checked for the possible toxicity of the herbal mixture using both *in vitro* and *in vivo* assays. The results showed that the toxicity level of the HM extract placed it in category 4 (medium toxicity, between 500 and 2000 mg/kg), which is less toxic than commonly used substances like caffeine, aspirin, or ibuprofen (Tables 6 and 7). Lemon balm and St. John's wort are antispasmodic and antidiarrheal and are used to alleviate abdominal discomfort.[32,33] Therefore, it is possible that at higher HM doses, abdominal distension and diarrhea are absent because of these effects.

CONCLUSION

The diverse array of secondary metabolites found in plant extracts has unlimited potential and possibilities. In the last few decades, using plant extracts and products to treat various diseases has been successful in many cases, and the results in this area appear promising. Therapeutic strategies using phytopharmaceuticals provide a new perspective to address the void that chemical drug design and manufacturing worldwide have been unable to fill. HM is a new formulation of the combined hydroethanolic extracts of Lemon balm and St. John's wort, which was analyzed for its phytochemical properties and cell and animal toxicities in the present study. HM contains flavonoids at high concentrations. No microbial growth was observed in the microbiological tests performed on the HM. At concentrations of up to 1% *v/v*, HM did not cause toxicity in the NIH/3T3 cell line, and it did not interfere with the MTT assay. Higher concentrations of HM seem to have interfered with the MTT assay and resulted in greater cell viability than the control. PROBIT analysis of the acute oral toxicity of HM extract in Wistar rats indicated an LD_{50} of 695.2 mg/kg body weight, which places HM in toxicity category 4 (moderate toxicity). Considering all the results, a range of 1-5% of the maximum dose of HM without any indications of toxicity in the animal model (*i.e.*, 3.81-19.1 mg/kg/day) is suggested for pharmacological testing in clinical trials.

Acknowledgements

The authors express their deepest gratitude to Professor Gholamreza Amin at the Tehran University of Medical Sciences

and Yas Daru Herbal Pharmaceutical Company, Tehran, for their guidance and technical support.

Ethics

Ethics Committee Approval: Animal procedures were approved by the Payame Noor University Research Ethics Committee (approval number: IR.PNU.REC.1401.082, date: 15.05.2022).

Informed Consent: Not required.

Authorship Contributions

Concept: F.F., S.F., S.D., Design: F.F., S.F., Data Collection or Processing: S.F., Analysis or Interpretation: S.F., Literature Search: M.Z., Writing: M.Z., S.D.

Conflict of Interest: No conflict of interest was declared by the authors.

Financial Disclosure: The authors declared that this study received no financial support.

REFERENCES

1. Yuan H, Ma Q, Ye L, Piao G. The traditional medicine and modern medicine from natural products. Molecules. 2016;21:559.
2. Dini S, Chen Q, Fatemi F, Asri Y. Phytochemical and biological activities of some Iranian medicinal plants. Pharm Biol. 2022;60:664-689.
3. Fatemi F, Golbodagh A, Hojihosseini R, Dadkhah A, Akbarzadeh K, Dini S, Malayeri MRM. Anti-inflammatory Effects of deuterium-depleted water plus rosa damascena mill. Essential oil *via* cyclooxygenase-2 pathway in rats. Turk J Pharm Sci. 2020;17:99-107.
4. Malayeri MR, Dadkhah A, Fatemi F, Dini S, Torabi F, Tavajjoh MM, Rabiei J. Chemotherapeutic effect of Berberis integerrima hydroalcoholic extract on colon cancer development in the 1,2-dimethyl hydrazine rat model. Z Naturforsch C J Biosci. 2016;71:225-232.
5. Torabi F, Dadkhah A, Fatemi F, Dini S, Taghizadeh M, Malayeri MR. Prevention and therapy of 1, 2-dimethyl hydrazine induced colon carcinogenesis by Ferula assafoetida hydroalcoholic extract. Turkish J Biochem. 2015;40:390-400.
6. Rasooli A, Fatemi F, Hajihosseini R, Vaziri A, Akbarzadeh K, Mohammadi Malayeri MR, Dini S, Foroutanrad M. Synergistic effects of deuterium depleted water and *Mentha longifolia* L. essential oils on sepsis-induced liver injuries through regulation of cyclooxygenase-2. Pharm Biol. 2019;57:125-132.
7. Atanasov AG, Waltenberger B, Pferschy-Wenzig EM, Linder T, Wawrosch C, Uhrin P, Temml V, Wang L, Schwaiger S, Heiss EH, Rollinger JM, Schuster D, Breuss JM, Bochkov V, Mihovilovic MD, Kopp B, Bauer R, Dirsch VM, Stuppner H. Discovery and resupply of pharmacologically active plant-derived natural products: A review. Biotechnol Adv. 2015;33:1582-1614.
8. Fatemi F, Dadkhah A, Rezaei MB, Dini S. Effect of γ-irradiation on the chemical composition and antioxidant properties of cumin extracts. J Food Biochem. 2013;37:432-439.
9. Miraj S, Rafieian-Kopaei, Kiani S. Melissa officinalis L: A review study with an antioxidant prospective. J Evid Based Complementary Altern Med. 2017;22:385-394.
10. Longevity OMAC. Retracted: Phytochemical constituents, biological activities, and health-promoting effects of the *Melissa officinalis*. Oxid Med Cell Longev. 2024;2024:9842453.
11. Petrisor G, Motelica L, Craciun LN, Oprea OC, Ficai D, Ficai A. *Melissa officinalis*: Composition, Pharmacological effects and derived release systems-a review. Int J Mol Sci. 2022;23:3591.
12. Zarei A, Changizi-Ashtiyani S, Taheri S, Hosseini N. A brief overview of the effects of *Melissa officinalis* L. extract on the function of various body organs. J Res Med Sci. 2015;17.
13. Caldeira GI, Gouveia LP, Serrano R, Silva OD. Hypericum genus as a natural source for biologically active compounds. Plants. 2022;11:2509.
14. Szewczyk B, Pochwat B, Muszyńska B, Opoka W, Krakowska A, Rafało-Ulińska A, Friedland K, Nowak G. Antidepressant-like activity of hyperforin and changes in BDNF and zinc levels in mice exposed to chronic unpredictable mild stress. Behav Brain Res. 2019;372:112045.
15. Chen H, Muhammad I, Zhang Y, Ren Y, Zhang R, Huang X, Diao L, Liu H, Li X, Sun X, Abbas G, Li G. Antiviral activity against infectious bronchitis virus and bioactive components of *Hypericum perforatum* L. Front Pharmacol. 2019;10:1272.
16. Mohamed FF, Anhlan D, Schöfbänker M, Schreiber A, Classen N, Hensel A, Hempel G, Scholz W, Kühn J, Hrincius ER, Ludwig S. Hypericum perforatum and its ingredients hypericin and pseudohypericin demonstrate an antiviral activity against SARS-CoV-2. Pharmaceuticals (Basel). 2022;15:530.
17. Javid A, Motevalli Haghi N, Emami SA, Ansari A, Zojaji SA, Khoshkhui M, Ahanchian H. Short-course administration of a traditional herbal mixture ameliorates asthma symptoms of the common cold in children. Avicenna J Phytomed. 2019;9:126-133.
18. Martinelli M, Ummarino D, Giugliano FP, Sciorio E, Tortora C, Bruzzese D, De Giovanni D, Rutigliano I, Valenti S, Romano C, Campanozzi A, Miele E, Staiano A. Efficacy of a standardized extract of *Matricariae chamomilla* L., *Melissa officinalis* L. and tyndallized *Lactobacillus acidophilus* (HA122) in infantile colic: An open randomized controlled trial. Neurogastroenterol Motil. 2017;29.
19. Chang CC, Yang MH, Wen HM, Chern JC. Estimation of total flavonoid content in propolis by two complementary colorimetric methods. J Food Drug Anal. 2002;10.
20. Zeliou K, Kontaxis NI, Margianni E, Petrou C, Lamari FN. Optimized and validated HPLC analysis of St. John's wort extract and final products by simultaneous determination of major ingredients. J Chromatogr Sci. 2017;55:805-812.
21. Danihelová M, Veverka M, Sturdík E, Jantová S. Antioxidant action and cytotoxicity on HeLa and NIH-3T3 cells of new quercetin derivatives. Interdiscip Toxicol. 2013;6:209-216.
22. Attaran HR, Fatemi F, Rasooli A, Dadkhah A, Mohammadi Malayeri MR, Dini S. *Zataria multiflora* essential oil prevent iron oxide nanoparticles-induced liver toxicity in rat model. Journal of Medicinal plants and By-Products, 7, 15-24.
23. Dadkhah A, Fatemi F, Mohammadi Malayeri MR, Torabi F, Sarbazi M, Dini S. The hepatoprotective activity of caraway essential oil (*Carum carvi* L.) against iron oxide nanoparticles induced toxicity in Wistar rats. J Anim Res (Iranian Journal of Biology). 32, 188-197.
24. Fatemi F, Dini S, Rezaei MB, Dadkhah A, Dabbagh R, Naij S. The effect of γ-irradiation on the chemical composition and antioxidant activities of peppermint essential oil and extract. J Essent Oil Res. 26, 97-104.
25. Irandoust F, Dini S. A new perspective of aroma face mask on COVID-19 pandemic. J Med Eng Technol. 2022;46:198-208
26. Arceusz A, Wesolowski M, Ulewicz-Magulska B. Flavonoids and phenolic acids in methanolic extracts, infusions and tinctures from commercial samples of lemon balm. Nat Prod Commun. 2015;10:977-981.

27. Germ M, Stibilj V, Kreft S, Gaberščik A, Kreft I. Flavonoid, tannin and hypericin concentrations in the leaves of St. John's wort (*Hypericum perforatum* L.) are affected by UV-B radiation levels. Food Chem. 2010;122:471-474.

28. Qaderi MM, Martel AB, Strugnell CA. Environmental factors regulate plant secondary metabolites. Plants (Basel). 2023;12:447.

29. Aghakarim, Fahimeh, Hassan Sarikhani, and Ali Azizi. Effects of supplemental light quality at the end of day on herb production and some phytochemical properties of lemon balm (*Melissa officinalis* L.). Int J Hortic Sci. 2023;66-88.

30. Mohagheghzadeh A, Badr P, Mohagheghzadeh A, Hemmati S. *Hypericum perforatum* L. and the underlying molecular mechanisms for its choleretic, cholagogue, and regenerative properties. Pharmaceuticals. 2023;16,887.

31. Stojanović NM, Randjelović PJ, Mladenović MZ, Ilić IR, Petrović V, Stojiljković N, Ilić S, Radulović NS. Toxic essential oils, part VI: Acute oral toxicity of lemon balm (*Melissa officinalis* L.) essential oil in BALB/c mice. Food Chem Toxicol. 2019;133:110794.

32. Wang H, Chen Y, Wang L, Liu Q, Yang S, Wang C. Advancing herbal medicine: enhancing product quality and safety through robust quality control practices. Front Pharmacol. 2023;14:1265178.

33. Xiuying P, Jianping L, Ruofeng S, Liye Z, Xuehong W, Yan L. Therapeutic efficacy of *Hypericum perforatum* L. extract for mice infected with an influenzaa virus. Can J Physiol Pharmacol. 2012;90:123-130.

Turk J Pharm Sci 2024;21(4):348-354
DOI: 10.4274/tjps.galenos.2023.50723

ORIGINAL ARTICLE

Timolol Maleate *in Situ* Ophthalmic Mucoadhesive-Thermosensitive Gel: Development and Characterization

Özlem KRAL[1,2], Eda TURAN AYHAN[3], Sibel ILBASMIS-TAMER[1]*, Fahriye Figen TIRNAKSIZ[1]

[1]Gazi University Faculty of Pharmacy, Department of Pharmaceutical Technology, Ankara, Türkiye
[2]Ağrı İbrahim Çeçen University Faculty of Pharmacy, Department of Pharmaceutical Technology, Ağrı, Türkiye
[3]Adıyaman University Faculty of Pharmacy, Department of Pharmaceutical Microbiology, Adıyaman, Türkiye

ABSTRACT

Objectives: The aim of this study was to prepare a sustained-delivery mucoadhesive-thermosensitive formulation containing poloxamer 338 (P338), poloxamer 188 (P188), and mucoadhesive agents, such as chitosan (CHT) and carboxymethylcellulose (CMC), to increase the ophthalmic bioavailability of timolol maleate (TM).

Materials and Methods: Gels were prepared by mixing different amounts of P338, P188, and a mucoadhesive agent in cold isotonic water using a magnetic stirrer. The sol-gel gelation time of the gels was determined using the test tube inversion method. Viscosity measurements and analysis of the mechanical properties of the gel formulations were performed. *In vitro* release using dialysis membranes and *ex vivo* permeation studies using fresh-warmed cow eyes were performed.

Results: The gelation times of formulations containing 20:2.5 (P338:P188) and 0.1% CMC and formulations containing 20:2.5 (P338:P188) and 0.1% CHT were 35 s and 26.67 s, respectively. An optimally selected CHT mucoadhesive-thermosensitive *in situ* gelling system can successfully control the release of moderately hydrophilic drugs, such as TM. In the viscosity study, both formulations showed Newtonian fluid, and the CHT gel's viscosity was found to be higher. The CHT gel showed better mechanical properties than the CMC gel. The amount of TM penetrating the cow cornea after 24 hours was 73.38%, 71.80%, 67.25%, and 60.55% from the CHT gel, CMC gel, TM solution, and commercial preparation, respectively.

Conclusion: The improved mucoadhesive-thermosensitive *in situ* gelling system successfully controlled the release of TM. The significantly lower drainage of TM into the circulation compared with eye drops is an advantage in treating glaucoma, and the use of mucoadhesive agents increases drug penetration.

Keywords: Timolol maleate, mucoadhesive-thermosensitive, poloxamer, chitosan, carboxymethyl cellulose, ophthalmic gel

INTRODUCTION

Glaucoma is an eye disease that occurs when the balance between the amount of intraocular fluid produced and the amount drained out is disrupted, and it can cause irreversible blindness if left undiagnosed and untreated.[1,2] Timolol maleate (TM) in the form of eye drops is one of the most commonly used drugs in the treatment of open-angle glaucoma. An increase in the ocular bioavailability of TM eye drops is important for the treatment of glaucoma. This can be achieved by ensuring that eye drops do not drain and enhancing the residence time of eye drops.[3,4]

Many ophthalmic drugs are used at high doses or for longer periods to increase ocular bioavailability, but this increases the likelihood of causing ocular and systemic side effects.[5] Popular conventional ocular dosage forms, such as solution or suspension, have several limitations, notably a large drainage factor, short residence time, and poor bioavailability due to high tear fluid turnover.[1] Such causes usually result in an ocular bioavailability of less than 10%.[6] We are able to list the desired properties in an ophthalmic formulation as follows: be in the form of drops, not cause blurred vision or irritation, be able to withstand dilution of lacrimal fluid without rapid precorneal

*Correspondence: ilbasm@yahoo.com, Phone: +90 505 319 63 20, ORCID-ID: orcid.org/0000-0003-0361-7105
Received: 07.06.2023, Accepted: 03.09.2023

elimination after administration, and have a mucoadhesive property suitable for improving drug retention in the precorneal space.[6]

Different approaches, such as hydrogels, *in situ* gelling systems, microparticles, and colloidal carriers, are used to improve the therapeutic efficacy of ophthalmic pharmaceutical formulations and improve the bioavailability of administered drugs by increasing pre-corneal residence time and corneal penetration.[7] Gupta et al.[8] developed a temperature- and pH-triggered gel system using chitosan (CHT) and poloxamer 407. The formulation developed in this study showed significantly higher drug transport across the corneal membrane and increased ocular retention time. In the present study, different types (P338, P188) and ratios of poloxamers were tested, and characterization studies were conducted. Furthermore, the effects of mucoadhesive agents such as CHT and carboxymethylcellulose (CMC) were evaluated in terms of gelation time, viscosity, and mechanical properties. The effect of the gel formulations was demonstrated by *in vitro* release and *ex vivo* permeation compared with the commercial product in our study.[8]

Numerous studies have been conducted on systems based on solution gelling *in situ* using various polymers that undergo sol-gel phase transitions as a result of physical/chemical changes depending on pH, temperature, or a particular ion.[9-13] Poloxamers are thermosensitive, non-ionic polyoxyethylene-polyoxypropylene-polyoxyethylene (PEO n-PPO n-PEO n) tri-block copolymers.[14,15] It transforms from a low-viscosity solution to a gel at room temperature when its aqueous solution is 18% (*w/w*) or higher. Because the solution has a low poloxamer concentration, it loses its gelling ability after dilution with a lacrimal fluid, and this requires a higher poloxamer concentration [25% (*w/w*)]. In this case, the gelling temperature (GT) is lower than room temperature, and the solution must be stored in a refrigerator, making it difficult to prepare and use. Therefore, adding an analog of the poloxamer, for example, poloxamer 188 (P188), is a good alternative to increase the GT.[6]

The present study aim to prepare TM gel formulations containing poloxamer 338 (P338), poloxamer 188 (P188), and a mucoadhesive agent (CHT, CMC) to provide a sustained effect and a mucoadhesive thermosensitive formulation that gels in the eye when liquid at room temperature develops. It is aimed that the developed formulation is in the form of drops and can be applied easily, gels can be applied at eye temperature, and contact with the eye for a longer time. With its mucoadhesive feature, it is aimed to improve drug retention in the pre-corneal space. Thus, the drug stays in the eye for a longer time and increase its bioavailability.

MATERIALS AND METHODS

Materials

All chemicals and reagents used were of pharmaceutical and analytical grade. P338 and P188 were provided by BASF (Germany). CHT (low molecular weight) was purchased from Sigma-Aldrich (Steinheim, Germany), and CMC was provided by Aklar Chemistry (Ankara, Türkiye). The commercial product containing an equal amount of TM is a subsidiary of Bilim Pharmaceuticals (Türkiye). Active ingredient TM was obtained from Merck, USA.

Method

Preparation of gel formulations

Different concentrations of P338 and P188 were dissolved in cold isotonic water by mixing with a magnetic stirrer at 500 rpm in an ice bath for 20 minutes. The mucoadhesive agents (CHT, CMC) were added and dissolved. The formulations were refrigerated for at least 24 hours to ensure complete dissolution. Then, TM was added.

Drug content

Here, 0,5 g of the gel formulation was weighed and stirred in 100 mL of tear fluid for 24 hours at room temperature and 100 rpm on a magnetic stirrer. The TM concentration was measured at 295 nm using an ultraviolet (UV) spectrophotometer.[16]

pH determination

The pH values of the gel formulations were measured using a pH meter (Ohaus Corporatıion, USA) after being allowed to stand at room temperature for 1 hour. The pH of the developed gel formulations was adjusted to 7.4.

Viscosity measurement

Viscosity measurements of the gels were performed using a stress-controlled cone and plate rheometer (Brookfield, DV-III Rheometer). 0.5 mL sample was used and measurement was performed with spindle type CPE-52. The study was conducted in two different situations with and without the addition of an active ingredient, and three replicates were performed.

Determination sol-gel time

The test-tube inverting technique was used to determine the samples' sol-gel gelation times.[17] Briefly, a 10 mL test tube with a diameter of 1.0 cm was filled with 2 mL of the solution, and time measurements were started when the test tube was placed in a digital water bath at 34 °C. The flowability of the sample was monitored every 5 s by tilting the tubes. The gelation time was determined as the moment the samples' flow ceased, and the values were noted (Figure 1).

Texture profile analysis (TPA)

A TA-XT Plus Texture Analyzer (Stable Micro Systems, London, UK) was used to analyze the mechanical properties of the gels. The study was performed by attaching a penetrometer (moving probe) probe to the device. Approximately 50 mL of the gel formulation was placed in a beaker (100 mL). A pressure of 2 mm/s and a depth of 15 mm were applied twice on the gels with a 10 mm-diameter probe. The interval between the two compressions was adjusted to 15 s in each period.[18] Data obtained from Texture Exponent 2.0.6.0. calculated with a software. The mechanical properties of the gel formulations, including hardness, tackiness, cohesiveness, and elasticity, were determined.

In vitro release study

Franz diffusion cells were used in the *in vitro* release study and 0.5 mL of the formulation was transferred to the donor chamber. Artificial tear fluid was filled into the receptor chamber, which has a 2.5 mL volume, and stirred continuously using a small magnetic bar. The molecular weight of the dialysis membrane used to separate the donor and acceptor chambers was 12,000-14,000 Da. The experiment was conducted at 34 °C ± 2 °C. Samples were collected at specified time points (0.25 hours, 0.5 hours, 1 hour, 2 hours, 3 hours, 4 hours, 6 hours, 8 hours, 10 hours, and 24 hours) and replaced with an equal volume of artificial tear fluid. Samples were analyzed by UV spectrophotometer at 295 nm (n= 3). The release profile was created by plotting the cumulative amount of TM released from the formulations over time. The artificial tear fluid's ingredients were filtered water (*q.s.* 100 g), sodium bicarbonate (0.220 g), sodium chloride (0.670 g), and calcium chloride dehydrate (0.008 g). This fluid was used to simulate tear fluid.[8]

Ex vivo permeability study

Ex vivo experiments were performed using corneas from cow eyeballs collected from slaughterhouses immediately after the animal was sacrificed.[19] The cornea was carefully removed with 4-5 mm of surrounding scleral tissue. The removed corneas were cleaned with cold saline and stored in fresh simulated tear fluid before use (Figure 2).[20] The corneas were placed between the donor and receptor compartments of the Franz diffusion cell, with the endothelium facing the receptor compartment. The temperature was maintained constant at 34 ± 2 °C throughout the experiment. A volume of 0.5 mL of each formulation was administered, and the experiment was performed in triplicate (n= 3). Subsequently, the same procedures used in the *in vitro* release study were applied to the *ex vivo* permeation study. Permeated amount of TM (%) from the cow cornea versus time was plotted.

Statistical analysis

GraphPad Prism 5.0 Software was used in statistical analyses. One-Way ANOVA test was used for group comparisons. In the analyses, a significant difference was determined as $P < 0.05$.

RESULTS

Gelation time study

Different combinations of P338, P188, CMC, and CHT were studied to prepare the mucoadhesive thermosensitive gel formulations. The gelling times were found to be 26.67 seconds for the CHT gel and 35 seconds for the CMC gel to be the most suitable (Table 1).

Viscosity measurement

Viscosity measurements of the ophthalmic gel formulations were performed with and without TM. While the viscosity of the CHT gel formulation was 1572.66 mPa.s, that of the CMC gel

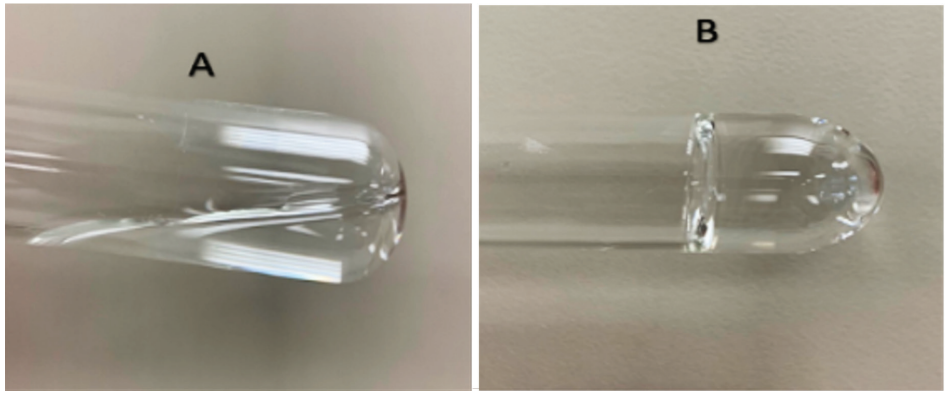

Figure 1. The figure shows the gels in solution form at 25 °C (A) and transformed into gels at 34 °C (B)

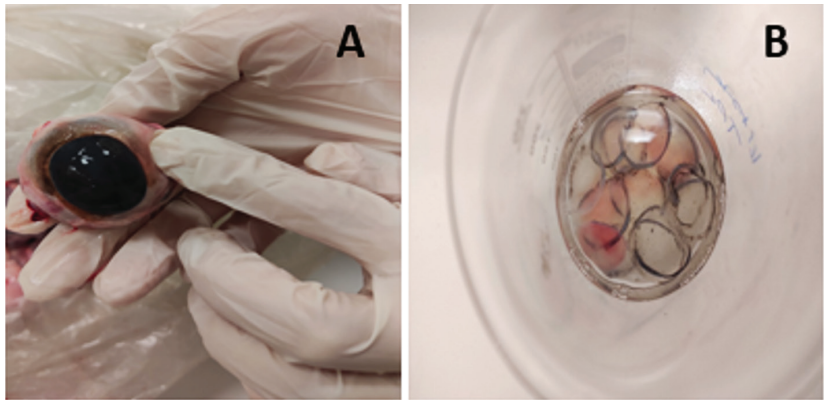

Figure 2. Freshly harvested cow eyes (A) and removed corneas (B)

formulation was 915 mPa.s, and the viscosity values increased with the addition of the drug. The gel formulation rheograms showed Newtonian fluid behavior at 25 °C when shear stress was plotted against shear rate (Figure 3).

Texture profile analysis

The mechanical properties of CHT and CMC gels were examined by texture profile analysis. The hardness, adhesiveness, cohesiveness and elasticity values obtained at the end of the study are given in Table 2. According to the texture profile analysis results, the mechanical properties of both systems were found to be similar.

In vitro release and ex vivo permeation studies

The *in vitro* drug release profiles of the CMC gel, CHT gel, commercial product, and TM solution are shown in Figure 4A. At the end of 24 hours, drug release was obtained at approximately the same percentage for the gels. At the end of 24 hours, TM released from the commercial products comprised 82% of the dose.

Figure 4B displays the results of *ex vivo* permeation tests. The amount of TM penetrating the cow cornea after 24 hours was 73.38%, 71.80%, 67.25%, and 60.55% from the CHT gel, CMC gel, TM solution, and commercial preparation, respectively.

Table 1. Gelation times of different *in situ* ophthalmic gel formulations at 34 °C

System	P338:188 (*w/v* %)	CMC (*w/v* %)	CHT (*w/v* %)	Gelation time (second)
CMC gel	18:2.5	0.1	-	98.33
	20:2.5	0.1	-	35
	22:2.5	0.1	-	gel
CHT gel	18:2.5	-	0.1	68.33
	20:2.5	-	0.1	26.67
	22:2.5	-	0.1	gel

CMC: Chitosan, CHT: Carboxymethylcellulose

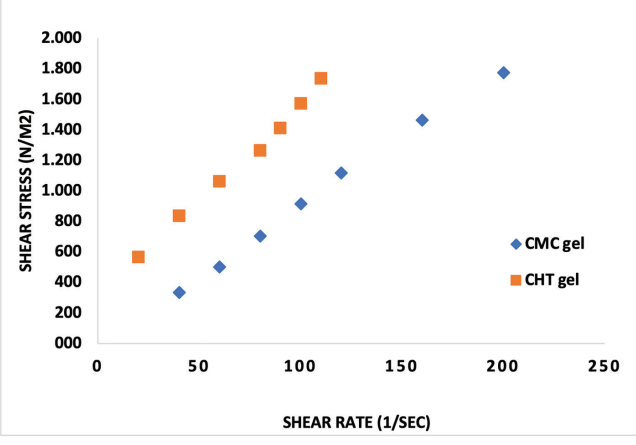

Figure 3. Viscosity measurements of the formulations at 25 °C
CMC: Carboxymethylcellulose, CHT: Chitosan

DISCUSSION

Poloxamers with thermogenic properties are non-ionic triblock copolymers consisting of one unit of polypropylene and two units of polyoxyethylene. The gelation process depends on the critical micelle concentration and temperature. At physiological temperatures and concentrations, the aqueous solution returns to a gel state *in situ*.

Different poloxamers can be used together to adjust the GT. Mucoadhesive polymer-and poloxamer-containing gels are systems that are being studied extensively as drug delivery systems. Poloxamer-based mucoadhesive gels have two main advantages: they have both gelation and mucoadhesion properties at physiological temperatures. The presence of a mucoadhesive polymer in an aqueous poloxamer solution may change the sol-gel transition temperature, gelation time, rheological properties, and release properties of the active substance. Similarly, the addition of poloxamer may affect the mucoadhesive properties of the mucoadhesive gel.[21]

In the present study, a poloxamer-based (two different types combined) mucoadhesive thermosensitive system was investigated. The aim is to prepare thermogel systems whose GTs are close to the corneal temperature. A combination of different poloxamers at different concentrations was used for suitable temperatures. According to the literature, the preferred mucoadhesive polymers, CHT and CMC, act as penetration enhancers to promote the drug's transcorneal permeability.[8]

Additionally, poloxamer, which are marketed as pluronic, have all the characteristics-including good thermal gelling, non-irritating eyes, and tolerance-that make them acceptable for ocular administration.[22]

The retention time of poloxamer-based gels is directly influenced by their mechanical and rheological characteristics. In the case of weak mechanical strength and low viscosity, rapid elimination occurs, whereas in the case of high viscosity, gel flow becomes problematic.[23] To evaluate these properties, we performed gelling time, viscosity and TPA analyses.

It was found that the polymer composition affected the physicochemical properties of *in situ* gel formulations, including TM. The formulation's Tsol-gel reduced when the P338 content was increased. The difference in the mucoadhesive agent also affected the gelation time. Soriano-Ruiz et al.[24] reported the preparation gels using different ratios of poloxamer to CHT and measured the gelation times. The gelling time was 1.16 min when 20% poloxamer/0.5 CHT was used and 0.86 minute when the poloxamer ratio was 22%. Gratieri et al.[25] assessed the gelation temperatures of gels using 16% poloxamer and 0.5%, 1%, and 1.5% CHT as 33 ± 0.8 °C, 32 ± 1.7 °C, 31 ± 1.3 °C, respectively. Morsi et al.[26] developed a ketorolac tromethamine-loaded thermosensitive *in situ* gel system for the treatment of postoperative ocular inflammation. Different concentrations of poloxamer and hydroxypropyl methylcellulose were used in the gel systems. Similar to our study, it was determined that as the poloxamer concentration increased, the gelation time and gelation temperature decreases.[26]

Table 2. Mechanical properties of the gel formulations

	Hardness (g) ± SD	Adhesiveness (g.second) ± SD	Cohesiveness ± SD	Elasticity ± SD
CHT gel	19.349 ± 0.452	-16.097 ± 0.179	0.882 ± 0.016	0.559 ± 0.014
CMC gel	20.857 ± 1.482	-14.999 ± 2.982	0.916 ± 0.047	0.544 ± 0.025

CMC: Chitosan, CHT: Carboxymethylcellulose, SD: Standard deviation

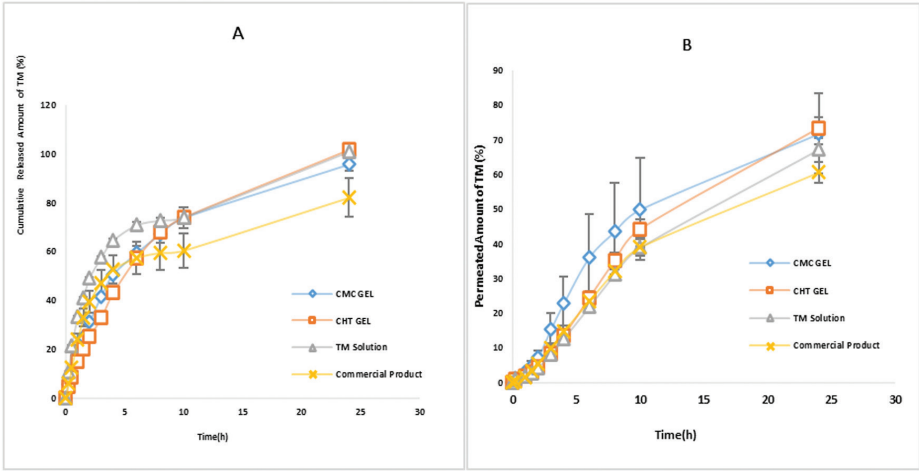

Figure 4. TM release and permeation profiles from TM-containing in situ ophthalmic gels through dialysis membranes (A) and cow corneas (B) ($p > 0.05$)
TM: Timolol maleate

As a result of viscosity studies performed at 25 °C, CHT and CMC gels show Newtonian fluid. Similar to our study, Tirnaksiz et al.[21] in their study, they concluded that the poloxamer solutions they prepared at different concentrations (10%, 12.5% and 15%) showed Newtonian fluid at three temperatures (25 °C, 30 °C and 35 °C).

In order to examine the mechanical properties of the gels, hardness, adhesiveness, cohesiveness and elasticity values were obtained. The amount of work needed to separate the probe from the formulation was defined by the adhesiveness value, which is related to the adhesive characteristics. The aim is to increase the residence time of the drug in the eye; therefore, a high adhesive value indicates stronger adhesion on the surface. According to the experimental results, the CHT gel formulation, which also exhibits higher gel strength properties, achieved the maximum adhesiveness. Cohesiveness indicates the difficulty in breaking down the internal structure of the gel and the effect of repeated stresses. The elasticity feature is that the gel is structurally restored after compression and deformation. A low numerical value indicates high product flexibility.[27] Hardness is defined as the force required to achieve a certain deformation, and it refers to the applicability of the gel to the desired area.[28] It is desirable to have low hardness values for the formulations so that they can be easily taken from the container and applied to the mucosal area.[29] In our study, the hardness of the CHT gel was lower than that of the CMC gel. It has been stated in the literature that there is a correlation between viscosity and hardness.[30] We found that the hardness value of the CHT gel, which has a lower viscosity, was also lower than that of the CMC gel, in line with the literature. Higher adhesive properties in CHT gels are important parameters in mucoadhesive gel design because better gel contact and retention will improve clinical efficacy.

The *in vitro* release properties of CMC gel, CHT gel, commercial product and TM solution were investigated using dialysis membrane. As expected, there was a faster release in the TM solution in the first hours compared with the other formulations, and the release rate was lower for the gel systems. The release of the drug from the gels and TM solution was characterized by an initial phase of high release (burst effect).[31]

The cumulative percentage of drug release through the corneal membrane was slightly lower than that through the dialysis membrane. This might be because the dialysis membrane acts as a basic mechanical barrier, whereas the cornea's epithelium, stroma, and endothelium act as a lipophilic hydrophilic barrier for corneal penetration.[31]

Although the difference between the groups was found to be statistically insignificant as a result of the *ex vivo* permeation study ($p > 0.05$), the permeability of the gel formulation was higher than the solution and commercial product. Owing to its thermosensitive, mucoadhesive gel formulations, TM penetrated the cornea more effectively for a longer period. Thermosensitive *in situ* hydrogels may increase ocular bioavailability by prolonging drug release.[32]

In our study, *in vitro* release and *ex vivo* permeability studies of the developed gels were performed and compared with gel formulations, solutions and commercial products. Thus, it was observed that TM gel systems prolonged the release and increased the retention time in the eye. In particular, different types of poloxamer (P338 and P188) have been used

in combination instead of the poloxamer 407 used in many studies. At the same time, different gel formulations have been developed with the addition of mucoadhesive agents.[25,33-35]

In another study, an ocular gel system sensitive to temperature and pH was developed using poloxamer and CHT polymers. In the *in vitro* transcorneal permeability study, the gel system developed with the drug solution was compared. After 4 hours, the permeability of the drug through the goat cornea was 42.11% ± 2.1% for the solution and 63.41% ± 2.6% for the gel system. This situation was interpreted as being explained by the good transmucosal enhancer properties of CHT.[8]

Similar to our study, one study concluded that an ophthalmic gel developed *in situ* gel showed significantly improved bioavailability compared with a commercial aqueous solution. The developed *in situ* gel formulation was noted to show potential for use as a delivery system for carteolol hydrochloride with superior ocular bioavailability.[36] Gratieri et al.[25] in their study developed a thermosensitive gel formulation by experimenting with different ratios of poloxamer to CHT. The results showed that CHT improved the mechanical strength and tissue properties of the poloxamer formulations. It has been reported that the poloxamer/CHT gel makes contact with the corneal surface four times more than a conventional solution. It was concluded that the developed *in situ* shaping gel is a promising tool for the topical treatment of ocular diseases.

The ocular bioavailability and retention time of TM can be increased with *in situ* gel formulations prepared using polymers other than those used in this study, such as carbopol, polycarbophil, cellulose acetophthalate latex, gellan gum, alginate, ethyl (hydroxyethyl) cellulose, methylcellulose, and Smart Hydrogel™. It can be suggested that the effectiveness of the developed gel formulations can be supported by *in vivo* studies.

CONCLUSION

In this study, thermosensitive-mucoadhesive ophthalmic gel formulations were developed using different types and concentrations of poloxamers and mucoadhesive polymers. The developed gel formulations are liquid at room temperature, and when applied to the cornea, they can form in a short time, such as 26.67 (CHT gel) or 35 seconds (CMC gel). Mucoadhesive and thermosensitive polymer types and concentrations affect gelation time. In the TPA analysis, the hardness value of the CHT gel was found to be lower than that of the CMC gel in relation to viscosity. As a result of *in vitro* release, faster drug release was observed in the TM solution compared with the other formulations in the first hours, but at the end of 24 hours, approximately the same percentage of drug release was obtained with the gels. According to an *ex vivo* permeation study, TM penetrated the cornea longer and more effectively because of the thermosensitive, mucoadhesive gel formulations. The developed gel systems effectively controlled the release of relatively hydrophilic drugs, such as timolol maleate, compared to eye drops and increased drug permeability when using mucoadhesive polymers. Thermosensitive-mucoadhesive hydrogels are effective systems for increasing ocular bioavailability and reducing the frequency of drug application by prolonging drug release. It was concluded that the developed gel formulations are better in contact with the corneal surface than a commercial solution, making them a promising tool for the topical treatment of ocular diseases and improving patient compliance.

Ethics

Ethics Committee Approval: Not required.

Informed Consent: There is not any animal or human experiment in our study.

Authorship Contributions

Surgical and Medical Practices: Ö.K., E.T.A., S.I-T. Concept: Ö.K., E.T.A., S.I-T. F.F.T., Design: Ö.K., E.T.A., S.I-T. F.F.T., Data Collection or Processing: Ö.K., E.T.A., S.I-T. F.F.T., Analysis or Interpretation: Ö.K., E.T.A., S.I-T. Literature Search: Ö.K., E.T.A., S.I-T. F.F.T., Writing: Ö.K., E.T.A., S.I-T. F.F.T.

Conflict of Interest: The authors declare that they have no conflict of interest.

Financial Disclosure: The authors declare no competing financial interest.

REFERENCES

1. Khattab A, Marzok S, Ibrahim M. Development of optimized mucoadhesive thermosensitive pluronic based in situ gel for controlled delivery of Latanoprost: Antiglaucoma efficacy and stability approaches. J Drug Deliv Sci Technol. 2019;53:101134.
2. Lee DA, Higginbotham EJ. Glaucoma and its treatment: A review. Am J Heal Pharm. 2005;62:691-699.
3. Kamel AH El. In vitro and *in vivo* evaluation of Pluronic F127-based ocular delivery system for timolol maleate. Int J Pharm. 2002;241:47-55.
4. Aggarwal D, Kaur IP. Improved pharmacodynamics of timolol maleate from a mucoadhesive niosomal ophthalmic drug delivery system. Int J Pharm. 2005;290:155-159.
5. Urtti A, Rouhiainen H, Kaila T, Saano V. Controlled ocular timolol delivery: systemic absorption and intraocular pressure effects in humans. Pharm Res. 1994;11:1278-1282.
6. Qi H, Chen W, Huang C, Li L, Chen C, Li W, Wu C. Development of a poloxamer analogs/carbopol-based *in situ* gelling and mucoadhesive ophthalmic delivery system for puerarin. Int J Pharm. 2007;337:178-187.
7. Almeida H, Amaral MH, Lobão P, Silva AC, Loboa JM. Applications of polymeric and lipid nanoparticles in ophthalmic pharmaceutical formulations: present and future considerations. J Pharm Pharm Sci. 2014;17:278-293.
8. Gupta H, Jain S, Mathur R, Mishra P, Mishra AK, Velpandian T. Sustained ocular drug delivery from a temperature and pH triggered novel *in situ* gel system. Drug Deliv. 2007;14:507-515.
9. Zhu M, Wang J, Li N. A novel thermo-sensitive hydrogel-based on poly(N-isopropylacrylamide)/hyaluronic acid of ketoconazole for ophthalmic delivery. Artif Cells Nanomed Biotechnol. 2018;46:1282-1287.
10. Allam A, Elsabahy M, El Badry M, Eleraky NE. Betaxolol-loaded niosomes integrated within pH-sensitive *in situ* forming gel for management of glaucoma. Int J Pharm. 2021;598:120380.

11. Hsiue GH, Hsu SH, Yang CC, Lee SH, Yang IK. Preparation of controlled release ophthalmic drops, for glaucoma therapy using thermosensitive poly-N-isopropylacrylamide. Biomaterials. 2002;23:457-462.
12. Zhu Q, Cheng H, Huo Y, Mao S. Sustained ophthalmic delivery of highly soluble drug using pH-triggered inner layer-embedded contact lens. Int J Pharm. 2018;544:100-111.
13. Ho AY, Olm-Shipman M, Zhang Z, Siu CT, Wilgucki M, Phung A, Arnold BB, Porinchak M, Lacouture M, McCormick B, Powell SN, Gelblum DY. A randomized trial of mometasone furoate 0.1% to reduce high-grade acute radiation dermatitis in breast cancer patients receiving postmastectomy radiation. Int J Radiat Oncol Biol Phys. 2018;101:325-333.
14. Çulcu Ö, Tunçel E, İlbasmış Tamer S, Tırnaksız FF. Characterization of thermosensitive gels for the sustained delivery of dexketoprofen trometamol for dermal applications. J Gazi Univ Heal Sci Inst. 2(2), 1-12.
15. Almeida H, Lobão P, Frigerio C, Fonseca J, Silva R, Quaresma P. Development of mucoadhesive and thermosensitive eyedrops to improve the ophthalmic bioavailability of ibuprofen. J Drug Deliv Sci Technol. 2016;35:69-80.
16. Gupta S, Vyas SP. Carbopol/chitosan based pH triggered *in situ* gelling system for ocular delivery of timolol maleate. Sci Pharm. 2010;78:959-976.
17. Chen X, Zhi F, Jia X, Zhang X, Ambardekar R, Meng Z, Paradkar AR, Hu Y, Yang Y. Enhanced brain targeting of curcumin by intranasal administration of a thermosensitive poloxamer hydrogel. J Pharm Pharmacol. 2013;65:807-816.
18. Tuğcu-Demiröz F, Acartürk F, Özkul A. Preparation and characterization of bioadhesive controlled-release gels of cidofovir for vaginal delivery. J Biomater Sci Polym Ed. 2015;26:1237-1255.
19. Barse R, Kokare C, Tagalpallewar A. Influence of hydroxypropylmethylcellulose and poloxamer composite on developed ophthalmic in situ gel: *Ex vivo* and *in vivo* characterization. Journal of Drug Delivery Science and Technology. 2016;33:66-74.
20. Kouchak M, Mahmoodzadeh M, Farrahi F. Designing of a pH-triggered carbopol®/HPMC *in situ* gel for ocular delivery of dorzolamide HCl: *in vitro, in vivo*, and *ex vivo* evaluation. AAPS PharmSciTech. 2019;20:210.
21. Tirnaksiz F, Robinson JR. Rheological, mucoadhesive and release properties of pluronic F-127 gel and pluronic F-127/polycarbophil mixed gel systems. Pharmazie. 2005;60:518-523.
22. Wu Y, Liu Y, Li X, Kebebe D, Zhang B, Ren J, Lu J, Li J, Du S, Liu Z. Research progress of *in situ* gelling ophthalmic drug delivery system. Asian J Pharm Sci. 2019;14:1-15.
23. Soliman KA, Ullah K, Shah A, Jones DS, Singh TRR. Poloxamer-based *in situ* gelling thermoresponsive systems for ocular drug delivery applications. Drug Discov Today. 2019;24:1575-1586.
24. Soriano-Ruiz JL, Calpena-Campmany AC, Silva-Abreu M, Halbout-Bellowa L, Bozal-de Febrer N, Rodríguez-Lagunas MJ, Clares-Naveros B. Design and evaluation of a multifunctional thermosensitive poloxamer-chitosan-hyaluronic acid gel for the treatment of skin burns. Int J Biol Macromol. 2020;142:412-422.
25. Gratieri T, Gelfuso GM, Rocha EM, Sarmento VH, de Freitas O, Lopez RF. A poloxamer/chitosan in situ forming a gel with prolonged retention time for ocular delivery. Eur J Pharm Biopharm. 2010;75:186-193.
26. Morsi N, Ghorab D, Refai H, Teba H. Ketoroloac tromethamine loaded nanodispersion incorporated into thermosensitive *in situ* gel for prolonged ocular delivery. Int J Pharm. 2016;506:57-67.
27. Ustundag Okur N, Yozgatli V, Senyigit Z. Formulation and detailed characterization of voriconazole loaded *in situ* gels for ocular application. Ankara Univ Eczac Fak Derg. 2020;44:33-49.
28. Jones DS, Woolfson AD, Brown AF. Textural analysis and flow rheometry of novel, bioadhesive antimicrobial oral gels. Pharm Res. 1997;14:450-457.
29. Rençber S, Karavana SY, Şenyiğit ZA, Eraç B, Limoncu MH, Baloğlu E. Mucoadhesive *in situ* gel formulation for vaginal delivery of clotrimazole: formulation, preparation, and *in vitro/in vivo* evaluation. Pharm Dev Technol. 2017;22:551-561.
30. Tuğcu-Demiröz F, Acartürk F, Erdoğan D. Development of long-acting bioadhesive vaginal gels of oxybutynin: formulation, *in vitro* and *in vivo* evaluations. Int J Pharm. 2013;457:25-39.
31. Sawant D, Dandagi PM, Gadad AP. Formulation and evaluation of sparfloxacin emulsomes-loaded thermosensitive *in situ* gel for ophthalmic delivery. J Sol-Gel Sci Technol. 2016;77:654-665.
32. Huang W, Zhang N, Hua H, Liu T, Tang Y, Fu L, Yang Y, Ma X, Zhao Y. Preparation, pharmacokinetics and pharmacodynamics of ophthalmic thermosensitive *in situ* hydrogel of betaxolol hydrochloride. Biomed Pharmacother. 2016;83:107-113.
33. Gratieri T, Gelfuso GM, de Freitas O, Rocha EM, Lopez RF. Enhancing and sustaining the topical ocular delivery of fluconazole using chitosan solution and poloxamer/chitosan *in situ* forming gel. Eur J Pharm Biopharm. 2011;79:320-327.
34. Varshosaz J, Tabbakhian M, Salmani Z. Designing of a thermosensitive chitosan/poloxamer *in situ* gel for ocular delivery of ciprofloxacin. The Open Drug Delivery J. 2008;2:61-70.
35. Edsman K, Carlfors J, Petersson R. Rheological evaluation of poloxamer as an *in situ* gel for ophthalmic use. Eur J Pharm Sci. 1998;6:105-112.
36. El-Kamel A, Al-Dosari H, Al-Jenoobi F. Environmentally responsive ophthalmic gel formulation of carteolol hydrochloride. Drug Deliv J Deliv Target Ther Agents. 2006;13:55-59.

Turk J Pharm Sci 2024;21(4):355-366
DOI: 10.4274/tjps.galenos.2023.62293

ORIGINAL ARTICLE

Hemagglutinin from the Root Tuber of *Dioscorea preussii* Pax

Oludele Olayemi ODEKANYIN*, Sunday Isaiah AKANNI

Obafemi Awolowo University, Faculty of Science, Department of Biochemistry and Molecular Biology, Ile-Ife, Nigeria

ABSTRACT

Objectives: In this study, *Dioscorea preussii* root tuber hemagglutinin was purified and its physicochemical properties were determined. The antioxidative and anti-hemolytic activities of the hemagglutinin were also investigated.

Materials and Methods: The hemagglutinating assay was used to detect the presence of lectin in the phosphate-buffered saline extract of the *D. preussii* root tuber. The lectin was purified using ammonium sulfate fractionation and molecular sieve chromatography. The optimum pH and temperature were determined. In addition, antioxidant activity was assessed using 2,2 diphenylpicrylhydrazyl (DPPH) radical scavenging, metal chelating, ferric reducing antioxidant power (FRAP), and lipid peroxidation inhibition assays. Red blood cells subjected to oxidative damage caused by H_2O_2 were employed to evaluate their antihemolytic ability.

Results: Starch inhibited hemagglutinin activity. *Dioscorea preussii* hemagglutinin (DPH) maintained full hemagglutinating activity from 30 °C to 60 °C and pH 5-13. Ethylene diamine tetraacetic acid did not affect the hemagglutinating activity of hemagglutinin. All denaturing agents (Guanidine-HCl, urea, and β-mercaptoethanol) reduced the hemagglutinating activity of the hemagglutinin to different degrees. The hemagglutinin scavenged the DPPH radical and chelated iron metal with half maximum inhibitory concentration (IC_{50}) of 0.727 ± 0.035 mg/mL and 0.583 ± 0.078 mg/mL, respectively, while the FRAP assay showed that it contained 76 mg of ascorbic acid equivalent per gram of the purified hemagglutinin. In the absence of hemolytic agents and at lower concentration tested, hemagglutinin showed positive membrane integrity protection.

Conclusion: This study provides information on the antioxidant properties of *D. preussii* root tuber hemagglutinin as well as its cell membrane protective ability. The lectin is a starch-binding, which makes it a novel lectin.

Keywords: *Dioscorea preussii*, hemagglutinin, antioxidant, anti-hemolytic, lectin

INTRODUCTION

Dioscorea preussii as a genus belongs to the family *Dioscoreaceae*, which is the most recognized among all families under the order *Dioscoreae*. This genus is primarily found in West Africa, tropical America, and Southeast Asia. *Dioscorea* spp. (*Dioscoreaceae*), which are commonly referred to as Yams in English, are tuberous plants with stems that climb and twine either to the right or left. The Yorubas, Igbos, and Hausas in Nigeria refer to yam as is, ji, and dopa, respectively.[1] Food and health issues continue to be the main challenges in developing countries. Many wild crops are still unexplored; unfortunately, great medicinal and nutritional solutions that the world is looking for might just be locked up in some of these crops. Therefore, scientific research must address these problems robustly by looking for other food and medicinal sources.[2]

There are many wild medicinal and edible products that nature has provided like tubers, stems, nuts, roots, fruits, and flowers.[3,4] Apart from the significant roles of yam in fighting the scarcity of food, literature has shown that *Dioscorea* species possess biological activities like antiproliferative, antioxidant, androgenic, lectin, antimicrobial, and immunomodulatory activities, among others.[5-7]

Very little is known about *D. preussii* Pax, as extremely few studies[8,9] have been conducted on this wild plant. It is a climber whose stem twines left-handed, with the ability to go up to 24 m from its narrow cylindrical tuber. The tuber, which is usually deeply buried, can be as long as 40 cm, with horizontal branches that can also be as long as 30 cm long. Tuberculosis is mostly eaten in some places during famine.[10,11] In Nigeria, the tuber is

*Correspondence: dekanyin@gmail.com, Phone: +08062879457, ORCID-ID: orcid.org/0000-0003-2676-2241
Received: 08.07.2023, Accepted: 07.09.2023

known as ainyelo, igiruesi, and esuru-igbo among the Igbo, Edo, and Yoruba people, respectively.[10,12] The extract of *D. preussii* has been reported to exhibit *in vitro* cytotoxicity, antileishmanial, and antifungal activities.[13] Tabopda et al.[8] isolated and characterized three important steroidal saponins from this tuber.

During cellular metabolism, which is a form of normal cellular activity, free radicals are produced. These free radicals can simply be described as atoms or molecules containing a single electron or more in their outer orbits, making these atoms or molecules unstable and highly reactive. These reactive species at low or moderate levels perform beneficial roles in immunity, redox regulation, cellular signaling pathways and in mitogenic response.[14] At higher concentrations, reactive oxygen species (ROS) cause oxidative stress, whereas reactive nitrogen species cause nitrosative stress, which destroys biomolecules. Biomolecules such as deoxyribonucleic acid (DNA), lipids, and proteins could have their integrity damaged by excess ROS, thereby causing an upsurge in the imbalance in oxidant-antioxidant levels found in different diseases in humans such as cardiovascular diseases, diabetes mellitus, cataracts, rheumatoid arthritis and others.[14]

To prevent the destructive effects of free radicals, the human body has devised different mechanisms to combat them through certain agents known as antioxidants.[15] Antioxidants are molecules that neutralize free radicals to prevent their cellular damage. They do this by donating electron(s) to reactive species, chelating metals, hydrogen donation, enzyme inhibition, and peroxide decomposition.[15,16]

Hemolysis is the rupturing of the erythrocytes.[17] Red blood cells are known to possess abundant polyunsaturated fatty acids, high oxygen, hemoglobin, and membrane proteins. Because erythrocytes are more exposed to oxygen than any other cell or tissue in the body, they are more vulnerable to oxidative destruction; thus, they are frequently and widely used in the study of oxidative damage in membranes. Moreover, although hemoglobins present in erythrocytes are strong catalysts that can lead to the initiation of lipid peroxidation, the invasion of the membranes of erythrocytes by peroxidases can also result in cell hemolysis.[18,19] This is resulted in peroxidation of unsaturated membrane fatty acids leads to disruption of the usual organization of membrane lipids, membrane pore formation and water permeability alteration, eventually damaging the membrane structure leading to hemolysis.[20] Because of its relatively high stability and diffusion of hydrogen peroxide, it is considered an excellent oxidant model for investigating both the hemolytic and anti-hemolytic activities of various samples.[19] Different natural substances have been proposed as therapeutic agents to prevent hemolysis, some of which have anti-hemolytic potential linked to their free radical scavenging activity.[21,22]

Lectins are ubiquitous (glyco) proteins that possess at least one binding site for carbohydrate or their derivatives, have no catalytic function, and are also of non-immunoglobulin origin.[23] All of these proteins were initially referred to as hemagglutinin, a term currently used only for those whose sugar specificity is unknown or unknown. Plants are a great source of lectins, and they are also the major source from which lectins that are analyzed are isolated. Lectins are known to have many biological properties including antifungal, antitumor, antibacterial, antiviral, germicidal, and insecticidal activities.[24] Lectins are also known to perform various roles including storage, transport, signaling,[25,26] cell recognition, cell migration, endocytosis, complement activation, cell adhesion, intracellular translocation processes, apoptosis activation, cell signaling, immune regulation, and defense against pathogens.[25,27]

Under the condition of severe redox imbalance, erythrocytes become vulnerable and cellular defense does not offer full defense against the attack of reactive and free radicals, which could lead to oxidative damage-related diseases such as cardiovascular disease. Recently hemagglutinin, which possesses antioxidant activity, has been reported[28,29] from plant sources and protects erythrocytes from hemolysis. The literature search indicated that there is a need for more plant-derived proteins with such activity. Therefore, identifying hemagglutinin with antioxidant potential and protective effects on erythrocytes that have little or no side effects will be of great benefit. This study led to the purification of a novel hemagglutinin from the root tuber of *D. preussii* and the determination of its physicochemical properties. This study also investigated the antioxidant and anti-hemolytic activities of hemagglutinin with a view to exploring its therapeutic potential.

MATERIALS AND METHODS

All experiments, or otherwise stated, were carried out in the Protein Science Laboratory, Biochemistry, and Molecular Biology Department, Obafemi Awolowo University, Ile-Ife, Nigeria.

Blood collection

Different blood groups under the ABO blood group classification were drawn from apparently healthy human donors into heparinized bottles. Erythrocytes were also obtained from healthy rabbits purchased from Teaching and Research Farm, Obafemi Awolowo University, Ile-Ife, Nigeria.

Preparation of D. preussii crude extracts

Root tubers of *D. preussii* were collected from a farm in Obafemi Awolowo University, Ile-Ife, Nigeria. The root tubers of *D. preussii* were thoroughly washed to remove sand particles and then peeled. The peeled tubers were minced into very small pieces and ground into a fine paste. Ground tubers were extracted at 4 °C overnight in phosphate-buffered saline (PBS, pH 7.2) at a ratio of 1:10 *w/v*. The mixture was sieved with cheesecloth; the filtrate was later centrifuged at 4 °C and 10,000 rpm for 20 minutes using a cold centrifuge (Centurion Scientific LTD. 8880, R-Series). The resulting supernatant is hereafter termed the crude extract.

Glutaraldehyde fixation in erythrocytes

To fix the erythrocytes, blood samples were collected from humans and animals into heparinized bottles. The samples were immediately centrifuged at 3,000 rpm using a centrifuge

(Hospibrand 0502-1) for 15 minutes to obtain the erythrocytes. The erythrocytes were washed five times with PBS and then fixed in chilled 1% glutaraldehyde-PBS solution for 1 hour at 4 °C with intermittent mixing. After fixation, the mixture was centrifuged for 5 minutes at 3000 rpm to collect the fixed erythrocytes. The fixed erythrocytes were extensively washed with PBS to remove glutaraldehyde. Two percent of the erythrocytes were prepared in PBS containing 0.02% sodium azide. This was stored in a refrigerator for further use.

Hemagglutinating assay

The presence of lectin in the crude extracts of *D. preussii* and its various fractions was determined using a modified hemagglutinating assay procedure involving Odekanyin and Kuku.[30] The assay was performed in a 96-well U-shaped microtiter plate. PBS (100 µL) was sequentially pipetted into all wells of the microtiter plate. After this, 100 µL of the crude extract or any fraction was added to the first well in the first row, and the mixture was serially diluted up to the 24th well (2 rows). Fifty microliters of the fixed erythrocyte suspension (50 µL) were pipetted into each well. The plate was left undisturbed for 2 hours on a laboratory bench and then observed for any visible hemagglutination. The control experiment did not extract any fractions. Haemagglutination titer unit was taken as the highest dilution reciprocal of the crude extract or any of the fractions producing visible haemagglutination. Specific activity is the haemagglutination titer unit number per mg protein expressed as hemagglutinating units/mg.

Sugar specificity test

The sugar specificity of *D. preussii* hemagglutinin (DPH) was determined by comparing the abilities of different sugars to inhibit the hemagglutinating activity of the hemagglutinin. First, the serial dilution of the hemagglutinin was carried out as described in hemagglutinating assay section until the last dilution at which hemagglutination was observed. Sugar solution (0.2 M, 50 µL) was added to each well, whereas PBS-supplemented sugar solution was added to the control wells. The microtiter plate was then incubated at room temperature for 2 hours. The erythrocyte suspension (50 µL) was added to each well. The plate was left undisturbed for 2 hours on a laboratory bench and then observed for any visible hemagglutination. The tested sugars were glucosamine HCl, lactose, maltose, sorbose, starch, mannitol, galactose, N-acetyl-D-glucosamine, xylose, arabinose, glucose, dulcitol, α-D-methyl glucopyranoside, and 2-deoxy-D-glucose.

Protein concentration determination

Lowry method[31] of protein concentration determination was adopted to determine the total protein concentration of the crude extract and other fractions. Bovine serum albumin was used as the standard.

Purification of lectin

Ammonium sulfate fractionation

Solid ammonium sulfate (16.4 g/100 mL) was mixed with a known volume of the crude extract with gentle stirring to reach a solution containing 30% ammonium sulfate saturation. After 24 hours, the mixture was centrifuged at 4,000 rpm for 10 minutes to collect the precipitate. This precipitate represents the 30% ammonium sulfate fraction. The ammonium sulfate saturation of the supernatant was then increased to 60% through slow addition with gentle stirring of solid ammonium sulfate (18.1 g/100 mL). The precipitate was also collected and represented a 60% ammonium sulfate precipitate fraction. Again, the ammonium sulfate saturation of the supernatant was increased to 90% by slowly adding solid ammonium sulfate (20.1 g/100 mL). The precipitate representing 90% of the fraction was also collected. All precipitates were separately dialyzed against PBS exhaustively, and the dialysate of each fraction was tested for hemagglutinating activity. The dialysates were later stored in a deep freezer (below -4 °C)

Gel filtration on Sephadex G-100

Approximately 15 g of Sephadex G-100 was preswollen in PBS (200 mL) at room temperature for 72 hours. A column (2.5 x 40 cm) was packed with the preswollen resin and equilibrated with PBS (500 mL, 25 mM, pH 7.2). 5 mL of *D. preussii* ammonium sulfate dialysate was layered on the packed column, the same buffer (PBS) used for eluting proteins while collecting 5 mL fractions at a 20 mL/h flow rate. The hemagglutinating activity and protein concentration of these fractions were evaluated. Fractions with high hemagglutinating activity were pooled together, dialyzed exhaustively in phosphate buffer (pH 7.2, 0.01 M), and finally freeze-dried for further use.

Physicochemical characterization of lectin

Temperature effect on hemagglutinating activity

The purified hemagglutinin was incubated at various temperatures (30 °C-100 °C) for 60 minutes. Aliquots of the hemagglutinin at each temperature at 30 and 60 min and thereafter subjected to hemagglutinating assay.

pH effect on hemagglutinating activity

An Aliquot of the purified hemagglutinin was incubated for 1 hour with various buffers with different pH values to evaluate the effect of pH on the hemagglutinating activity of purified hemagglutinin. The same concentration (0.2 M) of the different buffers was used, and their pH ranges were as follows: Glycine-HCl buffer (pH 1-3), Acetate buffer (pH 4-6); Tris-HCl buffer (pH 7-8) and Glycine-NaOH buffer (pH 9-13). The incubated aliquots of hemagglutinin were subjected to a hemagglutinating assay after incubation to determine residual activity.

Denaturants effect on hemagglutinating activity

An aliquot of the purified hemagglutinin was incubated for 6 hours in 2-8 M concentrations of different denaturants (Guanidine HCl, urea and Mercaptoethanol) to determine the effects of the denaturants on the lectin activity of the purified hemagglutinin. The hemagglutinin incubated in PBS served as the control. The incubated mixtures were then assayed for hemagglutinating activity before and after dialyzing against PBS.

Chelating agents' effect on hemagglutinating activity

Purified hemagglutinin was dialyzed against two different concentrations of ethylene diamine tetraacetic acid (EDTA) (10 mM and 50 mM) separately for approximately 24 hours at 4 °C to determine the effect of EDTA on DPH. Subsequently, it was assayed for hemagglutinating activity.

Antioxidants assays

Scavenging of DPPH radicals

The purified hemagglutinin was assessed for its ability to scavenge DPPH radicals according to the method of Huh and Han.[32] Three-tenths millimolar DPPH in methanol (1 mL) was mixed with varying concentrations of the hemagglutinin (sample)/ascorbic acid (standard), after which the mixture was incubated for half an hour in a dark cupboard. Absorbance was measured at 517 nm using a Biobase ultraviolet-visible spectrophotometer BK-D5 series compared with a control in which the sample/standard was substituted with methanol.

The following formula was used to calculate the percentage inhibition:

$$\text{Percentage DPPH}^{\bullet}\text{ inhibition} = \frac{(A_{control}\text{-}A_{sample})}{A_{control}} \times 100$$

Here, $A_{control}$ denotes the absorbance of the control, and A_{sample} denotes the absorbance of the tested samples.

Ferric reducing antioxidant power (FRAP) assay

To prepare the FRAP reagent according to Benzie and Strain,[33] 300 mM acetate buffer (pH 3.6), 2,4,6-tri-(2-pyridyl)-1,3,5-triazine (TPTZ, 10 mM, in 40 mM HCl), and 20 mM $FeCl.6H_2O$ at a ratio of 10:1:1 were mixed. Varying concentrations of ascorbic acid (50 µL, 0.02-0.1 mg/mL) or hemagglutinin (50 µL of 0.1 mg/mL) were added to FRAP (1 mL). Ten minutes after mixing, absorbance was measured at 593 nm against a blank reagent. The samples were protected from direct sunlight. The ascorbic acid equivalent (AAE) of the sample was estimated. The equivalent concentration was used to express the reducing power.

Lipid peroxidation inhibition assay

This assay was performed in accordance with the previously described procedure of Masao et al.[34] Butylated hydroxyltoluene (BHT) was used as the positive control. Egg homogenate (0.25 mL of 10%) was mixed with 0.1 mL Tris-HCl buffer (150 mM, pH 7.2), 0.05 mL of 1 % (*w/v*) ascorbic acid, 0.05 mL of 0.07 M $FeSO_4$, and various concentrations of the sample/standard, after which the mixture was incubated at 37 °C for an hour. After that, 0.67% thiobarbituric acid (TBA, 2.0 mL) was added. The mixtures were incubated for 30 minutes at 100 °C, allowed to cool, with the subsequent addition of butane-1-ol (2.0 mL), and centrifuged for 10 minutes at 3000 rpm. The absorbance of the supernatant was measured with the reagent blank as a reference at 532 nm.

The percentage inhibition of lipid peroxidation was estimated using the equation below:

$$\text{Lipid peroxidation inhibition} = \frac{A - B}{A} \times 100$$

Where A represents the absorbance of the control (without test sample), B represents the absorbance of the tested samples.

Metal-chelating activity assay

The ability of the DPH to form a complex with iron was determined using a metal chelating assay. The method proposed by Singh and Rajini[35] was used with minor modifications. Stock solutions of 2 mM $FeSO_4{\cdot}7H_2O$ and 5 mM ferrozine were diluted 20 times. $FeSO{\cdot}7H_2O$ (1 mL) was combined with various concentrations of hemagglutinin (1 mL)/EDTA (1 mL). After incubating for 5 minutes, ferrozine (1 mL) was added to start the reaction, and the reaction mixture was vortexed and incubated for another 10 minutes. The absorbance of the solution was then measured at 562 nm spectrophotometrically. The formula below was used to calculate the percentage inhibition of the formation of ferrozine-Fe^{2+}:

$$\text{Percentage Chelation} = \frac{(A_{control}\text{-}A_{sample})}{A_{control}} \times 100$$

Anti-hemolytic activity assay

The human blood group O-positive specimen used in this assay was first prepared before use. The blood drawn from a healthy donor was washed five times with PBS *via* centrifugation. Five percent (5%) of the washed erythrocytes were then prepared in PBS. Ebrahimzadeh et al.[36] procedure was adopted with little modification to determine the anti-hemolytic activity. Fifty microliters of different concentrations of hemagglutinin/ standard (ascorbic acid) were added to the erythrocyte suspension in PBS (5%, 100 µL). After 30 minutes of incubation, 100 µL of H_2O_2 (1.77 M) was added to the mixture. Subsequently, incubation for 3 hours at 37 °C followed by gentle shaking of the mixture. After incubation, the reaction mixture was centrifuged for 10 minutes at 2500 rpm. The supernatant was collected, and the absorbance was read at 540 nm to estimate the amount of hemoglobin released. The erythrocytes were also treated as described above, but without the hemagglutinin to obtain complete hemolysis taken as 100%.

To evaluate hemolysis induced by the sample (hemagglutinin), red blood cells were pre-incubated with the sample (hemagglutinin, 50 µL), after which the amount of hemoglobin released was determined. The percentage of hemolysis was calculated using the following formula:

The following formula was used to calculate the percentage of anti-hemolysis:

$$\text{Percentage anti-hemolysis} = \frac{A_2 - A_1}{A_2} \times 100$$

$$\text{Percentage hemolysis} = \frac{A_1}{A_2} \times 100$$

Hemolysis due to H_2O_2 (100 µL) was taken as 100% hemolysis. A_1 represents the absorbance of the tested samples. A_2 represents absorbance at 100% hemolysis.

Statistical analysis

The experiments were performed in triplicate, and the results were expressed as mean ± standard error of the mean and were analyzed using one-way analysis of variance for multiple measurements. GraphPad Prism statistical software version 7.0 (San Diego, California, 92108, United States) was used for all statistical analyses.

Ethical approval

The study approved by the Obafemi Awolowo University Departmental Health Research Ethic Committee (approval number: OAUBCH/HREC/2024/005, date: l4.08.2024).

RESULTS

The crude extract of *D. preussii* tubers agglutinated all the human blood group (ABO) and rabbit erythrocytes non-specifically. It displayed equal preference for all the erythrocytes tested (Table 1).

The binding specificity of *D. preussii* hemagglutinin to carbohydrates was investigated by reacting it with different sugars, none of them was able to completely inhibit the hemagglutinating activity of the haemagglutinin except a polysaccaharide, starch. The hemagglutinating activity was slightly inhibited by glucose, lactose, mannitol and ducitol, while fructose, galactose, maltose, arabinose, and methyl α-D-glucopyranoside had no effect on the hemagglutinating activity. Xylose and N-acetylglucosamine activated the hemagglutinating activity of the haemagglutinin.

The dialysate of the 60% ammonium sulphate precipitate was found to have higher activity than the dialysates of the 30% and 90% ammonium sulphate precipitates (Table 2).

Table 1. Blood group specificity of *Dioscorea preussii* crude extract

Blood type (Erythrocyte)		Hemagglutinating titer
Human blood group	A	2^{11}
	B	2^{11}
	O	2^{11}
	AB	2^{11}
Rabbit		2^{11}

Table 2. Hemagglutinating activities of dialysates with 30%, 60%, and 90% ammonium sulfate precipitates of *Dioscorea preussii*

Dialysates	Hemagglutinating titer
30%	2^6
60%	2^{10}
90%	2^5

The three ammonium sulphate fractions (30%, 60% and 90%) were subjected to gel filtration on Sephadex G-100. Sixty percent (60%) ammonium sulphate precipitate dialysate gave one major protein peak with 2 minor peaks. The haemagglutinating activity was found to reside in the major protein peak. The fractions of the activity peak were pooled. The specific activity and purification fold were 118.5 and 13.48 respectively (Table 3). The typical chromatogram of gel filtration on Sephadex G-100 of dialysate of 60% ammonium sulphate precipitate is shown in Figure 1A. The 30% and 90% ammonium sulphate precipitate dialysate were also gel filtered. Typical chromatogram of the gel filtration of 30% and 90% ammonium sulphate precipitate dialysates are shown in Figures 1B and 1C respectively. The active fractions were pooled and had insignificant hemagglutinating activity.

The hemagglutinating activity of *D. preussii* hemagglutinin was found to be completely stable up to 60 °C, there was a slight reduction of its activity at 70-90 °C, but totally lost its activity at 100 °C (Figure 2A).

The optimum pH of the hemagglutinin was between pH 5 and pH 13, which cover the neutral and basic pH range. It was noticed that the activity at the acidic pH range increases with increase in pH up to pH 5 (Figure 2B).

EDTA at two different concentrations (10 mM and 50 mM) had no effect on the hemagglutinating activity of the hemagglutinin after prolong dialysis.

Result revealed that all the denaturing agents were able to reduce the hemagglutinating activity of the hemagglutinin to different degrees as shown in Figure 2C. Mercaptoethanol at 1M to 7M was found to reduce the activity of the haemagglutinin to 50%, while 8M further reduced the activity to 25%. The hemagglutinating activity of *D. preussii* hemagglutinin was also found to have been reduced by Guanidine HCl at 4M and 5M to 50%, which was further reduced to 25% at 6M to 8M. Urea was found to reduce the hemagglutinating activity of the haemagglutinin at 8M by 50%.

Figure 3A shows the DPPH radical scavenging activity of *D. preussii* hemagglutinin. The haemagglutinin was found to possess DPPH radical scavenging activity in a concentration dependent manner, with an IC_{50} of 0.727 ± 0.035 mg/mL which was lower in activity than that of the standard (Ascorbic acid) having an IC_{50} of 0.022 ± 0.001 mg/mL.

The result of the metal chelating assay revealed that *D. preussii* was able to chelate iron in a dose dependent manner (Figure 3B). The IC_{50} of the haemagglutinin was found to be 0.583 ± 0.078 mg/mL which was lower in activity when compared with that of the standard (EDTA) possessing an IC_{50} of 0.041 ± 0.006 mg/mL.

D. preussii hemagglutinin unlike the standard (Butylated hydroxyltoluene) possessed no anti-lipid peroxidation activity. The level of lipid peroxidation was however found to increase as the concentration of the hemagglutinin increased, while the opposite was observed for the standard, that is, as the concentration of BHT increased, the percentage inhibition of lipid peroxidation also increased (Figure 3C).

D. preussii haemagglutinin exhibited high antihemolytic activity in the absence of hemolytic agent. Up to 90% antihemolytic activity was recorded and the activity was concentration related. The lower concentration of the hemagglutinin also protected the cell membrane integrity against oxidative stress caused by hydrogen peroxide.

DISCUSSION

In this study, the crude protein extract obtained from the root tubers of *D. preussii* contained hemagglutinin. The isolated and purified hemagglutinin was termed DPH. DPH hemagglutinating activity was non-specific against all types of red blood cells, as it agglutinated all the human blood group (ABO) and rabbit erythrocytes. This result showed that lectin possessed blood

Table 3. Purification table of hemagglutinin from *Dioscorea preussii* tuber

Fractions	Total protein level (mg)	Total activity (HU)	Specific activity (HU/mg)	Yield %	Purification fold
Crude extract	233.10	2048	8.79	100	1
Ammonium Sulfate precipitates dialysate (60%)	33.50	1024	30.57	50	3.48
Gel filtration (Sephadex G-100)	2.16	256	118.5	12.5	13.48

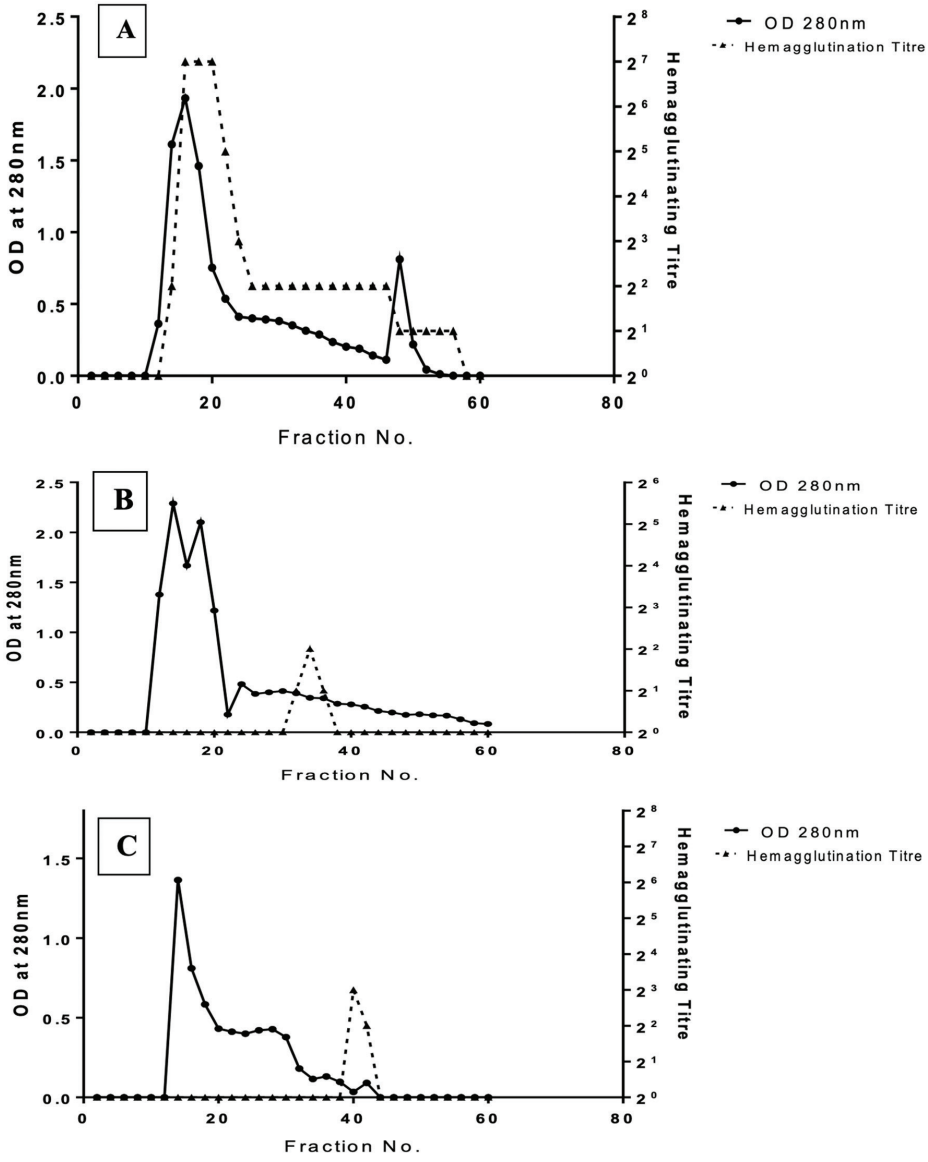

Figure 1. Gel Filtration Chromatogram of the Dialysate of the 60% (A), 30% (B), and 90% (C) $(NH_4)_2SO_4$ precipitate of *Dioscorea preussii* crude extract on Sephadex G-100

group specificity that was different from that of most tuber lectins. Tuber lectins are majorly rabbit erythrocytes specific. Tuber lectins from *Arisaema utile* Hook. F. Scott,[37] *Caladium bicolor* (Aiton) Vent.,[38] and *Dioscorea bulbifera* L.[39] have all been reported to agglutinate rabbit erythrocytes but are unreactive to human ABO blood group erythrocytes. Recently, a contrary report was published by Akinyoola et al.[40] Their report showed that the tuber lectin of *Dioscorea mangenotiana* J. Miège agglutinated all the human blood group (ABO) and rabbit erythrocytes non-specifically. These findings are consistent with the results reported in this study. In support of this, Sharma et al.[41] published isolation and purification of *Adenia hondala* (Gaertn.) de Wilde tuber lectin, a human blood group non-specific antibody that agglutinated rabbit erythrocytes.

A hapten inhibition assay, which determines the ability of sugars to inhibit the hemagglutinating activity of *D. preussii* tuber hemagglutinin, was performed. Different sugars including monosaccharides, disaccharides, and their derivatives along

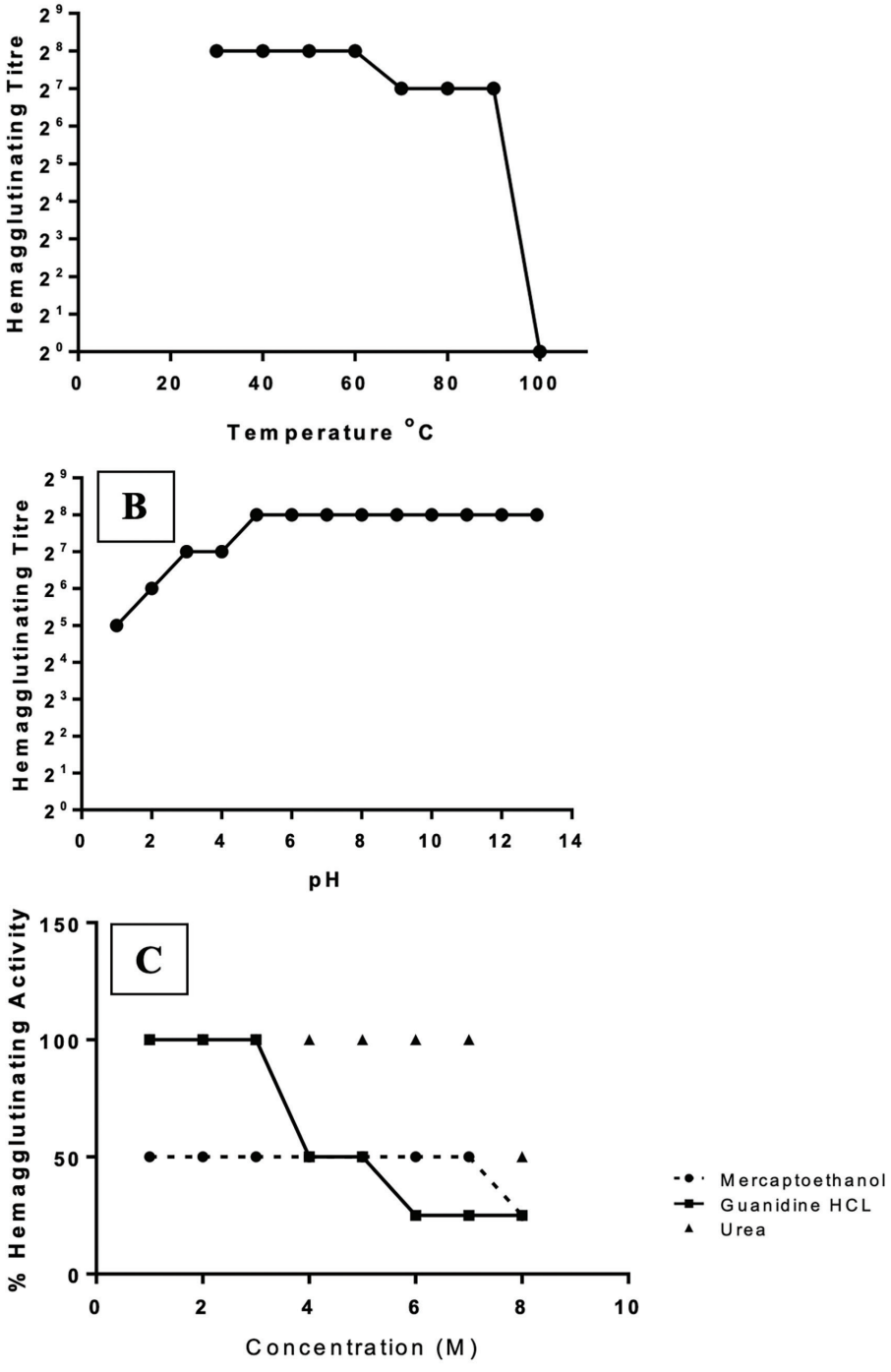

Figure 2. Effects of temperature, pH, and denaturing agents on DPH hemagglutinating activity
DPH: *Dioscorea preussii* hemagglutinin

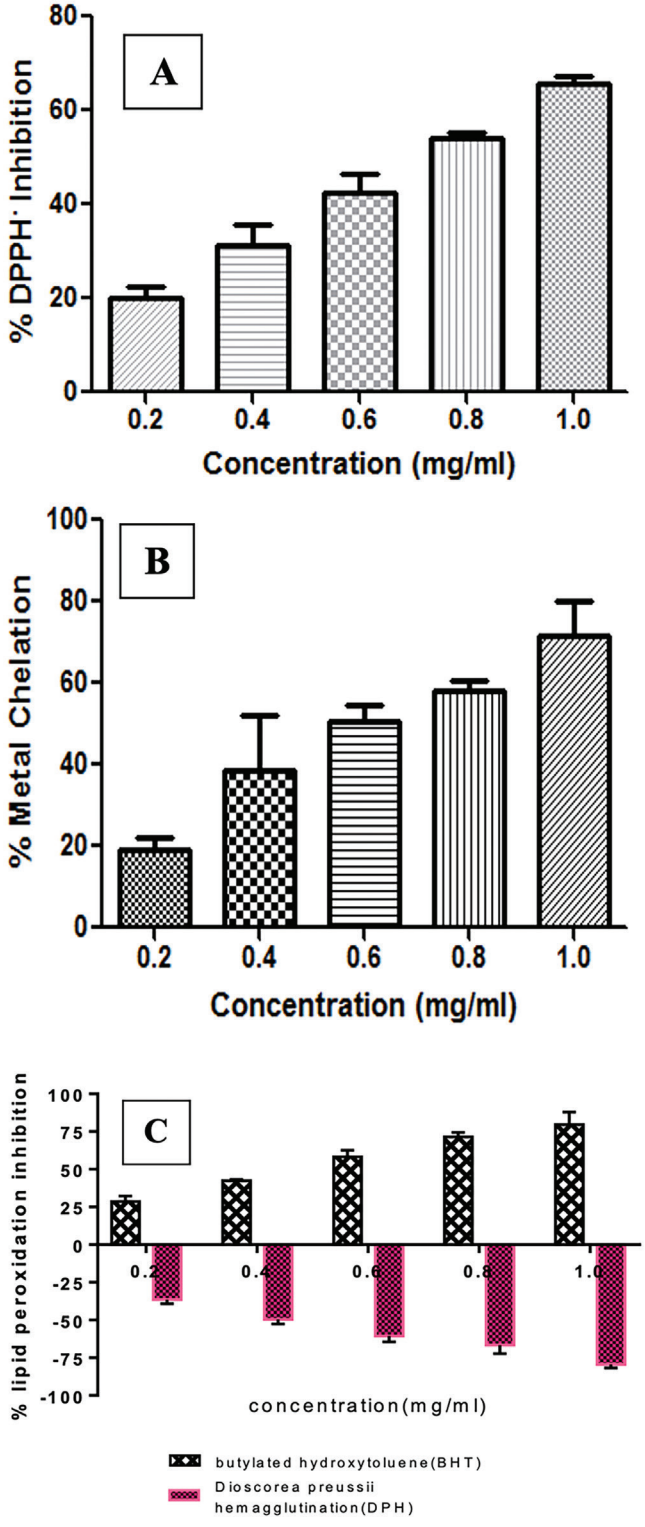

Figure 3. Antioxidant activity of *Dioscorea preussii* hemagglutinin. A) DPPH radical-scavenging activity, B) metal-chelating activity, C) anti-lipid peroxidation activity

DPPH: 2,2 diphenylpicrylhydrazyl

with some polysaccharides were used for this study, but none of the sugars inhibited the hemagglutinating activity of hemagglutinin except starch. This is compatible with the result of Sharma et al.[39] It was reported that all of the tested simple sugar derivatives and the simple sugar themselves did not inhibit the hemagglutinating activity of the aerial tuber of *D. bulbifera* lectin. Pereira et al.[42] reported that all the tested sample sugars did not inhibit the hemagglutinating activity of *Colocasia esculenta* lectin. Contrary to this, Akinyoola et al.[40] reported that glucose and N-acetylglucosamine inhibited *D. mangenotiana* tuber lectin activity. Galactose was also found to inhibit the activity of *Dioscorea opposita* tuber lectin.[43] It was discovered in the current study that a polysaccharide of plant origin (starch) inhibited the hemagglutinating activity of *D. preussii* tuber hemagglutinin.

We subjected the crude lectin extract from the root tubers of *D. preussii* to salt fractionation using ammonium sulfate. The dialysate of the 60% ammonium sulfate precipitate was found to have higher hemagglutinating activity than the dialysates of the 30% and 90% ammonium sulfate precipitates (Table 2). Therefore, it was purified and used for further studies. Also, 60% ammonium sulfate precipitate dialysate gave one major protein peak with 2 minor peaks when gel-filtered on a Sephadex G-100 column. The hemagglutinating activity was found to reside in the major protein peak. The fractions of activity peaks were pooled. The specific activities and fold purifications were 118.5 and 13.48, respectively (Table 3). The typical chromatogram of gel filtration on Sephadex G-100 of dialysate with 60% ammonium sulfate precipitate is shown in Figure 1A. Dialysates with 30% and 90% ammonium sulfate precipitate were also gel-filtered. The active fractions were pooled and had insignificant hemagglutinating activity (Figure 1B and 1C). Purity of protein is initially determined by the specific activity of the protein and later by electrophoresis. Specific activity is the amount or activity of such protein per milligram of whole protein in the sample. The higher the specific activity the better the purity of the protein. Pure protein is obtainable through the usage of chromatographic techniques. A single step or combination of different chromatographic methods can be adopted for purification procedure. In this study, a single step chromatographic technique (gel filtration) was adopted. The process produced hemagglutinin with specific activity of 118.5 HU/mg and purification fold of 13.48. Similar procedure was employed by Akinyoola et al.[40] and lower value of specific activity (0.25 HU/mg) and purification fold (3.1) were obtained. In another publication by Podder et al.,[29] a single purification step was used for purification of *Manikara zapota* lectin. The lectin was purified on affinity chromatographic column and higher value of specific activity (420 HU/mg) and purification fold (17.5) were reported. Chan and Ng[43] engaged anion exchange chromatography and gel filtration for the purification of *D. opposite* tuber lectin. The specific activity was higher than reported value in the current study.

DPH was found to resist heat denaturation up to 60 °C, as it was found to maintain full hemagglutinating activity up to 60 °C even after heating for one hour. Although, at 70 °C, the hemagglutinin lost 50% of its hemagglutinating activity after 1 hour of incubation but was still found to maintain its native hemagglutinating activity after heating for 30 minutesat this temperature and up to 90 °C before totally losing it at 100 °C

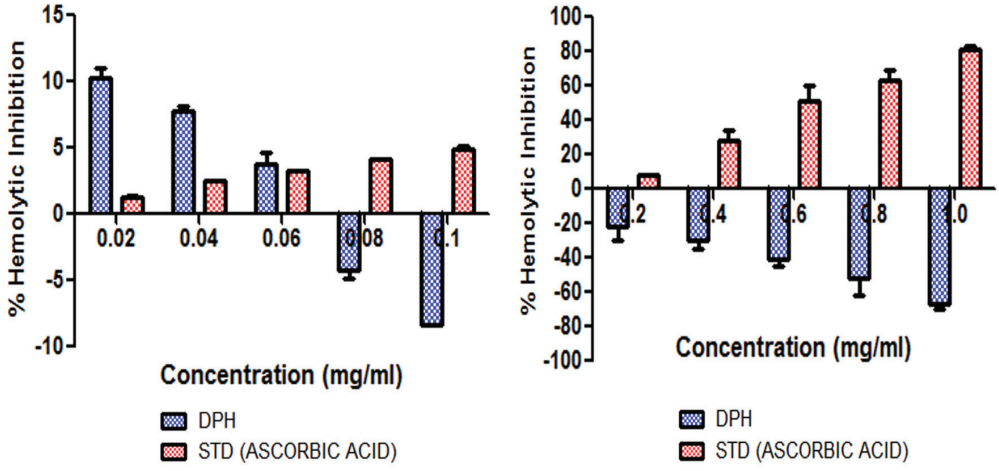

Figure 4. Anti-hemolytic potential of DPH
DPH: *Dioscorea preussii* hemagglutinin

(Figure 2A). Lectins isolated from *D. opposita by* Chan and Ng,[43] *Arisaema helleborifolium* Scott. by Kaur et al.,[44] and *Nymphaea nouchali* var. caerulea by Kabir et al.[45] were all shown to resist thermal inactivation till up to 60 °C. The loss of hemagglutinating activity of *D. preussii* at high temperatures might be since the weak interactions responsible for maintaining the structural integrity of hemagglutinin were disrupted, thereby altering its native conformation responsible for its activity.[46,47]

The pH is a consequence of the amino acid composition of the protein and is noticed in almost all enzyme reactions and in some proteins' functions. Hydrogen or hydroxyl ions are highly reactive and can interact with the most ionizable groups present at the surface of the protein molecule, possibly at the active center. Therefore, any pH alteration is connected to a change in the ionization state of the molecule, which in turn regulates the binding forces between the enzyme and substrate.[48] DPH was found to show high tolerance to a wide pH range. Although it had 50% hemagglutinating activity at pH 3 and 4, it was found to maintain full hemagglutinating activity at pH 5-13 (Figure 2B). It can be speculated that an increase in hydroxyl ions favored lectin better ionization, thereby promoting good binding forces between hemagglutinin and the erythrocyte membrane, which eventually led to the stability of hemagglutinating activity. This is close to what was reported for *D. opposita* tuber lectin, whose stability was manifested over a wide range of pH (pH 2-13), but lost 50% of its activity at pH 0-1.[43] Kaur et al.[38] also documented that the tuber lectin of *C. bicolor* exhibits hemagglutinating activity in a wide pH range of 2.5-12.5. DPH has a wider pH range stability than *D. mangenotiana* tuber lectin, which was reported by Akinyoola et al.[40] *D. mangenotiana* lectin activity was stable between pH 3 and 8, and lost approximately 12.5% of its activity at pH 9 and above.

While some lectins are known to require the presence of one or more metal ions, especially divalent cations, to exhibit their full hemagglutinating activity,[29,49,50] others do not require them because they still possess their optimal activities even in the absence of these metals. Using chelating agents like EDTA may lead to a decrease in or complete loss of hemagglutinating activity if the lectin requires a metal ion for its activity. In the chelating study conducted in this research, it was discovered that the hemagglutinating activity of DPH was not affected by the treatment of the metal chelating agent EDTA (10 mM and 50 mM). It might be an indication that DPH does not require the presence of metal ions in order to carry out its hemagglutinating activity or that these metal ions are too tightly bound to the hemagglutinin so much that EDTA could not remove them. This is comparable to the observations of Dhuna et al.,[37] Akinyoola et al.[40] and Pereira et al.[42] on tuber lectins from *A. utile, D. mangenotiana,* and *C. esculenta.* The authors documented the inability of EDTA to affect the hemagglutinating activity of lectins extracted from the tubers. Contrary to the above reports, Kabir et al.[45] reveals that the hemagglutinating activity of *N. nouchali* tuber lectin requires the presence of Ca^{2+}, Ba^{2+}, or Mg^{2+}.

A protein's tertiary structure is maintained by both covalent and non-covalent interactions, which include hydrogen bonds, hydrophobic bonds, ionic interactions, van der Waal's forces, and disulfide linkages. Introducing certain denaturing agents, such as a disulfide bond breaking agent (β-Mercaptoethanol) and chaotropic agents (guanidine-HCl and Urea) might give an insight into some structural properties of the protein. All denaturing agents used in this study reduced the hemagglutinating activity of hemagglutinin to different degrees, as shown in Figure 2C. The decrease in activity observed with the addition of β-Mercaptoethanol, might be an indication that the hemagglutinin contains a disulfide bond crucial to its hemagglutinating activity, which β-Mercaptoethanol reduces. The reduction in the hemagglutinating activity of hemagglutinin due to chaotropic agents (guanidine-HCl and urea) might indicate that hemagglutinin is a globular protein whose hydrogen bonds and hydrophobic interactions are disrupted by these agents.[51] The findings of the present study are consistent with those of other researchers on tuber lectins.[37,38,40,45,47]

During metabolic reactions, different free radicals are generated, but the most significant are those produced from oxygen, which are designated as ROS. Major biomolecules (DNA, lipids and proteins) can have their integrity damaged

by excess ROS, thereby causing an increase in the oxidative stress found in different human disease conditions.[14] In order to prevent these destructive effects of free radicals, the human body uses antioxidants, which can be endogenous (produced within the body) or exogenous (supplied to the body from foods and supplements), to neutralize them through different mechanisms, including donating electron(s) to reactive species, chelating metals, hydrogen donation, enzyme inhibition, and peroxide decomposition.[15,16]

The DPPH radical scavenging assay is one of the most widely used antioxidant assays for determining the antioxidant activity of natural samples/compounds. 2,2-diphenyl-1-picrylhydrazyl, which is the radical form of DPPH, accepts a proton from a donor to become the stable form 2,2-diphenyl-1-picrylhydrazine, which is accompanied by a change of color from deep violet to yellow.[52] This assay takes advantage of this color change that occurred only after the reduction of DPPH to monitor spectrophotometrically at 517 nm the radical scavenging capacity of a sample.[52] DPH was evaluated to have a dose-dependent free radical-scavenging activity (Figure 3A) with an IC_{50} of 0.727 ± 0.035 mg/mL, which was lower in activity than that of ascorbic acid, which had an IC_{50} of 0.022 ± 0.001 mg/mL.

A reducing power assay is typically used to assess the ability of a substance to donate an electron. DPH was observed to reduce Fe^{3+}/ferriccyanide complex to the Fe^{2+}/ferrouscyanide form, as seen through the change in color to blue measured at 593 nm. The FRAP assay showed that hemagglutinin contained 76 mg of AAE per gram of partially purified hemagglutinin.

The ability of DPH to chelate ferrous (a transition metallic ion) was determined using a metal chelating activity assay. Ferrous, like Cu^{+}, is a prooxidant known to be capable of generating hydroxyl radicals, very destructive ROS, from hydrogen peroxide through a reaction known as the Fenton reaction. A ferrozine-Fe^{2+} complex is formed when Fe^{2+} and ferrozine react together.[53] The addition of hemagglutinin disrupted complex formation, reducing the strength of the color that was measured at 562 nm. The reduction in color intensity was an indication that the hemagglutinin was able to chelate ferrous ions, thereby showing the potential to prevent the formation of dangerous hydroxyl free radicals. DPH was able to chelate iron in a dose-dependent manner (Figure 3B) with an IC_{50} of 0.583 ± 0.078 mg/mL, whereas the standard (EDTA) had an IC_{50} of 0.041 ± 0.006 mg/mL.

The ability of hemagglutinin to prevent lipid peroxidation was also investigated as a potential antioxidant. When lipid peroxidation, which is known to disrupt the cell membrane and lead to cell damage, occurs in the biological system, aldehydes such as malondialdehyde (MDA) are produced.[54,55] MDA is known to be very reactive, and it is typically used as an indicator of tissue damage. The colorless MDA can react with thiobarbituric acid to produce a pink adduct that can be measured at 532 nm spectrophotometrically. In the presence of an antioxidant, oxidation is inhibited, resulting in a reduction in absorbance. It was observed from the result of this assay that DPH, unlike the standard (BHT), was not found to possess anti-lipid peroxidation activity. Hemagglutinin could not inhibit lipid peroxidation. Lipid peroxidation levels increased as the amount of hemagglutinin increased from 0.2 to 1 mg/mL (Figure 3C). Unlike BHT, it prevents lipid peroxidation in a dose-related manner. The concentration of BHT increased with increasing percentage inhibition of lipid peroxidation.

Erythrocytes are known to have membranes containing abundant unsaturated fatty acids. The concentrations of oxygen they contain are very high; therefore, they are exposed to oxygen more than any other tissue in the body, making them more vulnerable to oxidative injury. They are therefore universal candidates for studying membrane hemolysis due to free radical attack. Exposure of erythrocytes to oxidative stress can result in protein damage, lipid peroxidation, and eventually hemolysis. Hydrogen peroxide is a well-known ROS that is highly stable and involved in signaling cascades and diffusion, making it to be considered an attractive oxidant model.[18,19,56] The antihemolytic assay gave biphasic results. At lower concentrations, hemagglutinin inhibited cell membrane hemolysis in the presence of an oxidative stress agent, as the concentration increased, this ability was aborted. The amount of hemoglobin released when H_2O_2 was introduced continued to increase as the hemagglutinin concentration increased (Figure 4). Although in the simple hemolytic assay conducted in the absence of a hemolytic agent, hemagglutinin provided a reasonable level of cell membrane protection with 4.2%-7.0% hemoglobin released in the concentration range of 0.2-1.0 mg/mL.

CONCLUSION

In conclusion, this study reported a novel hemagglutinin from the root tuber of *D. preussii*, which is a starch-binding lectin that showed physicochemical properties similar to those of other *Dioscorea* species lectins and also possessed antioxidant and cell membrane protective activities, which can be of great health benefit.

Ethics

Ethics Committee Approval: The study approved by the Obafemi Awolowo University Departmental Health Research Ethic Committee (approval number: OAUBCH/HREC/2024/005, date: l4.08.2024).

Informed Consent: Not required.

Authorship Contributions

Concept: O.O.O., Design: O.O.O., S.I.A., Data Collection or Processing: S.I.A., Analysis or Interpretation: O.O.O., S.I.A., Literature Search: O.O.O., S.I.A., Writing: O.O.O.

Conflict of Interest: No conflict of interest was declared by the authors.

Financial Disclosure: The authors declared that this study received no financial support.

REFERENCES

1. Suleiman MA, Agbo EB, Wasa, AA. Isolation and identification of microorganisms associated with yam rot of yam sold in Bauchi markets, Nigeria. *J Microbiol Res*. 2015;3:25-29.
2. Kumar S, Das G, Shin HS, Patra JK. Dioscorea spp. (A Wild Edible Tuber): A study on its ethnopharmacological potential and traditional use by the local people of similipal biosphere reserve, India. Front Pharmacol. 2017;8:52.
3. Chandrasekara A, Josheph Kumar T. Roots and tuber crops as functional foods: a review on phytochemical constituents and their potential health benefits. Int J Food Sci. 2016;2016:3631647.
4. Hailu AA, Addis G. The content and bioavailability of mineral nutrients of selected wild and traditional edible plants as affected by household preparation methods practiced by local community in Benishangul Gumuz Regional State, Ethiopia. Int J Food Sci. 2016;2016:7615853.
5. Kumar S, Das G, Shin HS, Patra JK. *Dioscorea* spp. (A Wild Edible Tuber): A study on its ethnopharmacological potential and traditional use by the local people of similipal biosphere reserve, India Front Pharmacol. 2017;8:52.
6. Kaur B, Khatun S, Suttee A. Current highlights on biochemical and pharmacological profile of *Dioscorea* alata: A review. Plant Arch. 2021; 21:552-559.
7. Adomėnienė A, Venskutonis PR. *Dioscorea* spp.: Comprehensive review of antioxidant properties and their relation to phytochemicals and health benefits. Molecules. 2022; 27:2530.
8. Tabopda TK, Mitaine-Offer AC, Tanaka C, Miyamoto T, Mirjolet JF, Duchamp O, Ngadjui BT, Lacaille-Dubois MA. Steroidal saponins from *Dioscorea preussii*. Fitoterapia. 2014;97:198-203.
9. Ali MS, Iqbal S, Lateef M, Joseph N. Preussiate, a new urease inhibitory chalcone from *Dioscorea preussii* Pax. Natural Product Research. 2023; 14:1-8.
10. Milne-Redhead E. Dioscoreaceae. In: crown agents for oversea governments and administrations, Polhill RM (eds.) Flora of tropical East Africa. Crown Agents, London, 1975, p. 26.
11. Burkill HM. The useful plants of Tropical West Africa. Royal Botanic Gardens. 1985, 254-257.
12. Bown D, Common plants of IITA. International Institute of Tropical Agriculture (IITA). Ibadan, Nigeria, 2012:64-65.
13. Lamidi M, DiGiorgio C, Delmas F, Favel A, Mve-Mba CE, Rondi ML, Ollivier E, Nze-Ekekang L, Balansard G. *In vitro* cytotoxic, antileishmanial and antifungal activities of ethnopharmacologically selected Gabonese plants. J Ethnopharmacol. 2005;102:185-190.
14. Phaniendra A, Jestadi DB, Periyasamy L. Free radicals: properties, sources, targets, and their implication in various diseases. Indian J Clin Biochem. 2015;30:11-26.
15. Bhattacharya S. Reactive oxygen species and cellular defense system. Free radicals in human health and disease. 2015:17-29.
16. Lobo V, Patil A, Phatak A, Chandra N. Free radicals, antioxidants and functional foods: Impact on human health. Pharmacogn Rev. 2010;4:118-126.
17. Vijayraja D, Jeyaprakash K. Phytochemical analysis, *in vitro* antioxidant and anti-haemolysis activity of *Turbinaria ornata* (turner) J. Agardh. *Int Adv Res J Sci Eng Technol. 2015;2*:45-49.
18. Asgary S, Naderi G, Askari N. Protective effect of flavonoids against red blood cell hemolysis by free radicals. Exp Clin Cardiol. 2005;10:88-90.
19. Alves MGDCF, Dore CMPG, Castro AJG, do Nascimento MS, Cruz AKM, Soriano EM, Benevides NMB, Leite EL. Antioxidant, cytotoxic and haemolytic effects of sulfated galactans from edible red alga *Hypnea musciformis*. J Appl Phycol. 2012;24:1217-1227.
20. Nur E, Biemond BJ, Otten HM, Brandjes DP, Schnog JJ; CURAMA Study Group. Oxidative stress in sickle cell disease; pathophysiology and potential implications for disease management. Am J Hematol. 2011;86:484-489.
21. Yang HL, Chen SC, Chang NW, Chang JM, Lee ML, Tsai PC, Fu HH, Kao WW, Chiang HC, Wang HH, Hseu YC. Protection from oxidative damage using Bidens pilosa extracts in normal human erythrocytes. Food Chem Toxicol. 2006;44:1513-1521.
22. Iuchi, Y. (2012). Anemia Caused by Oxidative Stress. InTech.
23. Hamid R, Masood A, Wani IH, Rafiq S. Lectins: Proteins with diverse applications. *J Appl Pharm Sci. 2013;*3:S93-S103.
24. Silva MC, de Paula CA, Ferreira JG, Paredes-Gamero EJ, Vaz AM, Sampaio MU, Correia MT, Oliva ML. *Bauhinia forficata* lectin (BfL) induces cell death and inhibits integrin-mediated adhesion on MCF7 human breast cancer cells. Biochim Biophys Acta. 2014;1840:2262-2271.
25. Santos AF, da Silva MDC, Napoleão TH, Paiva PMG, Correia MDS, Coelho LCBB. Lectins: Function, structure, biological properties and potential applications. *Curr Top Pept Protein* Res. 2014;15:41-62.
26. Dias Rde O, Machado Ldos S, Migliolo L, Franco OL. Insights into animal and plant lectins with antimicrobial activities. Molecules. 2015;20:519-541.
27. Loh SH, Park JY, Cho EH, Nah SY, Kang YS. Animal lectins: potential receptors for ginseng polysaccharides. J Ginseng Res. 2017;41:1-9.
28. Odekanyin OO, Kayode AS, Adewuyi JO. Purification, characterization and antioxidant potential of a novel lectin from *Pterocarpus soyauxii* taub seeds. Not Sci Biol. 2019;11:112-121.
29. Podder MK, Hossain MM, Kabir SR, Asaduzzaman AKM, Hasan I. Antimicrobial, antioxidant and antiproliferative activities of a galactose-binding seed lectin from *Manilkara zapota*. Heliyon. 2024;10:e24592.
30. Odekanyin OO, Kuku A. Characterization of galactose-specific lectin from the skin mucus of African catfish Clarias gariepinus. *Sci Res Essays. 2014;9*:869-879.
31. Lowry OH, Rosebrough NJ, Farr AL, Randall RJ. Protein measurement with the Folin phenol reagent. J Biol Chem. 1951;193:265-275.
32. Huh MK, Han MD. Inhibitory effect of hyaluronidase and DPPH radical scavening activity using extraction of *Equisetum arvens*. Eur J Adv Res Biol Life Sci. 2015;3:47-51.
33. Benzie IF, Strain JJ. Ferric reducing/antioxidant power assay: direct measure of total antioxidant activity of biological fluids and modified version for simultaneous measurement of total antioxidant power and ascorbic acid concentration. Methods Enzymol. 1999;299:15-27.
34. Masao H, Yang XW, Miyashiro H, Namba T. Inhibitory effects of monomeric and dimeric phenylpropanoids from mace on lipid peroxidation *in vivo* and *in vitro*. *Phytother Res. 1993;*7:395-401.
35. Singh N, Rajini PS. Free radical scavenging activity of an aqueous extract of potato peel. Food Chem. 2004;85:611-616.
36. Ebrahimzadeh MA, Nabavi SF, Nabavi SM, Eslami B. Antioxidant and antihaemolytic activities of *Mentha piperita*. Pharmacology Online. 2010;1:744-752.

37. Dhuna V, Dhuna K, Singh J, Saxena AK, Agrawal SK, Kamboj SS. Isolation, purification and characterization of an N-acetyl-D-lactosamine binding mitogenic and anti-proliferative lectin from tubers of a cobra lily Arisaema utile Schott. *Adv Biosci Biotechnol. 2010;*1:79-90.

38. Kaur K, Singh J, Kamboj SS, Saxena AK. A Lectin with Anti-proliferative, Mitogenic and anti-insect potential from the Tubers of Caladium bicolor Vent. *Asian Australas J Plant Sci Biotechnol. 2011;*5:1-9.

39. Sharma M, Hotpet V, Sindhura BR, Kamalanathan AS, Swamy BM, Inamdar SR. Purification, characterization and biological significance of mannose binding lectin from *Dioscorea bulbifera* bulbils. Int J Biol Macromol. 2017;102:1146-1155.

40. Akinyoola KA, Odekanyin OO, Kuku A, Sosan MB. Anti-insect potential of a lectin from the tuber, Dioscorea mangenotiana towards *Eldana saccharina* (Lepidoptera: Pyralidae). *Int J Agric Biotechnol Sustain* Dev. 2016;8:16-26.

41. Sharma M, Hedge P, Hiremath K, Reddy V, Kamalanathan AS, Swamy BM, Inamdar SR. Purification, characterization and fine sugar specificity of a N- Acetylgalactosamine specific lectin from *Adenia hondala*. Glycoconj J. 2018;35:511-523.

42. Pereira PR, Silva JT, Verícimo MA, Paschoalin VM, Teixeira GA. Crude extract from taro (*Colocasia esculenta*) as a natural source of bioactive proteins able to stimulate haematopoietic cells in two murine models. J Funct Foods. 2015;18:333-343.

43. Chan YS, Ng TB. A lectin with highly potent inhibitory activity toward breast cancer cells from edible tubers of Dioscorea opposita cv. nagaimo. PLoS One. 2013;8:e54212.

44. Kaur M, Singh K, Rup PJ, Saxena AK, Khan RH, Ashraf MT, Kamboj SS, Singh J. A tuber lectin from *Arisaema helleborifolium* Schott with anti-insect activity against melon fruit fly, *Bactrocera cucurbitae* (Coquillett) and anti-cancer effect on human cancer cell lines. Arch Biochem Biophys. 2006;445:156-165.

45. Kabir SR, Zubair MA, Nurujjaman M, Haque MA, Hasan I, Islam MF, Hossain MT, Hossain MA, Rakib MA, Alam MT, Shaha RK. Purification and characterization of a Ca^{2+}-dependent novel lectin from *Nymphaea nouchali* tuber with antiproliferative activities. Biosci Rep. 2011;3:465-475.

46. Singh AP, Saxena KD. Biological activity of purified *Momardica charantia* lectin. *Chem Sci Trans.* 2013;2:258-262.

47. Odekanyin OO, Akande OO. In-vitro Antioxidant and antibacterial potential of mannose/glucose-binding *Pterocarpus osun* craib. Seeds Lectin. *J Appl Life Sci*. 2019;22:1-14.

48. Adolph L, Lorenz RD. Enzyme diagnosis in diseases of the heart, liver and pancreas. John Wiley and Sons Inc. New York, USA, 1982.

49. Konozy EH, Bernardes ES, Rosa C, Faca V, Greene LJ, Ward RJ. Isolation, purification, and physicochemical characterization of a D-galactose-binding lectin from seeds of *Erythrina speciosa*. Arch Biochem Biophy. 2003; 410:222-9.

50. Sangha MK, Bala M, Sharma S. Purification, Characterization and bioefficacy of legume lectins against mustard aphid. Legume Research. 2024; 47:645-651.

51. Lehninger AL, Nelson DL, Cox MN. The three dimensional structure of proteins. In: Principles of Biochemistry, 5th ed. Macmillon Worth Publishers, New York, USA, 2001;159-202.

52. Ganaie AA, Mishra RP, Allaie AH. Isolation and purification of a lectin from seeds of a drought resistant plant, *Caragana gerardiana* and evaluation of its antimicrobial and antioxidant activities. *World J Pharm Res.* 2017;6:493-506.

53. Torres-Fuentes C, Alaiz M, Vioque J. Iron-chelating activity of chickpea protein hydrolysate peptides. Food Chem. 2012;134:1585-1588.

54. Qingming Y, Xianhui P, Weibao K, Hong Y, Yidan S, Li Z, Yanan Z, Yuling Y, Lan D, Guoan L. Antioxidant activities of malt extract from barley (*Hordeum vulgare* L.) toward various oxidative stress *in vitro* and *in vivo*. Food Chem. 2010;118:84-89.

55. Sandesh P, Velu V, Singh RP. Antioxidant activities of tamarind (*Tamarindus indica*) seed coat extract using *in vitro* and *in vivo* models. *J Food Sci Technol.* 2014;51:1965-1973.

56. Ugartondo V, Mitjans M, Torres JL, Vinardell MP. Biobased epicatechin conjugates protect erythrocytes and nontumoral cell lines from H_2O_2-induced oxidative stress. J Agric Food Chem. 2009;57:4459-4465.

Turk J Pharm Sci 2024;21(4):367-375
DOI: 10.4274/tjps.galenos.2023.98572

ORIGINAL ARTICLE

Analysis of Anticancer Taxanes in Turkish Hazelnut (*Corylus avellana* L.) Genotypes Using High-Performance Liquid Chromatography

Gülbahar Zehra KUTLUTÜRK[1], Elif Sine DÜVENCİ[2], Bora KARAGÜL[2], Baki YAMAN[1], Halil İbrahim UĞRAŞ[2], Ümit SERDAR[3], Şule ARI[1]*

[1]İstanbul University Faculty of Science, Department of Molecular Biology and Genetics, İstanbul, Türkiye
[2]Düzce University Faculty of Science and Arts, Department of Chemistry, Düzce, Türkiye
[3]Ondokuz Mayıs University Faculty of Agriculture, Department of Horticulture, Samsun, Türkiye

ABSTRACT

Objectives: This study aimed to investigate the anticancer taxane profiles of edible and non-edible parts of seven Turkish hazelnut (*Corylus avellana* L.) genotypes. Hazelnut is one of the healthy foods rich in nutrients and antioxidants. Its regular consumption is associated with a reduced risk of coronary heart disease and cancer. Hazelnut has been described as a plant source that produces taxanes which are widely used in many cancers. Türkiye is a homeland of hazelnut culture and has its own cultivars. Investigation of anticancer taxane profiles in different parts of Turkish hazelnut genotypes is important to show the potential and value of this plant from the perspective of the pharmaceutical and food industries.

Materials and Methods: In this study, green leafy covers (GLCs) and hard shells (HSs) (non-edible parts), skinless kernels (SKs), brown-skins (BSs), and brown-skinned kernels (BSKs) (edible parts) of Çakıldak, Sivri, Tombul, Palaz, and Kalınkara as standard and Ham and Sivri Yağlı as local genotypes were used. The five parts of each genotype were ground to powder and eliminated to a size of less than 80 mesh. Each part was extracted using hexane and methanol for 10-deacetylbaccatin III (10-DAB III), baccatin III (BAC III), cephalomannine, and paclitaxel analyses in three replicates. Samples and standards were analyzed by acetonitrile: water gradient method on NOVA Spher 100 Phenyl-Hexyl C18 column inhigh-performance liquid chromatography reverse phase system with 228 nm ultraviolet detector and 1.0 mL/min flow rate. Microsoft Office Excel, 2016, and analysis of variance Jamovi Version 2.3 were used for statistical and data analysis, consecutively.

Results: Hazelnut parts differed to a very high degree from each other in terms of the highest amount of 10- DAB III (Ham HSs, 9,15 µg/g), BAC III (Kalınkara BSs, 7.24 µg/g), cephalomannine (Sivri Yağlı BSs, 6.37 µg/g), and paclitaxel (Ham BSKs, 4.36 µg/g) they contained. While HSs, BSKs, and BSs were rich in taxanes in all of the analyzed genotypes, SKs, and GLCs remain limited for anticancer taxanes.

Conclusion: This is the first report that revealed the differences in taxane contents of Turkish hazelnuts including previously untested standard and local genotypes and their parts. Significant differences between genotype and hazelnut parts are expected to highlight the health benefits of consuming raw Turkish hazelnut with BSs and their possible use as a functional food. These results add more information to elucidate the bioactive potential of Turkish hazelnuts and their by-products and provide a promising resource for the food and pharmaceutical industry with an anticancer perspective.

Keywords: *Corylus avellana*, taxanes, anticancer, functional foods, by-products

INTRODUCTION

Among nut species, Turkish hazelnut (*Corylus avellana* L.), is the most valuable tree nut crop worldwide.[1] Hazelnut species exhibit distribution mainly in Türkiye, Italy, Spain, Portugal, France, and some parts of the USA.[2] For the cultivation of high-quality hazelnut varieties, Türkiye has suitable growing conditions.[3] With 80% of cultivated hazelnut area in the world, Turkey is the leading producer and alone meets about 69% of global hazelnut production (776 thousand tonnes).[4]

*Correspondence: sari@istanbul.edu.tr, Phone: +90 532 303 41 90, ORCID-ID: orcid.org/0000-0002-7386-4657
Received: 26.08.2023, Accepted: 23.12.2023

Hazelnut fruit is divided into three parts; these are green leafy cover (GLC), hard shell (HS), and hazelnut kernel which can be consumed raw [with brown-skin (BS)] or roasted (without BS). In addition to their role as a popular snack both in Türkiye and worldwide, approximately 90% of hazelnuts are utilized as an ingredient in a variety of processed foods, especially in confectionery and bakery products.[5] The kernel, a main product of hazelnuts, plays a special role in human nutrition and health due to its particular composition.[6-8] The distinctive nutritional and sensory characteristics of hazelnuts render them an incomparable and optimal ingredient for food products. However, the kernel constitutes less than 50% of the total nut weight, and substantial by-products (GLC, HS, and BS) are removed during harvesting and processing.[1,9] Among these by-products, none has nearly significant commercial value. The HS, a majority of the by-products, is mainly used as a low-value heating source, and the GLCs are rarely used as organic fertilizers.[3,5,10] The use of by-products as readily available in diverse bioactive compounds and functional food ingredients could become a valuable source.[9,10] Therefore, in recent years, the number of studies that focused on investigating the utilization of hazelnut by-products has increased.[10-12] Studies on HSs and BSs mainly investigate the extraction, characterization, and identification of substantial bioactive molecules such as phenolic compounds, dietary fiber, cellulosic compounds, activated carbon, and pigments.[5,13-15] In addition, researchers found that GLC extracts contained bioactive compounds that have high antioxidant, antibacterial, and free radical scavenger properties.[3,16] It has been shown that hazelnut is also a source of anti-cancer taxanes.[17-21]

Paclitaxel, also known as Taxol® is a representative of a class of diterpenes taxanes, which are widely used as a chemotherapeutic agent to stabilize microtubules in many types of cancer. Since the discovery of its antitumoral activity, Taxol® has been approved as a chemotherapeutic drug for the treatment of ovarian, breast, lung, bladder, prostate, melanoma, esophageal, and other types of solid tumors.[22] It has also been used to treat acquired immunodeficiency syndrome-related Kaposi sarcoma.[23] Taxol® is originally extracted in low yield from the bark of *Taxus brevifolia*. Chemical and partial synthesis of Taxol® from its precursors, 10-deacetylbaccatin III (10-DAB III), baccatin III (BAC III), and cephalomannine are also very expensive and time-consuming.[19] Although it was generally considered a particular metabolite of *Taxus* spp., paclitaxel extraction was carried out from hazelnuts.[17] For more than two decades hazelnut and its by-products have been studied from the aspect of anticancer taxane contents.[17] In addition to paclitaxel, 10-DAB III, BAC III, and cephalomannine were isolated from hazelnut HSs, GLCs, and leaves.[18-20,24] As an alternative to taxol, the synthetic analog, taxotere™ (generic name Docetaxel), was acquired by semi-synthesis from BAC III and 10-DAB III, two taxol precursor molecules. The American Food and Drug Administration authorized the use of Paclitaxel and Docetaxel for treating ovarian and breast cancers.[25] On the other hand, the natural congener of paclitaxel, cephalomannine has shown anti-tumor activity in several different cell lines.[26] The cytotoxic effects of cephalomannine were first demonstrated in human glioblastoma cells.[27] Later on, Zhang et al.[28] demonstrated that cephalomannine significantly attenuates hepatocellular carcinoma progression *in vitro* and *in vivo* and bone metastasis in prostate cancer *in vivo*.[29] Therefore, cephalomannine has recently been evaluated as an anti-cancer drug candidate.[28-32]

Among Turkish hazelnut (*C. avellana* L.) genotypes (Tombul, Palaz, Çakıldak, Sivri, Kalınkara, Ham, and Sivri Yağlı) used in this study, Tombul, Palaz and Çakıldak categorized as standard and are most grown in Türkiye. However, the cultivation of Tombul and Palaz decreased because they start to leaf early in the spring, while the cultivation of the Çakıldak has increased because it leaves late and is, therefore, more resistant to spring frost. Sivri and Kalınkara, which are standard genotypes, are generally preferred as pollinators due to their lower nut quality. Local genotypes, Ham and Sivri Yağlı, are available only as pollinators in the orchard. Within the 18 cultivars grown in Türkiye, the Tombul is considered the first-quality hazelnut due to its high oil content, distinctive taste, and aroma, and easily and quickly removable BS during roasting.[33] Since it, beings, the most consumed cultivar both nationally and internationally, Tombul hazelnut leaves, HSs and GLCs have been studied for their taxane contents.[6,19] In addition to Tombul, the present work is aimed to investigate the taxane content of other hazels grown in Türkiye, in terms of genotype and hazelnut parts for the first time. Thus, taxane contents of 7 different hazelnuts (Çakıldak, Sivri, Tombul, Palaz, and Kalınkara as standard and Ham, Sivri Yağlı local genotypes) parts [GLCs, HSs, skinless kernels (SKs), BSs, and BSKs] were analyzed by high-performance liquid chromatography (HPLC). Results were discussed from the perspective of functional foods and promising resources for the pharmaceutical industry.

MATERIALS AND METHODS

Plant materials and chemicals

In this study, GLCs and HSs (non-edible parts), SKs, BSs, and BSKs (edible parts) of Çakıldak, Sivri, Tombul, Palaz, and Kalınkara as standard and Ham, and Sivri Yağlı as local hazelnut (*C. avellana L.)* genotypes were used. Tombul, Palaz, and Çakıldak were selected as they were the most grown in Türkiye. The others are preferred as pollinators, but they have not yet been studied. Hazelnut samples were harvested in August 2017 in the Fatsa district of Ordu province (40°59'27.9"N 37°35'01.6"E), Türkiye.The samples were kept in cloth bags at room temperature until analyses were carried out.

HPLC grade of acetonitrile (› 99.93%), methanol (99.99%), and hexane for organic trace analysis UniSolv® were obtained from Merck (Darmstadt, Germany). All the standard reference compounds; 10-DAB III (› 95.0%), BAC III (› 95.0%), cephalomannine (› 97.0%), and paclitaxel (› 95.0%) were acquired from Sigma-Aldrich (Germany).

Taxane extraction

Oil and methanol extractions were adapted from Oguzkan et al.[21] and performed as follows. Five parts (GLCs, HSs, BSKs, SKs, and BSs,) of 7 different Turkish hazelnuts were used as

experimental material. HSs, BSKs SKs, and BSs were separately grounded by the Sinbo SCM 2934 coffee grinder while GLCs were grounded by the Loyka LKD 100 Sample Grinder Mill. GLCs, HSs, BSKs, and SKs were ground to a size of 10 g while BSs were 0.12 g. Then these parts were defatted with hexane in volumetric beakers at room temperature for 1 hour using a magnetic stirrer with a heater (25 °C, 400 rpm). Grounded GLCs, HSs, BSKs, and SKs were defatted with 20.0 mL hexane (1:20, *w/v*). Since the amount of ground BSs was small, the oil was removed with 10 mL of hexane (1:10, *w/v*). Solid-liquid extraction was performed by mixing the grounded samples with 99% methanol on a magnetic stirrer with a heater (25 °C, 400 rpm). The defatted GLCs, HSs, BSKs, and SKs of hazelnuts were extracted by 100.0 mL methanol (1:10, *w/v*) while the defatted BSs were extracted by 10.0 mL methanol (1:10, *w/v*) at room temperature for 24 hours. The resulting slurries were filtered through filter papers into the Erlenmeyer flasks. The solvent was then removed under vacuum at 40 °C at 300 rpm using a rotary evaporator (Heidolph™ Hei-Vap™). The residues were dissolved with 3.0 mL (BSs with 2.0 mL) methanol, and samples were stored at -20 °C in a freezer between analyses.

Sample preparation and HPLC-photo diode array (PDA) analysis of taxane diterpenoid

In this study, 10-DAB-III, BAC-III, cephalomannine, and paclitaxel, were used as standards for taxane analysis. All of the samples were filtered and brought to the condition to be analyzed by HPLC. Analyses were performed on Shimadzu CBM-20A/CBM-20A lite brand HPLC. OVA Spher 100 Phenyl-Hexyl C18 column (4.6 mm x 250 mm, 5 µm particle size) was used as a column. Mobile phase acetonitrile:water gradient system was adjusted. PDA was used as a detector.

Identification of taxane diterpenoids in hazelnut extracts was performed according to Oguzkan et al.[21] The samples were filtered through a 0.20 µm membrane filter into the new amber glass vials (1.5 mL) before being measured in HPLC. The resultant supernatants were pooled and analyzed. The taxane contents in the extracts of hazelnut were quantified by HPLC reverse phase (RP) system (the Shimadzu CBM-20A/CBM-20A lite) having NOVA Spher 100 Phenyl-Hexyl C18 column (4.6 mm x 250 mm, 5 µm particle size). 10-DAB III, BAC III, cephalomannine, and paclitaxel in hazelnut extracts were eluted with a linear gradient of acetonitrile and water (25:75-15 minute, 75-25-40 minute) at a flow rate of 1.0 mL/minute for 55 minute. The gradient method was preferred to separate impurities from plant-derived products and proportional changes were made in the gradient method during the analysis period. Acetonitrile and the water phase were preferred because the RP column is very effective in the separation of impurities. Depending on the polarity of the mobile phase, sharp and clear peaks of the sought compounds were obtained with the gradient method.

The injection volume was 20.0 µL and peak values were detected at 228 nm using a ultraviolet detector (PDA, Germany). Samples were injected into HPLC at 20.0 µL. Identification of taxanes was carried out by comparison of keeping times with standards. All analysis was performed in triplicate.

Calibration curves for 10-DAB III, BAC III, cephalomannine, and paclitaxel standards were prepared at different concentrations (50 mg/L; 25 mg/L; 10 mg/L; 5 mg/L; 2,5 mg/L and 1 mg/L). Calibration curves were prepared by plotting the peak area against the different standard concentrations. In the study for each hazelnut fraction, the standard solutions were first read and the standard curve was drawn. These different concentrations were analyzed by HPLC and retention times of 10-DAB III, BAC III, cephalomannine, and paclitaxel were determined. Chromatograms were monitored at 11-12 minute for 10-DAB III,16-17 min for BAC III, 25-26 minute for cephalomannine, and 26-27 minute for paclitaxel and were given in Figure 1.[33]

All environmental and personal safety precautions were taken during the experimental and analysis procedures. Protective equipment such as gloves, goggles, and aprons was used during these procedures. In the evaporation process, the pressure setting was controlled from the barometer.

Statistical analysis

All the tests were performed with three replicates. The results for each taxane of seven genotypes and their parts are presented as the mean ± standard deviation (SD, n= 3) by Microsoft Office Excel, 2016 Version16.71. Data were analyzed by One-Way analysis of variance (ANOVA) by using Jamovi Version 2.3. Five parts from seven hazelnuts were performed for each taxane. Statistical significance in mean taxane concentrations between genotypes and their parts was evaluated by One-Way (ANOVA) followed by Tukey's and Bonferroni correction correction as a post hoc-test for multiple comparisons in our analysis. These helped ensure the reliability of our statistical inferences. A p value less than 0.01 was considered statistically significant. The graphs were generated by Microsoft Office Excel, 2016 Version16.71. The bars of graphics were calculated as ± SD of the mean for each and total taxanes.

RESULTS

Herewith we report anticancer taxane contents of 5 standards and 2 local Turkish hazelnut genotypes both in their non-edible and edible parts for the first time. In addition to the total taxane contents of hazelnut genotypes (Figure 2), 10-DAB III, BAC III, cephalomannine, and paclitaxel contents are given separately for each hazelnut parts (GLC, HS, SK, BS, and BSK) in Figure

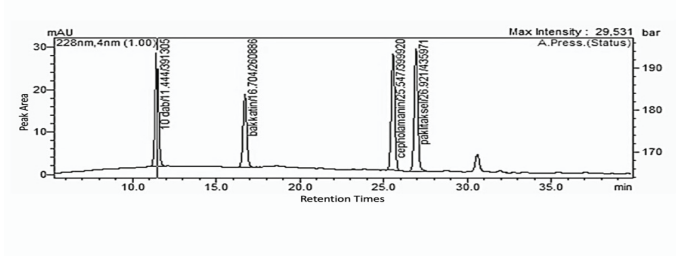

Figure 1. The chromatogram shows the peak areas and retention times of the taxane. 10-DAB III, 11,444 minute and peak area 391,305; BAC-III, 16,704 minute and peak area 260,886; cephalomannine, 25,547 minute and peak area 399,920; Paclitaxel, 26,921 minute and peak area 435,971

10-DAB III: 10-deacetylbaccatin III, BAC-III: Baccatin III

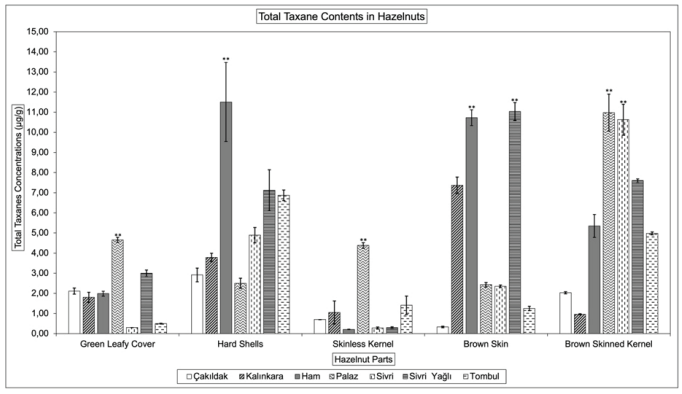

Figure 2. Total taxane contents in GLC, HS, SK, BS, and BSK of seven hazelnut genotypes. Statistical significance between hazelnut genotypes and their parts was determined using One-Way analysis of variance. $^{**}p < 0.01$, demonstrating significant differences in total taxane concentrations among hazelnut genotypes within each region. Bars represent the mean ± SD

GLC: Green leafy cover, HS: Hard shell, SK: Skinless kernel, BS: Brown-skin, BSK: Brown-skinned kernel, SD: Standard deviation

3-7. Concentrations of 10-DAB III, BAC III, cephalomannine, paclitaxel, and total taxane from GLC, HS, SK, BS, and BSK of seven hazelnut genotypes (Tombul, Palaz, Çakıldak, Sivri, Kalınkara, Ham and Sivri Yağlı) are given in Table 1.

Total taxane patterns in hazelnut parts of different genotypes

The distribution of total taxanes in hazelnut parts (GLC, HS, SK, BS, and BSK) for seven genotypes is given in Figure 2. Although total taxane profiles of hazelnut genotypes were found to be in a wide range (0.21 and 11.51 µg/g) in tested materials, average taxane contents of the hazelnut parts showed the following trend: BSK (6.08 µg/g) › HS (5.66 µg/g) › BS (5.07 µg/g) › GLC (2.05 µg/g) › SK (1.19 µg/g). Genotypes were ranked according to their total taxane contents in all parts as follows; Ham (29.78 µg/g), Sivri Yağlı (29.06 µg/g), Palaz (24.95 µg/g), Sivri (18.45 µg/g), Tombul (15.01 µg/g), Kalınkara (14.96 µg/g), Çakıldak (8.09 µg/g).

10-DAB III, BAC III, cephalomannine, paclitaxel, and total taxane content of green hazelnut leafy cover

10-DAB III, BAC III, cephalomannine, paclitaxel, and total taxane contents in the GLC of seven genotypes are given in Figure 3. HPLC results showed that extracts of GLCs mainly contained paclitaxel. The total amount of paclitaxel (7.46 µg/g) comprised 52% of total GLC's taxanes. Although this compound is substantially represented by Palaz, paclitaxel is found in nearly all tested genotypes. 10-DAB III was the second most abundant taxane and comprised 23% of total GLC's taxanes. On the other hand, cephalomannine is not detected and/or in small quantities for GLC extracts.

10-DAB III, BAC III, cephalomannine, paclitaxel, and total taxane content of hard HS

10-DAB III, BAC III, cephalomannine, paclitaxel, and total taxane contents in the HSs of the seven genotypes are illustrated in Figure 4. In the results obtained, total 10-DAB III (31.06 µg/g), an important intermediate for Taxol®, comprised 78% of total HS's taxane. BAC III was the second most abundant taxane and comprised 14% of total HS's taxane. The HSs of the seven genotypes nearly contained all taxane in their extracts and were the most advantageous parts for these molecules after BSKs.

10-DAB III, BAC III, cephalomannine, paclitaxel, and total taxane contents of hazelnut SK

10-DAB III, BAC III, cephalomannine, paclitaxel, and total taxane contents in skinless hazelnut kernels of the seven genotypes are presented in Figure 5. The HPLC results showed that the extracts of SKs mainly contained BAC III. The total amount of BAC III (5.67 µg/g) comprised 68% of total SK's taxane. Although this compound is substantially represented by Palaz, BAC III was found in all tested genotypes. Cephalomannine was the second most abundant taxane, constituting 31% of all SK taxanes. On the other hand, 10-DAB III and paclitaxel are not detected or are present in small quantities in the SK extracts.

10-DAB III, BAC III, cephalomannine, paclitaxel, and total taxane contents of hazelnut BS

10-DAB III, BAC III, cephalomannine, paclitaxel, and total taxane contents in kernel's BSs of seven genotypes are illustrated in Figure 6. In the results obtained, the taxane compound distribution of BS extracts showed parallelism with SKs. BAC III and cephalomannine contents comprised 68% and 32% of total BSs taxanes, respectively. 10-DAB III and paclitaxel were not detected in BS extracts for any tested hazelnut genotypes. However, BS extracts accumulated ~4-fold higher content than SKs for both BAC III and cephalomannine.

10-DAB III, BAC III, cephalomannine, paclitaxel, and total taxane content of hazelnut BSKs

10-DAB III, BAC III, cephalomannine, paclitaxel, and total taxane contents in BSKs of seven varieties are given in Figure 7. Our results show that BSK extracts showed significant differences from BS and SK extracts in distribution and quantity for taxane compounds. The BSK extracts represented the hazelnut part with the highest abundance of taxanes. While, BS and SK accumulated only BAC III and cephalomannine, nearly all taxanes were identified in BSK extracts. According to our results, extracts of BSK mainly contained cephalomannine (42%). BAC III, the main compound of BS and SK, was the second most abundant molecule in BSKs (32%). Despite 10-DAB III and paclitaxel molecules were not identified in both SK and BS, BSK extracts contained these taxanes at 13% and 14%, respectively.

DISCUSSION

Hazelnut kernels are a nutritious and health-promoting food because of their high content of sanitary lipids, vitamins, essential amino acids, dietary fibers, and specialized phytochemicals that own respectable biological activities. The health benefits of hazelnuts have taken a new significance after they were determined to produce anticancer taxanes.[1,34-36] Although antioxidant and phenolic compounds mainly represent phytochemicals in kernels, findings of paclitaxel and other taxanes also in them, generate a distinguished aspect of health-

Table 1. Concentrations of 10-DAB III, BAC III, cephalomannine, paclitaxel, and total taxane from GLC, HS, SK, BS, and BSK of seven hazelnut genotypes (Tombul, Palaz, Çakıldak, Sivri, Kalınkara, Ham and Sivri Yağlı)

H. parts	H. varieties	10-deacetyl BACIII (µg/g)	BAC III (µg/g)	Cephalomannine (µg/g)	Paclitaxel (µg/g)	Total (µg/g)
GLC	Çakıldak	ND	2.12 ± 0.15	ND	ND	2.12 ± 0.15
	Kalınkara	ND	ND	ND	1.80 ± 0.25	1.80 ± 0.25
	Ham	ND	ND	ND	1.99 ± 0.12	1.99 ± 0.12
	Palaz	1.29 ± 0.08	ND	ND	3.37 ±0.20	4.66 ± 0.13
	Sivri	ND	ND	ND	0.30 ± 0.00	0.30 ± 0.00
	Sivri Yağlı	1.96 ± 0.11	ND	1.04 ± 0.05	ND	3.00 ± 0.16
	Tombul	ND	0.35 ± 0.02	0.14 ± 0.01	ND	0.50 ± 0.02
HS	Çakıldak	2.26 ± 0.38	0.25 ± 0.05	0.40 ± 0.02	ND	2.91 ± 0.34
	Kalınkara	2.73 ± 0.27	0.54 ± 0.01	0.50 ± 0.05	0.02 ± 0.02	3.78 ± 0.21
	Ham	9.15 ± 1.98	1.31 ± 0.14	1.05 ± 0.03	ND	11.51 ± 1.96
	Palaz	2.13 ± 0.03	ND	0.33 ± 0.21	0.04 ± 0.00	2.50 ± 0.25
	Sivri	4.75 ± 0.37	ND	0.11 ± 0.02	0.03 ± 0.03	4.89 ± 0.38
	Sivri Yağlı	4.27 ± 0.32	2.47 ± 0.84	0.37 ± 0.21	0.02 ± 0.01	7.12 ± 1.02
	Tombul	5.77 ± 0.12	1.02 ± 0.15	0.07 ± 0.03	0.02 ± 0.00	6.87 ± 0.26
BS	Çakıldak	ND	ND	0.33 ± 0.04	ND	0.33 ± 0.04
	Kalınkara	ND	7.24 ± 0.43	0.13 ± 0.01	ND	7.37 ± 0.41
	Ham	ND	6.21 ± 0.38	4.52 ± 0.02	ND	10.73 ± 0.39
	Palaz	ND	2.43 ± 0.11	ND	ND	2.43 ± 0.11
	Sivri	ND	2.35 ± 0.06	ND	ND	2.35 ± 0.06
	Sivri Yağlı	ND	4.67 ± 0.41	6.37 ± 0.05	ND	11.04 ± 0.44
	Tombul	ND	1.25 ± 0.11	ND	ND	1.25 ± 0.11
SK	Çakıldak	ND	0.38 ± 0.07	0.32 ± 0.06	0.00	0.70 ± 0.03
	Kalınkara	ND	0.31 ± 0.00	0.73 ± 0.58	0.05 ± 0.00	1.05 ± 0.57
	Ham	ND	0.09 ± 0.00	0.13 ± 0.00	ND	0.21 ± 0.01
	Palaz	ND	3.71 ± 0.09	0.67 ± 0.06	ND	4.38 ± 0.14
	Sivri	ND	0.18 ± 0.00	0.10 ± 0.05	ND	0.28 ± 0.05
	Sivri Yağlı	ND	0.17 ± 0.02	0.11 ± 0.02	0.02 ± 0.00	0.30 ± 0.04
	Tombul	ND	0.83 ± 0.04	0.50 ± 0.40	0.07 ± 0.03	1.41 ± 0.46
BSK	Çakıldak	1.36 ± 0.08	ND	0.67 ± 0.06	ND	2.03 ± 0.05
	Kalınkara	0.24 ± 0.06	ND	0.72 ± 0.05	ND	0.96 ± 0.02
	Ham	0.99 ± 0.47	ND	ND	4.36 ± 0.16	5.35 ± 0.57
	Palaz	0.17 ± 0.02	5.78 ± 1.48	4.74 ± 0.78	0.29 ± 0.03	10.98 ± 0.92
	Sivri	0.42 ± 0.09	4.45 ± 0.72	5.14 ± 0.16	0.62 ± 0.06	10.63 ± 0.77
	Sivri Yağlı	2.26 ± 0.15	ND	5.34 ± 0.21	ND	7.68 ± 0.08
	Tombul	ND	3.22 ± 0.02	1.16 ± 0.02	0.60 ± 0.01	4.98 ± 0.07

All concentrations of taxane are presented as mean ± SD (µg/g dry weight)
10-DAB III: 10-deacetylbaccatin III, BAC-III: Baccatin III, GLC: Green leafy cover, HS: Hard shell, SK: Skinless kernel, BS: Brown-skin, BSK: Brown-skinned kernel, SD: Standard deviation, ND: Not peak was detected, H.: Hazelnut

promoting properties of this nut.[1,17-19,37] Together with kernel bioactivity studies, by-products (GLC, HSs, and BS) have been forwarded to significant research areas for phytochemicals.[35,36] The health benefits of hazelnuts expanded after they were determined to produce anticancer taxanes. Previous works concentrated on the recovery of paclitaxel from by-products of a few hazelnuts (Tombul, Ventimiglia, Genova, Alessandria, Gasaway), and little is known about whether non-edible and

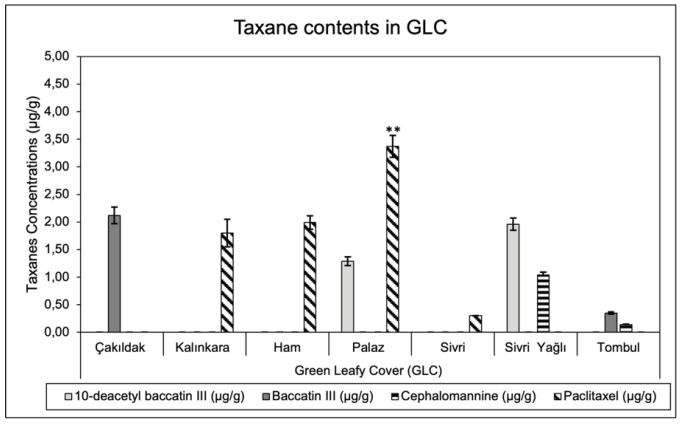

Figure 3. Concentrations of 10-DAB III, BAC III, cephalomannine, and paclitaxel from the GLC. Statistical significance between hazelnut genotypes was determined using a One-Way analysis of variance. **Indicates a p < value 0.01, demonstrating significant differences in the highest taxane concentration among the hazelnut genotypes and their parts. Bars represent the mean ± SD

10-DAB III: 10-deacetylbaccatin III, BAC-III: Baccatin III, GLC: Green leafy cover, SD: Standard deviation

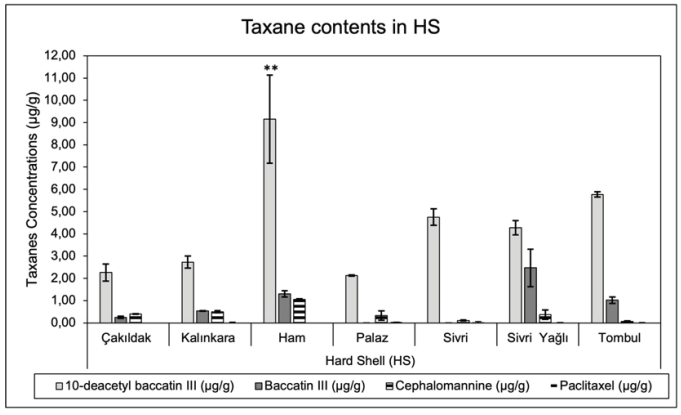

Figure 4. Concentrations of 10-DAB III, BAC III, cephalomannine, and paclitaxel from HS. Statistical significance between hazelnut genotypes was determined using a One-Way analysis of variance. **Indicates a p < 0.01, demonstrating significant differences in the highest taxane concentration among the hazelnut genotypes and their parts. Bars represent the mean ± SD

10-DAB III: 10-deacetylbaccatin III, BAC-III: Baccatin III, HS: Hard shell, SD: Standard deviation

edible parts contained taxanes in Turkish cultivars.[17-19,37]

This is the first report to analyze seven Turkish genotypes separately in terms of paclitaxel and its derivatives and evidenced taxane compounds reveal a high variability depending on the non-edible and edible parts of genotypes. This variability was particularly noticeable in terms of the total taxane content of the genotypes. While Palaz was detected as the most advantageous genotype for GLC (2.3 times higher than average), SK (3.7 times higher than average), and BSK (1.8 times higher than average) extracts, Ham (2 times higher than average) and Sivri Yağlı (2.2 times higher than average) had highest total taxanes of their HSs and BSs, respectively. According to the highest taxane contents, parts of Sivri, Kalınkara, and Çakıldak were ranked as BSK, BS, and HS. Our analysis showed Ham's HS has the

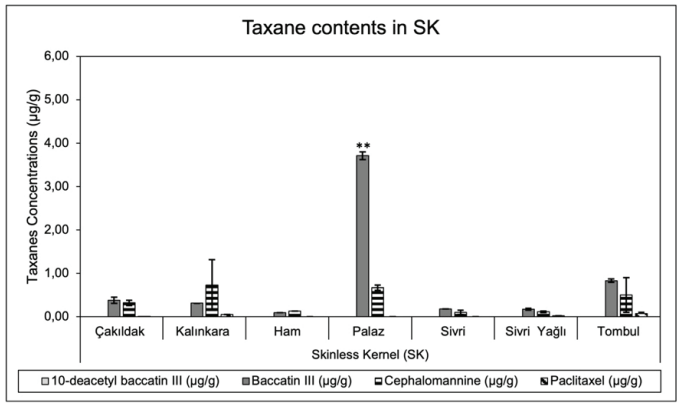

Figure 5. Concentrations of 10-DAB III, BAC III, cephalomannine, and paclitaxel from the SK. Statistical significance between hazelnut genotypes was determined using a One-Way analysis of variance. **Indicates a p < 0.01, demonstrating significant differences in the highest taxane concentration among the hazelnut genotypes and their parts. Bars represent the mean ± SD

10-DAB III: 10-deacetylbaccatin III, BAC-III: Baccatin III, SK: Skinless kernel, SD: Standard deviation

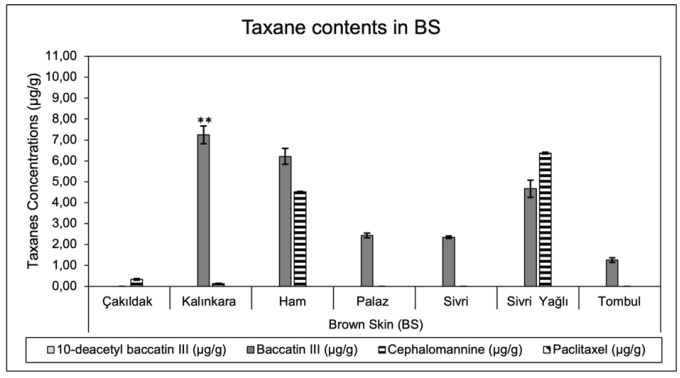

Figure 6. Concentrations of 10-DAB III, BAC III, cephalomannine, and paclitaxel from BS. Statistical significance between hazelnut genotypes was determined using a One-Way analysis of variance. **Indicates a p < 0.01, demonstrating significant differences in the highest taxane concentration among the hazelnut genotypes and their parts. Bars represent the mean ± SD

10-DAB III: 10-deacetylbaccatin III, BAC-III: Baccatin III, BS: Brown-skin, SD: Standard deviation

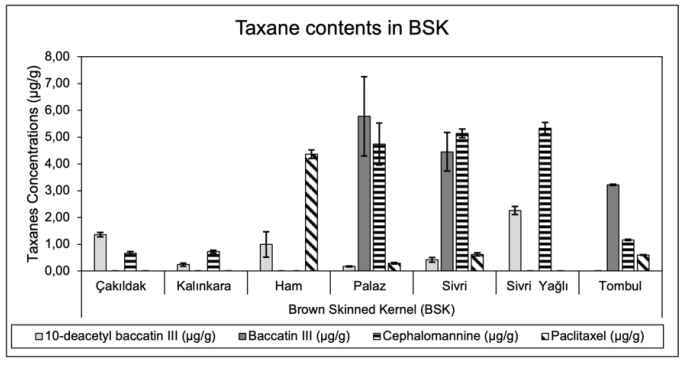

Figure 7. Concentrations of 10-DAB III, BAC III, cephalomannine, and paclitaxel from BSK. Statistical significance between hazelnut genotypes was determined using One-Way analysis of variance. Bars represent the mean ± SD

10-DAB III: 10-deacetylbaccatin III, BAC-III: Baccatin III, BSK: Brown-skinned kernel, SD: Standard deviation

highest total taxane content in all tested parts of genotypes. While the total taxane amount was significantly high in GLC and SK parts of Palaz, there was no difference when compared with Sivri for BSK. HSs of Ham had the highest total taxane content, however, in BS's there was no significant difference between with Sivri Yağlı. Moreover, Tombul, the most known hazelnut genotype in paclitaxel recovery studies, had relatively lower amounts of these compounds (Figure 2).

Since Hoffman et al.[17] discovered paclitaxel in *C. avellana*, HSs have become a prominent material for the investigation of paclitaxel and other taxanes. Hoffman and Shahidi[19] showed HSs contain more taxanes than GLC extracts. Oguzkan et al.[21] analyzed a mix of HS samples collected from different regions of Türkiye and they identified paclitaxel and its precursor BAC III. In the same study, GLCs were also investigated, and BAC III was to be the main taxane. Our analysis indicated that the highest level of total 10-DAB III content among all tested parts was found in the HSs of the hazelnuts. According to our data, GLC extracts contain the highest paclitaxel level in all tested parts. Furthermore, our analysis identifies Palaz as the richest genotype in paclitaxel content among the others. Interestingly, the GLC extracts from the Tombul are similar to the findings of a previous study conducted by Hoffman and Shahidi[19], which proposed that the GLC included only BAC III. These findings highlight the differences in the amount of paclitaxel present in various genotypes and their parts. Taxane contents are affected by multiple variables such as extraction methods, genotype, and growing conditions.[37] Although, these by-products are readily available natural resources for paclitaxel and its derivatives, because of the production of HSs and GLCs in thousands of tons each year.

Despite the kernels not being analyzed in detail, the current study indicated the presence of taxanes in the skinless kernel, its BS, and BSKs of Turkish hazelnut genotypes.[19,37] Among the analyzed hazelnut extracts, the BSK was the most advantageous part for the synthesis of taxane compounds. Together with the diversity present in the genotypes, BSKs contain almost all taxane compounds, and the second most abundant paclitaxel, which is mainly represented by the Ham genotype. Previous research indicated that BSK extracts were unfavorable for Tombul and there is not any knowledge of Ham for the recovery of taxane compounds. The SK extracts were found to have relatively lower taxane production compared to other parts.[19] Previous research emphasized that SK has a general trend showing a lower bioactive potential that is mostly contributed by phenolic compounds.[1] According to our results, skins of the kernels were discovered as the most accumulative part of the kernel for BAC III, an essential precursor compound for the semi-synthesis of Taxol® and a potent anticancer agent cephalomannine. This finding has significant implications for the fields of phytochemical and pharmaceutical research of hazelnuts. It highlights the significance that hazelnut skins are to the bioavailability of these beneficial anticancer compounds and, provides the possible relevance of this natural source in the production of pharmaceuticals.[32] It is known that taxanes such as paclitaxel, which exhibit certain cytotoxicity, prevent cancer cells from proliferating and inhibit the rate at which middle- and late-stage cells transform, are found in hazelnut shells, GLC, and leaves.[5] In addition, recent studies that investigated the activity of cephalomannine in cell viability considered that this compound is a promising natural agent for treating different cancer types.[32] It has also been proven that cephalomannine significantly attenuates hepatocellular carcinoma progression.[28] Li and Parry[38] monitored the antioxidant activities and antiproliferative effects of Turkish and Oregon hazelnut parts and demonstrated that extracts from roasted hazelnut skins suppressed the proliferation of cancer cells and exhibited free radical scavenging properties. Consuming the kernel with BS is strongly suggested for preventing the loss of bioactive compounds from the kernel, although there is no unanimous opinion about the kernel and its BS relationships in terms of bioactivity.[1,38,39]

This is the first report that revealed the differences in taxane contents of Turkish standard and local hazelnut genotypes in different edible and non-edible kernel parts. The data reveals that there are significant differences between genotype and hazelnut parts. Previous studies have demonstrated that the synthesis of taxane compounds in these plants can exhibit significant heterogeneity depending on conditions such as land compositions, height, climate, genotype, and tissue type. Türkiye with a wide-ranging collection of hazelnut genotypes and a leading position in global production has promising potential for the recovery of these compounds and a rich source of this functional food with an anticancer perspective.

Study limitations

In this study, 4 anticancer taxane compounds were analyzed separately in 5 different kernel parts of 7 Turkish hazelnut genotypes and were presented with comprehensive and detailed data for future research. However, in addition to the hazelnut parts analyzed in this study, enriching the results by analyzing leaf and stem samples, in the same way, may contribute to the overall assessment of taxane contents in Turkish hazelnut varieties.

CONCLUSION

Türkiye is a leading global hazelnut producer, resulting in being one of the countries with the highest amounts of by-products such as GLC and HSs. Identification of taxanes in hazelnut by-products which are commonly considered as discarded material and produced thousands of tonnes per year is a future alternative for obtaining these compounds from readily available natural resources. Moreover, our findings challenged previous knowledge about the recovery of taxanes from edible parts of hazelnuts. While HSs, BSKs, and BSs were rich in taxanes in all of the analyzed hazelnut genotypes, SKs, and GLCs remain limited for these anticancer taxanes. Surprisingly, BSKs of local genotypes were found rich in taxanes than skinless kernels of standard genotypes. Our study has revealed significant findings on the abundance of taxane compounds in Turkish hazelnuts including previously untested genotypes and their parts. These findings are expected to highlight the

health benefits of consuming raw Turkish hazelnuts with BSs and their possible use as a functional food. Perhaps regular consumption of a certain amount of the kernels of Ham, Palaz, Kalınkara, Sivri, and Tombul hazelnuts containing the paclitaxel compound can prevent the irregular proliferation of body cells. Collectively, the data presented in this study can be used not only in breeding projects aiming at choosing cultivars with higher levels of health-promoting compounds but also to expand the pharmaceutical potential of local genotypes with further studies based on using a holistic approach.

Acknowledgements

The authors acknowledge funding from the Scientific Research Projects of İstanbul University under Project No. FYL-2018-31616. We wish to thank Sabriye Perçin Özkorucuklu for being a scientific advisor at the beginning of the experiments.

Ethics

Ethics Committee Approval: Not required.

Informed Consent: Not required.

Authorship Contributions

Concept: Ş.A., Design: G.Z.K., E.S.D., B.K., H.İ.U., Ş.A., Data Collection or Processing: G.Z.K., E.S.D., B.K., Analysis or Interpretation: G.Z.K., B.Y., Literature Search: B.Y., H.İ.U., Ü.S., Ş.A., Writing: G.Z.K., B.Y., Ş.A.

Conflict of Interest: No conflict of interest was declared by the authors.

Financial Disclosure: The authors declared that this study received no financial support.

REFERENCES

1. Bottone A, Cerulli A, D'Urso G, Masullo M, Montoro P, Napolitano A, Piacente S. Plant speialized metabolites in hazelnut (*Corylus avellana*) kernel and byproducts: An update on chemistry, biological activity, and analytical aspects. Planta Med. 2019; 85 (11/12):840-855.
2. Çetin N, Yaman M, Karaman K, Demir B. Determination of some physicomechanical and biochemical parameters of hazelnut (*Corylus avellana* L.) cultivars. Turk J Agric. 2020;44:439-450.
3. Shahidi F, Alasalvar C, Liyana-Pathirana CM. Antioxidant phytochemicals in hazelnut kernel (*Corylus avellana* L.) and hazelnut byproducts. J Agric Food Chem. 2007;55:1212-1220.
4. Food and Agriculture Organization of the United Nations, FAOSTAT; 2021 Crops and Livestock Product. Avaible from: https://www.fao.org/faostat/en/#data/QCL [accessed 05.07.2023].
5. Zhao J, Wang X, Lin H, Lin Z. Hazelnut and its by-products: A comprehensive review of nutrition, phytochemical profile, extraction, bioactivities and applications. Food Chem. 2023;413:135576.
6. Alasalvar C, Shahidi F, Liyanapathirana CM, Ohshima T. Turkish Tombul hazelnut (*Corylus avellana* L). 1. Compositional characteristics. J Agric Food Chem. 2003;51:3790-3796.
7. U.S.Department of Agriculture, USDA; 2018. Food Composition Databases. Avaible from: https://fdc.nal.usda.gov [accessed 05.07.2023].
8. Tunçil YE. Dietary fibre profiles of Turkish Tombul hazelnut (*Corylus avellana* L.) and hazelnut skin. Food Chem. 2020;316:126338.
9. Ceylan FD, Adrar N, Bolling BW, Capanoglu E. Valorisation of hazelnut by-products: current applications and future potential. Biotechnol Genet Eng Rev. 2022:1-36.
10. Xu Y, Sismour EN, Parry J, Hanna MA, Li H. Nutritional composition and antioxidant activity in hazelnut shells from US-grown cultivars. Int J Food Sci Technol. 2012;47:940-946.
11. Saricaoglu FT, Gul O, Besir A, Atalar I. Effect of high pressure homogenization (HPH) on functional and rheological properties of hazelnut meal proteins obtained from hazelnut oil industry by-products. J Food Eng. 2018;233:98-108.
12. Puliga F, Leonardi P, Minutella F, Zambonelli A, Francioso O. Valorization of hazelnut shells as growing substrate for edible and medicinal mushrooms. Horticulturae. 2022;8:214.
13. Contini M, Baccelloni S, Frangipane MT, Merendino N, Massantini R. Increasing espresso coffee brew antioxidant capacity using phenolic extract recovered from hazelnut skin waste. J Funct Foods. 2012;4:137-146.
14. Özdemir KS, Yılmaz C, Durmaz G, Gökmen V. Hazelnut skin powder: A new brown colored functional ingredient. Food Res Int. 2014;65:291-297.
15. Hoşgün EZ, Bozan B. Effect of different types of thermochemical pretreatment on the enzymatic hydrolysis and the composition of hazelnut shells. Waste Biomass Valori. 2020;11:3739-3748.
16. Alasalvar C, Karamać M, Amarowicz R, Shahidi F. Antioxidant and antiradical activities in extracts of hazelnut kernel (*Corylus avellana* L.) and hazelnut green leafy cover. J Agric Food Chem. 2006;54:4826-4832.
17. Hoffman A, Khan W, Worapong J, Strobel G, Griffin D, Arbogast B, Zheng P, Boone RB, Ning L, Daley L, Strobel G, Barosfsky DF. Bioprospecting for taxol in angiosperm plant extracts-using high performance liquid chromatography thermospray mass spectroscopy to detect the anticancer agent and its related metabolites in Filbert trees. Spectrosc.1998;13:22-32.
18. Ottaggio L, Bestoso F, Armirotti A, Balbi A, Damonte G, Mazzei M, Sancandi M, Miele M. Taxanes from shells and leaves of *Corylus avellana*. J Nat Prod. 2008;71:58-60.
19. Hoffman A, Shahidi F. Paclitaxel and other taxanes in hazelnut. J Funct Foods. 2009;1:33-37.
20. Oguzkan SB, Karadeniz S, Karagul B, Uzun A, Aksoy ES, Guler OO, Cakir U, Ugras HI. Effects of some adsorbents on the pre-purification of taxol (Anticancer drug) from hazelnut nutshells. Int J Pharmacol. 2018;14:835-840.
21. Oguzkan SB, Karagul B, Aksoy ES, Uzun A, Can M, Yilmaz H, Ugras HI, Binici B, Goren AC. Determination of taxanes by validated LC-MS/MS method in hazelnut collected from different regions and altitudes in Turkey. J Chem Metrol. 2018;12:26-33.
22. Fitzpatrick FA, Wheeler R. The immunopharmacology of paclitaxel (Taxol), docetaxel (Taxotere), and related agents. Int Immunopharmacol. 2003;3:1699-1714.
23. Swamy MK, Pullaiah T, Chen ZS. Paclitaxel: Sources, chemistry, anticancer actions, and current biotechnology. Elsevier. 2021;2-45. https://doi.org/10.1016/C2020-0-02897-5
24. Oguzkan SB, Karagul B, Uzun A, Güler ÖÖ, Ugras HI. Pre-purification of an anticancer drug (Paclitaxel) obtained from nut husks. Int J Pharmacol. 2018;14:76-82.
25. Panchagnula P. Pharmaceutical aspects of paclitaxel. Int J Pharm.1998;1-15.

26. Ohtsu H, Nakanishi Y, Bastow KF, Lee FY, Lee KH. Antitumor agents 216. Synthesis and evaluation of paclitaxel-camptothecin conjugates as novel cytotoxic agents. Bioorg Med Chem. 2003;11:1851-1857.

27. Helson L. Cephalomannine and 10-deacetyltaxol cytotoxicity in human glial and neuroblastoma cell-lines. Int J Oncol. 1993;2:297-299.

28. Zhang RY, Liu ZK, Wei D, Yong YL, Lin P, Li H, Liu M, Zheng NS, Liu K, Hu CX, Yang XZ, Chen ZN, Bian H. UBE2S interacting with TRIM28 in the nucleus accelerates the cell cycle by ubiquitination of p27 to promote hepatocellular carcinoma development. Signal Transduct Target Ther. 2021;6:64.

29. Peng S, Chen X, Huang C, Yang C, Situ M, Zhou Q, Ling Y, Huang H, Huang M, Zhang Y, Cheng L, Zhang Q, Guo Z, Lai Y, Huang J. UBE2S as a novel ubiquitinated regulator of p16 and β-catenin to promote bone metastasis of prostate cancer. Int J Biol Sci. 2022;18:3528-3543

30. Qiao Z, Kondo T. Identification of cephalomannine as a drug candidate for glioblastoma *via* high-throughput drug screening. J Electrophor. 2018;62:17-20.

31. Dell'Anno I, Melani A, Martin SA, Barbarino M, Silvestri R, Cipollini M, Giordano A, Mutti L, Nicolini A, Luzzi L, Aiello R, Gemignani F, Landi S. Drug screening revealed novel potential agents against malignant pleural mesothelioma. Cancers (Basel). 2022;14:2527.

32. Ullah A, Leong SW, Wang J, Wu Q, Ghauri MA, Sarwar A, Su Q, Zhang Y. Cephalomannine inhibits hypoxia-induced cellular function *via* the suppression of APEX1/HIF-1α interaction in lung cancer. Cell Death Dis. 2021;12:490.

33. Kutluturk GZ. Analysis of anticancer taxanes in hazelnuts (*Corylus avellana* L.) grown in Türkiye, Master Thesis. İstanbul University Institute of Science and Technology; 2019.

34. İslam A. Hazelnut culture in Türkiye. Akademik Ziraat Derg. 2018;7:259-266.

35. Alasalvar C, Shahidi F. Natural antioxidants in tree nuts. Eur J Lipid Sci Technol. 2009;111:1056-1062.

36. Di Nunzio M. Hazelnuts as source of bioactive compounds and health value underestimated. Curr Res Nutr Food Sci. 2019;7:17-28.

37. Phuc DTH, Popovich DG. Screening for paclitaxel and other taxanes in kernel and shell of *Corylus avellana* (Hazelnut). J pharmacogn Phytochem. 2017;6:247-254.

38. Li H, Parry JW. Phytochemical compositions, antioxidant properties, and colon cancer antiproliferation effects of Turkish and Oregon hazelnut. Food Sci Nutr. 2011;2:1142-1149.

39. Taş NG, Gökmen V. Bioactive compounds in different hazelnut varieties and their skins. J Food Compos Anal. 2015;43:203-208.